REALIZATION SPACES

OF POLYTOPES

by

Jürgen Richter-Gebert
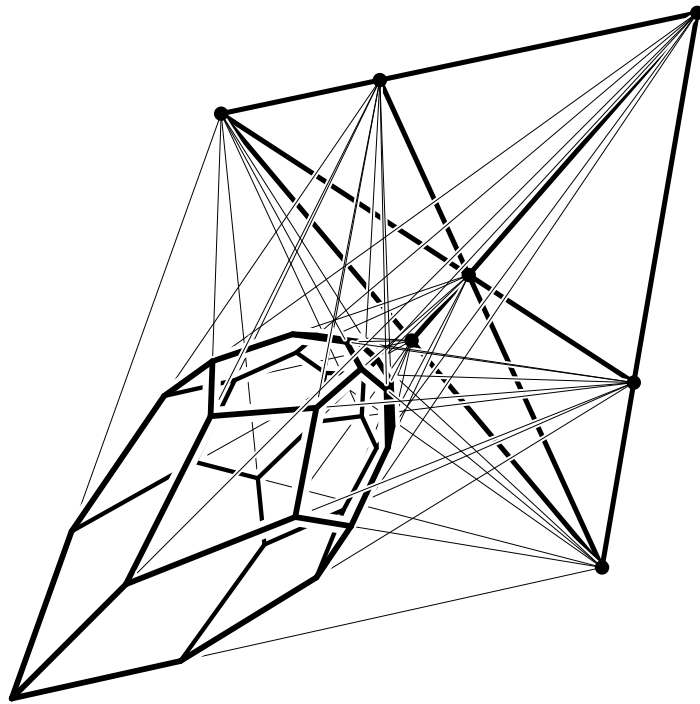
Technische Universität Berlin, 1996

Author's address: Dr. Dr. Jürgen Richter-Gebert

Technische Universität Berlin,

FB Mathematik, Sekr. 6-1,

Straße des 17. Juni 136,

D-10623 Berlin, Germany

e-mail: `richter@math.tu-berlin.de`
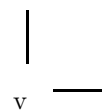
For Ingrid and Angela-Sophia,

who helped me so much.

Steinitz's Theorem (proved in 1922) is one of the oldest and most prominent results in polytope theory. It gives a completely combinatorial characterization of the face lattices of 3-dimensional polytopes. Steinitz observed that the technique of proving his theorem also implies that for any 3-dimensional polytope the set of all its *realizations* is a trivial topological set. In other words: *realization spaces of 3-dimensional polytopes are contractible.* For a long time it was an open problem whether there exist similar results in spaces of dimension greater than three. It was proved by Mnëv in 1986 that the contrary is the case. As a consequence of his famous Universality Theorem for oriented matroids he showed that *realization spaces of polytopes with dimension-plus-four vertices can have arbitrary homotopy type.* The present research monograph studies the structure of realization spaces of polytopes in *fixed dimension*. The main result that is obtained is a Universality Theorem for 4-polytopes. It states that *for every primary basic semialgebraic set V there exists a 4-dimensional polytope whose realization space is stably equivalent to V*.

This research monograph has three goals. First of all it serves as a comprehensive source for all results that I have been able to obtain in connection to the Universality Theorem for 4-polytopes. It includes complete proofs of all these results including a proof of the Universality Theorem itself. Secondly, it is (as the title says) meant as an introduction to the beautiful theory of realization spaces of polytopes. For that purpose also a treatment of Steinitz's Theorem is included. Although the result is classical the proof presented here contains some new and fresh elements. In particular, we provide a new proof for Tutte's Theorem on equilibrium representations of planar graphs. We also give a complete proof of Mnëv's Universality Theorem for oriented matroids (and of its generalization: the Universal Partition Theorem). Last but not least, this monograph is written for the sake of enjoyment of geometric constructions. Most of the concepts and constructions that are needed here are elementary in nature. The final construction for the Universality Theorem is obtained by building larger and larger polytopal units of increasing geometric and algebraic complexity. We start from small incidence configurations, go to polytopes for addition and multiplication, and end up with polytopes that encode entire polynomial inequality systems. I hope that the reader can feel the fun that lies in these constructions.

There are many alternative ways of approaching the main results of this monograph. In particular, there are several different ways to build up the proof

of the Universality Theorem for 4-polytopes. However, all the approaches kown to me rely on similar principles:

- first construct small and useful polytopes (using *Lawrence Extensions* or similar techniques) that have non-prescribable facets (or vertex figures),
- use *connected sums* to join these polytopes to larger units that are capable of encoding arithmetic operations,
- finally use *connected sums* to join these arithmetic units into even larger polytopes that encode entire polynomial inequality systems.

Here I have chosen an approach that is very modular. The basic building blocks are *very* simple polytopes, and the whole complexity is governed by the way of composing these blocks.

In order to obtain the strongest possible results it was necessary to set up a new concept of *stable equivalence* that compares realization spaces with other semialgebraic sets. The reader may excuse the fact that whenever stable equivalence between two spaces is proved the exposition becomes a bit technical. Everywhere else I used concrete geometric approaches rather than abstract settings. Whenever it is possible the constructions are carried out in an explicit manner.

Part I to Part III are based on my Habilitationsschrift at the Technical University Berlin, 1995. The typesetting of this monograph relies on LaTeX. Most of the drawings are done with *Cinderella*.

There are many people who have made the writing of this monograph possible. First of all I want to thank Günter M. Ziegler for offering me a position where I could concentrate mainly on this work. I am extremely grateful to him for his careful reading of every page and for the uncountably many valuable suggestions, discussions, comments and protests that encouraged me to go always one step further than I had already done.

Also I am very grateful to Anders Björner, Marie-Françoise Coste-Roy, Henry Crapo, Eva-Maria Feichtner, Eli Goodman, Martin Henk, Peter Kleinschmidt, Ulli H. Kortenkamp, Peter McMullen, Ricky Pollack, Jörg Rambau, and Bernd Sturmfels for many inspiring discussions and valuable comments on my manuscript in its various stages.

I especially, want to thank my wife Ingrid and my little daughter Angela-Sophia, who was born on the day of the "breakthrough" for the main theorem. Angela-Sophia's inspiring presence definitely helped me to keep my thoughts as simple as possible. Without Ingrid I would have never been able to write all this. She always had an open ear for me that helped me to clarify my ideas, and she accompanied me through all the "dead ends" that are unavoidable in such a kind of work.

Berlin, October 1996   JÜRGEN RICHTER-GEBERT

Contents

1 Polytopes and their Realizations

Polytopes have a long tradition as objects of mathematical study. Their historical roots reach back to the ancient Greek mathematicians, having a first highlight in their enumeration of the famous Platonic Solids. Already at this point strong impetus came from the fact that polytopes intimately connect topics from geometry and from combinatorics (the Platonic Solids solve a first enumerative question in polytopal geometry, to find all polytopes with a *flag transitive* symmetry group — a combinatorial concept). The work presented in this research monograph is also motivated from questions that are on the borderline of geometry, algebra and combinatorics. We investigate the structure of the *realization spaces* of polytopes with fixed combinatorial types. Our aim is to exhibit a radical contrast between the behavior of realization spaces for polytopes in dimensions three and four.

For three-dimensional polytopes the structure of the realization spaces turns out to be rather simple (a consequence of the classical *Steinitz's Theorem* that was already known in 1922). However, realization spaces of four-dimensional polytopes can behave as complicated as one can think of (as a consequence of the *Universality Theorem* first presented in this monograph). We will give complete proofs of these two theorems and explore their far reaching consequences.

1.1 Polytopes

Formally, polytopes are the convex hulls of finite point sets in $\mathbb{R}^d$:

<u>Definition 1.</u> Let $\boldsymbol{P} = (\boldsymbol{p}_1, \ldots, \boldsymbol{p}_n) \in \mathbb{R}^{d \cdot n}$ be a finite collection of points that affinely span $\mathbb{R}^d$. The set

$$P = \mathbf{conv}(\boldsymbol{P}) := \Big\{ \sum_{i=1}^{n} \lambda_i \boldsymbol{p}_i \mid \sum_{i=1}^{n} \lambda_i = 1 \text{ and } \lambda_i \geq 0 \text{ for } i = 1, \ldots, n \Big\},$$

the *convex hull* of the point set $\boldsymbol{P}$, is called a *d-dimensional polytope* (a *"d-polytope"* for short). The *faces* of P are P itself and the intersections $P \cap A$, such that A is an affine hyperplane that does not meet the interior of P. The *face lattice* of P is the set of all faces of P, partially ordered by inclusion.

(a)   (b)
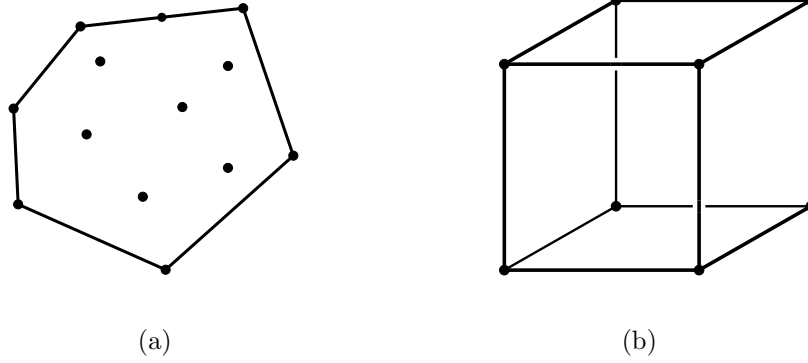
Figure 1:   A convex polygon and a cube. Two simple examples of polytopes.

While a polytope is a geometric object, its face lattice is purely combi-
natorial in nature. Figure 1(a) illustrates a 2-polytope as the convex hull of a
finite number of points in the plane. We see that those points that are not in
an extreme position make no contribution to the polytope itself. The points in
extreme position (i.e., the 0-dimensional faces) are the *vertices* of a polytope.
Figure 1(b) shows a cube as an example of a 3-dimensional polytope. The face
lattice of the cube consists of the cube itself, 6 facets, 12 edges, 8 vertices and
the empty set.

The need to structure the set of all polytopes of a fixed dimension leads to
two main lines of study:

- to list all possible combinatorial types of polytopes (in other words, to
  determine which finite lattices correspond to face lattices of polytopes, and
  which do not),
- to describe the set of all realizations of a given combinatorial type.

The "set of all realizations" of a combinatorial type is formalized below by
the concept of the *realization space* of a polytope. Besides their intrinsic impor-
tance for questions of real discrete geometry, such spaces appear in subjects as
diverse as algebraic geometry (moduli spaces), differential topology (see Cairns'
smoothing theory [21]), and nonlinear optimization (see Günzel et al. [33]).

Assume that in Definition 1 each point $\boldsymbol{p}_i$ for $i = 1, \ldots, n$ is a vertex of P.
A *realization* of a polytope P is a polytope $Q = \mathbf{conv}(\boldsymbol{q}_1, \ldots, \boldsymbol{q}_n)$ such that the
face lattices of P and Q are isomorphic under the correspondence $\boldsymbol{p}_i \to \boldsymbol{q}_i$. The
sequence of vertices $B = (\boldsymbol{p}_1, \ldots, \boldsymbol{p}_{d+1})$ is a *basis* of $\boldsymbol{P}$ if these points are affinely
independent in any realization of P.

<u>DEFINITION 2.</u> Let $P = \mathbf{conv}(\boldsymbol{p}_1, \ldots, \boldsymbol{p}_n) \subset \mathbb{R}^d$ be a d-polytope with n vertices and with a basis $B = (\boldsymbol{p}_1, \ldots, \boldsymbol{p}_{d+1})$. The *realization space* $\mathcal{R}(P, B)$ is the set of all matrices $\boldsymbol{Q} = (\boldsymbol{q}_1, \ldots, \boldsymbol{q}_n) \in \mathbb{R}^{d \cdot n}$ for which $\mathbf{conv}(\boldsymbol{Q})$ is a realization of P and $\boldsymbol{q}_i = \boldsymbol{p}_i$ for $i = 1, \ldots, d + 1$.

By the choice of a certain basis for which the points have to stay fixed, we factor out components in the set of all realizations of a polytope that come from rotations and translations. It turns out that the realization space $\mathcal{R}(P, B)$ is essentially (up to "stable equivalence," see below) independent of the choice of an admissible basis. Hence it makes sense to speak of *the* realization space $\mathcal{R}(P)$ of a polytope.

Every realization space is a *primary basic semialgebraic set*: it is the set of solutions of a finite system of polynomial equations $f_i(x) = 0$ and strict inequalities $g_j(x) > 0$, where the f_i and g_j are polynomials with integer coefficients on $\mathbb{R}^{d \cdot n}$. To see this, one checks that the realization space is the set of all matrices $\boldsymbol{Q} \in \mathbb{R}^{d \cdot n}$ for which some entries are fixed, and the determinants of certain $d \times d$ minors have to be positive, negative, or zero.

Our main aim here is a Universality Theorem for 4-polytopes, stating that for every primary semialgebraic V set there exists a 4-polytope whose realization space is "stably equivalent" to V. The concept of *stable equivalence* will be clarified in Section 2. It can be considered as a strengthened version of homotopy equivalence that preserves also information on the underlying algebraic structure. In particular, if two semialgebraic sets V and V' are stably equivalent and V contains non-rational points, then V' contains non-rational points as well.

1.2 History I: Steinitz's Theorem

What does the realization space of a polytope look like? Which algebraic numbers are needed to coordinatize the vertex set of a given d-dimensional polytope? How can one tell whether a finite lattice is the face lattice of a polytope or not?

For 3-dimensional polytopes, Steinitz's work [56, 55] answered the basic questions about realization spaces more then seventy years ago. In particular, Steinitz's "Fundamentalsatz der konvexen Typen" (today known as *Steinitz's Theorem*) and its modern relatives (see [31] and [65]) provide complete answers to the above questions for this special case.

<u>STEINITZ'S THEOREM (1922):</u> *A graph G is the edge graph of a 3-polytope if and only if G is simple, planar and 3-connected.*

The classical proof by Steinitz is done by a clever combinatorial reduction technique that allows one to generate larger 3-polytopes from smaller ones. Alternatively, Steinitz's Theorem can be proved using the *Koebe-Andreev-Thurston Circle Packing Theorem* (see [65]), or by arguments using the concept of *self-stresses of planar graphs* (see [23, 36, 47], and Part IV). The statements in the

following list can be derived from a careful inspection of the known proofs of
Steinitz's Theorem.

- For every 3-polytope $P \subseteq \mathbb{R}^3$ the realization space $\mathcal{R}(P)$ is a smooth open
  ball. (This ball has dimension $e - 6$, if P has e edges.)
- For every 3-polytope P the space $\mathcal{R}(P)$ contains rational points, that is,
  every 3-polytope can be realized with integral vertex coordinates.
- Every combinatorial 2-sphere is polytopal.
- BARNETTE, GRÜNBAUM, 1970, [12]: The shape of one 2-face in the bound-
  ary of a 3-polytope P can be arbitrarily prescribed, that is, the canonical
  map $\mathcal{R}(P) \to \mathcal{R}(F)$ is surjective for every facet $F \subseteq P$.
- ONN, STURMFELS, 1992, [51]: If a 3-polytope has n vertices then it can be
  realized with integral coefficients smaller than n^{169n^3}.

In Part IV of this monograph we will present a proof of Steinitz's Theorem that is
based on the self stress approach. This approach also proves that the realization
space of any 3-polytope is contractible, and that it contains rational points. In
particular, our treatment will improve the bound given by Sturmfels and Onn.

- Any 3-polytope P with n vertices can be realized with integral coordinates
  smaller than 2^{18n^2}.
- If P furthermore contains a triangle, then it can be realized with integral
  coordinates smaller than 43^n.

One can prove statements similar to the above corollaries for d-polytopes
that have at most $d + 3$ vertices. Under (affine) Gale duality these polytopes are
encoded by certain point arrangements on a line. This fact leads to a classification
method that allows one to analyze these polytopes. Most of this analysis has been
done by Mani [44] and Kleinschmidt [41].

- Every combinatorial $(d-1)$-sphere with $d + 3$ vertices is polytopal.
- Every d-polytope with $d+3$ vertices can be realized with integral coefficients.
- The realization space of every d-polytope with $d+3$ vertices is contractible.

1.3   History II: Polytopes in Dimension Higher than 3

Over the years, it became clear that no similar positive answer could be expected
for high-dimensional polytopes. The situation becomes much more complicated
if either the dimension or the codimension exceeds three. We first discuss the
case of fixed dimension. There are several d-polytopes (with $d \geq 3$) known that
behave differently from 3-polytopes with respect to realizability. The following
list summarizes chronologically the counterexamples that are found to contrast
with the 3-dimensional case.

- PERLES, 1967, [31]:
  Non-rational 8-polytope (12 vertices, 28 facets).

- BARNETTE, 1971, [8]:
  Non-polytopal combinatorial 3-sphere (8 vertices, 19 facets).
- KLEINSCHMIDT, 1976, [40]:
  4-polytope with non-prescribable 3-face (10 vertices, 15 facets).
- BARNETTE, 1980, [11]:
  4-polytope with non-prescribable 3-face (12 vertices, 7 facets).
- BOKOWSKI, EWALD, KLEINSCHMIDT, 1984, [15, 16]:
  4-polytope with disconnected realization space (10 vertices, 28 facets).
- ZIEGLER, 1992, [65]:
  5-polytope with non-prescribable 2-face (12 vertices, 10 facets).

Besides these "sporadic examples," no general construction technique was known to produce polytopes with a "controllably bad" behavior for any fixed dimension. The σ-construction presented in [57] for that purpose turned out to be incorrect [65].

If we investigate the case of codimension four much more is known and general tools are applicable. In 1986 N.E. Mnëv proved a *Universality Theorem for oriented matroids* of rank 3 (see [7, 33, 52, 48, 49]). This result leads, via Gale diagram techniques, to a universality theorem for d-polytopes with $d+4$ vertices: in general for such polytopes the realization spaces can be arbitrarily complicated. In technical terms the Universality Theorem can be stated as:

MNËV'S UNIVERSALITY THEOREM (1986):

(i) *For every primary basic semi-algebraic set V defined over $\mathbb{Z}$ there is a rank 3 oriented matroid whose realization space is stably equivalent to V.*

(ii) *For every primary basic semi-algebraic set V defined over $\mathbb{Z}$ there is an integer $d > 1$ and a d-polytope P with $d+4$ vertices whose realization space is stably equivalent to V.*

Stable equivalence is a strong concept of topological equivalence, that in particular preserves homotopy type and the algebraic complexity of test points. So Mnëv's construction implies:

- The realizability problem for d-polytopes with $d+4$ vertices is (polynomial time) equivalent to the "Existential Theory of the Reals."
- The realizability problem for d-polytopes with $d+4$ vertices is NP-hard.
- All algebraic numbers are needed to coordinatize all d-polytopes with $d+4$ vertices.
- For every finite simplicial complex Δ there is a d-polytope with $d+4$ vertices whose realization space is homotopy equivalent to Δ.

It will be the main purpose of this monograph to establish similar results for the case of polytopes in fixed dimension $d = 4$.

1.4   New Results on 4-Polytopes

We will constructively prove that the realization spaces of 4-polytopes can be "arbitrarily ugly," in a well defined sense.

<u>Universality Theorem for 4-Polytopes:</u>
For every primary basic semi-algebraic set V defined over $\mathbb{Z}$, there is a 4-polytope P whose realization space is stably equivalent to V. The face lattice of P can be generated from defining equations of V in polynomial time.

The following new results are corollaries of the Universality Theorem or consequences of the construction we provide for it.

  (i) There is a non-rational 4-polytope with 33 vertices.

 (ii) All algebraic numbers are needed to coordinatize all 4-polytopes.

(iii) The realizability problem for 4-polytopes is NP-hard.

(iv) The realizability problem for 4-polytopes is (polynomial time) equivalent to the "Existential Theory of the Reals" (see [53]).

 (v) For every finite simplicial complex Δ, there is a 4-polytope whose realization space is homotopy equivalent to Δ.

(vi) There is a 4-polytope for which the shape of some 2-face cannot be arbitrarily prescribed.

(vii) Polytopality of 3-spheres cannot be characterized by excluding a finite set of "forbidden minors".

(viii) In order to realize all combinatorial types of integral 4-polytopes with n vertices in the integer grid $\{1, 2, \ldots, f(n)\}^4$, the "coordinate size" function $f(n)$ has to be at least doubly exponential in n.

In particular these consequences solve all the problems that were recently emphasized in Ziegler's article *"Three problems about 4-polytopes"* [64].

The proof of the Universality Theorem is constructive. We will describe 4-polytopes that model *addition* and *multiplication* by the non-prescribability of a 2-dimensional face. The addition- and multiplication-polytopes will be joined into larger units that model systems of polynomial equations and inequalities.

Our approach is in some sense analogous to Mnëv's original proof of his Universality Theorem for oriented matroids. He uses the classical *von Staudt constructions* (which model addition and multiplication for points on a line in the projective plane) to compose large planar incidence structures that model arbitrary polynomial computations. The main difficulty in Mnëv's proof is to organize the construction in a way such that different basic calculations do not interfere and such that the underlying oriented matroid stays invariant for all instances of a geometric computation. *Our* main difficulty will be the construction of polytopes for addition and multiplication.

1.5 Polytopal Tools

Lawrence extensions and connected sums are elementary geometric operations on polytopes that form the basis for the constructions we need in order to prove the Universality Theorem. They are very simple and innocent looking operations, but they are very powerful.

For *Lawrence extensions* the basic operation is the following: take a point p in a d-dimensional point configuration, and replace it by two new points $\overline{p}$ and $\underline{p}$ that lie on a ray that starts at the original point and leaves the d-dimensional space spanned by the point configuration in a "new" direction of $(d + 1)$-dimensional space (see Figure 2).
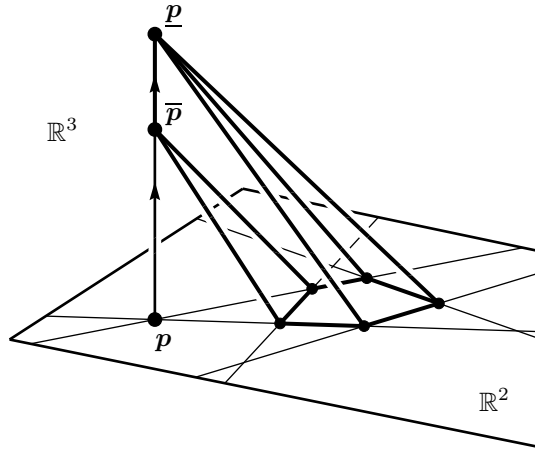
Figure 2: A Lawrence extension of a pentagon.

Every such Lawrence extension increases both the dimension of a point configuration and its number of points by 1. Note that although the original point is deleted in the construction, it is still implicitly present: it can be "reconstructed" as the intersection of the line spanned by the two new points with the d-hyperplane spanned by the original point configuration.

The "classical" use of Lawrence extensions [13, 6, 49] starts with a 2-dimensional configuration of n points, and performs Lawrence extensions on all these points, one by one. The resulting configuration of $2n$ points is the vertex set of an $(n+2)$-dimensional polytope, the *Lawrence polytope* of the point configuration. Every realization of the Lawrence polytope determines a realization of the original point configuration, including all collinearities and all orientations of triples. In fact, the realization spaces of the Lawrence polytope and the planar configuration are stably equivalent. This can be used to lift Mnëv's Universality Theorem from planar point configurations (oriented matroids) to d-polytopes.

If one wants to stay within the realm of 4-polytopes, then it is not permissible to use more than two Lawrence extensions. However, careful use of just one

or two Lawrence extensions on some points outside a 2- or 3-polytope leads to extremely interesting and useful polytopes — such as the basic building blocks for the Universality Theorem (see Section 5).

Connected sums are the operations that compose these basic building blocks into larger units. They are performed as follows: Assume that one is given two d-polytopes P_1 and P_2 that have projectively equivalent facets F_1 resp. F_2. We use F to denote the combinatorial type of $F_1 \cong F_2$. Then, using a projective transformation, one can "merge" P_1 and P_2 into a more complicated polytope, the *connected sum* $Q := P_1 \#_F P_2$. The polytope Q has all the facets of P_1 and P_2, except for F_1 and F_2. However, the boundary complex ∂F, consisting of all the proper faces of F, is still present in Q (Figure 3).

$$P_1 \qquad\qquad\qquad P_2 \qquad\qquad\qquad P_1 \#_F P_2$$
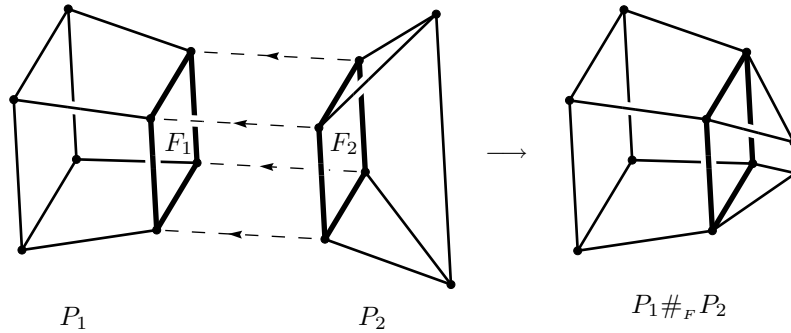
Figure 3:   The connected sum of a cube and a triangular prism.

Now, if one takes an arbitrary realization of Q, then it is not in general true that this realization arises as a connected sum of realizations of P_1 and of P_2: in a "bad" realization of Q the boundary complex ∂F may not be flat. In fact, in dimension $d = 3$ one can see that the complex ∂F in Q is necessarily flat if and only if F is a triangular facet. In dimension 4, there are much more different types of facets that are "necessarily flat," among them pyramids, prisms, and "tents." Only such necessarily flat facets are used in connected sum operations for the proof of the Universality Theorem.

1.6   Sketch of the Proof of the Universality Theorem

Our proof starts from the defining equations of a primary basic semialgebraic set, and uses them explicitly to construct the face lattice of a 4-polytope. A result of Shor [53] is used, which states that every primary semialgebraic set V is stably equivalent to a semialgebraic set $V' \in \mathbb{R}^n$ whose variables

$$1 = x_1 < x_2 < x_3 < \ldots < x_n$$

are totally ordered and for which all defining equations have the form

$$x_i + x_j = x_k \quad \text{or} \quad x_i \cdot x_j = x_k$$

for certain $1 \leq i \leq j < k \leq n$. Such a set of defining equations and inequalities is a *Shor normal form* of V. Thus only elementary addition and multiplication have to be modeled: they are encoded into the non-prescribability of a 2-face in certain polytopes.

In the following we briefly describe how a polytope $P(V)$ can be constructed, whose realization space is stably equivalent to a given primary semialgebraic set V described by a Shor normal form. While Lawrence extensions are used to generate "basic building blocks," the connected sum operation is used to combine these blocks into larger semantic units.

(i) The initial building blocks generated by Lawrence extensions are

• a 4-polytope X that contains a hexagonal 2-face with vertices $1, \ldots, 6$, in this order, such that in every realization of X the lines $1 \vee 4$, $2 \vee 3$ and $5 \vee 6$, are concurrent (see Section 5, Figure 5.4.1),

• "forgetful transmitter" polytopes T_n that contain an n-gon G and an $(n-1)$-gon G' such that in every realization of T_n the edge supporting lines of G' are projectively equivalent to edge supporting lines of G, and

• polytopes C_n that serve as "connectors" and contain three n-gons G_1, G_2 and G_3 that are projectively equivalent in every realization of C_n.

(ii) These basic building blocks are composed by applying connected sum operations to polytopes P^+ and $P^\times$ that model addition and multiplication. These two polytopes both contain 12-gons G with edges labeled by

$$0, 1, i, j, k, \infty, 0', 1', i', j', k', \infty',$$

in this order. In each realization of P^+ or $P^\times$ the six intersections $\alpha^* = \alpha \cap \alpha'$ of opposite edge supporting lines of G lie on a line ℓ. The points 0^*, 1^* and ∞^* define a projective scale σ on ℓ. Furthermore P^+ (resp. $P^\times$) is realizable if and only if $\sigma(i^*) + \sigma(j^*) = \sigma(k^*)$ (resp. $\sigma(i^*) \cdot \sigma(j^*) = \sigma(k^*)$). (Special care has to be taken in the case $i = j$.)

(iii) Again by applying connected sum operations these addition and multiplication polytopes are composed to the polytope $P(V)$ that contains an $(2n+6)$-gon G with edges labeled by

$$0, 1, 2, \ldots, n, \infty, 0', 1', 2', \ldots, n', \infty',$$

in this order. In each realization of $P(V)$ the $n+3$ intersections $\alpha^* = \alpha \cap \alpha'$ of opposite edge supporting lines of G lie on a line ℓ. The points 0^*, 1^* and ∞^* define a projective scale σ on ℓ. Addition and multiplication polytopes are added in correspondence to the defining equations of V. By this the points of V are in one-to-one correspondence to the values $\sigma(1^*), \ldots, \sigma(n^*)$ in possible realizations of $P(V)$.

Thus $P(V)$ contains a centrally symmetric $(2n+6)$-gon whose "slopes" of opposite edges in any realization of $P(V)$ encode the coordinates of the corresponding point in the semialgebraic set V. Each realization of $P(V)$ corresponds to a single point in V. Conversely, each point in V corresponds to a (contractible) set of realizations of $P(V)$.

1.7   Outline of the Monograph

This monograph consists of six main parts.

Part I is entitled "The Objects and the Tools". It is dedicated to the foundation of the results presented here. In Section 2 we first set up precise definitions of the concepts that are needed: *polytopes, cones, affine, linear* and *projective transformations, realization spaces, semialgebraic sets* and *stable equivalence.* Section 3 is devoted to the basic construction techniques that are needed for the Universality Theorem. After introducing *prisms, pyramids* and *tents* we present the two main tools: *connected sums* and *Lawrence extensions.*

Part II "The Universality Theorem" carefully develops the Universality Theorem step by step. In Section 4 we explain the basic facts about Shor normal forms, and describe how we will encode defining equations of a semialgebraic set $V \in \mathbb{R}^n$ into polytopes. In Section 5 the basic building blocks of our construction are presented in terms of Lawrence extensions. The essential properties of these basic building blocks are proved. Section 6 describes how the basic building blocks can be used to construct a polytope $\boldsymbol{H}$ that forces a harmonic relation on the edge slopes of a 2-face. Section 7 describes how we can construct addition- and multiplication-polytopes from the basic building blocks and the polytope $\boldsymbol{H}$. Section 8 describes how the desired polytope $\boldsymbol{P}(\mathcal{S})$ for a Shor normal form $\mathcal{S}$ is composed from addition- and multiplication-polytopes. We then prove that the realization space of $\boldsymbol{P}(\mathcal{S})$ is indeed stably equivalent to the semialgebraic set associated with $\mathcal{S}$. This completes the proof of the Universality Theorem.

Part III "Applications of Universality" is dedicated to consequences and to results that are related to the Universality Theorem. Section 9 presents complexity theoretic implications. There we will prove algorithmic complexity results, prove results on the topological structure of realization spaces, describe constructions of infinite classes of non-polytopal combinatorial spheres and present constructions for small non-rational polytopes. We also show that the maximal required grid size to realize all integral polytopes with n vertices grows doubly exponential with n. In Section 10 we will transfer our universality results from 4-polytopes to 3-dimensional diagrams and 4-dimensional fans. We will prove that nearly all our results on 4-polytopes (universality of realization spaces, NP-completeness, impossibility of local characterizations, algebraic complexity and doubly exponential growth of size) are also valid for a corresponding setup for 3-diagrams and 4-fans. Section 11 describes an interesting generalization of the Universality Theorem: the *Universal Partition Theorem for* 4-*polytopes.* While the Universality Theorem dealt with a single primary semialgebraic set, the Universal Partition Theorem is concerned with a family of such sets that are nested

in a complicated way. The main statement of the Universal Partition Theorem is that (up to stable equivalence) one can recover this family of semialgebraic sets as a family of realization spaces of polytopes. These realization spaces are nested in a way that is topologically equivalent to the nesting of the original semialgebraic sets. This section also includes a proof of the Universal Partition Theorem for oriented matroids.

In Part IV "Three-dimensional Polytopes" we give a proof of Steinitz's Theorem about 3-polytopes. This part is accessible already after Section 2 is read. The proof that is presented here is based on the relation of polytopes and stressed graphs. A theorem of Tutte [59] (that states that a self stress representation of a planar 3-connected graph always has convex non-overlapping cells) is a basic ingredient in this proof. We present also a complete proof of Tutte's Theorem (using a technique that is different from Tutte's original approach). Then we prove that realization spaces of 3-polytopes are trivial (i.e. in particular contractible). We also show that all combinatorial types of 3-polytopes with integer vertices can be embedded on the integer grid $\{1, 2, \ldots, f(n)\}^3$ where $f(n)$ is singly exponential in n^2 (resp. singly exponential in n for the simplicial case).

Part V presents "Alternative Construction Techniques" that lead to similar (but weaker) results as our Universality Theorem. These techniques are presented here since they contain construction principles (different from the previous ones) that are of interest on their own right. We first prove a Non-Steinitz Theorem in dimension 5. The proof is based on the combination of Ziegler's polytope that has a non-prescribable 2-face and an incidence theorem about conics on 2-manifolds. After this we describe how Mnëv's Universality Theorem for oriented matroids can be transfered to a Universality Theorem for 6-polytopes. This proof nicely relates several concepts from oriented matroid theory and from polytope theory: (universality of oriented matroids, "flat" oriented matroids, zonotopes, polars of projections, Lawrence extensions, and connected sums). The proof obtained there is considerably shorter than the proof for the Universality Theorem 4-polytopes. The construction even leads to a closed formula that associates with an oriented matroid $\mathcal{M}$ (that arises from Mnëv's constructions) a polytope $P(\mathcal{M})$ whose realization space is stably equivalent to that of $\mathcal{M}$.

Finally, Part VI gives a collection of "Open Problems" related to realization spaces of polytopes. There we will also collect further comments and related results.

PART I: THE OBJECTS AND THE TOOLS

2 Polytopes and Realization Spaces

In this Section we present the basic notions and concepts on which all further investigations are based. Our philosophy thereby is of a "puristic" nature. We want to have the suitcase in which we carry the relevant concepts "as light as possible." For that reason we concentrate on four relevant concepts:

- polytopes and their combinatorial nature,
- geometric transformations of polytopes,
- realization spaces,
- semialgebraic sets and stable equivalence.

The interrelation between these concepts is the core issue of this monograph. The reader who wants to have a broader introduction into the theory of polytopes can find excellent treatments in the classical book of Grünbaum [31] and in the recently published book of Ziegler [65].

2.1 Notational Conventions

Our polytopes will be embedded in real vector spaces, and they will often be represented by the coordinates of their vertices. A vector $\boldsymbol{p} = (p_1, \ldots, p_d)^T \in \mathbb{R}^d$ is usually interpreted as a column vector. The origin of $\mathbb{R}^d$ is $\boldsymbol{0} := (0, \ldots, 0)^T$. The standard operations that will be used on this level are *addition* $\boldsymbol{p} + \boldsymbol{q}$ of vectors, *multiplication* $\lambda \cdot \boldsymbol{p}$ with a real scalar $\lambda \in \mathbb{R}$, and the canonical *scalar product* $\langle \boldsymbol{p}, \boldsymbol{q} \rangle$, and the *cross product* $\boldsymbol{p} \times \boldsymbol{q}$ of two vectors in $\mathbb{R}^3$. The scalar product and cross product are defined by

$$\langle \begin{pmatrix} p_1 \\ p_2 \\ \vdots \\ p_d \end{pmatrix}, \begin{pmatrix} q_1 \\ q_2 \\ \vdots \\ q_d \end{pmatrix} \rangle := \sum_{i=1}^{d} p_i q_i, \qquad \begin{pmatrix} p_1 \\ p_2 \\ p_3 \end{pmatrix} \times \begin{pmatrix} q_1 \\ q_2 \\ q_3 \end{pmatrix} := \begin{pmatrix} p_2 q_3 - p_3 q_2 \\ p_3 q_1 - p_1 q_3 \\ p_1 q_2 - p_2 q_1 \end{pmatrix} .$$

The *euclidean length* is defined as $||\boldsymbol{p}|| := \sqrt{\langle \boldsymbol{p}, \boldsymbol{p} \rangle}$.

We assume that the reader is familiar with basic concepts of linear algebra (in particular with linear and affine functionals and transformations and with

their representation by matrices). A linear functional $f\colon \mathbb{R}^d \to \mathbb{R}$ may be always expressed as $f(\boldsymbol{p}) = \langle \boldsymbol{x}, \boldsymbol{p} \rangle$ for a suitable vector $\boldsymbol{x} \in \mathbb{R}^d$. Equivalently, it may be expressed an element $f \in (\mathbb{R}^d)^*$ in the dual vector space. We then have $f(\boldsymbol{p}) = f \cdot \boldsymbol{p}$. A linear transformation $L\colon \mathbb{R}^d \to \mathbb{R}^d$ may be always expressed as $L(\boldsymbol{p}) = M \cdot \boldsymbol{p}$ for a suitable (real) $d \times d$ matrix M. An affine functional $f\colon \mathbb{R}^d \to \mathbb{R}$ may be always expressed as $f(\boldsymbol{p}) = \langle \boldsymbol{x}, \boldsymbol{p} \rangle + t$ for a suitable vector $\boldsymbol{x} \in \mathbb{R}^d$ and a scalar $t \in \mathbb{R}$. An affine transformation $A\colon \mathbb{R}^d \to \mathbb{R}^d$ may be always expressed as $A(\boldsymbol{p}) = M \cdot \boldsymbol{p} + \boldsymbol{t}$ for a suitable (real) $d \times d$ matrix M and a vector $\boldsymbol{t} \in \mathbb{R}^d$.

We deal with *convex polytopes* considered as objects in *affine spaces* as well as their projective counterparts, the *polyhedral cones*, objects in *linear vector spaces*. The *affine, convex, linear* and *positive hulls* of a set $S \subseteq \mathbb{R}^d$ are defined as follows:

$$\mathbf{aff}(S) := \Big\{ \boldsymbol{x} {=} \sum_{i=1}^{n} \lambda_i \boldsymbol{x}_i \mid n {\in} \mathbb{N};\ \lambda_i {\in} \mathbb{R};\ \boldsymbol{x}_i {\in} S \text{ for } i {=} 1, \ldots, n;\ \sum_{i=0}^{n} \lambda_i {=} 1 \Big\},$$

$$\mathbf{conv}(S) := \Big\{ \boldsymbol{x} {=} \sum_{i=1}^{n} \lambda_i \boldsymbol{x}_i \mid n {\in} \mathbb{N};\ \boldsymbol{x}_i {\in} S \text{ and } \lambda_i \geq 0 \text{ for } i {=} 1, \ldots, n;\ \sum_{i=1}^{n} \lambda_i {=} 1 \Big\},$$

$$\mathbf{lin}(S) := \Big\{ \boldsymbol{x} {=} \sum_{i=1}^{n} \lambda_i \boldsymbol{x}_i \mid n {\in} \mathbb{N};\ \lambda_i {\in} \mathbb{R};\ \boldsymbol{x}_i {\in} S \text{ for } i {=} 1, \ldots, n \Big\},$$

$$\mathbf{pos}(S) := \Big\{ \boldsymbol{x} {=} \sum_{i=1}^{n} \lambda_i \boldsymbol{x}_i \mid n {\in} \mathbb{N};\ \boldsymbol{x}_i {\in} S \text{ and } \lambda_i \geq 0 \text{ for } i {=} 1, \ldots, n \Big\}.$$

Throughout this monograph we deal with polytopes, and with various operations that produce larger polytopes from smaller ones. All the polytopes will have labeled vertices, and we have to keep track of vertex labelings under all our operations. A point $\boldsymbol{p}_i \in \mathbb{R}^d$ is considered as a labeled point. The index i (which is taken from some arbitrary finite index set) plays the role of the label. We usually will consider *point configurations*

$$\boldsymbol{P} = (\boldsymbol{p}_i)_{i \in X} \subseteq \mathbb{R}^{d \cdot |X|}$$

that are collections of labeled points with a finite index set X. Point configurations will sometimes be considered as finite subsets $\{\boldsymbol{p}_i\}_{i \in X}$ of $\mathbb{R}^d$. Thus it makes sense to write $\mathbf{conv}(\boldsymbol{P})$, $\mathbf{aff}(\boldsymbol{P})$, etc. For $Y \subseteq X$ the *restriction* of $\boldsymbol{P}$ to Y is denoted by

$$\boldsymbol{P}\big|_Y = (\boldsymbol{p}_i)_{i \in Y}.$$

Within a given point configuration we always assume that each label occurs at most once. However, two points $\boldsymbol{p}_i$ and $\boldsymbol{q}_i$ in different point configurations $\boldsymbol{P}$ and $\boldsymbol{Q}$ may have the same label. This will sometimes be used to emphasize a correspondence between points. In a similar way we will label lines, hyperplanes, etc. The points of a configuration $\boldsymbol{P}$ may also appear as the rows of a $n \times d$ matrix. In this case the labels will be indicated by letters preceding the rows.

We will sometimes consider point configurations as *affine* configurations and sometimes as *linear* configurations. For *affine* configurations the point coordinates are interpreted literally as positions in some $\mathbb{R}^d$. The flats considered are the *affine* hulls of subsets of points. For *linear* configurations the coordinates are always interpreted as *homogeneous coordinates* in $\mathbb{R}^{d+1}$ of point sets in $\mathbb{R}^d$. In this case a point $\boldsymbol{p}$ is considered as a representant of the ray $\{\lambda \boldsymbol{p} \mid \lambda \geq 0\}$. The flats considered in the linear situation are the *linear* hulls of subsets of points. The *affine dimension* of a point configuration $\boldsymbol{P}$ is $\mathbf{dim}(\mathbf{aff}(\boldsymbol{P}))$. The *linear dimension* of a point configuration $\boldsymbol{P}$ is $\mathbf{dim}(\mathbf{lin}(\boldsymbol{P}))$.

For an affine configuration $\boldsymbol{P} \in \mathbb{R}^{d \cdot n}$ we get its *homogenization* $\boldsymbol{P}^{\mathrm{hom}} \in \mathbb{R}^{(d+1) \cdot n}$ by embedding it into an affine hyperplane of $\mathbb{R}^{d+1}$, using the canonical map

$$\boldsymbol{p} = (p_1, \ldots, p_d)^T \longmapsto \boldsymbol{p}^{\mathrm{hom}} := (p_1, \ldots, p_d, 1)^T.$$

We then interpret the resulting points in homogeneous coordinates. If $\boldsymbol{P}^{\mathrm{hom}}$ is generated in this way, we will always have $\mathbf{pos}(\boldsymbol{P}^{\mathrm{hom}}) \neq \mathbb{R}^{d+1}$. The affine hyperplane H defined by $x_{d+1} = 1$ intersects $\mathbf{pos}(\boldsymbol{P}^{\mathrm{hom}})$ in a bounded region, the convex hull of $\boldsymbol{P}$. Conversely, if for a linear configuration $\boldsymbol{P} \in \mathbb{R}^{(d+1) \cdot n}$ there exists an affine hyperplane H (that does not contain the origin) such that $\mathbf{pos}(\boldsymbol{P}^{\mathrm{hom}}) \cap H$ is a bounded region, then we get a *dehomogenization* by intersecting $\mathbf{pos}(\boldsymbol{p})$ with H for each point $\boldsymbol{p}$ of $\boldsymbol{P}$. Such a hyperplane H is called *admissible*.

For an affine point configuration $\boldsymbol{P}$ an *admissible projective transformation* is given by a homogenization step followed by a non-degenerate linear transformation followed by a dehomogenization step. Admissible projective transformations have the property that convex sets spanned by points of $\boldsymbol{P}$ are mapped to convex sets.

2.2   Polytopes, Cones and Combinatorial Polytopes

A *convex polytope* is the convex hull of a finite set of points. A *polyhedral cone* is the positive hull of a finite set of points. The extreme points (resp. rays) of polytopes (resp. cones) are the *vertices*. By slight abuse of notation (compare Definition 1) we here identify a polytope (or cone) with the corresponding point configuration given by its vertex set. This is justified since the positions of the vertices completely determine the polytope. This will later on avoid unnecessary technicalities when we relate point configurations to polytopes via Lawrence extensions.

DEFINITION 2.2.1.

- A point configuration $\boldsymbol{P} = (\boldsymbol{p}_i)_{i \in X}$ is a *d-polytope* if for every $i \in X$ we have $\mathbf{conv}(\boldsymbol{P}) \neq \mathbf{conv}(\boldsymbol{P}\big|_{X-\{i\}})$, and $\boldsymbol{P}$ has affine dimension d.

- A point configuration $\boldsymbol{P} = (\boldsymbol{p}_i)_{i \in X}$ is a *d-cone* if for every $i \in X$ we have $\mathbf{pos}(\boldsymbol{P}) \neq \mathbf{pos}(\boldsymbol{P}\big|_{X-\{i\}})$, and $\boldsymbol{P}$ has linear dimension d.

- For a polytope $\boldsymbol{P} \in \mathbb{R}^{d \cdot n}$ the *associated cone* is $\boldsymbol{P}^{\mathrm{hom}} \in \mathbb{R}^{(d+1) \cdot n}$.

- The *faces* of a $(d+1)$-cone $\boldsymbol{P}$ are sets $F = \{i \in X \mid h(\boldsymbol{p}_i) = 0\}$ where $h: \mathbb{R}^{d+1} \to \mathbb{R}$ is a linear functional with $h(\boldsymbol{p}_i) \geq 0$ for all $\boldsymbol{p}_i \in \boldsymbol{P}$.

- The *faces* of a d-polytope $\boldsymbol{P}$ are the faces of the associated $(d+1)$-cone $\boldsymbol{P}^{\mathrm{hom}}$.

By this definition the polytope is identified with its set of vertices. The faces of a polytope are given by the set of their vertex labels. By this (slightly non-standard) notion we will avoid technical difficulties later on. We consider a face F as representing the point configuration $\boldsymbol{P}\big|_F$, the restriction of $\boldsymbol{P}$ to F. A *k-face* F of a polytope is a face for which $\boldsymbol{P}\big|_F$ has affine dimension k. A *facet* of a d-polytope is a $(d-1)$-face. The vertices of a d-polytope are the 0-faces. We denote the sets of faces, facets and vertices of a polytope $\boldsymbol{P}$ by $\mathbf{faces}(\boldsymbol{P})$, $\mathbf{facets}(\boldsymbol{P})$, and $\mathbf{vert}(\boldsymbol{P})$, respectively.

<u>REMARK 2.2.2.</u>   The set X itself and the empty set $\emptyset$ are faces of a polytope $\boldsymbol{P} = (\boldsymbol{p}_i)_{i \in X}$. The face X is generated by the zero-functional $h = \mathbf{0}$. The face $\emptyset$ is generated by any functional that is strictly positive on all points in $\boldsymbol{P}$.

The *combinatorial structure* of a polytope $\boldsymbol{P}$ is given by the face lattice of $\boldsymbol{P}$:

<u>DEFINITION 2.2.3.</u>   The *face lattice* $\mathrm{FL}(\boldsymbol{P})$ of a d-polytope $\boldsymbol{P}$ is the lattice

$$\mathrm{FL}(\boldsymbol{P}) = (\mathbf{faces}(\boldsymbol{P}), \subseteq)$$

where the set system of faces is ordered by inclusion. The face lattice $\mathrm{FL}(\boldsymbol{P})$ is also called the *combinatorial type* of $\boldsymbol{P}$. A finite lattice L that is isomorphic to the face lattice $\mathrm{FL}(\boldsymbol{P})$ of some polytope $\boldsymbol{P}$ is called *polytopal*.

For any partially ordered set system $(\mathcal{F}, \subseteq)$ with $\mathcal{F} \subseteq 2^X$, the *closure* $\overline{B}$ of a set $B \subseteq X$ is the smallest element of $\mathcal{F}$ that contains B. In the case of polytopal face lattices this operation models the affine closure of vertices.

<u>REMARK 2.2.4.</u>   The *face lattice* of a d-polytope $\boldsymbol{P} = (\boldsymbol{p}_i)_{i \in X}$ is a graded atomic and coatomic lattice. The set X is the maximal element, $\emptyset$ is the minimal element, the vertices are the atoms and the facets are the coatoms.

The face lattice $FL(\boldsymbol{P})$ is completely described by the list of facets

$$P := \mathbf{facets}(\boldsymbol{P}).$$

All faces of lower dimensions can be generated as the intersections of finite subsets of $\mathbf{facets}(\boldsymbol{P})$. If $F \subseteq X$ is a face of $\boldsymbol{P}$ then

$$P\big|_F := \{F \cap F' \mid F' \in \mathbf{facets}(\boldsymbol{P})\}$$

describes the face lattice of F. By means of this P becomes a complete description of the combinatorial structure of $\boldsymbol{P}$. We will call P a *combinatorial polytope*. However, our definition of combinatorial polytopes will be more general and will also include facet lists P where no corresponding realization $\boldsymbol{P}$ can be found. The following definition describes a combinatorial polytope by a collection of the index sets that correspond to the facets.

<u>DEFINITION 2.2.5.</u> A *combinatorial d-polytope* $P \subseteq 2^X$ on a finite index set X is recursively defined by the following two operations:

(i) For a d-polytope $\boldsymbol{P}$ the facet list **facets**$(\boldsymbol{P})$ is a combinatorial d-polytope.

(ii) If P and Q are combinatorial d-polytopes on index sets X_P and X_Q, respectively and

$$P \cap Q = \{F\} = \{X_P \cap X_Q\} \quad \text{with} \quad P\big|_F = Q\big|_F,$$

then $P \cup Q - \{F\}$ is a combinatorial d-polytope on the index set $X_P \cup X_Q$.

Part (ii) of this definition says that whenever two combinatorial d-polytopes P and Q contain exactly one combinatorially isomorphic facet F, one can remove F from both polytopes, glue the remaining parts of P and Q along the generated holes and will again obtain a combinatorial d-polytope. By this gluing operation we can generate face lattices that are no longer polytopal, but still describe combinatorial PL-spheres (cf. Hudson [37], Zeeman [63], Björner [14]).

<u>EXAMPLE 2.2.6.</u> As a running example in this chapter we use the cube and its face lattice. A 2-dimensional projection of the standard cube with vertex coordinates

$$\Big\{ (i,j,k) \mid i,j,j \in \{0,1\} \Big\} \subseteq \mathbb{R}^3$$

is given in Figure 2.2.1. The table lists all members of its face lattice. One dimensional faces are, as usual, called edges.
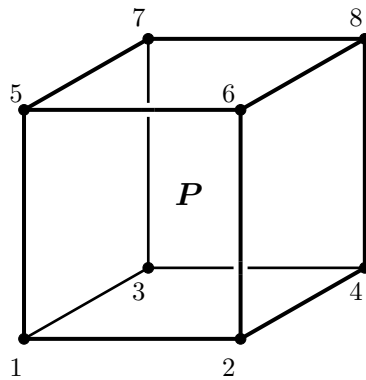
Figure 2.2.1: The cube and its face lattice.

2.3 Affine and Projective Equivalence

A realization of a polytope $\boldsymbol{P}$ is a polytope $\boldsymbol{P}'$ with $\mathrm{FL}(\boldsymbol{P}) = \mathrm{FL}(\boldsymbol{P}')$ (i.e. a polytope combinatorially isomorphic to $\boldsymbol{P}$). We will investigate the set of all such realizations considered as a topological space. It is reasonable to factor out components of realization spaces that arise from transformation groups in $\mathbb{R}^d$ (rotations, translations, affine transformations, etc.). These transformations always maintain the combinatorial structure of $\boldsymbol{P}$. For that purpose we will use a definition of realization spaces that takes care of these effects and avoids these factors that are trivially the same for all d-polytopes.

For any transformation $T \colon \mathbb{R}^d \to \mathbb{R}^d$ and a point configuration $\boldsymbol{P}$ embedded in $\mathbb{R}^d$ we define $T(\boldsymbol{P})$ such that the image $T(\boldsymbol{p}_i)$ of a point $\boldsymbol{p}_i$ has the label i in $T(\boldsymbol{P})$.

<u>DEFINITION 2.3.1.</u>   Two d-polytopes $\boldsymbol{P}$ and $\boldsymbol{P}'$ embedded in $\mathbb{R}^d$ are *affinely equivalent* if there exists an affine transformation $A(\boldsymbol{x}) := M(\boldsymbol{x}) + \boldsymbol{t}$ with $M \in \mathbf{GL}(d)$ and $\boldsymbol{t} \in \mathbb{R}^d$ such that $A(\boldsymbol{P}) = \boldsymbol{P}'$. We then write $\boldsymbol{P} \overset{\mathrm{aff}}{\simeq} \boldsymbol{P}'$.

Two d-cones $\boldsymbol{P}$ and $\boldsymbol{P}'$ in $\mathbb{R}^d$ are *linearly equivalent* if there exists a linear transformation $L \in \mathbf{GL}(d)$ such that $\mathbf{pos}(L(\boldsymbol{P})) = \mathbf{pos}(\boldsymbol{P}')$. We then write $\boldsymbol{P} \overset{\mathrm{lin}}{\simeq} \boldsymbol{P}'$.

<u>REMARK 2.3.2.</u>   Affinely equivalent polytopes $\boldsymbol{P}$ and $\boldsymbol{P}'$ satisfy $\mathrm{FL}(\boldsymbol{P}) = \mathrm{FL}(\boldsymbol{P}')$. In particular, $\boldsymbol{P}$ and $\boldsymbol{P}'$ have the same set of vertices.

Linear equivalence of cones induces another concept of equivalence for polytopes: *projective equivalence*. However, this equivalence concept is not directly generated by a group action, since not every linear transformation of a cone corresponds to an admissible projective transformation of a corresponding polytope.

<u>DEFINITION 2.3.3.</u>   Two d-polytopes $\boldsymbol{P}$ and $\boldsymbol{P}'$ are *projectively equivalent* if the cones spanned by $\boldsymbol{P}^{\mathrm{hom}}$ and $(\boldsymbol{P}')^{\mathrm{hom}}$ are linearly equivalent.

In particular, affinely equivalent polytopes are also projectively equivalent.

<u>EXAMPLE 3.3.4.</u>   Figure 2.3.1 shows parallel projections of a few transformations of the 3-dimensional cube. The first row of pictures consists only of affine transformations, while the second row shows proper projective transformations.
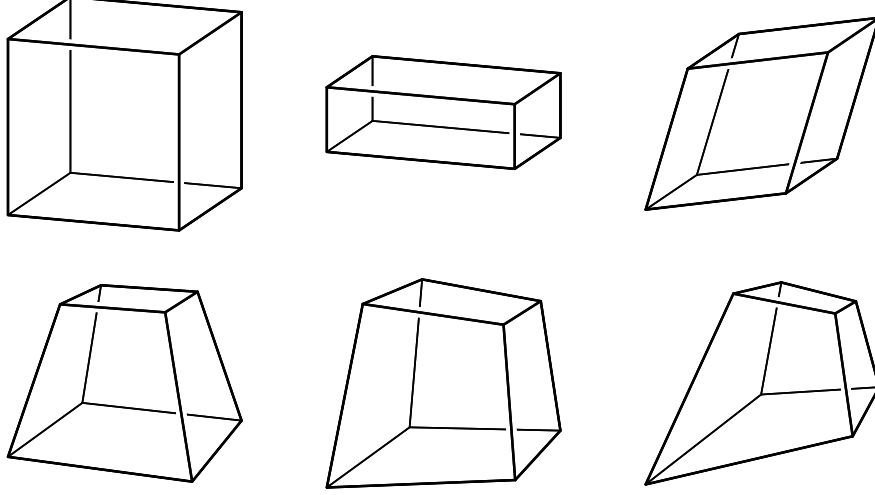
Figure 2.3.1: Affine and projective transformations of the cube.

2.4 Realization Spaces

We now study realization spaces of polytopes. A *realization* of a d-polytope $\boldsymbol{P}$ is a polytope $\boldsymbol{P}'$ in $\mathbb{R}^d$ with $\mathrm{FL}(\boldsymbol{P}) = \mathrm{FL}(\boldsymbol{P}')$. Roughly speaking, the realization space of a polytope $\boldsymbol{P}$ is the space of all realizations of $\boldsymbol{P}$ modulo affine transformations.

An *affine basis* of a d-polytope $\boldsymbol{P} = (\boldsymbol{p}_i)_{i \in X}$ is a set consisting of $d+1$ vertex labels

$$B = \{b_0, \dots, b_d\} \in X$$

such that the vertices $\boldsymbol{p}_{b_i}$ are necessarily affinely independent in every realization of $\boldsymbol{P}$. We get a particular basis of $\boldsymbol{P}$ if we choose $b_0, \dots, b_d$ such that

$$\mathbf{aff}(\{\boldsymbol{p}_{b_0}, \dots, \boldsymbol{p}_{b_k}\}) = \mathbf{aff}(\boldsymbol{P}\big|_F)$$

for a k-face F of $\boldsymbol{P}$ for all $k = 1, \dots, d$. This choice of a basis is purely combinatorial in the sense that the sequence

$$\overline{\{b_0\}}, \quad \overline{\{b_0, b_1\}}, \quad \overline{\{b_0, b_1, b_2\}}, \dots, \quad \overline{\{b_0, \dots, b_d\}}$$

forms a chain of faces in the face lattice $\mathrm{FL}(\boldsymbol{P})$ starting with a vertex b_1 and ending with the index set of the whole polytope X.

<u>DEFINITION 2.4.1.</u>   Let $\boldsymbol{P}$ be a d-polytope and let $B = \{b_1, \ldots, b_{d+1}\}$ be a basis of $\boldsymbol{P}$. The *realization space* $\mathcal{R}(\boldsymbol{P}, B)$ is the set of all polytopes $\boldsymbol{P}'$ with $\mathrm{FL}(\boldsymbol{P}) = \mathrm{FL}(\boldsymbol{P}')$ and $\boldsymbol{p}_i = \boldsymbol{p}'_i$ for $i \in B$.

Thus the realization space of a polytope $\boldsymbol{P}$ with respect to a given basis is the set of all realizations of $\boldsymbol{P} \in \mathbb{R}^d$ with the extra restriction that the points in the basis stay fixed. This definition factors out the affine transformations. We will see that in a precise sense the structure of the realization space is identical for each choice of a basis B.

<u>EXAMPLE 2.4.2.</u>   In the case of the cube, the vertices $(1, 2, 3, 5)$ form an affine basis. We assume that we have $\boldsymbol{p}_1 = (0, 0, 0)$, $\boldsymbol{p}_2 = (1, 0, 0)$, $\boldsymbol{p}_3 = (0, 0, 1)$, $\boldsymbol{p}_5 = (0, 1, 0)$. Since by these coordinates already the positions of the (supporting hyperplanes of the) facets $(1, 2, 3, 4)$, $(1, 2, 5, 6)$, and $(1, 3, 5, 7)$ are determined the positions of the vertices 4, 6, and 7 are of the form $\boldsymbol{p}_4 = (x_4, 0, z_4)$, $\boldsymbol{p}_6 = (x_6, y_6, 0)$, and $\boldsymbol{p}_7 = (0, y_7, z_7)$. All the involved parameters must be greater than one, to satisfy the convexity requirements. Furthermore we must have $x_4 + z_4 > 1$, $x_6 + y_6 > 1$, and $y_7 + z_7 > 1$. After fixing these points, the positions of the (supporting hyperplanes of the) facets $(2, 4, 6, 8)$, $(3, 4, 7, 8)$, and $(5, 6, 7, 8)$ are determined. Their intersection gives the position of $\boldsymbol{p}_8$. Again, convexity has to be preserved. This defines an additional (open) obstruction for the parameters $x_4, \ldots, z_7$. This constraint is a (large) polynomial inequality in $x_4, \ldots, z_7$. It turns out that the possible choices for these parameters form an open contractible set of dimension 6. (We will see in Part IV that this is just a special case of a general result for 3-polytopes). Figure 2.4.1 shows three elements from $\mathcal{R}(\textbf{cube}, (1, 2, 3, 5))$. The parameters for these three cases are

$$\begin{aligned}
&x_4 = 1, \quad\ z_4 = 1, \quad\ x_6 = 0.7, \quad y_6 = 1, \quad\ y_7 = 1, \quad\ z_7 = 1 \\
&x_4 = 0.8, \quad z_4 = 1, \quad\ x_6 = 1, \quad\ y_6 = 0.8, \quad y_7 = 1, \quad\ z_7 = 0.8 \\
&x_4 = 1.1, \quad z_4 = 1.1, \quad x_6 = 1.1, \quad y_6 = 1.1, \quad y_7 = 1.1, \quad z_7 = 1.1
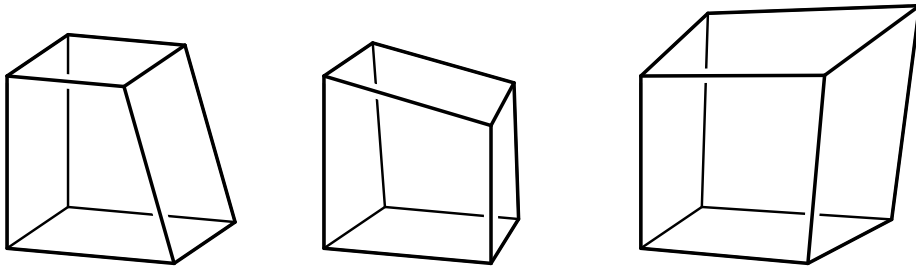\end{aligned}$$

Figure 2.4.1:   Elements from the realization space of the cube.

2.5 Semialgebraic Sets and Stable Equivalence

Let $\Omega = (\{f_i\}_{0 < i \le r}, \{g_i\}_{0 < i \le s}, \{h_i\}_{0 < i \le t})$ be a finite collection of polynomials

$$f_1, \ldots, f_r, g_1, \ldots, g_s, h_1, \ldots, h_t \in \mathbb{Z}[x_1, \ldots, x_n]$$

with integer coefficients. The *basic semialgebraic set* $V(\Omega) \in \mathbb{R}^n$ is the set

$$V = V(\Omega) := \Big\{ \boldsymbol{x} \in \mathbb{R}^n \mid \quad f_i(\boldsymbol{x}) = 0 \text{ for } i = 1, \ldots, r$$
$$g_i(\boldsymbol{x}) < 0 \text{ for } i = 1, \ldots, s$$
$$h_i(\boldsymbol{x}) \le 0 \text{ for } i = 1, \ldots, t \Big\}$$

defined as the solution of a finite number of polynomial equations and polynomial inequalities. A basic semialgebraic set is called *primary*, if the defining equations contain no non-strict inequalities (i.e. $t = 0$ in the above notion). Thus, for example, the set $\{0, 1\}$ and the open interval $]0, 1[\subset \mathbb{R}$ are primary basic semialgebraic sets, while the closed interval $[0, 1]$ is a basic semialgebraic set in $\mathbb{R}$ that is not primary. Semialgebraic sets form a general setting to define subsets of $\mathbb{R}^n$ by polynomial equations and inequalities. In particular any rational polytope, its interior and its boundary can be easily identified as semialgebraic sets. To see that the realization space of a polytope is a (primary) semialgebraic set as well one checks that the realization space is the set of all matrices $\boldsymbol{Q} \in \mathbb{R}^{d \cdot n}$ for which some entries are fixed, and the determinants of certain $d \times d$ minors have to be positive, negative or zero (compare [7]).

We will prove that primary semialgebraic sets generally form a good object of comparison for realization spaces. The Universality Theorem will state that for every primary semialgebraic set V there is a 4-polytope whose realization space is "stably equivalent" to V.

The concept of *stable equivalence* that we use to compare realization spaces with general primary semialgebraic sets has been used by different authors. However, the precise definitions they used (see [33, 34, 49, 50, 53]) vary substantially in their technical content. The common idea is that semialgebraic sets that only differ by a "trivial fibration" and a rational change of coordinates should be considered as stably equivalent, while semialgebraic sets that differ in certain "characteristic properties" should not turn out to be stably equivalent. In particular, stable equivalence should preserve the homotopy type, and respect the algebraic complexity and the singularity structure. We now present a concept of stable equivalence that is stronger than all previously used notions.

Let $V \subseteq \mathbb{R}^n$ and $W \subseteq \mathbb{R}^{n+d}$ be basic semialgebraic sets with $\pi(W) = V$, where π is the canonical projection $\pi \colon \mathbb{R}^{n+d} \to \mathbb{R}^n$ that deletes the last d coordinates. V is a *stable projection* of W if W has the form

$$W = \Big\{ (\boldsymbol{v}, \boldsymbol{v}') \in \mathbb{R}^{n+d} \mid \boldsymbol{v} \in V \text{ and } \phi_i^{\boldsymbol{v}}(\boldsymbol{v}') > 0; \, \psi_j^{\boldsymbol{v}}(\boldsymbol{v}') = 0 \text{ for all } i \in X; \, j \in Y \Big\}.$$

Here X and Y denote finite (possibly empty) index sets. For $i \in X$ and $j \in Y$ the functions $\phi_i^{\boldsymbol{v}}$ and $\psi_j^{\boldsymbol{v}}$ are affine functionals whose parameters depend polynomially on V. Thus we have

$$\phi_i^{\boldsymbol{v}}(\boldsymbol{v}') = \langle (\phi_i^1(\boldsymbol{v}), \ldots, \phi_i^d(\boldsymbol{v}))^T, \boldsymbol{v}' \rangle + \phi_i^{d+1}(\boldsymbol{v})$$

$$\psi_j^{\boldsymbol{v}}(\boldsymbol{v}') = \langle (\psi_j^1(\boldsymbol{v}), \ldots, \psi_j^d(\boldsymbol{v}))^T, \boldsymbol{v}' \rangle + \psi_j^{d+1}(\boldsymbol{v})$$

with polynomial functions $\phi_i^1(\boldsymbol{v}), \ldots, \phi_i^{d+1}(\boldsymbol{v})$ and $\psi_j^1(\boldsymbol{v}), \ldots, \psi_j^{d+1}(\boldsymbol{v})$.

If V is a stable projection of W, then all the fibers $\pi^{-1}(\boldsymbol{v})$ are the (non-empty) relative interiors of *polyhedra* (i.e. sets that are obtained by intersecting a finite number of open halfspaces and hyperplanes). In particular, if the sets X and Y are empty we get $W = V \times \mathbb{R}^d$. If the functionals ϕ_i and ψ_i are constant and V is the interior of a convex polytope then W is itself the interior of a polyhedral set, that projects onto V.
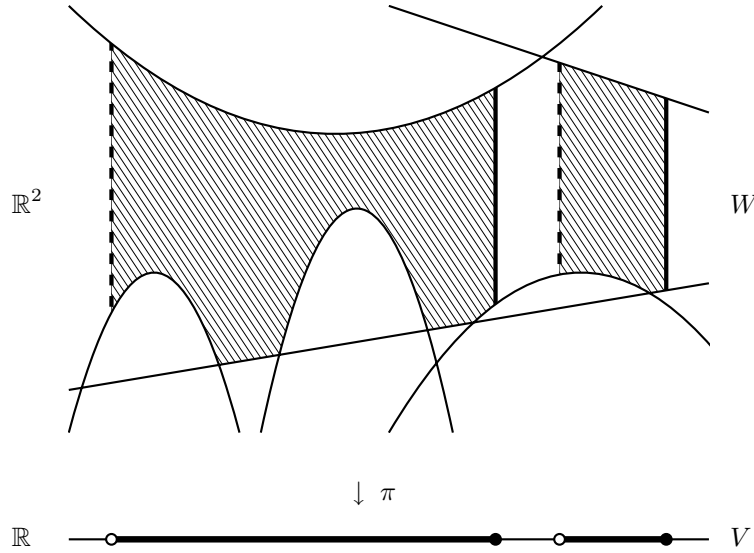
Figure 2.5.1: A stable projection from $\mathbb{R}^2$ to $\mathbb{R}$.

In Figure 2.5.1 the concept of stable projections is illustrated by an example in which $V = \pi(W)$ consists of two halfopen intervals (the darkened lines). The set W (the shaded area) is constrained by a set of inequalities $\phi_i^{\boldsymbol{v}}(\boldsymbol{v}') > 0$. The set of equations $\psi_j^{\boldsymbol{v}}$ is empty.

Two basic semialgebraic sets V and W are *rationally equivalent* if there exist a homeomorphism $f\colon V \to W$ such that both functions f and f^{-1} are rational functions (with rational coefficients). We may consider a rational equivalence as a kind of "reparametrization" of the set.

DEFINITION 2.5.1.   Two basic semialgebraic sets V and W are *stably equivalent* if they lie in the equivalence class generated by stable projections and rational equivalence. We then write $V \approx W$.

A basic semialgebraic set that is stably equivalent to the singleton $\{0\} \subseteq \mathbb{R}^1$ is called *trivial*. The following lemma collects some properties that are in fact "stable" under stable equivalence.

LEMMA 2.5.2. *Let $V \in \mathbb{R}^n$ and $W \in \mathbb{R}^m$ be a pair of stably equivalent semialgebraic sets and let A be a subfield of the algebraic numbers of characteristic zero. We have*

(i) *V and W are homotopy equivalent.*
(ii) *$V \cap A^n = \emptyset \iff W \cap A^m = \emptyset$.*

PROOF. Part (i) is a direct consequence of the fact that stable projections and rational equivalences do not change the homotopy type. For part (ii) we first prove that property (ii) holds if $V = \pi(W)$ is a stable projection of W. If $V \cap A^n = \emptyset$ then $W \cap A^m = \emptyset$, since π just deletes the last $m - n$ coordinates. Conversely, if $\boldsymbol{v} \in V \cap A^n$ we find a point $(\boldsymbol{v}, \boldsymbol{v}') \in W \cap (A^n \times \mathbb{Q}^{m-n}) \subseteq W \cap A^m$. This is the case since the constraints for the vector $\boldsymbol{v}'$ are given by equations $\psi_j^{\boldsymbol{v}}(\boldsymbol{v}') = 0$ and inequalities $\phi_i^{\boldsymbol{v}}(\boldsymbol{v}') > 0$, in which the coefficients of $\psi_j^{\boldsymbol{v}}$ and $\phi_i^{\boldsymbol{v}}$ are rational. The solution set of $\psi_j^{\boldsymbol{v}}(\boldsymbol{v}') = 0$ is a vector space for which we can find a rational basis. Since the remaining obstructions are strict inequalities only and the fiber $\pi^{-1}(\boldsymbol{v})$ is by definition not empty, we can always find a rational point. Property (ii) holds also for rational equivalence, since evaluating a rational function with integer coefficients cannot increase the algebraic complexity. By Definition 2.5.1 this proves part (ii). $\qquad\square$

We now collect some results about stable equivalence that are useful for the special situations of polytopes and realization spaces that will be needed later.

LEMMA 2.5.3.

(i) *For a semialgebraic set $V \subseteq \mathbb{R}^n$ we have $V \approx \{\lambda \boldsymbol{v} \in \mathbb{R}^{n+1} \mid \boldsymbol{v} \in V^{\mathrm{hom}},\ \lambda > 0\}$.*
(ii) *Non-empty sets defined by a collection of strict affine inequalities and equations are trivial.*
(iii) *The interior of a polytope is trivial.*

PROOF. For (i) we explicitly give a stable projection $\pi\colon V' \to V$ and a rational homeomorphism f such that

$$f(V') = \{\lambda \boldsymbol{v} \in \mathbb{R}^{n+1} \mid \boldsymbol{v} \in V^{\mathrm{hom}},\ \lambda > 0\}$$

and f^{-1} is a rational function. We set $V' = \{(\boldsymbol{v}, \lambda) \mid \boldsymbol{v} \in V \text{ and } \lambda > 0\}$ and $f(\boldsymbol{v}, \lambda) = (\lambda \boldsymbol{v}, \lambda)$. We have $f^{-1}(\boldsymbol{w}, \lambda) = (\boldsymbol{w}/\lambda, \lambda)$, which is a well defined rational function on V' since λ is always positive.

For (ii) let $V \in \mathbb{R}^n$ be a semialgebraic set defined by strict affine inequalities and equations (i.e. the relative interior of a polyhedral set). We apply (i) and prove that $V' = \{\lambda \boldsymbol{v} \in \mathbb{R}^{n+1} \mid \boldsymbol{v} \in V^{\mathrm{hom}},\ \lambda > 0\}$ is trivial. The cone V' is a

stable projection of $V' \times \{0\}$. The cone V' is defined by strict *linear* inequalities and equations only. Therefore $\{0\}$ is a stable projection of $V' \times \{0\}$. This proves (ii).

Part (iii) is an immediate consequence of part (ii), since interiors of polytopes are non-empty sets defined by strict affine inequalities. □

<u>LEMMA 2.5.4.</u> *Let B_1 and B_2 be two affine bases of a d-polytope $\boldsymbol{P}$. Then we have*
$$\mathcal{R}(\boldsymbol{P}, B_1) \approx \mathcal{R}(\boldsymbol{P}, B_2).$$

PROOF. We assume that the vertices of $\boldsymbol{P} = (\boldsymbol{p}_i)_{i \in X}$ are indexed by a label set X. For any element $\boldsymbol{Q} = (\boldsymbol{q}_i)_{i \in X} \in \mathcal{R}(\boldsymbol{P}, B_1)$ the vertices $(\boldsymbol{q}_i)_{i \in B_2}$ are affinely independent, since B_2 is a basis of $\boldsymbol{P}$. Hence for each $\boldsymbol{Q} \in \mathcal{R}(\boldsymbol{P}, B_1)$ there exists a unique non-degenerate affine transformation $A_{\boldsymbol{Q}}:\mathbb{R}^d \to \mathbb{R}^d$ such that $A_{\boldsymbol{Q}}(\boldsymbol{q}_i) = \boldsymbol{p}_i$ for all $i \in B_2$. We have $A_{\boldsymbol{Q}}(\boldsymbol{Q}) \in \mathcal{R}(\boldsymbol{P}, B_2)$. The coefficients of $A_{\boldsymbol{Q}}$ are rational functions of the coordinates of $\boldsymbol{Q}$. Furthermore, no two elements in $\mathcal{R}(\boldsymbol{P}, B_1)$ (resp. in $\mathcal{R}(\boldsymbol{P}, B_2)$) are affinely equivalent, therefore the map
$$\begin{aligned} f:\mathcal{R}(\boldsymbol{P}, B_1) &\longrightarrow \mathcal{R}(\boldsymbol{P}, B_2) \\ \boldsymbol{Q} &\longmapsto A_{\boldsymbol{Q}}(\boldsymbol{Q}) \end{aligned}$$

forms a rational homeomorphism between the two realization spaces. The inverse f^{-1} is also a rational function, since it can be defined in the same way by interchanging the roles of $\mathcal{R}(\boldsymbol{P}, B_1)$ and $\mathcal{R}(\boldsymbol{P}, B_2)$. □

The last lemma allows us to speak (modulo stable equivalence) of *the* realization space $\mathcal{R}(\boldsymbol{P})$ of a polytope $\boldsymbol{P}$, since for any choice of a basis we obtain rationally equivalent realization spaces. The lemma also allows us to speak of the realization space $\mathcal{R}(P)$ of a combinatorial polytope P, which is empty if P is not polytopal, and $\mathcal{R}(\boldsymbol{P})$ otherwise, where $\boldsymbol{P}$ is any realization of P.

2.6   Polarity

Polarity is one of the most important concepts in polytope theory. In a certain sense it is the polyhedral counterpart of the well known *duality* operator from projective geometry. We will need the concept of polarity later on in Part IV, when we investigate the realization spaces of 3-polytopes.

<u>DEFINITION 2.6.1.</u> For a set $A \subset \mathbb{R}^d$ we define the polar by
$$A^{\Delta} := \Big\{ \boldsymbol{x} \in \mathbb{R}^d \mid \langle \boldsymbol{x}, \boldsymbol{a} \rangle \leq 1 \text{ for all } \boldsymbol{a} \in A \Big\}.$$

The polarity operator assigns to a set A all vectors $\boldsymbol{x}$ that represent linear functionals $f(\boldsymbol{a}) = \langle \boldsymbol{x}, \boldsymbol{a} \rangle - 1$ that are negative on all elements of A. It is easy to

check that, $\mathbf{conv}(A)$ does not contain the origin $\mathbf{0}$, if and only if A^Δ is unbounded. We will apply the polarity operator only to polytopes (considered as convex sets $\mathbf{conv}(\boldsymbol{P}) = \mathbf{conv}(\boldsymbol{p}_0, \ldots, \boldsymbol{p}_n) \subseteq \mathbb{R}^d$) that contain the origin in their interior. The set $\mathbf{conv}(\boldsymbol{P})^\Delta$ is again a polytope that contains the origin (for a proof of this non-trivial fact we refer to [64]). Since we represented polytopes just by the set of their vertices, we have to slightly adapt the definition of polarity. For this let $\boldsymbol{P} = (\boldsymbol{p}_0, \ldots, \boldsymbol{p}_n)$ and $\boldsymbol{Q} = (\boldsymbol{q}_0, \ldots, \boldsymbol{q}_m)$ be two d-polytopes given by their vertices. $\boldsymbol{Q}$ is the polar of $\boldsymbol{P}$ if $\mathbf{conv}(\boldsymbol{P})^\Delta = \mathbf{conv}(\boldsymbol{Q})$. We then write $\boldsymbol{Q} = \boldsymbol{P}^\Delta$. The following Theorem collects the crucial facts for that case.

THEOREM 2.6.2. *Let $\boldsymbol{P}$ be a polytope that (considered as convex set) contains the origin and let $\boldsymbol{P}^\Delta$ be its polar.*

(i) *The face lattice of $\boldsymbol{P}^\Delta$ is anti-isomorphic to the face lattice of $\boldsymbol{P}$ (i.e. it is obtained from $\mathrm{FL}(\boldsymbol{P})$ by reversing the order relation),*

(ii) *The vertices of $\boldsymbol{P}^\Delta$, can be computed from the vertices of $\boldsymbol{P}$ by rational functions,*

(iii) $\boldsymbol{P}^{\Delta\Delta} = \boldsymbol{P}$,

(iv) *if $\boldsymbol{P} = M \cdot \boldsymbol{P}'$ for some non-degenerate linear transformation M then $\boldsymbol{P}'^\Delta = (M^T)^{-1} \boldsymbol{P}^\Delta$.*

PROOF. The proofs for (i)–(iii) can be found in [64, Chapter 2.3]. For (iv) we prove more generally, if $A \in \mathbb{R}^d$ is any set and M is a non-degenerate linear transformation, then $(M(A))^\Delta = (M^T)^{-1}(A^\Delta)$. We have

$$
\begin{aligned}
\boldsymbol{x} \in (M(A))^\Delta &\iff \langle \boldsymbol{x}, M \cdot \boldsymbol{a} \rangle \leq 1 \text{ for all } \boldsymbol{a} \in A \\
&\iff \langle M^T \cdot \boldsymbol{x}, \boldsymbol{a} \rangle \leq 1 \text{ for all } \boldsymbol{a} \in A \\
&\iff M^T \cdot \boldsymbol{x} \in A^\Delta \\
&\iff \boldsymbol{x} \in (M^T)^{-1}(A^\Delta).
\end{aligned}
$$

This proves the claim. □

Thus, for a polytopal face lattice $\mathrm{FL} = \mathrm{FL}(\boldsymbol{P})$ we can uniquely define the polar face lattice by $\mathrm{FL}^\Delta = \mathrm{FL}(\boldsymbol{P}^\Delta)$. If I is the vertex/facet incidence matrix of FL, then I^T (the transposed matrix) is the vertex/facet incidence matrix of FL^Δ. Each vertex of FL corresponds to a facet in FL^Δ, and vice versa. For our study of realization spaces the following fact is relevant.

THEOREM 2.6.3. *Let $\boldsymbol{P}$ be a d-polytope that contains the origin and let $\boldsymbol{P}^\Delta$ be its polar.*

(i) $\mathcal{R}(\boldsymbol{P}) \approx \mathcal{R}(\boldsymbol{P}^\Delta)$,

(ii) $\mathcal{R}(\boldsymbol{P})$ *and $\mathcal{R}(\boldsymbol{P}^\Delta)$ have the same (topological) dimension.*

PROOF. Assume that $\boldsymbol{P} = (\boldsymbol{p}_0, \ldots, \boldsymbol{p}_n)$ and that w.l.o.g $B = (0, 1, \ldots, d)$ is an affine basis of $\boldsymbol{P}$. We also assume that $\boldsymbol{P}^\Delta = \boldsymbol{Q} = (\boldsymbol{q}_0, \ldots, \boldsymbol{q}_m)$ and that w.l.o.g the index set $B = (0, 1, \ldots, d)$ is as well an affine basis of $\boldsymbol{Q}$.

For this proof we need a concept of realization spaces that behaves "friendly" with respect to polarity. The space $\mathcal{R}_{\mathrm{lin}}(\boldsymbol{P}, B)$ is the set of all polytopes $\boldsymbol{P}'$ with $\mathrm{FL}(P) = \mathrm{FL}(P')$, and $\boldsymbol{p}_i - \boldsymbol{p}_0 = \boldsymbol{p}'_i - \boldsymbol{p}'_0$ for $i = 1, \dots, d$, and $\boldsymbol{0} \in \mathbf{conv}(\boldsymbol{P}')$. The elements of $\mathcal{R}_{\mathrm{lin}}(\boldsymbol{P}, B)$ are all elements of the form

$$(\boldsymbol{p}_0 - \boldsymbol{t}, \dots, \boldsymbol{p}_n - \boldsymbol{t}) \text{ such that } \boldsymbol{P}' = (\boldsymbol{p}_0, \dots, \boldsymbol{p}_n) \in \mathcal{R}(\boldsymbol{P}, B) \text{ and } \boldsymbol{t} \in \mathbf{int}(\mathbf{conv}(\boldsymbol{P}'))$$

Since the interior of a polytope $\boldsymbol{P}$ is bounded by affine halfspaces that depend polynomially on the coordinates of $\boldsymbol{P}$, the spaces $\mathcal{R}_{\mathrm{lin}}(\boldsymbol{P}, B)$ and $\mathcal{R}(\boldsymbol{P}, B)$ are stably equivalent. The (topological) dimension of $\mathcal{R}_{\mathrm{lin}}(\boldsymbol{P}, B)$ is the (topological) dimension of $\mathcal{R}(\boldsymbol{P}, B)$ increased by d (the number of degrees of freedom for the choice of the vector $\boldsymbol{t}$). The elements in $\mathcal{R}_{\mathrm{lin}}(\boldsymbol{P}, B)$ are pairwise not linearly equivalent. For every realization $\boldsymbol{P}'$ of $\boldsymbol{P}$ that contains the origin (in the interior of its convex hull) there is a unique linear transformation M such that $M \cdot \boldsymbol{P}' \in \mathcal{R}_{\mathrm{lin}}(\boldsymbol{P}, B)$

We prove our theorem by showing that $\mathcal{R}_{\mathrm{lin}}(\boldsymbol{P}, B)$ is rationally equivalent to $\mathcal{R}_{\mathrm{lin}}(\boldsymbol{P}^{\Delta}, B)$. Let $\boldsymbol{P}' \in \mathcal{R}_{\mathrm{lin}}(\boldsymbol{P}, B)$ be a realization of $\boldsymbol{P}$. For $\boldsymbol{P}'^{\Delta}$ there is a unique linear transformation M such that $M \cdot \boldsymbol{P}'^{\Delta} = \boldsymbol{Q}' \in \mathcal{R}_{\mathrm{lin}}(\boldsymbol{P}^{\Delta}, B)$. The vertex coordinates of $\boldsymbol{Q}'$ can be computed from $\boldsymbol{P}'$ by means of a rational function $f: \mathcal{R}_{\mathrm{lin}}(\boldsymbol{P}, B) \to \mathcal{R}_{\mathrm{lin}}(\boldsymbol{P}^{\Delta}, B)$. This function f is injective: If we have $f(\boldsymbol{P}'_1) = f(\boldsymbol{P}'_2)$ then $\boldsymbol{P}'^{\Delta}_1$ and $\boldsymbol{P}'^{\Delta}_2$ are linearly equivalent. By Theorem 2.6.2(iii) and (iv) $\boldsymbol{P}'_1 = \boldsymbol{P}'^{\Delta\Delta}_1$ and $\boldsymbol{P}'_2 = \boldsymbol{P}'^{\Delta\Delta}_2$ are linearly equivalent. Thus we have $\boldsymbol{P}'_1 = \boldsymbol{P}'_2$. The function f is also surjective: Let $\boldsymbol{Q}'$ be any polytope in $\mathcal{R}_{\mathrm{lin}}(\boldsymbol{P}^{\Delta}, B)$. Then $\boldsymbol{Q}'^{\Delta}$ is a realization of $\boldsymbol{P}$ that contains the origin in its interior. Thus there is a linear transformation M with $\boldsymbol{P}' = M \cdot \boldsymbol{Q}'^{\Delta} \in \mathcal{R}_{\mathrm{lin}}(\boldsymbol{P}, B)$. Again by Theorem 2.6.2(iv) we have $f(\boldsymbol{P}') = \boldsymbol{Q}'$. This proves that f is a homeomorphism. Since polarity is a completely symmetric concept the inverse f^{-1} is also a rational function. Thus f provides a rational equivalence. $\qquad\square$

2.7   Visualization of 4-Polytopes: Schlegel Diagrams

Although the construction techniques that will be presented here are a purely formal process, it will be useful to have a good imagination of what is going on. *Schlegel diagrams* are a very effective tool to represent d-dimensional polytopes in $(d-1)$-space. Here we are in the lucky situation to deal almost exclusively with 4-dimensional polytopes which can still be nicely represented in 3-dimensional space via Schlegel diagrams.

The idea behind Schlegel diagrams is easy: if one wants to represent a d-polytope $\boldsymbol{P}$ in $(d - 1)$-space, then one chooses a facet F of $\boldsymbol{P}$ and a point $\boldsymbol{p}$ that is outside $\boldsymbol{P}$ but still very close to the center of F. Then one projects the boundary of the polytope, using F as "projection screen" and $\boldsymbol{p}$ as center of the projection. The facet F is called the *basis* of the Schlegel diagram.
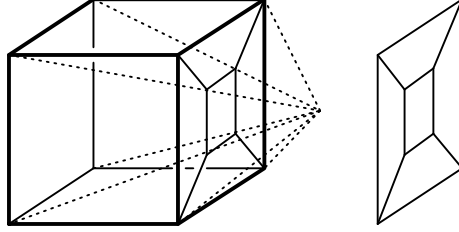
Figure 2.7.1: Construction of the Schlegel diagram of a the cube.

By this procedure, the images of the facets **facets**($\boldsymbol{P}$) − F induce a complete polytopal subdivision of F, a *Schlegel Diagram* of $\boldsymbol{P}$ (a geometric object in $(d-1)$-space). We can read off the complete face lattice of $\boldsymbol{P}$ from a Schlegel Diagram $\mathcal{S}$ with basis F (the facets of $\boldsymbol{P}$ correspond to the cells of the subdivision together with F itself). Although a lot of information about the concrete geometric realization of $\boldsymbol{P}$ seems to be lost, being a Schlegel Diagram is a very strong criterion. In general, most polytopal subdivisions of F that are combinatorially isomorphic to a Schlegel Diagram with basis F are actually not a Schlegel Diagram. In Part IV we will learn more about these connections.

We omit a more formal definition of Schlegel Diagrams here, and instead show some pictures. Figure 3.6.1 demonstrates how a Schlegel Diagram of a 3-dimensional cube is constructed. Figure 3.6.2 (read as 3-dimensional objects) shows Schlegel diagrams of several simple 4-polytopes: the simplex, the 4-cube and the product of two triangles.

simplex   **hypercube** $\boldsymbol{\Delta_2 \times \Delta_2}$
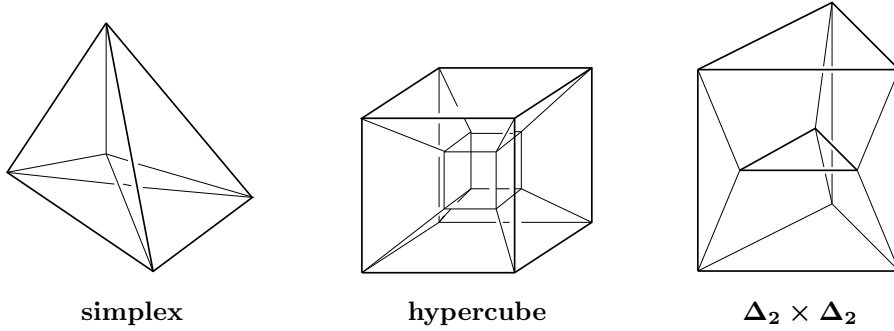
Figure 2.7.2: Schlegel diagrams of some 4-dimensional polytopes.

3   Polytopal Constructions

In this section we describe the different constructions needed for the proof of the Universality Theorem. Special care is taken of the realization spaces of the resulting polytopes. Again we take the puristic standpoint and give only concepts that are relevant in relation to our main theorems.

3.1   Pyramids, Prisms and Tents

Among the most trivial standard operations for polytopes are the constructions of *pyramids* and *prisms*. They will be recalled here briefly on the level of their face lattices. For a finite label set $X = \{1, \ldots, n\}$, we define $X' = \{1', \ldots, n'\}$. Remember that combinatorial polytopes are represented by a list of their facets. Each entry of the list consists of the vertex labels on the corresponding facet.

<u>DEFINITION 3.1.1.</u>   Let P be a combinatorial d-polytope over the index set X and let $y \notin X$ be a new label. The *pyramid* $\mathbf{pyr}(P, y)$ is the combinatorial $(d{+}1)$-polytope

$$\mathbf{pyr}(P, y) := \Big\{ F \cup \{y\} \mid F \in P \Big\} \cup \{X\}.$$

In the realizable case a pyramid over a d-polytope $\boldsymbol{P}$ is obtained by embedding $\boldsymbol{P}$ in an affine hyperplane of $\mathbb{R}^{d+1}$ and then taking the convex hull with a point $\boldsymbol{p}_y$ outside $\mathbf{aff}(\boldsymbol{P})$. All possible choices of $\boldsymbol{p}_y$ are affinely equivalent. Therefore $\mathbf{pyr}(P, y)$ has a realization space that is isomorphic to that of P.

<u>DEFINITION 3.1.2.</u>   Let P be a combinatorial d-polytope over the index set X. The *prism* $\mathbf{prism}(P)$ is the combinatorial $(d{+}1)$-polytope

$$\mathbf{prism}(P) := \Big\{ F \cup F' \mid F \in P \Big\} \cup X \cup X'.$$

In the realizable case a prism over a d-polytope $\boldsymbol{P}$ is obtained by embedding $\boldsymbol{P}$ in a suitable hyperplane H of $\mathbb{R}^{d+1}$, then projecting $\boldsymbol{P}$ on a hyperplane H' that does not meet $\mathbf{conv}(\boldsymbol{P})$, and then taking the convex hull of $\boldsymbol{P}$ and its image.

Finally, we need the concept of a *tent* over an n-gon:

<u>DEFINITION 3.1.3.</u>   Let $P = \{\{1, 2\}, \{2, 3\}, \ldots, \{n{-}1, n\}, \{n, 1\}\}$ be an n-gon with $n \geq 4$ and $\{n, 1\}, \{i, i{+}1\} \in P$ be two non-adjacent edges with $2 \leq i \leq n{-}2$, and let a, b be two new labels. The *tent* $\mathbf{tent}^{\{n,1\},\{i,i+1\}}(P, a, b)$ is the combinatorial 3-polytope

$$
\begin{aligned}
\mathbf{tent}^{\{n,1\},\{i,i+1\}}(P, a, b) \quad = \quad & \Big\{ \{j, j{+}1, a\} \mid 1 \leq j \leq i \Big\} \\
\cup \quad & \Big\{ \{j, j{+}1, b\} \mid i{+}1 \leq j \leq n{-}1 \Big\} \\
\cup \quad & \Big\{ \{n, 1, a, b\}, \; \{i, i{+}1, a, b\} \Big\}.
\end{aligned}
$$

We can realize a tent if we take an n-gon $\boldsymbol{G}$ in the xy-plane of $\mathbb{R}^3$, where the edges $\{n, 1\}$ and $\{i, i+1\}$ are parallel to the x-axis. We then add two points $\boldsymbol{p}_a = (0, 0, 1)$ and $\boldsymbol{p}_b = (1, 0, 1)$ and take the convex hull.
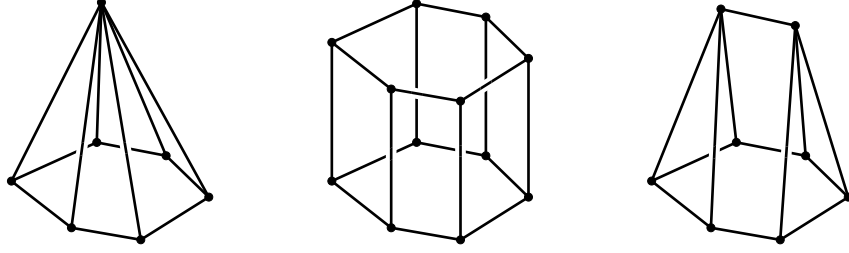
Figure 3.2.1: A pyramid, a prism and a tent over a hexagon.

3.2   Connected Sums

Our first more complicated construction is "gluing" two polytopes of the same dimension along a common facet. We will describe this polytopal operation (the connected sum) directly on the level of the underlying combinatorial polytopes. The essence of the connected sum of two combinatorial polytopes was already represented by part (ii) of Definition 2.2.5, where combinatorial polytopes are defined. We will restrict our consideration of the resulting realization spaces to what is needed for this article. However, it should be mentioned that the "connected sum" operation composes the realization spaces of the summands in a highly non-trivial way. For our purposes it is *the* way to obtain complicated realization spaces from simple ones (although we just use the "tip of the iceberg" of the power of connected sum operations).

Let P and Q be combinatorial polytopes indexed by X and Y, respectively. We assume that P contains a facet $F_P \in P$ and Q contains a facet $F_Q \in Q$ such that $P\big|_{F_P}$ and $Q\big|_{F_Q}$ are related by a combinatorial isomorphism $\alpha \colon F_P \to F_Q$. (Indeed, there might exist many combinatorial isomorphisms between F_P and F_Q if the group of combinatorial automorphisms of F_P is non-trivial. We assume that α is a particular fixed one.)

We furthermore assume that the isomorphism between F_P and F_Q is already expressed by the labeling of the vertices. The combinatorial polytopes P and Q should be labeled such that

$$X \cap Y = F_P = F_Q \text{ and } \alpha(i) = i \text{ for } i \in F_P.$$

With this we can write $F = F_P = F_Q$.

<u>DEFINITION 3.2.1.</u>   With the above settings we define the *connected sum* $P \#_F Q$ as the combinatorial d-polytope: $P \#_F Q = (P \cup Q) - \{F\}$ indexed by $X \cup Y$.

<u>REMARK 3.2.2.</u>   The above definition implies the following characterization of
the faces of $P\#_F Q$:

$$\mathbf{faces}(P\#_F Q) = (\mathbf{faces}(P) \cup \mathbf{faces}(Q) \cup \{X \cup Y\}) - \{F, X, Y\}.$$

where

$$\mathbf{faces}(P) \cap \mathbf{faces}(Q) = \mathbf{faces}(F).$$

The next definition represents the geometric counterpart of Definition 3.2.1
and describes how concrete polytopes in $\mathbb{R}^d$ behave under connected sum oper-
ations.

<u>DEFINITION 3.2.3.</u>   If we have $\mathrm{FL}(\boldsymbol{P}) = P$, $\mathrm{FL}(\boldsymbol{Q}) = Q$ and $\mathrm{FL}(\boldsymbol{R}) = P\#_F Q$,
then $\boldsymbol{R}$ is a *connected sum* of $\boldsymbol{P}$ and $\boldsymbol{Q}$ if

$$\boldsymbol{R}\big|_X = \tau_P(\boldsymbol{P}) \quad \text{and} \quad \boldsymbol{R}\big|_Y = \tau_Q(\boldsymbol{Q})$$

for admissible projective transformations τ_P and τ_Q.
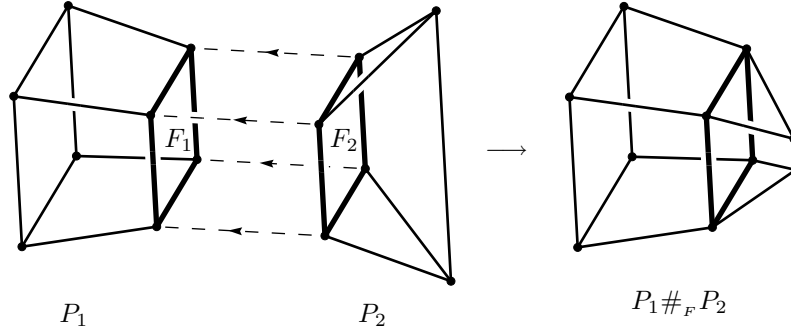
Figure 3.2.1: Connected sum of a cube and a triangular prism.

Figure 3.2.1 illustrates the operation of building the connected sum of a
triangular prism and a cube along a quadrangle. It can be seen that in the
geometric case a projective transformation might be necessary in order to obtain
a convex polytope again. The picture also demonstrates how the face F along
which the gluing is performed disappears in the resulting polytope.

The next lemma is in some sense the counterpart of Definition 3.2.3, and
tells us that if for $P\#_F Q$ and realizations $\boldsymbol{P}$ and $\boldsymbol{Q}$ the facets $\boldsymbol{P}\big|_F$ and $\boldsymbol{Q}\big|_F$ have
"the right shape", then $\boldsymbol{P}$ and $\boldsymbol{Q}$ can always be composed to form a realization
of $P\#_F Q$.

<u>LEMMA 3.2.4.</u> *Let $R = P \#_F Q$ and let $\boldsymbol{P}$ and $\boldsymbol{Q}$ be realizations of combinatorial d-polytopes P and Q, respectively. If the facet $\boldsymbol{P}\big|_F$ is projectively equivalent to the facet $\boldsymbol{Q}\big|_F$, then there exists a projective transformation τ such that $\mathbf{conv}(\boldsymbol{P} \cup \tau(\boldsymbol{Q}))$ is a realization of R.*

PROOF. We may assume that $\boldsymbol{Q}$ is already realized in such a way that $\mathbf{conv}(\boldsymbol{Q}) \cap \mathbf{conv}(\boldsymbol{P}) = \mathbf{conv}(\boldsymbol{Q}\big|_F) = \mathbf{conv}(\boldsymbol{P}\big|_F)$. Let $H_0, H_1, \ldots, H_r$ be the facet-defining affine hyperplanes for $\boldsymbol{Q}$, where H_0 corresponds to the facet F. We equip the hyperplanes with orientations, such that the positive halfspaces point to the interior of $\boldsymbol{Q}$. Now we choose a point $\boldsymbol{q}$ on the negative side of H_0 and on the positive side of all other hyperplanes $H_1, \ldots, H_r$. Similarly we choose a point $\boldsymbol{p}$ for the polytope $\boldsymbol{P}$ on the opposite side to $\mathbf{interior}(\mathbf{conv}(\boldsymbol{P}))$ of the hyperplane spanning F and on the same side for all other facet-defining hyperplanes.

We now choose a projective transformation τ, that maps $\boldsymbol{q}$ to $\boldsymbol{p}$, leaves $\boldsymbol{Q}\big|_F$ invariant and maps $\boldsymbol{Q}$ into the pyramid $\mathbf{conv}((\boldsymbol{P}\big|_F) \cup \{\boldsymbol{p}\})$. This transformation always exists and has the properties required in the theorem, as can be easily checked.   □

Looking at Figure 3.2.1, one observes that there might be realizations of $P \#_F Q$ that cannot be sectioned by a hyperplane into the former summands again. This happens since, in the realization of $P \#_F Q$, the vertices that used to be in F no longer have to stay on a common hyperplane. We will only deal with the case where this cannot happen due to the structure of F: in this case the facet F is called *necessarily flat*. If F is necessarily flat, then in every realization of $P \#_F Q$ we can find realizations of P and of Q as substructures.

The k-skeleton of a d-polytope $\boldsymbol{P}$ is the polyhedral complex (see [64]) generated by all k-faces of $\boldsymbol{P}$. For instance, the 1-skeleton is the edge graph, and the d-skeleton is $\boldsymbol{P}$ itself.

<u>DEFINITION 3.2.5.</u> A d-polytope $\boldsymbol{P}$ is *necessarily flat* if every polyhedral embedding of its $(d-1)$-skeleton in $\mathbb{R}^n$; $d < n$ has affine dimension at most d.

In fact, in dimension $d = 2$ one can see that a polytope $\boldsymbol{P}$ is necessarily flat if and only if $\boldsymbol{P}$ is a triangle. In dimension 3, there are many more different types of polytopes that are "necessarily flat," as the next lemma shows.

<u>LEMMA 3.2.6.</u> *Pyramids, prisms, and tents over n-gons are necessarily flat.*

PROOF. A pyramid $P = \mathbf{pyr}(Q, y)$ contains Q as a facet. Except for Q, the pyramid P has just one additional point y. Thus the affine dimension of the $(d-1)$-skeleton of P has dimension at most d.

Let $\boldsymbol{P} \subseteq \mathbb{R}^m$ be a realization of the $(d-1)$-skeleton of $\mathbf{prism}(G)$, a prism over an n-gon G labeled by $1, \ldots, n$ in this order. The opposite n-gon G' in $\mathbf{prism}(G)$ is labeled canonically by $1', \ldots, n'$. The vertices $1, 2, 3, 1'$ form an affine basis of

$\boldsymbol{P}$. Since $\{1, 1', 2, 2'\}$ is a facet, the point $2'$ lies in the affine hull of $\boldsymbol{p}_1, \boldsymbol{p}_2, \boldsymbol{p}_{1'}$. Since $\{2, 2', 3, 3'\}$ is a facet, the point $3'$ lies in the affine hull of $\boldsymbol{p}_2, \boldsymbol{p}_3, \boldsymbol{p}_{2'}$. Points $4, \ldots, n$ and $4', \ldots, n'$ lie in the affine hulls of $1, 2, 3$ and $1', 2', 3'$, respectively. This proves that $\mathbf{aff}(\boldsymbol{P}) = \mathbf{aff}(\{\boldsymbol{p}_1, \boldsymbol{p}_2, \boldsymbol{p}_3, \boldsymbol{p}_{1'}\})$.

Let $\boldsymbol{P} \subseteq \mathbb{R}^m$ be a realization of the $(d-1)$-skeleton of $\mathbf{tent}^{e_1, e_2}(G, a, b)$, a tent over an n-gon G with disjoint edges e_1 and e_2. All points of $\boldsymbol{P}$ lie either on the plane that supports G or on the plane spanned by the edge e_1, a and b. These two planes have a one-dimensional intersection, since they both contain e_1. Therefore $\boldsymbol{P}$ has affine dimension at most 3. □

Finally, we discuss the effect of connected sum operations on realization spaces. Assume that the facet F along which the two summands are glued is necessarily flat. Furthermore assume that the shape of F cannot be arbitrarily chosen for realizations of P as well as for realizations of Q. Any realization $\boldsymbol{R}$ of $P \#_F Q$ can be sectioned by a hyperplane spanned by the points of F into two pieces that form realizations of P and Q. Therefore $\boldsymbol{R}$ must be compatible with both obstructions (those coming from P and those coming from Q) at the same time. More formally, we choose bases $B_P = (b_0, \ldots, b_d, b_{d+1})$ and $B_Q = (b_0, \ldots, b_d, b'_{d+1})$ for P and Q respectively, such that $B_F = (b_0, \ldots, b_d)$ is a basis of the facet F. We furthermore define deletion maps

$$\pi_P \colon \mathcal{R}(P, B_P) \to \mathcal{R}(F, B_F),$$
$$\pi_Q \colon \mathcal{R}(Q, B_Q) \to \mathcal{R}(F, B_F),$$
$$\pi_R \colon \mathcal{R}(P \#_F Q, B_P) \to \mathcal{R}(F, B_F)$$

The fact that the shape of F cannot be arbitrary chosen in P and Q translates to the fact that π_P and π_Q are not surjective. For the shape of the points of F in $P \#_F Q$ we get

$$\pi_R(\mathcal{R}(P \#_F Q, B_P)) = \pi_P(\mathcal{R}(P, B_P)) \cap \pi_Q(\mathcal{R}(Q, B_Q))$$

Thus the realization space of $P \#_F Q$ may be "complicated" if the above intersection is not trivial.

3.3 Lawrence Extensions

While face lattices encode the combinatorial boundary structure of polytopes and cones, the combinatorial structure of general point configurations is modeled by *oriented matroids* (for an introduction to the theory of oriented matroids see [7]).

The oriented matroid $\mathcal{M}(\boldsymbol{P})$ of a (linear) point configuration in $\mathbb{R}^d$ is a list of all point partitions on $\boldsymbol{P}$ induced by linear hyperplanes in $\mathbb{R}^d$. The realization space of the oriented matroid $\mathcal{M}(\boldsymbol{P})$ is the space of all point configurations in $\mathbb{R}^d$ that generate the same partitions as $\boldsymbol{P}$ does. In particular, oriented matroids contain complete information about the incidence structure of $\boldsymbol{P}$ (i.e. which point

sets in $\boldsymbol{P}$ are linearly dependent). One can also describe oriented matroids on the level of "signed" *affine* point configurations and partitions by *affine* hyperplanes.

In 1980, J. Lawrence developed a method that, for a given oriented matroid $\mathcal{M}$, generates a polytope $\boldsymbol{P}_{\mathcal{M}}$ whose realization space is stably equivalent to the realization space of $\mathcal{M}$. One way to interpret the *Lawrence construction* is that (in the affine picture) each point of a point configuration $\boldsymbol{P}$ is doubled and the two resulting points are lifted with different "speed" into a new direction of space. By this means a configuration of n points that affinely spans $\mathbb{R}^d$ gets translated into a configuration of $2n$ points in affine dimension $d+n$. The resulting $2n$ points form the vertex set of an $(n+d)$-polytope. The resulting polytope is called the *Lawrence polytope* of $\boldsymbol{P}$. Dependences in the original point configuration are represented by faces (i.e. dependent points in convex position) of the resulting polytope.

The dimension of the Lawrence polytope grows with the number of points in the original point configuration. Since our aim is to obtain a construction where the dimension stays fixed, we will not make use of the complete Lawrence construction. Instead we will very *selectively* apply the lifting process to single points in planar or 3-dimensional configurations. If one wants to stay within the realm of 4-polytopes, then it is not permissible to use more than two such "Lawrence extensions". However, careful use of just one or two Lawrence extensions on some points outside a 2- or 3-polytope leads to extremely interesting and useful polytopes — such as the basic building blocks for the proof of the Universality Theorem.

We will introduce Lawrence extensions on the level of linear point configurations and cones. Thus point coordinates are considered as homogeneous coordinates, and the hyperplanes under consideration are linear hyperplanes. However, it is always possible to switch to the affine picture by simply "cutting" the whole configuration with an admissible dehomogenization hyperplane.

In what follows, we will always assume that $\boldsymbol{P} = (\boldsymbol{p}_i)_{i \in X}$ and $\boldsymbol{Q} = (\boldsymbol{q}_i)_{i \in Y}$ are point configurations on disjoint index sets $X = \{\mathrm{a}, \mathrm{b}, \dots, \mathrm{z}\}$ and $Y = \{1, \dots, k\}$ given by *homogeneous* coordinates.

<u>DEFINITION 3.3.1.</u> Let $\boldsymbol{P} = (\boldsymbol{p}_i)_{i \in X} \in \mathbb{R}^{d \cdot |X|}$ be a cone and let $\boldsymbol{Q} = (\boldsymbol{q}_1, \dots, \boldsymbol{q}_k) \in \mathbb{R}^{d \cdot k}$ be some additional points with $\boldsymbol{q}_i \notin \mathbf{pos}(\boldsymbol{P})$. The *Lawrence extension* $\boldsymbol{\Lambda}(\boldsymbol{P}, \boldsymbol{Q})$ is defined by the following $(|X|+2k) \times (d+k)$ matrix of homogeneous coordinates:

$$
\mathbf{\Lambda}(\boldsymbol{P},\boldsymbol{Q}) :=
\begin{array}{c}
\mathrm{a} \\ \vdots \\ \mathrm{z} \\ \overline{1} \\ \overline{2} \\ \vdots \\ \overline{k} \\ \underline{1} \\ \underline{2} \\ \vdots \\ \underline{k}
\end{array}
\left(
\begin{array}{ccccc}
\boldsymbol{p}_{\mathrm{a}} & 0 & 0 & \dots & 0 \\
\vdots & \vdots & \vdots & & \vdots \\
\boldsymbol{p}_{\mathrm{z}} & 0 & 0 & \dots & 0 \\
\boldsymbol{q}_1 & 1 & 0 & \vdots & 0 \\
\boldsymbol{q}_2 & 0 & 1 & \vdots & 0 \\
\vdots & \vdots & \vdots & \ddots & \vdots \\
\boldsymbol{q}_k & 0 & 0 & \vdots & 1 \\
-\boldsymbol{q}_1 & 1 & 0 & \vdots & 0 \\
-\boldsymbol{q}_2 & 0 & 1 & \vdots & 0 \\
\vdots & \vdots & \vdots & \ddots & \vdots \\
-\boldsymbol{q}_k & 0 & 0 & \vdots & 1
\end{array}
\right)
$$

Each of the points $\boldsymbol{q}_i$ with $i = 1, \dots, k$ generates two new points $\boldsymbol{q}_{\overline{i}}$ and $\boldsymbol{q}_{\underline{i}}$ using a new direction of space for each of the points $\boldsymbol{q}_i$. We have $\boldsymbol{q}_{\overline{i}} - \boldsymbol{q}_{\underline{i}} = 2\boldsymbol{q}_i$.

<u>REMARK 3.3.2.</u> We get the usual Lawrence construction as defined in [6], if $\boldsymbol{P}$ is empty.

It is easy to see that the points of $\mathbf{\Lambda}(\boldsymbol{P},\boldsymbol{Q})$ can be dehomogenized by a suitable affine hyperplane. For this we have to find a linear functional $h' \in (\mathbb{R}^{d+k})^*$ such that $h' \cdot \boldsymbol{p} > 0$ for all points $\boldsymbol{p} \in \mathbf{\Lambda}(\boldsymbol{P},\boldsymbol{Q})$. Since $\boldsymbol{P}$ is a cone in $\mathbb{R}^d$, there is a linear functional $h = (h_1, \dots, h_d) \in (\mathbb{R}^d)^*$ that is positive on all points of $\boldsymbol{P}$. Defining $h' = (h_1, \dots, h_d, N, \dots, N)$, where $N > 0$ is a sufficiently large number, gives the desired linear functional in $(\mathbb{R}^{d+k})^*$.

The following lemma shows that $\mathbf{\Lambda}(\boldsymbol{P},\boldsymbol{Q})$ is indeed a $(d+k)$-cone, and describes the structure of its face lattice. For a linear functional $h \in (\mathbb{R}^d)^*$ and a point configuration $\boldsymbol{P} = (\boldsymbol{p}_i)_{i \in X}$ of linear dimension d, we denote by $\boldsymbol{P}_h^+$, $\boldsymbol{P}_h^-$ and $\boldsymbol{P}_h^0$ the sets of all indices $i \in X$ for which the functional $h \cdot \boldsymbol{p}_i$ is positive, negative, or zero, respectively. The functional h is a *cocircuit* of $\boldsymbol{P}$ if there is no non-zero functional $h' \neq \boldsymbol{0}$ satisfying $\boldsymbol{P}_h^0 \subset \boldsymbol{P}_{h'}^0$. Cocircuits describe the hyperplanes spanned by points in $\boldsymbol{P}$. For a point configuration $\boldsymbol{P} \cup \boldsymbol{Q}$ we say that a cocircuit h is *external to* $\boldsymbol{P}$ if $\boldsymbol{P}_h^- = \emptyset$. The hyperplanes defined by external cocircuits do not intersect the interior of $\mathbf{pos}(\boldsymbol{P})$. For an arbitrary index set Y we set $\overline{Y} = \{\overline{i} \mid i \in Y\}$ and $\underline{Y} = \{\underline{i} \mid i \in Y\}$.

<u>LEMMA 3.3.3.</u> *Let $h \in (\mathbb{R}^d)^*$ be a cocircuit of $\boldsymbol{P} \cup \boldsymbol{Q}$ that is external to $\boldsymbol{P}$. Then*

$$\boldsymbol{P}_h^0 \ \cup \ \{\overline{i} \mid i \notin \boldsymbol{Q}_h^-\} \ \cup \ \{\underline{i} \mid i \notin \boldsymbol{Q}_h^+\}$$

defines a facet of $\mathbf{pos}(\mathbf{\Lambda}(\boldsymbol{P},\boldsymbol{Q}))$. Furthermore,

$$(X \cup \overline{Y} \cup \underline{Y}) - \{\overline{i}, \underline{i}\},$$

are facets of $\mathbf{pos}(\mathbf{\Lambda}(\boldsymbol{P}, \boldsymbol{Q}))$, *for* $i = 1, \dots, k$. *All facets are generated in these two ways. This implies that* $\mathbf{\Lambda}(\boldsymbol{P}, \boldsymbol{Q})$ *is a cone (i.e., the vertices are in extreme position).*

PROOF. We set $\mathbf{\Lambda} = \mathbf{\Lambda}(\boldsymbol{P}, \boldsymbol{Q})$. We analyze the structure of the face lattice of $\mathbf{pos}(\mathbf{\Lambda})$. In order to get a complete list of all facets of $\mathbf{\Lambda}$, we need a list of all linear functionals $h' \in (\mathbb{R}^{d+k})^*$ that are non-negative on all points of $\mathbf{\Lambda}$ and which are zero on a maximal set of such points. The zero-sets of these linear functionals exactly define the facets of $\mathbf{pos}(\mathbf{\Lambda})$. Let $h' = (h_1, \dots, h_{d+k})$ be such a facet-defining functional. By the structure of $\mathbf{\Lambda}$, the first d entries $h = (h_1, \dots, h_d) \in (\mathbb{R}^d)^*$ of h', interpreted as a linear functional on $\mathbb{R}^d$, are non-negative on all points $\boldsymbol{p}_1, \dots, \boldsymbol{p}_n$. For $h \neq \mathbf{0}$, we get a unique facet-defining linear functional of $\mathbf{\Lambda}$ by the choice:

$$h' = (\, h_1, \dots, h_d, \; |h \cdot \boldsymbol{q}_1|, \; |h \cdot \boldsymbol{q}_2|, \dots, |h \cdot \boldsymbol{q}_k| \,).$$

Here $|h' \cdot \boldsymbol{q}|$ denotes the absolute value of the inner product of h and $\boldsymbol{q}$. It is easy to check that h defined this way is non-negative on all points of $\mathbf{\Lambda}$ and generates a maximal number of zero values on $\mathbf{\Lambda}$ for given h. The overall number of points that are zero on h' is then maximal if h was chosen to be a cocircuit of $\boldsymbol{P} \cup \boldsymbol{Q}$. For $i \in \{1, \dots, k\}$ we have

$$\mathbf{sign}(h' \cdot \boldsymbol{q}_{\overline{i}}) = \begin{cases} 1, & \text{if } h \cdot \boldsymbol{q}_i > 0, \\ 0, & \text{if } h \cdot \boldsymbol{q}_i \leq 0, \end{cases} \quad \text{and} \quad \mathbf{sign}(h' \cdot \boldsymbol{q}_{\underline{i}}) = \begin{cases} 1, & \text{if } \boldsymbol{q}_i \cdot h < 0, \\ 0, & \text{if } \boldsymbol{q}_i \cdot h \geq 0. \end{cases}$$

This determines the structure of these facets, as claimed in the lemma.

The remaining facets must have $h = \mathbf{0}^d$. Here $\mathbf{0}^d$ denotes the d-dimensional zero-vector. These facet-defining functionals are then given by the vectors $h_1 = (\mathbf{0}^d, 1, 0, \dots, 0)$, $h_2 = (\mathbf{0}^d, 0, 1, \dots, 0)$ etc., up to $h_k = (\mathbf{0}^d, 0, 0, \dots, 1)$. The functional h_i is non-zero only on the points labeled $\overline{i}$ and $\underline{i}$. This proves the lemma. $\quad\square$

Figure 3.3.1 shows the effect of a single Lawrence extension of a pentagon $\boldsymbol{P}$ in an affine picture. The additional point $\boldsymbol{q}_1$ was chosen on the intersection of two of the edge-supporting lines l_1 and l_2 of $\boldsymbol{P}$. Notice that this generates two quadrangular 2-faces $\boldsymbol{F}_1$ and $\boldsymbol{F}_2$ in the resulting Lawrence extension $\mathbf{\Lambda}(\boldsymbol{P}, \{\boldsymbol{q}_1\})$.
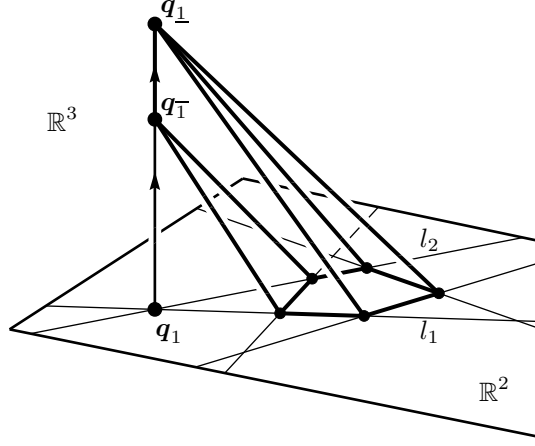
Figure 3.3.1: Lawrence extension of a pentagon.

Conversely, in every realization of $\mathbf{\Lambda}(\boldsymbol{P}, \{\boldsymbol{q}_1\})$, the line supporting $\boldsymbol{q}_{\overline{1}}$ and $\boldsymbol{q}_{\underline{1}}$ meets the intersection of l_1 and l_2 since the supporting planes of $\boldsymbol{P}$, $\boldsymbol{F}_1$ and $\boldsymbol{F}_2$ have exactly one point in common.

The important fact about a Lawrence extension is that its realization space is directly related to the realization space of the underlying point configuration $\boldsymbol{P} \cup \boldsymbol{Q}$ (interpreted in an appropriate way). For this we again let $\boldsymbol{P} \subset \mathbb{R}^d$ be a cone and let $\boldsymbol{Q} \subset \mathbb{R}^d$ be additional points not in $\mathbf{pos}(\boldsymbol{P})$. Another pair of such point configurations $(\boldsymbol{P}', \boldsymbol{Q}')$ is called *Lawrence equivalent* to $(\boldsymbol{P}, \boldsymbol{Q})$ if we have

$$\left\{ (\boldsymbol{P}_h^+ \cup \boldsymbol{Q}_h^+, \ \boldsymbol{P}_h^- \cup \boldsymbol{Q}_h^-) \mid h \in (\mathbb{R}^d)^*; \ h \text{ non-negative on } \boldsymbol{P} \right\}$$
$$= \quad \left\{ (\boldsymbol{P'}_h^+ \cup \boldsymbol{Q'}_h^+, \ \boldsymbol{P'}_h^- \cup \boldsymbol{Q'}_h^-) \mid h \in (\mathbb{R}^d)^*; \ h \text{ non-negative on } \boldsymbol{P}' \right\}.$$

REMARK 3.3.4. In the special case $\boldsymbol{P} = \boldsymbol{P}' = \emptyset$ we get the usual Lawrence construction. Then in the case of Lawrence equivalence the oriented matroids $\mathcal{M}(\boldsymbol{Q})$ and $\mathcal{M}(\boldsymbol{Q}')$ are identical.

LEMMA 3.3.5.   *With the notation above let*

$$\mathbf{\Lambda}' = \boldsymbol{P}' \cup \{\boldsymbol{q}'_{\overline{1}}, \ldots, \boldsymbol{q}'_{\overline{k}}, \ \boldsymbol{q}'_{\underline{1}}, \ldots, \boldsymbol{q}'_{\underline{k}}\}$$

be a realization of the Lawrence extension $\mathbf{\Lambda}(\boldsymbol{P}, \boldsymbol{Q})$. Then there exist points

$$\boldsymbol{Q}' = \{\boldsymbol{q}'_1, \ldots, \boldsymbol{q}'_k\}$$

such that $(\boldsymbol{P}', \boldsymbol{Q}')$ is Lawrence equivalent to $(\boldsymbol{P}, \boldsymbol{Q})$.

PROOF. By Lemma 3.3.3 the sets

$$\boldsymbol{F}_i \ = \ (X \ \cup \ \overline{Y} \ \cup \ \underline{Y}) - \{\overline{i}, \underline{i}\}$$

are facets of $\boldsymbol{\Lambda}'$, for $i = 1, \ldots, k$. By intersecting $k - 1$ of these facets we see that in particular

$$\boldsymbol{f}_i \ = \ X \ \cup \ \{\overline{i}, \underline{i}\}$$

is a $d+1$-face of $\boldsymbol{\Lambda}'$. Intersecting all $\boldsymbol{F}_i$ we see that X itself is a d-face. Furthermore $\{\overline{i}, \underline{i}\}$ is an edge. This proves that the intersection

$$A_i = \mathbf{lin}(\{\boldsymbol{q}'_{\overline{i}}, \boldsymbol{q}'_{\underline{i}}\}) \ \cap \mathbf{lin}(\boldsymbol{P})$$

is a 1-dimensional subspace. For $i = 1, \ldots, k$ let $\boldsymbol{q}' \in A_i \backslash \{\boldsymbol{0}\}$ be a point satisfying

$$\boldsymbol{q}'_i = \boldsymbol{q}'_{\overline{i}} - \alpha_i \boldsymbol{q}'_{\underline{i}}$$

with positive scalars α_i. Such scalars can be chosen to be positive since $A_i \cap \mathbf{pos}(\{\boldsymbol{q}'_{\overline{i}}, \boldsymbol{q}'_{\underline{i}}\}) = \emptyset$. The points $\boldsymbol{q}'_1, \ldots, \boldsymbol{q}'_k$ satisfy the requirements of the lemma. To see this let $\boldsymbol{F}$ be a facet of $\boldsymbol{\Lambda}'$ with $X \not\subset \boldsymbol{F}$. For every $i = 1, \ldots, k$ we have $\overline{i} \in \boldsymbol{F}$ or $\underline{i} \in \boldsymbol{F}$ or both. This facet has a corresponding facet-defining linear functional $h' \in (\mathbb{R}^{d+k})^*$, which is non-negative on all points of $\boldsymbol{\Lambda}'$ and zero on a maximal number of such points. The first d entries $h = (h_1, \ldots, h_d) \in (\mathbb{R}^d)^*$, interpreted as a linear functional on $\mathbb{R}^d$, are non-negative on all points $\boldsymbol{P}'$. Moreover, h defines a cocircuit of $\boldsymbol{P}' \cup \boldsymbol{Q}'$ since otherwise for h' there would be a way furthermore to increase the set $(\boldsymbol{\Lambda}')^0_{h'}$. This would contradict the fact that h' defines a facet. By our definition of $\boldsymbol{q}'_i$ we have

$$\boldsymbol{q}'_i \cdot h \ = \ \boldsymbol{q}'_i \cdot h' \ = \ \boldsymbol{q}'_{\overline{i}} \cdot h' - \alpha_i \boldsymbol{q}'_{\underline{i}} \cdot h'.$$

We get

$$\mathbf{sign}(h' \cdot \boldsymbol{q}'_i) = \left\{ \begin{array}{rl} 1 & \text{if } \overline{i} \notin \boldsymbol{F} \text{ and } \underline{i} \in \boldsymbol{F}, \\ 0 & \text{if } \overline{i} \in \boldsymbol{F} \text{ and } \underline{i} \in \boldsymbol{F}, \\ -1 & \text{if } \overline{i} \in \boldsymbol{F} \text{ and } \underline{i} \notin \boldsymbol{F}. \end{array} \right.$$

This finally proves that $(\boldsymbol{P}', \boldsymbol{Q}')$ defined this way is Lawrence equivalent to $(\boldsymbol{P}', \boldsymbol{Q}')$. $\qquad \square$

3.4 Examples

In the literature on polytopes one has several examples of polytopes for which some face cannot have arbitrary shape. It is an amazing fact that although these constructions were made independently by different authors with different techniques, they can all be explained by the tool of Lawrence extensions.

<u>EXAMPLE 3.4.1.</u>   Kleinschmidt's non-prescribable 3-face of a 4-polytope   In [40], P. Kleinschmidt constructed an example of a 4-polytope $\boldsymbol{P}_{\mathrm{K}}$ for which the shape of an octahedral 3-face $\mathcal{O}$ cannot be arbitrarily chosen. The polytope $\boldsymbol{P}_{\mathrm{K}}$ can be constructed in the following way. Consider an octahedron $\mathcal{O}$ realized in a way such that there is a point $\boldsymbol{q}_y$ such that the "shadow boundary of $\mathcal{O}$ seen from $\boldsymbol{q}_y$" is the edge path that is shown in Figure 3.4.2(a). A projection of such a realization of the octahedron is shown in Figure 3.4.2(b). In such a realization the three diagonals of $\mathcal{O}$ cannot meet in a point.
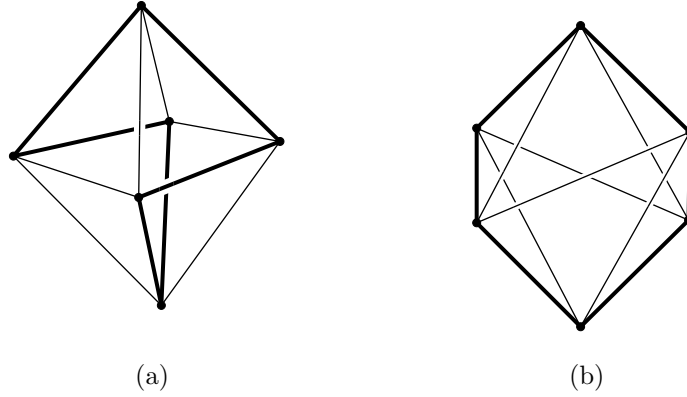

(a)   (b)

Figure 3.4.1: Construction of Kleinschmidt's polytope.

The Lawrence extension $\boldsymbol{P}_{\mathrm{K}} = \boldsymbol{\Lambda}(\mathcal{O}, \boldsymbol{q}_y)$ encodes this property into an octahedral facet. Kleinschmidt's polytope was used to construct the celebrated Bokowski-Ewald-Kleinschmidt polytope $\boldsymbol{P}_{\mathrm{BEK}}$ that was the only known example of a 4-polytope with a disconnected realization space ([15, 16]). The polytope $\boldsymbol{P}_{\mathrm{BEK}}$ is obtained by building the connected sum of $\boldsymbol{P}_{\mathrm{K}}$ and a mirror image of $\boldsymbol{P}_{\mathrm{K}}$ along the common octahedral facet. It is instructive to analyze why $\boldsymbol{P}_{\mathrm{BEK}}$ has a non-trivial realization space. After performing the connected sum operation of $\boldsymbol{P}_K$ with its mirror image $-\boldsymbol{P}_K$ the vertices of $\mathcal{O}$ no longer form a facet of the sum $\boldsymbol{P}_{\mathrm{BEK}} = \boldsymbol{P}_{\mathrm{K}}\#_{\mathcal{O}}(-\boldsymbol{P}_{\mathrm{K}})$. The vertices of $\mathcal{O}$ cannot lie in a common hyperplane, since the two summands force conditions that are not compatible with each other. Therefore there cannot be a realization of $\boldsymbol{P}_{\mathrm{BEK}}$ that realizes the full combinatorial symmetry. By Smith's theory this implies that the realization space of $\boldsymbol{P}_{\mathrm{BEK}}$ is not contractible. The realization space of $\boldsymbol{P}_{\mathrm{BEK}}$ is disconnected because there are two different ways of orienting the perturbed octahedron.

<u>EXAMPLE 3.4.2.</u>   Barnette's non-prescribable 3-face of a 4-polytope
In [11], D. Barnette constructed an example of another 4-polytope $\boldsymbol{P}_{\mathrm{B}}$ where the shape of a cubical 3-face $\mathcal{C}$ cannot be arbitrarily chosen. The polytope $\boldsymbol{P}_{\mathrm{B}}$ can be constructed in the following way. Consider a cube $\mathcal{C}$ realized in a way

such that there is a point $\boldsymbol{q}_y$ on which the supporting lines of the four edges that are adjacent to one facet meet. The Lawrence extension $\boldsymbol{P}_\mathrm{B} = \boldsymbol{\Lambda}(\mathcal{C}, \boldsymbol{q}_y)$ is a 4-polytope that has a cubical facet where the 4 corresponding edges must meet in a point. A Schlegel diagram of $\boldsymbol{P}_\mathrm{B}$ together with the reconstructed point $\boldsymbol{q}_y$ is shown in Figure 3.4.1.
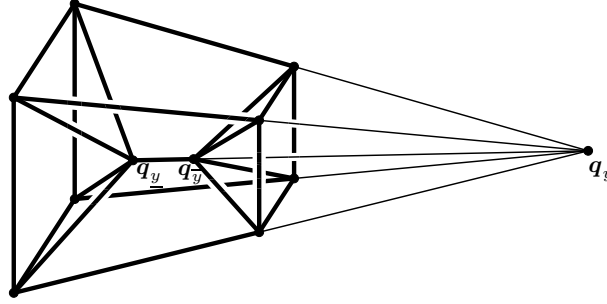

Figure 3.4.2: Construction of Barnette's polytope.

EXAMPLE 3.4.3.   Ziegler's non-prescribable 2-face of a 5-polytope

In [65], G.M. Ziegler constructed an example of a 5-polytope $\boldsymbol{P}_\mathrm{Z}$, where the shape of a hexagonal 2-face $\mathcal{H}$ cannot be arbitrarily chosen. In every realization of $\boldsymbol{P}_\mathrm{Z}$ the six vertices of $\mathcal{H}$ must lie on a conic (which is indeed a projective condition since five points uniquely determine a plane conic already). Ziegler generated $\boldsymbol{P}_\mathrm{Z}$ as the polar of a polytope associated to a 3-dimensional affine Gale diagram [58]. $\boldsymbol{P}_\mathrm{Z}$ can also be considered as a Lawrence extension in the following way. Start with a hexagon $\mathcal{H}$ whose vertices lie in an ellipse. Pascal's Theorem tells us that the intersections $\boldsymbol{q}_1, \boldsymbol{q}_2, \boldsymbol{q}_3$ of opposite sides lie on a line. Let $\boldsymbol{Q} = (\boldsymbol{q}_1, \boldsymbol{q}_2, \boldsymbol{q}_3)$. The polytope $\boldsymbol{P}_\mathrm{Z}$ is now obtained as the Lawrence extension $\boldsymbol{P}_\mathrm{Z} := \boldsymbol{\Lambda}(\mathcal{H}, \{\boldsymbol{q}_1, \boldsymbol{q}_2, \boldsymbol{q}_3\})$.
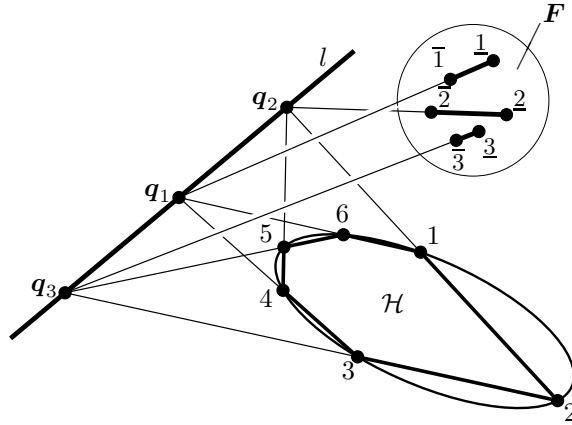

Figure 3.4.3: Construction of Ziegler's polytope.

The collinearity of the points in $\boldsymbol{Q}$ translates to the fact that the six new points $\overline{1}, \underline{1}, \overline{2}, 2, \overline{3}, \underline{3}$ lie on a common facet F.

The cocircuits of $\mathcal{H} \cup \boldsymbol{Q}$ are given by the edge-supporting lines of $\mathcal{H}$ and the line ℓ incident with $\boldsymbol{q}_1, \boldsymbol{q}_2, \boldsymbol{q}_3$. The combinatorial structure of these cocircuits is uniquely determined up to reorientation of the points $\boldsymbol{q}_i$. By Lemma 3.3.3 this uniquely determines the face lattice of $\boldsymbol{L}(\mathcal{H}, \boldsymbol{Q})$ (up to relabeling).

Conversely, from any realization of $\boldsymbol{P}_Z$ we can reconstruct the points $\boldsymbol{q}_1, \boldsymbol{q}_2, \boldsymbol{q}_3$ which have to be collinear by Lemma 3.3.5. Pascal's Theorem proves that the vertices of $\mathcal{H}$ again lie on a conic.
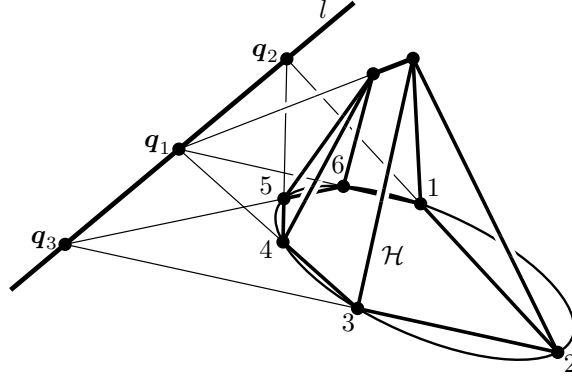

Figure 3.4.3: A 3-face of Ziegler's polytope.

Figure 3.4.4 shows one 3-face of $\boldsymbol{P}_Z$ (a tent over $\mathcal{H}$) that corresponds to a single Lawrence extension at one of the points in $\boldsymbol{Q}$. The polytope $\boldsymbol{P}_Z$ will play a crucial role in our alternative construction for a Non-Steinitz theorem given in Part V.

PART II: THE UNIVERSALITY THEOREM

4   Equations and Polytopes

4.1   Shor's Normal Form

In [53] P. Shor sketches an alternative proof of Mnëv's famous Universality The-
orem for oriented matroids [48]. His proof starts with a "preprocessing step"
that replaces the defining equations of an arbitrary primary semialgebraic set by
equations and inequalities (describing a stably equivalent set) of a particularly
simple kind: *all variables are linearly ordered and only elementary additions and
multiplications occur as equations.* The price that has to be paid for this reduc-
tion is that one has to introduce many new variables. The reduction to such a
Shor normal form will be the starting point for our construction, too. A sketch
of a non-constructive version of the following theorem is also implicit in Mnëv's
original work [48].

<u>DEFINITION 4.1.1.</u>   A *Shor normal form* is a triple $\mathcal{S} = (n, \mathbf{A}, \mathbf{M})$ where $n \in \mathbb{N}$
and $\mathbf{A}, \mathbf{M} \in \{1, \ldots, n\}^3$ such that for $(i, j, k) \in \mathbf{A} \cup \mathbf{M}$ we have $i \leq j < k$.

To every Shor normal form $\mathcal{S}$ we associate a semialgebraic set $V(\mathcal{S}) \in \mathbb{R}^n$
as the solution of the inequalities

$$1 < x_1 < x_2 < \ldots < x_n$$

and the equations

$$x_i + x_j = x_k \quad \text{for } (i, j, k) \in \mathbf{A} \text{ and}$$
$$x_i \cdot x_j = x_k \quad \text{for } (i, j, k) \in \mathbf{M}.$$

<u>THEOREM 4.1.2.</u>   (Shor [53].) *Let $W \subseteq \mathbb{R}^m$ be a primary basic semialgebraic
set defined over $\mathbb{Z}$. Then there exists a Shor normal form $\mathcal{S}(W) = \mathcal{S} = (n, \mathbf{A}, \mathbf{M})$
such that the semialgebraic set $V(\mathcal{S}) \subseteq \mathbb{R}^n$ is stably equivalent to W. Further-
more,*

(i) *$\mathcal{S}$ can be computed from the defining relations of W in a time that is
polynomially bounded in the coding length of the equations defining W,*

(ii) *there exists a polynomial function f such that $f(V(\mathcal{S}(W))) = W$.*

If one wants to consider also general (non-primary) semialgebraic sets $W \in \mathbb{R}^m$ one cannot expect the existence of a stably equivalent set given by a Shor normal form. However, one can construct a primary semialgebraic set $V \in \mathbb{R}^{m+k}$ such that $W = \pi(V)$ can be obtained as the image of a (non-stable) projection π. For this assume that in the defining equations of W we have k non-strict inequalities

$$a_i \leq b_i \quad \text{with} \quad a_i, \, b_i \in \mathbb{Z}[x_1, \ldots, x_m]$$

for $i = 1, \ldots, k$. To obtain the defining equations of V we simply replace these inequalities by equations

$$a_i = b_i + x_{m+i}^2,$$

with new variables $x_{m+1}, \ldots, x_{m+k}$.

4.2   Encoding Equations into Polygons

Shor uses his reduction to encode arbitrary semialgebraic sets by point sequences

$$\boldsymbol{p_0}, \boldsymbol{p_1}, \boldsymbol{p_{x_1}}, \ldots, \boldsymbol{p_{x_n}}, \boldsymbol{p_\infty}$$

on a line ℓ, in which the three points $\boldsymbol{p_0}, \boldsymbol{p_1}, \boldsymbol{p_\infty}$ define a projective scale on ℓ. The additions and multiplications are encoded by additional incidence configurations (essentially von Staudt constructions). The strict order of the variables assures that in the resulting point configuration the underlying oriented matroid is the same for every point of the semialgebraic set.

We will do something very similar: we will encode the values of the variables by the slopes of the lines of a $2(n+3)$-gon $\boldsymbol{G}$. The equations will be forced by additional polytopal constructions that are "adjacent" to $\boldsymbol{G}$. The order of the variables is represented by the ordering of the edge slopes of $\boldsymbol{G}$.

For a linearly ordered sequence of labels $X = (a_1, a_2, \ldots, a_n)$ we define $\boldsymbol{G}(X)$ to be an n-gon in which the edges are labeled by X in the given order. By $\boldsymbol{G}[X]$ we denote a $2n$-gon where the edges are labeled by

$$a_1, a_2, \ldots, a_n, a_1', a_2', \ldots, a_n'$$

in this order. A vertex v of $\boldsymbol{G}(X)$ is labeled $a \wedge b$ where a and b are the labels of the edges incident with v.

For the purpose of representing a Shor normal form $\mathcal{S} = (n, \mathbf{A}, \mathbf{M})$ we choose a label sequence $X = (\boldsymbol{0}, \boldsymbol{1}, x_1, x_2, \ldots, x_n, \boldsymbol{\infty})$. A $2(n+3)$-gon $\boldsymbol{G}[X]$, where the label set X has this form, is called a *computation frame*. Figure 4.1.1 shows the correct labeling for a computation frame with $n = 2$.
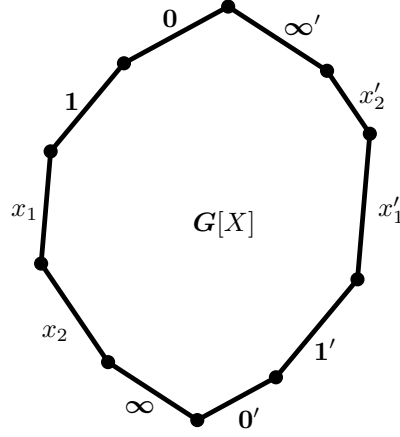
Figure 4.1.1:   The labeling of the computation frame.

In the following sections we will construct 4-polytopes $\boldsymbol{P}$ that contain computation frames $\boldsymbol{G}[X]$ as 2-faces. The shape of $\boldsymbol{G}[X]$ will not be arbitrarily prescribable. For every realization of $\boldsymbol{P}$ there exists a line ℓ such that the supporting lines of the sides a and a' of $\boldsymbol{G}[X]$ and ℓ intersect in a point $\boldsymbol{p}_a$ for all $a \in X$. Such a computation frame will be called *normal*. Figure 4.1.2 illustrates a normal computation frame for $n = 2$.

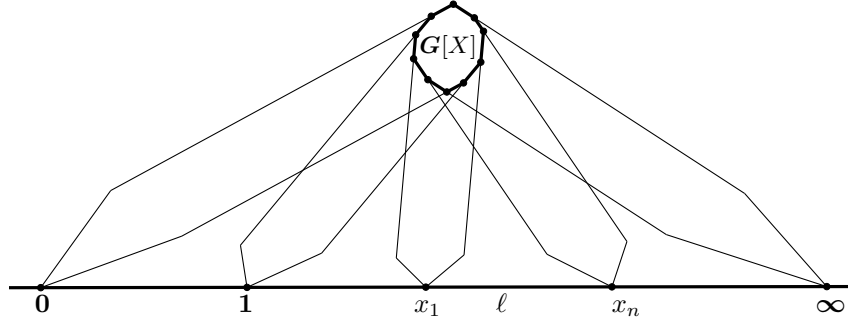**Figure 4.1.2:**   A normal computation frame and the line at infinity.

The *cross ratio* $(\boldsymbol{p}_1, \boldsymbol{p}_2 | \boldsymbol{p}_3, \boldsymbol{p}_4)$ of four points on a line ℓ is defined by

$$(\boldsymbol{p}_1, \boldsymbol{p}_2 | \boldsymbol{p}_3, \boldsymbol{p}_4) \; = \; \frac{|\boldsymbol{p}_1, \boldsymbol{p}_3| \cdot |\boldsymbol{p}_2, \boldsymbol{p}_4|}{|\boldsymbol{p}_1, \boldsymbol{p}_4| \cdot |\boldsymbol{p}_2, \boldsymbol{p}_3|}.$$

Here $|\boldsymbol{p}_i, \boldsymbol{p}_j|$ denotes the (oriented) euclidean distance of $\boldsymbol{p}_i$, and $\boldsymbol{p}_j$ and we assume that none of the points lies at infinity. The cross ratio is invariant under projective transformations; therefore we can also extend the above definition to the case where one or more of the points lies at infinity. In particular, if ℓ is equipped with an euclidean scale then we have $(x, 1 | 0, \infty) = x$. In other words,

after the choice of three distinct positions of $0, 1$ and ∞ on a line, the cross ratio exactly measures the euclidean scale. We say that $0, 1$ and ∞ define a *projective scale*.

For a normal computation frame $\boldsymbol{G}[X]$, we interpret the positions of the points $\boldsymbol{p_0}, \boldsymbol{p_1}$, and $\boldsymbol{p_\infty}$ as a projective scale representing the points $0, 1$, and ∞ on the line ℓ. The scalar value $\gamma(\boldsymbol{p})$ of a point $\boldsymbol{p}$ on ℓ is now defined by the cross ratio $(\boldsymbol{p}, \boldsymbol{p_1}|\boldsymbol{p_0}, \boldsymbol{p_\infty})$.

For a given Shor normal form $\mathcal{S} = (n, \mathbf{A}, \mathbf{M})$, we will construct a 4-polytope $\boldsymbol{P}(\mathcal{S})$ containing a 2-face $\boldsymbol{G}[\boldsymbol{0}, \boldsymbol{1}, x_1, x_2, \ldots, x_n, \boldsymbol{\infty}]$ that is a normal computation frame for every realization of $\boldsymbol{P}(\mathcal{S})$. Furthermore, $\boldsymbol{P}(\mathcal{S})$ satisfies:

 (i) in every realization of $\boldsymbol{P}(\mathcal{S})$ we have $\gamma(\boldsymbol{p}_{x_i}) < \gamma(\boldsymbol{p}_{x_j})$ for $i < j$;

 (ii) in every realization of $\boldsymbol{P}(\mathcal{S})$ we have $\gamma(\boldsymbol{p}_{x_i}) + \gamma(\boldsymbol{p}_{x_j}) = \gamma(\boldsymbol{p}_{x_k})$
     for $(i, j, k) \in \mathbf{A}$;

(iii) in every realization of $\boldsymbol{P}(\mathcal{S})$ we have $\gamma(\boldsymbol{p}_{x_i}) \cdot \gamma(\boldsymbol{p}_{x_j}) = \gamma(\boldsymbol{p}_{x_k})$
     for $(i, j, k) \in \mathbf{M}$;

(iv) for every point $(\boldsymbol{x}_1, \ldots, \boldsymbol{x}_n) \in V(\mathcal{S})$ there exists a realization of $\boldsymbol{P}(\mathcal{S})$ with
     $\gamma(\boldsymbol{p}_{x_i}) = \boldsymbol{x}_i$ for $i \in \{1, \ldots, n\}$.

Observe that part (i) is just a consequence of the label ordering on $\boldsymbol{G}[X]$.

Consider a normal $2n$-gon $\boldsymbol{G}[X]$ with $X = (a_1, \ldots, a_n)$. If we apply a projective transformation that maps the line ℓ to infinity, then the sides a and a' become parallel for $a \in X$. In this case we will call the $2n$-gon $\boldsymbol{G}[X]$ *pre-standardized*. After embedding a pre-standardized computation frame $\boldsymbol{G}[X]$ in a euclidean plane, it defines n different line slopes, one s_a for each label $a \in X$. The values of the slopes are in $\overline{\mathbb{R}} = \mathbb{R} \cup \{\infty\}$. A computation frame $\boldsymbol{G}[\boldsymbol{0}, \boldsymbol{1}, x_1, \ldots, x_n, \boldsymbol{\infty}]$ will be called *standardized* if we in addition have

$$s_{\boldsymbol{0}} = 0, \ s_{\boldsymbol{1}} = 1, \ s_{\boldsymbol{\infty}} = \infty.$$

For each slope s_a, we define a direction $\hat{a}$ by homogeneous coordinates:

$$\hat{a} = \begin{cases} (1, a) & \text{if } a \neq \infty, \\ (0, 1) & \text{if } a = \infty. \end{cases}$$

The cross ratio $(\boldsymbol{p}_a, \boldsymbol{p}_b|\boldsymbol{p}_c, \boldsymbol{p}_d)$ of four points on the line ℓ can also be defined in terms of the slopes:

$$(\boldsymbol{p}_a, \boldsymbol{p}_b|\boldsymbol{p}_c, \boldsymbol{p}_d) = \frac{\mathbf{det}(\hat{a}, \hat{c}) \cdot \mathbf{det}(\hat{b}, \hat{d})}{\mathbf{det}(\hat{a}, \hat{d}) \cdot \mathbf{det}(\hat{b}, \hat{c})}$$

In particular, we have $(0, \infty|a, b) = a/b$ and $(a, b|c, \infty) = (a - c)/(b - c)$.

The above conditions show that the points of $V(\mathcal{S}) \in \mathbb{R}^n$ are in one-to-one correspondence with the edge slopes of the standardized computation frame $\boldsymbol{G}[\boldsymbol{0}, \boldsymbol{1}, x_1, \ldots, x_n, \boldsymbol{\infty}]$. We will prove that under this encoding the realization space of $\boldsymbol{P}(\mathcal{S})$ is stably equivalent to $V(\mathcal{S})$, which is an even stronger condition.

5 The Basic Building Blocks

In our construction $\boldsymbol{P}(\mathcal{S})$ is composed from smaller polytopes that are glued via connected sum operations. The pieces that are glued together all fall into five different classes of 4-dimensional polytopes. This section presents these *basic building blocks* (BBBs) and discusses their properties. In each of the cases we describe the polytopes under consideration by explicitly describing realizations, then collecting the necessary results about the corresponding realization spaces. We will postpone the consideration of how the realization spaces behave under gluing operations until we have described the complete construction. We also describe how some of the BBBs are composed to form larger units that are used in the construction. These polytopes will be called *composed building blocks*.

The facets along which the BBBs are glued are all either pyramids over n-gons, prisms over n-gons, or tents over n-gons. One can consider the n-gons as a kind of "storage" for information and the basic blocks as "processing units". The particular n-gons that are used as storage will be called *information frames*. For book keeping purposes we will label the *edges* of these n-gons. We will consider the label set $X = (1, \ldots, n)$ of an n-gon as a cyclic sequence. If Y is obtained by deleting one label from X while maintaining the order of the remaining labels we write $Y \overset{\cdot}{\hookrightarrow} X$. If we have

$$Y \overset{\cdot}{\hookrightarrow} Y_1 \overset{\cdot}{\hookrightarrow} Y_2 \overset{\cdot}{\hookrightarrow} \ldots \overset{\cdot}{\hookrightarrow} Y_n \overset{\cdot}{\hookrightarrow} X$$

we write $Y \hookrightarrow X$. Then Y is a consistently ordered cyclic subsequence of X.

By an abuse of notation, we will use the symbol $\boldsymbol{P}$ both for the polytope $\boldsymbol{P}$ and its face lattice, provided no confusion can arise. During the process of gluing, we have to specify under which combinatorial isomorphism the two summands are joined along a facet $\boldsymbol{F}$ by a connected sum operation. For the case where $\boldsymbol{F}$ is a pyramid, a prism or a tent the combinatorial isomorphism is completely described by the edge labels of the n-gons involved. We will suppress all other information to avoid unnecessary technicalities.

- We denote (the face lattice of) a pyramid over $\boldsymbol{G}(X)$ by $\mathbf{pyr}(X)$.
- We denote (the face lattice of) a prism over $\boldsymbol{G}(X)$ by $\mathbf{prism}(X)$, where the edges of the n-gon opposite to $\boldsymbol{G}(X)$ are labeled by X'.
- We denote (the face lattice of) a tent over $\boldsymbol{G}(X)$ by $\mathbf{tent}^{x,y}(X)$, then the "parallel" edges are x and y.

We will describe our construction by *diagrams*, where the BBBs are represented by boxes and where a join between two blocks is represented by an edge between two boxes. Since the joins have three possible types (pyramid, prism, or tent), we use three different types of edges:

────── for pyramids, ══════ for prisms, and ══════ for tents.

5.1   A Transmitter

Our first BBB will be the polytope $\boldsymbol{T}_X$ containing two n-gons $\boldsymbol{G}(X)$ and $\boldsymbol{G}(X')$ that are projectively equivalent in every realization of $\boldsymbol{T}_X$. $\boldsymbol{T}_X$ is constructed in the following way.

- Start with the n-gon $\boldsymbol{G}(X)$ and let $\boldsymbol{P} = \mathbf{prism}(\boldsymbol{G}(X))$. This prism $\boldsymbol{P}$ contains a second n-gon $\boldsymbol{G}(X')$.
- The edges joining corresponding vertices of $\boldsymbol{G}(X)$ and $\boldsymbol{G}(X')$ are parallel, and therefore meet in a point $\boldsymbol{q}_y$ at infinity.
- Perform a Lawrence extension at $\boldsymbol{q}_y$. We define $\boldsymbol{T}_X = \boldsymbol{\Lambda}(\boldsymbol{P}, \{\boldsymbol{q}_y\})$.
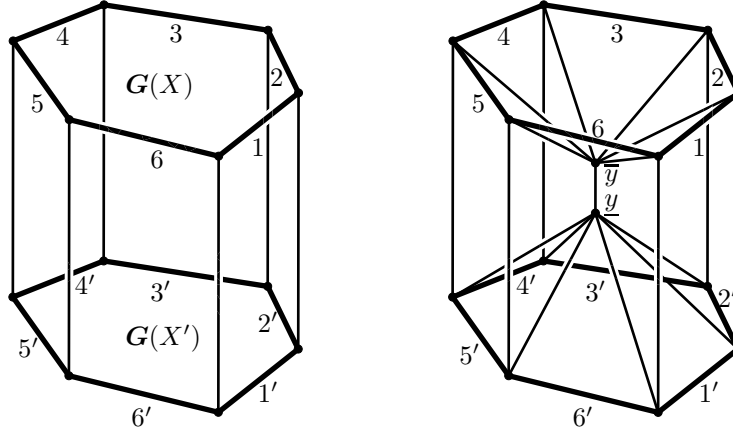
Figure 5.1.1: The construction of the transmitter.

Figure 5.1.1 shows $\boldsymbol{P}$ and a Schlegel diagram of $\boldsymbol{T}_X$. Observe that $\boldsymbol{T}_X$ could also be considered as a prism over a pyramid $\mathbf{pyr}(\boldsymbol{G}(X), y)$. The information frames of $\boldsymbol{T}_X$ are $\boldsymbol{G}(X)$ and $\boldsymbol{G}(X')$.

THEOREM 5.1.1.

(i) *The combinatorial type of $\boldsymbol{T}_X$ does not depend on the special choice of the points in the construction.*

(ii) *In every realization of $\boldsymbol{T}_X$, the n-gons $\boldsymbol{G}(X)$ and $\boldsymbol{G}(X')$ are projectively equivalent.*

PROOF. (i): The positive cocircuits of $\boldsymbol{P} \cup \{\boldsymbol{q}_y\}$ in the above construction that contain $\boldsymbol{q}_y$ are given by the supporting planes of the quadrangular faces of $\boldsymbol{P}$. The combinatorial structure of these cocircuits is uniquely determined up to reorientation of the point $\boldsymbol{q}_y$. By Lemma 3.3.3 this uniquely determines the face lattice of $\boldsymbol{T}_X$ (up to relabeling).

<u>(ii)</u>: Conversely, if $\boldsymbol{T}$ is a realization of $\boldsymbol{T}_X$, by Lemma 3.3.5 we can reconstruct a corresponding point $\boldsymbol{q}_y$ that forms the center of a projection of $\boldsymbol{G}(X)$ onto $\boldsymbol{G}(X')$. $\qquad\qquad\qquad\qquad\qquad\qquad\qquad\qquad\qquad\qquad\qquad\quad$ □

Observe that the transmitter $\boldsymbol{T}_X$ contains pyramids $\mathbf{pyr}(X)$ and $\mathbf{pyr}(X')$ as well as a prism $\mathbf{prism}(X)$ in the boundary. The transmitter will be represented by the box:
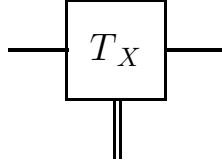

5.2   The Connector

We use two copies of transmitter $\boldsymbol{T}_X$ to build a first *composed* building block $\boldsymbol{C}_X$ that contains four different pyramids $\mathbf{pyr}(X)$ as facets, such that in every realization of $\boldsymbol{C}_X$ these four pyramids are projectively equivalent. This polytope $\boldsymbol{C}_X$ will be used as a "distributor" for information along which more than two processing units can be joined. We simply set

$$\boldsymbol{C}_X = \boldsymbol{T}_X \ \#_{\mathbf{prism}(X)} \ \boldsymbol{T}_X.$$

As diagram we can visualize $\boldsymbol{C}_X$ by:
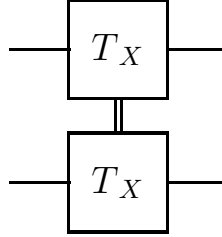
This polytope $\boldsymbol{C}_X$ contains two projectively equivalent n-gons $\boldsymbol{G}(X)$ and $\boldsymbol{G}(X')$, and has two pyramids adjacent to each of them. Although we could use all four possible connections we will – for reasons of simplicity – use only three of the pyramids of $\boldsymbol{C}_X$ as joins in our construction. Since the labeling along the n-gons $\boldsymbol{G}(X)$ is usually inherited from the neighbors in the construction, we often just write "$\boldsymbol{C}_n$" to represent a connector for an n-gon. In our diagrams, $\boldsymbol{C}_n$ will be represented by:
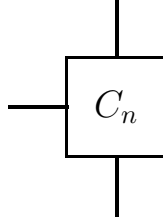
We assume that polytopes that are connected via $\boldsymbol{C}_n$ have consistent labelings on the n-gons.

5.3   A Forgetful Transmitter

The second BBB is very similar to $\boldsymbol{T}_X$, and is used to transmit projective conditions from an $(n+1)$-gon to an n-gon, thereby forgetting the position of one edge. We assume that $X = (1, \ldots, n)$ are the labels of the edges of an n-gon $\boldsymbol{G}(X)$ and $Y = (1', \ldots, (n+1)')$ are the labels of the edges of an $(n+1)$-gon $\boldsymbol{G}(Y)$. The "forgetful" transmitter $\boldsymbol{T}_X^Y$ is generated by the following procedure.

- Start with the n-gon $\boldsymbol{G}(X)$ and build $\boldsymbol{P} = \mathbf{prism}(\boldsymbol{G}(X))$. This polytope $\boldsymbol{P}$ contains a second n-gon $\boldsymbol{G}(X')$.

- Define $\boldsymbol{p}_y$ as the point at infinity in which the edges joining corresponding vertices of $\boldsymbol{G}(X)$ and $\boldsymbol{G}(X')$ meet.

- Truncate the vertex in which the edges $1'$ and n' meet. The new edge on $\boldsymbol{G}(X')$ will be labeled $(n+1)'$. Call the resulting polytope $\boldsymbol{P}'$.

- Perform a Lawrence extension at the point $\boldsymbol{q}_y$. We define

$$\boldsymbol{T}_X^Y = \boldsymbol{\Lambda}(\boldsymbol{P}', \{\boldsymbol{q}_y\}).$$

Figure 5.3.1 shows $\boldsymbol{P}'$ and a Schlegel diagram of $\boldsymbol{T}_X^Y$. The information frames of $\boldsymbol{T}_X^Y$ are $\boldsymbol{G}(X)$ and $\boldsymbol{G}(Y)$.
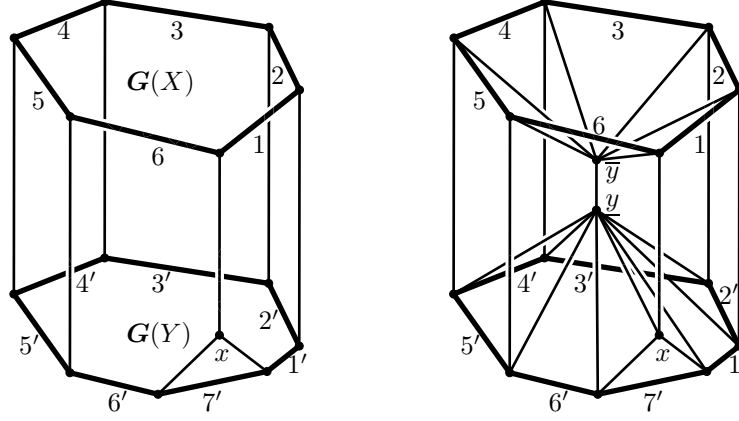
Figure 5.3.1: The construction of the forgetful transmitter.

<u>THEOREM 5.3.1.</u>

(i) *The combinatorial type of $\boldsymbol{T}_X^Y$ does not depend on the special choice of the points in the construction.*

(ii) *In every realization of $\boldsymbol{T}_X^Y$ the sets $\boldsymbol{L}_1$ and $\boldsymbol{L}_2$ of lines supporting the edges $1, \ldots, n$ and $1', \ldots, n'$, respectively, are projectively equivalent.*

PROOF. <u>(i)</u>: The positive cocircuits of $\boldsymbol{P}' \cup \{\boldsymbol{q}_y\}$ in the above construction that contain $\boldsymbol{q}_y$ are given by the supporting planes of the quadrangular faces of $\boldsymbol{P}$. The combinatorial structure of these cocircuits is uniquely determined up to reorientation of the point $\boldsymbol{q}_y$. By Lemma 3.3.3 this uniquely determines the face lattice of $\boldsymbol{T}_X^Y$ (up to relabeling).

<u>(ii)</u>: Conversely, if $\boldsymbol{T}$ is a realization of $\boldsymbol{T}_X^Y$, we can reconstruct a corresponding point $\boldsymbol{q}_y$ by Lemma 3.3.5 that forms the center of a projection of $\boldsymbol{L}_1$ onto $\boldsymbol{L}_2$. $\square$

The transmitter $\boldsymbol{T}_X^Y$ contains a pyramid $\mathbf{pyr}(X)$ over the n-gon $\boldsymbol{G}(X)$ and a pyramid $\mathbf{pyr}(Y)$ over the $(n{+}1)$-gon $\boldsymbol{G}(Y)$. These two facets will be used for connecting $\boldsymbol{T}_X^Y$ with other polytopes. The polytope $\boldsymbol{T}_X^Y$ is only defined for the case $X \hookrightarrow Y$. However if we have $X \hookrightarrow Y$ with

$$X \hookrightarrow Y_1 \hookrightarrow Y_2 \hookrightarrow \ldots \hookrightarrow Y_n \hookrightarrow Y$$

we can compose a chain of transmitters by connected sum operations. In this case we define a composed building block:

$$\boldsymbol{T}_X^Y \;=\; \boldsymbol{T}_X^{Y_1} \;\#_{\mathbf{pyr}(Y_1)}\; \boldsymbol{T}_{Y_1}^{Y_2} \;\#_{\mathbf{pyr}(Y_2)} \cdots \#_{\mathbf{pyr}(Y_n)}\; \boldsymbol{T}_{Y_n}^Y$$

The polytope $\boldsymbol{T}_X^Y$ contains the two pyramids $\mathbf{pyr}(X)$ and $\mathbf{pyr}(Y)$ such that in every realization the arrangements of lines supporting the edges labeled by X in both pyramids are projectively equivalent. In our diagrams the polytope $\boldsymbol{T}_X^Y$ will be represented by the box:

$$\longrightarrow \boxed{\quad X \;\hookrightarrow\; Y \quad} \longrightarrow$$
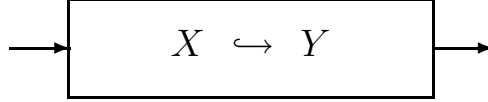
5.4   A 4-Polytope with Non-Prescribable 2-Face

Figure 5.4.1 shows a Schlegel diagram of a polytope $\boldsymbol{X}$ that contains a hexagon $\boldsymbol{G}_6 = \boldsymbol{G}(1,2,3,4,5,6)$ (the information frame) whose shape cannot be arbitrarily prescribed. In every realization of $\boldsymbol{X}$ the vertices $1 \wedge 4$, $2 \wedge 3$ and $5 \wedge 6$ are collinear. Here $a \wedge b$ denotes the intersection of the supporting lines of the two edges a and b. The polytope $\boldsymbol{X}$ is a basic building block and can be constructed by the following procedure:

- Start with a hexagon $\boldsymbol{G} = \boldsymbol{G}(1,\ldots,6)$, for which the points $1 \wedge 4$, $2 \wedge 3$ and $5 \wedge 6$ are collinear.
- Form $\boldsymbol{P} = \mathbf{tent}^{1,4}(\boldsymbol{G})$, a tent over $\boldsymbol{G}$. If, as in the drawing, a and b are the apices of the tent, then the lines $(2 \wedge 3) \vee a$ and $(5 \wedge 6) \vee b$ meet in a point $\boldsymbol{q}_y$.
- Perform a Lawrence extension at the point $\boldsymbol{q}_y$. We define

$$\boldsymbol{X} = \boldsymbol{\Lambda}(\boldsymbol{P}, \{\boldsymbol{q}_y\}).$$

THEOREM 5.4.1.

(i) *The combinatorial type of $\boldsymbol{X}$ does not depend on the special choice of the points in the construction.*

(ii) *In every realization of $\boldsymbol{X}$ the vertices $1 \wedge 4$, $2 \wedge 3$, and $5 \wedge 6$ are collinear.*

PROOF. (i): In $\boldsymbol{P}$ the lines $a \vee b$, 1, and 4 are concurrent, since they are the mutual intersections of three planes in $\mathbb{R}^3$. If furthermore $1 \wedge 4$, $2 \wedge 3$, and $5 \wedge 6$ are collinear, then a, b, $(2 \wedge 3)$, and $(5 \wedge 6)$ are coplanar. Therefore the lines $(2 \wedge 3) \vee a$ and $(5 \wedge 6) \vee b$ meet in a point which we call $\boldsymbol{q}_y$. The cocircuits of $\boldsymbol{P} \cup \{\boldsymbol{q}_y\}$ in the above construction that contain $\boldsymbol{q}_y$ are uniquely determined up to reorientation of the point $\boldsymbol{q}_y$. By Lemma 3.3.3 this uniquely determines the face lattice of $\boldsymbol{X}$ (up to relabeling).

(ii): Conversely, if $\boldsymbol{Y}$ is a realization of $\boldsymbol{X}$ we can reconstruct a corresponding point $\boldsymbol{q}_y$ on the lines $(2 \wedge 3) \vee a$ and $(5 \wedge 6) \vee b$ using Lemma 3.3.5. This implies that $(2 \wedge 3)$, $(5 \wedge 6)$, a and b are coplanar. By the concurrence of $a \vee b$, 1, and 4 this implies the theorem.   □
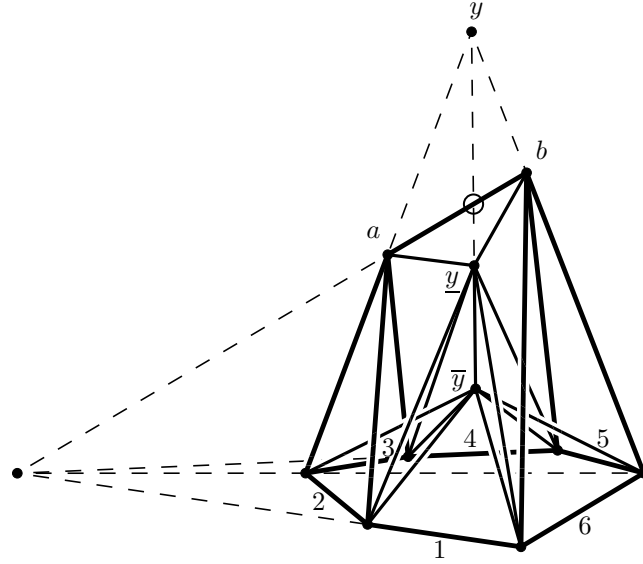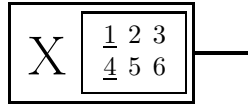
Figure 5.4.1: A 4-polytope with non-prescribable 2-face.

This solves Problem 6.11 in [65] where it was asked whether a 4-polytope with non-prescribable 2-face exists.

In particular, the polytope $\boldsymbol{X} = \boldsymbol{X}(1,2,3,4,5,6)$ contains a pyramid over the hexagon $\boldsymbol{G}(1,2,3,4,5,6)$ along which we may perform the gluing. In our diagrams the polytope $\boldsymbol{X}(1,\ldots,6)$ is represented by the box:


The letters $1,\ldots,6$ are labels of the edges of $\boldsymbol{G}(1,\ldots,6)$ in cyclic order. This representation is considered sensitive in the underlining of the points. In the polytope represented by the above box, we assume that $1 \wedge 4$, $2 \wedge 3$ and $5 \wedge 6$ are the collinear points.

5.5 An Adapter

Our next BBB $\boldsymbol{A}_8$ is almost trivial. It is an "adapter" containing a pyramid and a tent both sharing a common 8-gon $\boldsymbol{G}_8$, which plays the rôle of the information frame. It is used to connect a BBB that possesses a tent as join to another BBB that possesses a pyramid as join. We define

$$\boldsymbol{A}_8^{a,b} = \mathbf{pyr}(\mathbf{tent}^{a,b}(\boldsymbol{G}(1,2,3,4,5,6,7,8))).$$

In our diagrams $\boldsymbol{A}_8$ is represented by the box:
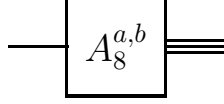
5.6   A Polytope for Partial Transmission of Information

Our fifth and last BBB $\boldsymbol{Y}_8^{1,5} = \boldsymbol{Y}(1,2,3,4,5,6,7,8)$ is also generated by
Lawrence extensions. It will be used in the composed building block that is de-
scribed in the next section. Here we describe its construction and its properties.
The polytope $\boldsymbol{Y}_8^{1,5}$ is constructed as follows.

- Start with an octagon $\boldsymbol{G}(1,\dots,8)$ where the edge-pair $(1,5)$ is parallel.
- In a plane parallel to $\boldsymbol{G}$ we choose another octagon $\boldsymbol{G}'$ such that the edge-
  pairs $(1,1')$ and $(5,5')$ meet in the same point $\boldsymbol{q}_y$.
- The convex hull $\boldsymbol{P}$ of $\boldsymbol{G}$ and $\boldsymbol{G}'$ has the combinatorial type of a prism over
  an 8-gon..
- We define $\boldsymbol{Y}_8^{1,5} = \boldsymbol{\Lambda}(\boldsymbol{P},\{\boldsymbol{q}_y\})$.

Figure 5.6.1 shows $\boldsymbol{P}$ and a Schlegel diagram of $\boldsymbol{Y}_8^{1,5}$. The information frames
of $\boldsymbol{Y}_8^{1,5}$ are the 8-gons $\boldsymbol{G}$ and $\boldsymbol{G}'$.

<u>Theorem 5.6.1.</u>

(i) *The combinatorial type of $\boldsymbol{Y}_8^{1,5}$ does not depend on the special choice of
the points in the construction.*

(ii) *In every realization of $\boldsymbol{Y}_8^{1,5}$, supporting lines of the edges $1, 1', 5$ and $5'$ meet
in a point.*

Proof. (i): Again, the Lawrence equivalence class of $(\boldsymbol{P},\{\boldsymbol{q}_y\})$ is uniquely de-
termined by the construction. By Lemma 3.3.3 this uniquely determines the face
lattice of $\boldsymbol{Y}_8^{1,5}$ (up to relabeling).

(ii): Conversely, if $\boldsymbol{Y}$ is a realization of $\boldsymbol{Y}_8^{1,5}$, we can reconstruct by Lemma 3.3.5
a corresponding point $\boldsymbol{q}_y$. This implies the theorem.   □
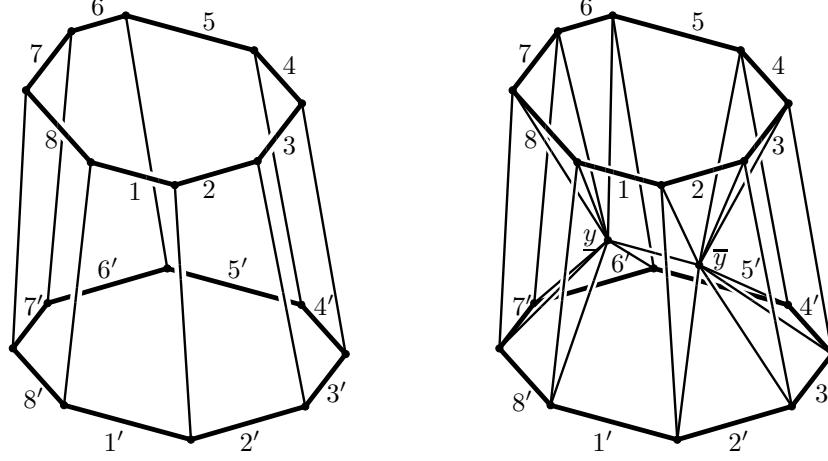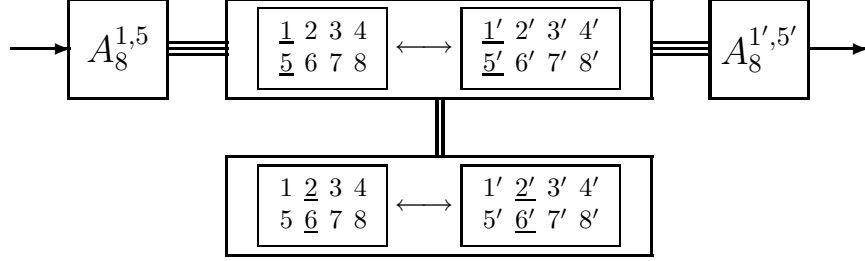
Figure 5.6.1: A "slope transmitter."

Observe that $\mathbf{tent}^{1,5}(\boldsymbol{G})$, $\mathbf{tent}^{1',5'}(\boldsymbol{G}')$ as well as the prism formed by $\boldsymbol{G}$ and $\boldsymbol{G}'$ are facets of $\boldsymbol{Y}_8^{1,5}$. In our diagrams the polytope $\boldsymbol{Y}_8^{1,5}$ is represented by the box:
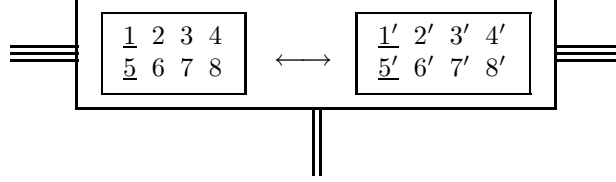
The letters $1, \ldots, 8$ are labels of the edges of $\boldsymbol{G}(1, \ldots, 8)$ in cyclic order. This representation is considered sensitive in the underlining of the points.

5.7 A Transmitter for Line Slopes

Our final (composed) building block $\boldsymbol{O}_8$ will be used to transmit projective conditions from one 8-gon $\boldsymbol{G} = \boldsymbol{G}(1, \ldots, 8)$ to another 8-gon $\boldsymbol{G}' = \boldsymbol{G}(1', \ldots, 8')$, thereby only transferring the information on the line slopes, while "forgetting" the concrete position of the edges. The polytope $\boldsymbol{O}_8$ is composed from two polytopes $\boldsymbol{Y}_8^{1,5}$ and $\boldsymbol{Y}_8^{2,6}$ and two adapters. The two polytopes $\boldsymbol{Y}_8^{1,5}$ and $\boldsymbol{Y}_8^{2,6}$ are joined along their prism, the adapters are glued to the tents $\mathbf{tent}^{1,5}(\boldsymbol{G})$ and $\mathbf{tent}^{1',5'}(\boldsymbol{G}')$ of $\boldsymbol{Y}_8^{1,5}$. The following diagram schematically describes the construction of $\boldsymbol{O}_8$:

$$
\begin{array}{ccc}
\rightarrow \boxed{A_8^{1,5}} & \boxed{\begin{array}{c} \underline{1}\ 2\ 3\ 4 \\ \underline{5}\ 6\ 7\ 8 \end{array} \longleftrightarrow \begin{array}{c} \underline{1'}\ 2'\ 3'\ 4' \\ \underline{5'}\ 6'\ 7'\ 8' \end{array}} & \boxed{A_8^{1',5'}} \rightarrow \\
& \boxed{\begin{array}{c} 1\ \underline{2}\ 3\ 4 \\ 5\ \underline{6}\ 7\ 8 \end{array} \longleftrightarrow \begin{array}{c} 1'\ \underline{2'}\ 3'\ 4' \\ 5'\ \underline{6'}\ 7'\ 8' \end{array}} &
\end{array}
$$

By construction the polytope $\boldsymbol{O}_8$ contains two octagonal 2-faces $\boldsymbol{G} = \boldsymbol{G}(1,\ldots,8)$ and $\boldsymbol{G}' = \boldsymbol{G}(1',\ldots,8')$. The main properties of $\boldsymbol{O}_8$ are summarized in the following theorem.

<u>THEOREM 5.7.1.</u>

(i) *If $\boldsymbol{G} = \boldsymbol{G}(1,\ldots,8)$ and $\boldsymbol{G}' = \boldsymbol{G}(1',\ldots,8')$ are two parallel 8-gons satisfying*

$$1 \wedge 5 = 1' \wedge 5', \quad 2 \wedge 6 = 2' \wedge 6', \quad 3 \wedge 7 = 3' \wedge 7', \quad 4 \wedge 8 = 4' \wedge 8',$$

then $\boldsymbol{G}$ and $\boldsymbol{G}'$ can be simultaneously chosen as the corresponding 8-gons of a realization of $\boldsymbol{O}_8$.
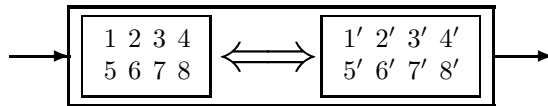
(ii) *If in a realization of $\boldsymbol{O}_8$ the intersections $A = (1 \wedge 5, 2 \wedge 6, 3 \wedge 7, 5 \wedge 8)$ of opposite edges of $\boldsymbol{G}$ are collinear, then we have*

$$1 \wedge 5 = 1' \wedge 5', \quad 2 \wedge 6 = 2' \wedge 6', \quad 3 \wedge 7 = 3' \wedge 7', \quad 4 \wedge 8 = 4' \wedge 8'.$$

PROOF. <u>(i)</u>: Assume that $\boldsymbol{G}$ and $\boldsymbol{G}'$ satisfy the hypotheses of (i). By Theorem 5.6.1(i) the convex hull of $\boldsymbol{G}$ and $\boldsymbol{G}'$ can be completed to realizations $\boldsymbol{P}_1$ and $\boldsymbol{P}_2$ of $\boldsymbol{Y}_8^{1,5}$ and $\boldsymbol{Y}_8^{2,6}$, respectively. By Lemma 3.2.4 the polytopes $\boldsymbol{P}_1$ and $\boldsymbol{P}_2$ can be composed using a connected sum operation along the prism. Applying Lemma 3.2.4 again, the resulting polytopes can be glued with suitable adapters to end up with a realization of $\boldsymbol{O}_8$.

<u>(ii)</u>: If in a realization of $\boldsymbol{P}_O$ the intersections $A = (1 \wedge 5, 2 \wedge 6, 3 \wedge 7, 5 \wedge 8)$ of opposite edges of $\boldsymbol{G}$ are collinear, we may w.l.o.g transform the points in A to infinity by a projective transformation. Applying Lemma 5.6.1(ii) we have $1 \wedge 5 = 1' \wedge 5'$ and $2 \wedge 6 = 2' \wedge 6'$. Hence the octagon $\boldsymbol{G}'$ is parallel to $\boldsymbol{G}$. The fact that $\boldsymbol{G} \cup \boldsymbol{G}'$ defines a combinatorial prism proves that, after this projective transformation, $\boldsymbol{G}$ and $\boldsymbol{G}'$ have identical edge slopes.   □

By this construction the polytope $\boldsymbol{O}_8$ contains two facets $\mathbf{pyr}(\boldsymbol{G})$ and $\mathbf{pyr}(\boldsymbol{G}')$. In the diagrams $\boldsymbol{O}_8$ is represented by the box:

$$
\rightarrow \boxed{\boxed{\begin{array}{c} 1\ 2\ 3\ 4 \\ 5\ 6\ 7\ 8 \end{array}} \Longleftrightarrow \boxed{\begin{array}{c} 1'\ 2'\ 3'\ 4' \\ 5'\ 6'\ 7'\ 8' \end{array}}} \rightarrow
$$

6   Harmonic Sets and Octagons

In this section, we will construct a polytope $\boldsymbol{H}(1,\ldots,8)$ that contains an octagonal 2-face $\boldsymbol{G} = \boldsymbol{G}(1,\ldots,8)$ whose shape cannot be prescribed arbitrarily. In every realization of $\boldsymbol{H}$ the intersections

$$A = \{1 \wedge 5,\ 2 \wedge 6,\ 3 \wedge 7,\ 4 \wedge 8\}$$

of opposite sides of $\mathcal{O}$ are collinear (with supporting line ℓ). Furthermore, these four points of intersection form a harmonic set, i.e.

$$(1 \wedge 5, 3 \wedge 7 \mid 2 \wedge 6, 4 \wedge 8) \ = \ -1.$$

6.1   A Line Configuration Forcing Harmonic Relations

Consider an 8-gon $\boldsymbol{G} = \boldsymbol{G}(1,\ldots,8)$ for which the supporting lines of the edges satisfy the following seven 3-point collinearities:

$$(1 \wedge 5, 8 \wedge 7, 2 \wedge 3),\ (1 \wedge 5, 7 \wedge 6, 3 \wedge 4),\ (3 \wedge 7, 2 \wedge 1, 4 \wedge 5),$$

$$(2 \wedge 5, 3 \wedge 4, 8 \wedge 7),\ (4 \wedge 1, 2 \wedge 3, 7 \wedge 6),\ (6 \wedge 1, 3 \wedge 4, 8 \wedge 7),\ (8 \wedge 5, 2 \wedge 3, 7 \wedge 6)$$
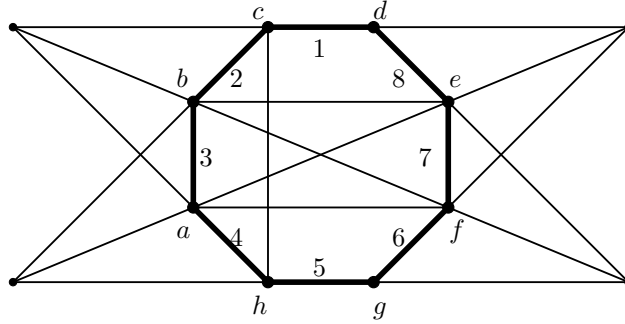

Figure 6.1.1: An incidence configuration that forces harmonic line slopes.

LEMMA 6.1.1. *An 8-gon $\boldsymbol{G}$ satisfying the collinearities described above is normal (i.e. the meets of opposite sides are collinear). After pre-standardization the slopes s_1, s_2, s_3, s_4 of the edges $1, 2, 3, 4$ satisfy $(s_1, s_3 | s_2, s_4) = -1$.*

PROOF. We embed $\boldsymbol{G}$ into the euclidean plane $\mathbb{R}^2$ and use homogeneous coordinates. A euclidean point (x, y) is represented by the vector $(x, y, 1) \in \mathbb{R}^3$. A euclidean line $\{(x, y) \mid ax + by + d = 0\}$ is represented by the vector $(a, b, d) \in \mathbb{R}^3$. Then both the *meet* operation "$\vee$" and the *join* operation "$\wedge$" are carried out by the standard *cross-product* in $\mathbb{R}^3$.

Up to projective equivalence we may assume that the lines $1, 3, 5$ and 7 are given by the equations $y = 1$, $x = -1$, $y = -1$ and $x = 1$, respectively (i.e. they are given by the coordinate vectors $((0, 1, -1)$, $(1, 0, -1)$, $(0, -1, -1)$ and $(-1, 0, -1))$. We assume that the vertices are labeled as shown in Figure 6.1.1. The collinearity $(1 \wedge 5, 7 \wedge 6, 3 \wedge 4)$ forces the join of the points a and f to be parallel to the x-axis. Similarly $(1 \wedge 5, 8 \wedge 7, 2 \wedge 3)$ implies that the join of the points b and e is parallel to the x-axis. We set

$$a = (-1, w, 1), \ b = (-1, x, 1), \ e = (1, x, 1), \ f = (1, w, 1)$$

with $-1 < w < x < 1$. Using the collinearities $(2 \wedge 5, 3 \wedge 4, 8 \wedge 7)$ and $(4 \wedge 1, 2 \wedge 3, 7 \wedge 6)$ we compute

$$c = 1 \wedge (b \vee (5 \wedge (a \vee e))) \quad \text{and} \quad h = 5 \wedge (a \vee (1 \wedge (b \vee f))).$$

Since the line $c \vee h$ has to be parallel to the y-axis, the second entry α of the vector $c \vee h$ must be zero. Inserting the coordinates of the points a, b, e and f we obtain (up to an integral factor)

$$\alpha = (w - 1)(w^2 - w^2 x - x^2 + x^3)$$

From $\alpha = 0$ and $-1 < w < x < 1$, we have

$$\alpha = 0 \quad \Longrightarrow \quad w^2(1 - x) = x^2(1 - x) \quad \Longrightarrow \quad 0 < x = -w < 1.$$

Since by this the points a and b lie symmetrically about the x-axis the construction implies that $\boldsymbol{G}$ is symmetric with respect to both coordinate axes. This implies that the line pairs $(4, 8)$ and $(2, 6)$ are parallel and that the slopes are in harmonic relation.   □

REMARK 6.1.2. The construction implies that the point c can be represented by homogeneous coordinates

$$c = (\ \frac{1 - 3x}{x + x^2}, \ 1, \ 1\ ).$$

Since (as a consequence of the symmetry) the first entry of this vector must lie between 0 and 1, we get realizations of $\boldsymbol{G}$ for a parameter range $x \in \ ]\frac{1}{3}, 1[$.

6.2   The Harmonic Polytope

In this section, we construct a polytope $\boldsymbol{H}(1, \ldots, 8)$ that has an octagonal 2-face $\mathcal{O} = \boldsymbol{G}(1, \ldots, 8)$. A construction diagram is presented below. The main properties of $\boldsymbol{H}(1, \ldots, 8)$ are collected in the following lemma.
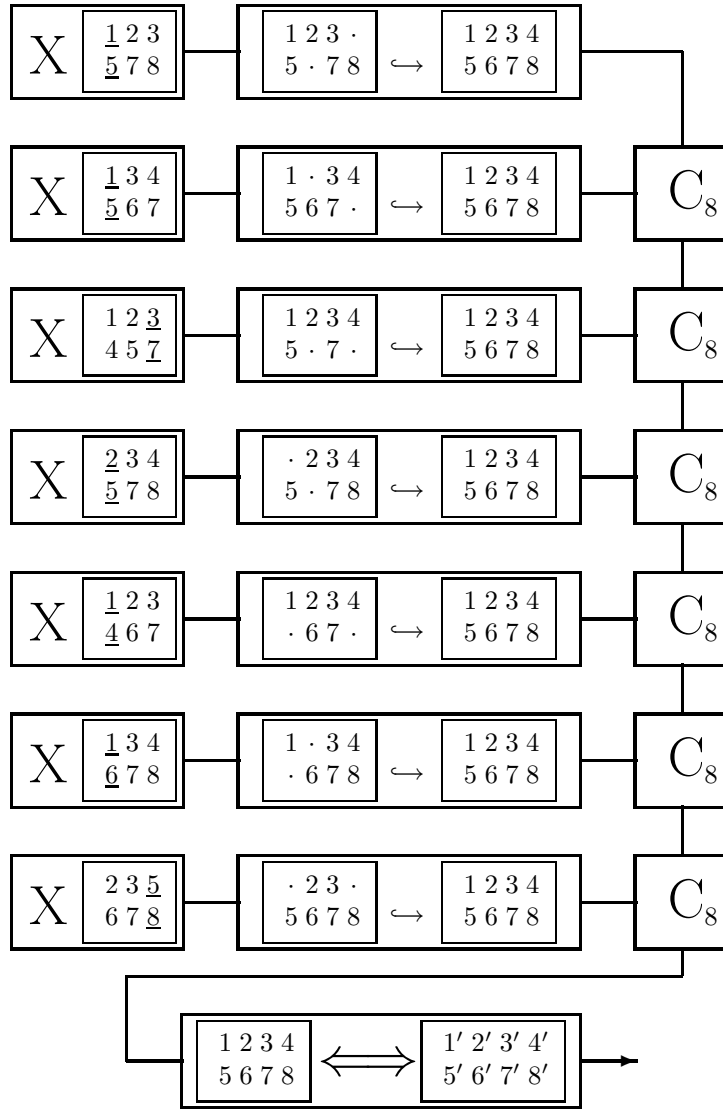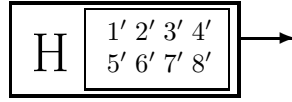
<u>LEMMA 6.2.1.</u>

(i) *In every realization of $\boldsymbol{H}(1,\ldots,8)$ the octagon $\mathcal{O}$ is normal.*

(ii) *If $\mathcal{O}$ is pre-standardized by a projective transformation, then we have $(s_1, s_3 | s_2, s_4) = -1$.*

(iii) *Every normal, pre-standardized octagon $\mathcal{O}$ with $(s_1, s_3 | s_2, s_4) = -1$ can be completed to a realization of $\boldsymbol{H}$.*

CONSTRUCTION AND PROOF. The polytope $\boldsymbol{H}(1',\ldots,8')$ is constructed by gluing basic building blocks according to the scheme given on the previous page. We construct a relabeled polytope with labels $1',\ldots,8'$ instead of $1,\ldots,8$. The seven $\boldsymbol{X}$-polytopes involved in the construction contain six different hexagons:

$$
\begin{aligned}
h_1 &= \boldsymbol{G}(\underline{1}, 2, 3, \underline{5}, 7, 8), \\
h_2 &= \boldsymbol{G}(\underline{1}, 3, 4, \underline{5}, 6, 7), \\
h_3 &= \boldsymbol{G}(\underline{3}, 4, 5, \underline{7}, 1, 2), \\
h_4 &= \boldsymbol{G}(\underline{2}, 3, 4, \underline{5}, 7, 8), \\
h_5 &= \boldsymbol{G}(\underline{1}, 2, 3, \underline{4}, 6, 7), \\
h_6 &= \boldsymbol{G}(\underline{1}, 3, 4, \underline{6}, 7, 8), \\
h_7 &= \boldsymbol{G}(\underline{5}, 6, 7, \underline{8}, 2, 3).
\end{aligned}
$$

The fact that they are $\boldsymbol{X}$-polytopes implies that collinearities corresponding to Theorem 5.4.1 occur. By suitable transmitters $\boldsymbol{T}_{h_i}^{(1,2,\ldots,8)}$ and connectors $\boldsymbol{C}_8$ the $\boldsymbol{X}$-polytopes are glued at (several copies of) a central 8-gon $\boldsymbol{G}(1,\ldots,8)$ while keeping the labeling consistent. This encodes exactly the incidence configuration of Lemma 6.1.1. Hence $\boldsymbol{G}(1,\ldots,8)$ is normal and after standardization the slopes are in harmonic position. We will call the construction up to this point $\boldsymbol{H}'(1,\ldots,8)$. Finally, the slopes of this 8-gon are transmitted to a octagon $\boldsymbol{G}(1',\ldots,8')$ by an $\boldsymbol{O}_8$-polytope. By Theorem 3.5.1 this 8-gon has the desired properties. This proves (i) and (ii).

For (iii) consider any octagon $\mathcal{O}' = (1',\ldots,8')$ that satisfies the conditions of (i) and (ii). Furthermore, consider any realization of $\boldsymbol{H}'(1,\ldots,8)$ containing the normal octagon $\mathcal{O}$ with slopes in harmonic position. By Theorem 5.3.1 there exists a polytope $\boldsymbol{O}$ such that the two contained octagons are projectively equivalent to $\mathcal{O}$ and $\mathcal{O}'$, respectively. By Lemma 3.2.4 we can perform a connected sum operation of $\mathcal{O}$ and $\boldsymbol{H}'(1,\ldots,8)$ to create the desired polytope. □

H | 1′ 2′ 3′ 4′ 5′ 6′ 7′ 8′ →

X | 1̲ 2 3 / 5̲ 7 8 — 1 2 3 · / 5 · 7 8 ↪ 1 2 3 4 / 5 6 7 8

X | 1̲ 3 4 / 5̲ 6 7 — 1 · 3 4 / 5 6 7 · ↪ 1 2 3 4 / 5 6 7 8 — C₈

X | 1 2 3̲ / 4 5 7̲ — 1 2 3 4 / 5 · 7 · ↪ 1 2 3 4 / 5 6 7 8 — C₈

X | 2̲ 3 4 / 5̲ 7 8 — · 2 3 4 / 5 · 7 8 ↪ 1 2 3 4 / 5 6 7 8 — C₈

X | 1̲ 2 3 / 4̲ 6 7 — 1 2 3 4 / · 6 7 · ↪ 1 2 3 4 / 5 6 7 8 — C₈

X | 1̲ 3 4 / 6̲ 7 8 — 1 · 3 4 / · 6 7 8 ↪ 1 2 3 4 / 5 6 7 8 — C₈

X | 2 3 5̲ / 6 7 8̲ — · 2 3 · / 5 6 7 8 ↪ 1 2 3 4 / 5 6 7 8 — C₈

1 2 3 4 / 5 6 7 8 ⟷ 1′ 2′ 3′ 4′ / 5′ 6′ 7′ 8′ →

7   Polytopes for Addition and Multiplication

In this section we describe polytopes that model addition and multiplication of real numbers by the non-prescribability of a normal $2n$-gon (computation frame) in a polytope. Recall that we denote the doubled sequence $(a, b, \ldots, z, a', b', \ldots, z')$ by $[a, b, \ldots, z]$.

7.1   Addition

We first describe the *addition polytopes*. We have to distinguish the two cases of modeling the equation $x + y = z$ with $x < y$, and the equation $x + x = z$, since in the second case the two summands are represented by the same edge pair of the computation frame.

As the polytope $\boldsymbol{P}^{2x}[\boldsymbol{0}, x, 2x, \boldsymbol{\infty}]$ that models $x + x = z$ we can simply take the harmonic polytope $\boldsymbol{H}[\boldsymbol{0}, x, 2x, \boldsymbol{\infty}]$, since

$$(0, 2x | x, \infty) = (0 - x)/(2x - x) = -1$$

holds for all $x > 0$. Observe that, since if we have $0 < x$, the sequence $0 < x < 2x < \infty$ has an order consistent with the order of the labeling of the computation frame. This allows us to define

$$\boldsymbol{P}^{2x}[\boldsymbol{0}, x, 2x, \boldsymbol{\infty}] := \boldsymbol{H}[\boldsymbol{0}, x, 2x, \boldsymbol{\infty}].$$

A construction diagram for the polytope $\boldsymbol{P}^{x+y}[\boldsymbol{0}, x, y, x+y, \boldsymbol{\infty}]$ modeling $x + y = z$ for $0 < x < y$ is given on the next page. Two harmonic polytopes

$$\boldsymbol{H}_1 = \boldsymbol{H}[x, \frac{x+y}{2}, y, \boldsymbol{\infty}] \quad \text{and} \quad \boldsymbol{H}_2 = \boldsymbol{H}[\boldsymbol{0}, \frac{x+y}{2}, x+y, \boldsymbol{\infty}]$$

are joined to a 12-gon

$$\boldsymbol{G} = \boldsymbol{G}[0, x, \frac{x+y}{2}, y, x+y, \infty]$$

using transmitters and connectors. Observe that $0 < x < y$ implies that

$$0 < x < \frac{x+y}{2} < y < x+y < \infty,$$

hence the order is consistent with the order of the edges of $\boldsymbol{G}_{12}$. Finally, a forgetful transmitter is used to delete the slope of the edge pair labeled $\frac{x+y}{2}$ and to transfer the result to a 10-gon $\boldsymbol{G}[\boldsymbol{0}, x, y, x+y, \boldsymbol{\infty}]$.

Theorem 7.1.1.

(i) *In every realization of $\boldsymbol{P}^{x+y}[\boldsymbol{0}, x, y, x+y, \boldsymbol{\infty}]$ the 10-gon $\boldsymbol{G}[\boldsymbol{0}, x, y, x+y, \boldsymbol{\infty}]$ is a normal computation frame. After standardization the slopes satisfy $s_x + s_y = s_{x+y}$.*

(ii) *Conversely, every standardized 10-gon $\boldsymbol{G}[\boldsymbol{0}, x, y, x+y, \boldsymbol{\infty}]$ satisfying $s_x + s_y = s_{x+y}$ can be completed to a realization of $\boldsymbol{P}^{x+y}[\boldsymbol{0}, x, y, x+y, \boldsymbol{\infty}]$.*

Proof. (i): Consider a realization of $\boldsymbol{P}^{x+y}[\boldsymbol{0}, x, y, x+y, \boldsymbol{\infty}]$, and assume that after standardization of $\boldsymbol{G}[\boldsymbol{0}, x, y, x+y, \boldsymbol{\infty}]$ the slopes s_x and s_y are given. The central 12-gon $\boldsymbol{G}[\boldsymbol{0}, x, \frac{x+y}{2}, y, x+y, \boldsymbol{\infty}]$ is called $\boldsymbol{G}'$. Via $\boldsymbol{G}'$ these slopes are transferred to the $\boldsymbol{H}$-polytopes $\boldsymbol{H}_1 = \boldsymbol{H}[x, \frac{x+y}{2}, y, \boldsymbol{\infty}]$ and $\boldsymbol{H}_2 = \boldsymbol{H}[\boldsymbol{0}, \frac{x+y}{2}, x+y, \boldsymbol{\infty}]$. By Lemma 6.2.1, H_1 determines the slope $s_{\frac{x+y}{2}}$ to be $\frac{x+y}{2}$ since $(x, y|z, \infty) = -1$ has the unique solution $z = \frac{x+y}{2}$. Similarly $\boldsymbol{H}_2$ determines the slope s_{x+y}, since $(0, z|\frac{x+y}{2}, \infty) = -1$ has the unique solution $z = x+y$. This proves (i).

(ii): For $0 < x < y$ consider a standardized computation frame $\boldsymbol{G} = \boldsymbol{G}[\boldsymbol{0}, x, y, x+y, \boldsymbol{\infty}]$ with line slopes

$$s_0 = 0, \; s_x = x, \; s_y = y, \; s_{x+y} = x + y, \; s_\infty = \infty.$$

Furthermore, consider a 12-gon $\boldsymbol{G}' = \boldsymbol{G}[\boldsymbol{0}, x, \frac{x+y}{2}, y, x + y, \boldsymbol{\infty}]$ that is obtained from $\boldsymbol{G}$ by introducing a new pair of parallel edges labeled $\frac{x+y}{2}$. For each of the "boxes" (= sub-polytopes) of our diagram, we provide a realization where the 2-faces along which the gluing is performed are obtained by deleting edges of $\boldsymbol{G}'$. Such realizations do exist according to Lemma 6.2.1(iii) and Theorem 5.2.1. Lemma 3.2.4 shows that these realizations can be composed by connected sum operations to form a realization of

$$\boldsymbol{P}^{x+y}[\boldsymbol{0}, x, y, x + y, \boldsymbol{\infty}].$$

This proves part (ii) of the theorem.   □

$$\mathrm{P}^{x+y} \left[\begin{array}{ccccc} 0 & x & y & x+y & \infty \end{array}\right] \longrightarrow$$

$$\mathrm{H} \left[\begin{array}{cccc} x & \frac{x+y}{2} & y & \infty \end{array}\right]$$

$$\left[\begin{array}{ccccc} \cdot & x & \frac{x+y}{2} & y & \cdot & \infty \end{array}\right]$$
$$\hookrightarrow$$
$$\left[\begin{array}{ccccc} 0 & x & \frac{x+y}{2} & y & x+y & \infty \end{array}\right]$$

$$\mathrm{H} \left[\begin{array}{cccc} 0 & \frac{x+y}{2} & x+y & \infty \end{array}\right]$$

$$\left[\begin{array}{ccccc} 0 & \cdot & \frac{x+y}{2} & \cdot & x+y & \infty \end{array}\right]$$
$$\hookrightarrow$$
$$\left[\begin{array}{ccccc} 0 & x & \frac{x+y}{2} & y & x+y & \infty \end{array}\right]$$

$$\mathrm{C}_{12}$$

$$\left[\begin{array}{ccccc} 0 & x & \frac{x+y}{2} & y & x+y & \infty \end{array}\right]$$
$$\hookrightarrow$$
$$\left[\begin{array}{ccccc} 0 & x & \cdot & y & x+y & \infty \end{array}\right] \longrightarrow$$
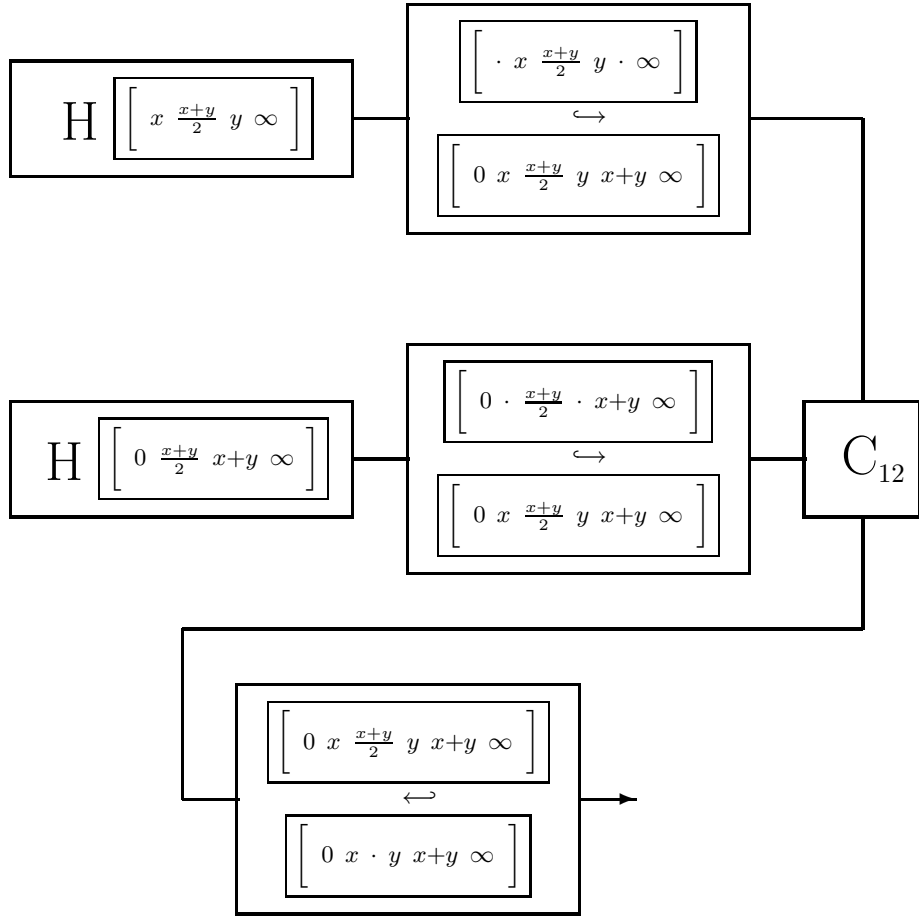
7.2 Multiplication

In a similar way we will construct *multiplication polytopes*. We have to distinguish the two cases of modeling the equation $x \cdot y = z$ with $x < y$ and the equation $x \cdot x = z$, since in the second case the two factors are represented by the same edge pair of the computation frame.

The polytope for $x \cdot x = z$ is constructed by gluing harmonic polytopes that model the operation. Eventually intermediate "indeterminants" are deleted by suitable forgetful transmitters. A construction diagram for the polytope

$$\boldsymbol{P}^{x^2}[\boldsymbol{0}, \boldsymbol{1}, x, x^2, \boldsymbol{\infty}]$$

is given on the next page. We have a theorem similar to Theorem 7.1.1:

THEOREM 7.2.1.

(i) *In every realization of* $\boldsymbol{P}^{x^2}[\boldsymbol{0}, \boldsymbol{1}, x, x^2, \boldsymbol{\infty}]$ *the 10-gon* $\boldsymbol{G}[\boldsymbol{0}, \boldsymbol{1}, x, x^2, \boldsymbol{\infty}]$ *is a normal computation frame. After standardization the slopes satisfy* $s_x^2 = s_{x^2}$.

(ii) *Conversely, every standardized 10-gon* $\boldsymbol{G}[\boldsymbol{0}, \boldsymbol{1}, x, x^2, \boldsymbol{\infty}]$ *satisfying* $s_x = s_{x^2}^2$ *can be completed to a realization of* $\boldsymbol{P}^{x^2}[\boldsymbol{0}, \boldsymbol{1}, x, x^2, \boldsymbol{\infty}]$.

PROOF. First observe that $1 < x < \infty$ implies

$$-x < 0 < 1 < x < x^2 < \infty,$$

therefore all occurring n-gons are consistently ordered.

The harmonic polytope $\boldsymbol{H}[-x, 0, x, \infty]$ uniquely determines the slope of the edge pair labeled by $-x$. We get $s_{-x} = -s_x$. The harmonic polytope $\boldsymbol{H}[-x, 1, x, x^2]$ uniquely determines the slope of the edge pair labeled by x^2. We then have $s_{x^2} = -s_x^2$. This is a consequence of the equation

$$(-x, x | 1, x^2) = \frac{(-x - 1)(x - x^2)}{(-x - x^2)(x - 1)} = \frac{-x + x^3}{x - x^3} = -1.$$

The rest of the proof is completely analogous to the proof of Theorem 7.1.1 and will not be repeated here. □

$$\mathrm{P}^{x^2} \left[\ 0\ 1\ x\ x^2\ \infty\ \right] \longrightarrow$$

$$\mathrm{H}\left[\ -x\ 0\ x\ \infty\ \right]$$

$$\left[\ -x\ 0\ \cdot\ x\ \cdot\ \infty\ \right]$$
$$\hookrightarrow$$
$$\left[\ -x\ 0\ 1\ x\ x^2\ \infty\ \right]$$

$$\mathrm{H}\left[\ -x\ 1\ x\ x^2\ \right]$$

$$\left[\ -x\ \cdot\ 1\ x\ x^2\ \cdot\ \right]$$
$$\hookrightarrow$$
$$\left[\ -x\ 0\ 1\ x\ x^2\ \infty\ \right]$$

$$\mathrm{C}_{12}$$

$$\left[\ -x\ 0\ 1\ x\ x^2\ \infty\ \right]$$
$$\hookleftarrow$$
$$\left[\ \cdot\ 0\ 1\ x\ x^2\ \infty\ \right] \longrightarrow$$
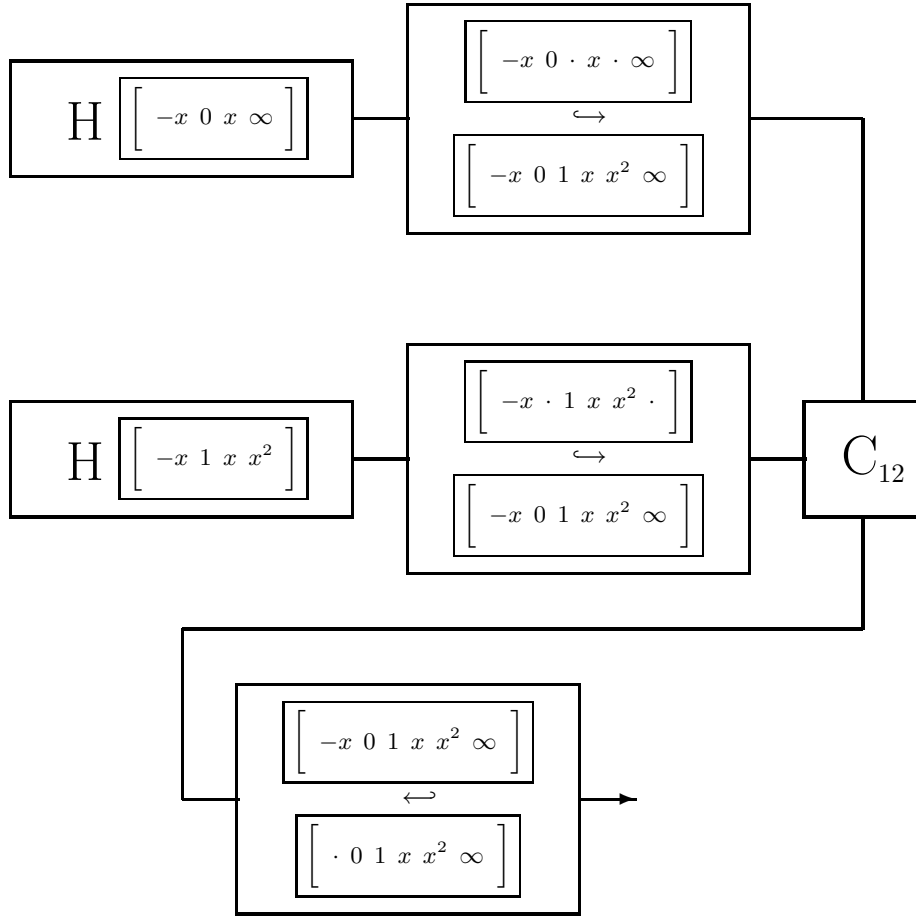
The multiplication $x \cdot y = z$ with $x < y$ is a bit more delicate. There is an analogous way of modeling this multiplication by connecting three harmonic relations. However, this computation introduces $\sqrt{x \cdot y}$ as an intermediate variable. We want to avoid this effect, since we intend to prove statements about stable equivalence which do not increase the algebraic complexity of the objects under considerations. For that reason we model the multiplication $x \cdot y = z$ by first squaring x and y (using polytopes $\boldsymbol{P}^{x^2}$) and then calculating $x \cdot y = \sqrt{x^2 \cdot y^2}$. We have to take some care which intermediate variables are simultaneously stored in an n-gon (computation frame), since we have no control on the linear order of the variables y and x^2.

The construction for the polytope

$$\boldsymbol{P}^{x \cdot y}[\boldsymbol{0}, \boldsymbol{1}, x, y, x \cdot y, \boldsymbol{\infty}]$$

is cut into two pieces and is represented on the following two pages. The first page describes the construction of a polytope

$$\boldsymbol{P}^{\sqrt{x^2 \cdot y^2}}[\boldsymbol{0}, \boldsymbol{1}, x^2, x \cdot y, y^2, \boldsymbol{\infty}]$$

that is used as a building block on the second page.

THEOREM 7.2.2.

(i) *In every realization of $\boldsymbol{P}^{x \cdot y}[\boldsymbol{0}, \boldsymbol{1}, x, y, x \cdot y, \boldsymbol{\infty}]$ the 12-gon $\boldsymbol{G}[\boldsymbol{0}, \boldsymbol{1}, x, y, x \cdot y, \boldsymbol{\infty}]$ is a normal computation frame. After standardization the slopes satisfy $s_x \cdot s_y = s_{x \cdot y}$.*

(ii) *Conversely, every standardized 12-gon $\boldsymbol{G}[\boldsymbol{0}, \boldsymbol{1}, x, y, x \cdot y, \boldsymbol{\infty}]$ satisfying $s_x \cdot s_y = s_{x \cdot y}$ can be completed to a realization of $\boldsymbol{P}^{x \cdot y}[\boldsymbol{0}, \boldsymbol{1}, x, y, x \cdot y, \boldsymbol{\infty}]$.*

PROOF. We first analyze the polytope $\boldsymbol{P}^{\sqrt{x^2 \cdot y^2}}[\boldsymbol{0}, \boldsymbol{1}, x^2, x \cdot y, y^2, \boldsymbol{\infty}]$. For this we assume that $1 < x^2 < y^2 < \infty$. This implies that all n-gons that occur are consistently ordered.

The harmonic polytope $\boldsymbol{H}[-x \cdot y, 0, x \cdot y, \infty]$ forces the relation $s_{-x \cdot y} = -s_{x \cdot y}$. Together with this the harmonic polytope $\boldsymbol{H}[-x \cdot y, x^2, x \cdot y, y^2]$ determines the corresponding line slopes. We have

$$s_{-x \cdot y} = -x \cdot y \quad \text{and} \quad s_{x \cdot y} = x \cdot y.$$

This is a consequence of the fact that the quadratic equation

$$(x^2, y^2 | -z, z) = \frac{(x^2 + z)(y^2 - z)}{(x^2 - z)(y^2 + z)} = \frac{x^2 y^2 - x^2 z + y^2 z - z^2}{x^2 y^2 + x^2 z - y^2 z - z^2} = -1$$

has two solutions, $z_1 = xy$ and $z_2 = -xy$, and of the induced ordering on the line slopes.

By arguments similar to Theorem 7.1.1 the polytope

$$\boldsymbol{P}^{\sqrt{x^2 \cdot y^2}}[\boldsymbol{0}, \boldsymbol{1}, x^2, x{\cdot}y, y^2, \boldsymbol{\infty}]$$

determines the slopes of the join $\mathbf{pyr}([\boldsymbol{0}, \boldsymbol{1}, x^2, x{\cdot}y, y^2, \boldsymbol{\infty}])$ and every pyramid having the right slopes can be completed to a realization of $\boldsymbol{P}^{\sqrt{x^2 \cdot y^2}}$.

The polytope $\boldsymbol{P}^{\sqrt{x^2 \cdot y^2}}$ is used as a kind of "subroutine" in the construction of the polytope $\boldsymbol{P}^{x{\cdot}y}[\boldsymbol{0}, \boldsymbol{1}, x, y, x{\cdot}y, \boldsymbol{\infty}]$. We assume that $1 < x < y < \infty$. This implies

$$0 < 1 < x < y < xy < y^2 < \infty \quad \text{and} \quad 0 < 1 < x < x^2 < xy < y^2 < \infty.$$

Hence all n-gons occurring in the construction of $\boldsymbol{P}^{x{\cdot}y}$ are ordered consistently. A polytope $\boldsymbol{P}^{x^2}[\boldsymbol{0}, \boldsymbol{1}, y, y^2, \boldsymbol{\infty}]$ attached to the 14-gon $\boldsymbol{G}[\boldsymbol{0}, \boldsymbol{1}, x, y, x{\cdot}y, y^2, \boldsymbol{\infty}]$ determines the slope s_{y^2}. Then by suitable forgetful transmitters the slope of y is "forgotten" and a new variable x^2 is introduced. A polytope $\boldsymbol{P}^{x^2}[\boldsymbol{0}, \boldsymbol{1}, x, x^2, \boldsymbol{\infty}]$ attached to the 14-gon $\boldsymbol{G}[\boldsymbol{0}, \boldsymbol{1}, x, x^2, x{\cdot}y, y^2, \boldsymbol{\infty}]$ determines the slope s_{x^2}. Finally, the slope of $x{\cdot}y$ is determined by the polytope $\boldsymbol{P}^{\sqrt{x^2 \cdot y^2}}[\boldsymbol{0}, \boldsymbol{1}, x^2, x{\cdot}y, y^2, \boldsymbol{\infty}]$. The proof is completely analogous to the proof of Theorem 7.1.1 and will not be repeated here. $\square$

$$\boxed{\mathrm{P}^{\sqrt{x^2y^2}} \ \left[\ 0\ 1\ x^2\ xy\ y^2\ \infty\ \right]} \longrightarrow$$

$$\mathrm{H}\ \left[\ -xy\ 0\ xy\ \infty\ \right] \quad \begin{array}{c} \left[\ -xy\ 0\ \cdot\ \cdot\ xy\ \cdot\ \infty\ \right] \\ \hookrightarrow \\ \left[\ -xy\ 0\ 1\ x^2\ xy\ y^2\ \infty\ \right] \end{array}$$

$$\mathrm{H}\ \left[\ -xy\ x^2\ xy\ y^2\ \right] \quad \begin{array}{c} \left[\ -xy\ \cdot\ \cdot\ x^2\ xy\ y^2\ \cdot\ \right] \\ \hookrightarrow \\ \left[\ -xy\ 0\ 1\ x^2\ xy\ y^2\ \infty\ \right] \end{array} \quad \mathrm{C}_{14}$$

$$\begin{array}{c} \left[\ -xy\ 0\ 1\ x^2\ xy\ y^2\ \infty\ \right] \\ \hookleftarrow \\ \left[\ \cdot\ 0\ 1\ x^2\ xy\ y^2\ \infty\ \right] \end{array} \longrightarrow$$

$$\mathrm{P}^{x\cdot y}\ \left[\ 0\ 1\ x\ y\ xy\ \infty\ \right]\ \longrightarrow$$

$$\mathrm{P}^{\sqrt{x^2y^2}}\ \left[\ 0\ 1\ x^2\ xy\ y^2\ \infty\ \right]$$

$$\frac{[\ 0\ 1\ \cdot\ x^2\ xy\ y^2\ \infty\ ]}{\hookrightarrow}$$
$$[\ 0\ 1\ x\ x^2\ xy\ y^2\ \infty\ ]$$

$$\mathrm{P}^{x^2}\ \left[\ 0\ 1\ x\ x^2\ \infty\ \right]$$

$$\frac{[\ 0\ 1\ x\ x^2\ \cdot\ \cdot\ \infty\ ]}{\hookrightarrow}$$
$$[\ 0\ 1\ x\ x^2\ xy\ y^2\ \infty\ ]$$

$$\mathrm{C}_{14}$$

$$\frac{[\ 0\ 1\ x\ y\ xy\ y^2\ \infty\ ]}{\hookleftarrow}$$
$$[\ 0\ 1\ x\ \cdot\ xy\ y^2\ \infty\ ]$$

$$\frac{[\ 0\ 1\ x\ \cdot\ xy\ y^2\ \infty\ ]}{\hookrightarrow}$$
$$[\ 0\ 1\ x\ x^2\ xy\ y^2\ \infty\ ]$$

$$\mathrm{C}_{14}$$

$$\frac{[\ 0\ 1\ x\ y\ xy\ y^2\ \infty\ ]}{\hookleftarrow}$$
$$[\ 0\ 1\ \cdot\ y\ \cdot\ y^2\ \infty\ ]$$

$$\mathrm{P}^{x^2}\ \left[\ 0\ 1\ y\ y^2\ \infty\ \right]$$

$$\frac{[\ 0\ 1\ x\ y\ xy\ y^2\ \infty\ ]}{\hookleftarrow}$$
$$[\ 0\ 1\ x\ y\ xy\ \cdot\ \infty\ ]\ \longrightarrow$$
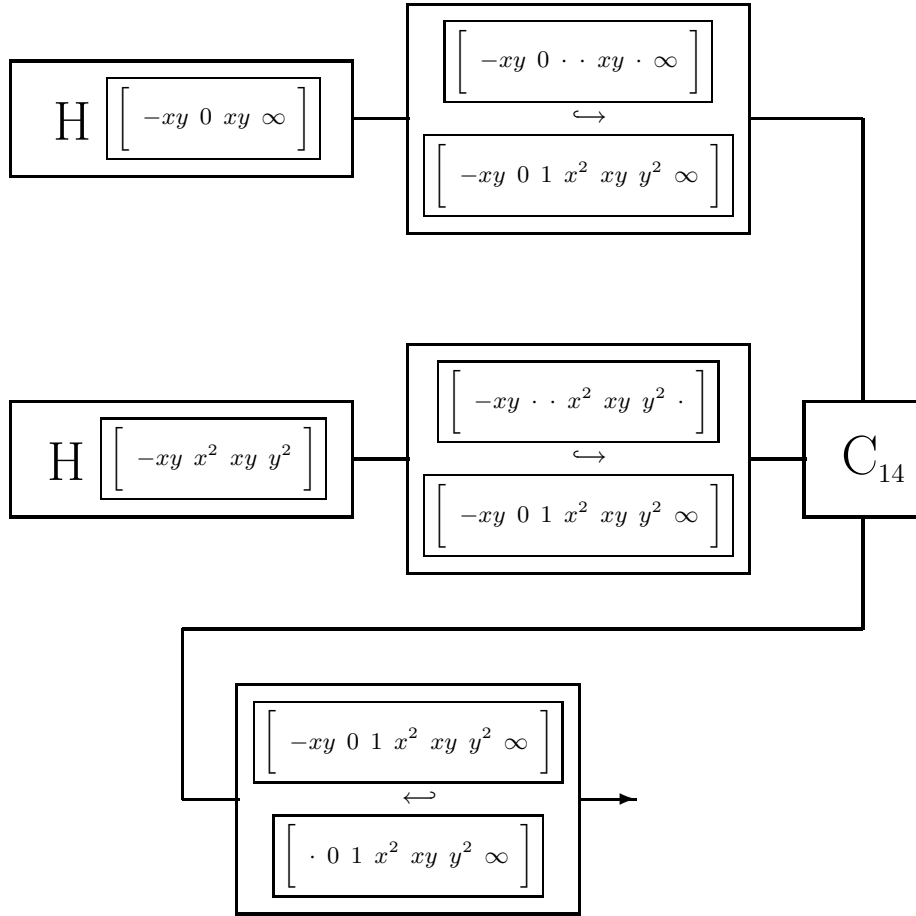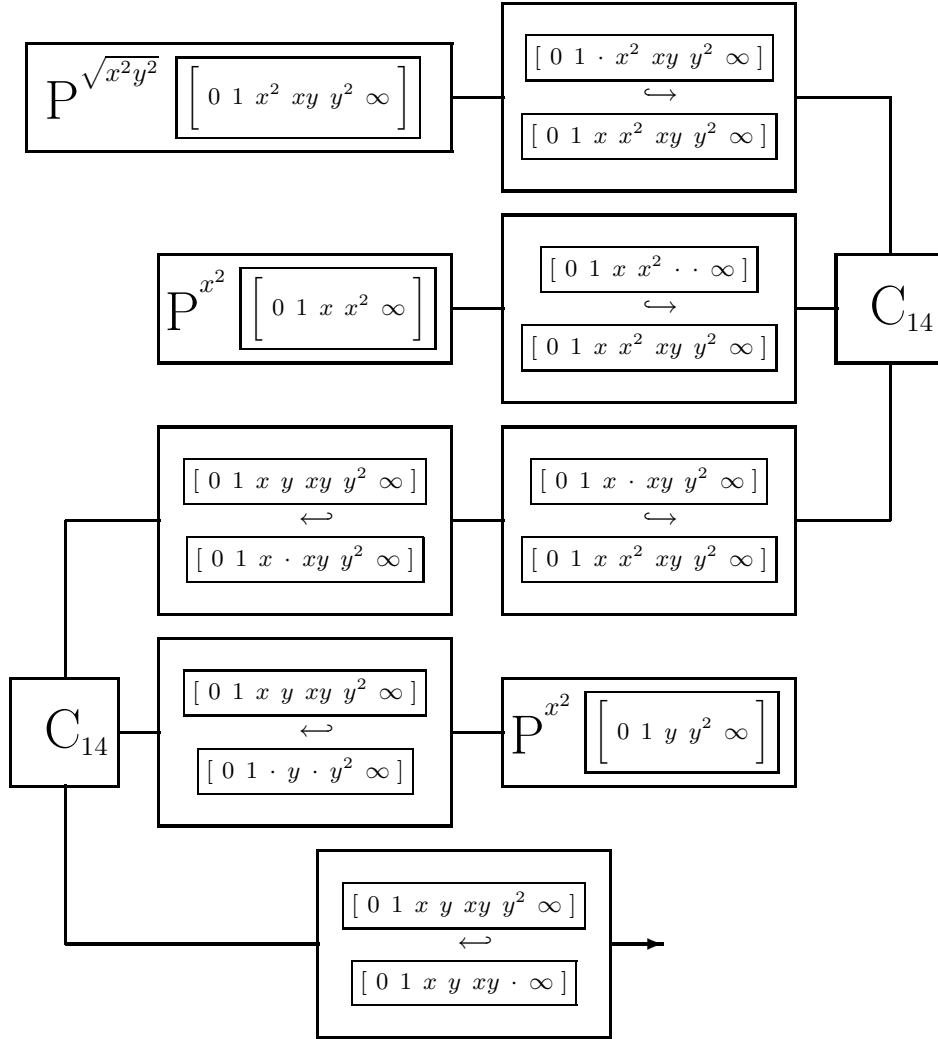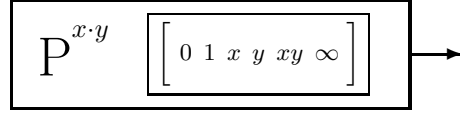
8   Putting the Pieces Together: The Universality Theorem

8.1   Encoding Semialgebraic Sets in Polytopes

So far we have managed to construct polytopes, which contain computation frames as 2-faces that model the operations $2x$, $x + y$, x^2 and $x \cdot y$. We now put these pieces together to obtain a polytope that models a given Shor normal form. Recall that a Shor normal form $\mathcal{S} = (n, \mathbf{A}, \mathbf{M})$ is given by n totally ordered variables

$$1 < x_1 < x_2 < \ldots < x_n < \infty$$

and a set of equations

$$x_i + x_j = x_k \text{ for } (i, j, k) \in \mathbf{A} \quad \text{and} \quad x_i \cdot x_j = x_k \text{ for } (i, j, k) \in \mathbf{M}.$$

We may assume that each of the variables appears at least once in an equation. Furthermore, we may assume that we have $i \leq j < k$ for $(i, j, k) \in \mathbf{A} \cup \mathbf{M}$. For a (from now on fixed) Shor normal form $\mathcal{S} = (n, \mathbf{A}, \mathbf{M})$ we set

$$X = [\mathbf{0}, \mathbf{1}, x_1, x_2, \ldots, x_n, \boldsymbol{\infty}].$$

The starting point of our construction is the doubly iterated pyramid

$$\boldsymbol{S}(\mathcal{S}) = \mathbf{pyr}(\mathbf{pyr}(\boldsymbol{G}(X))).$$

This 4-polytope $\boldsymbol{S}(\mathcal{S})$ in particular has a pyramid over the $2(n + 3)$-gon $\boldsymbol{G}(X)$ as a facet. We now produce the following collection $\mathcal{C}(\mathcal{S})$ of polytopes:

$$\left\{ \boldsymbol{P}^{2x}(Y) \;\#_{\mathbf{pyr}(Y)}\; \boldsymbol{T}_Y^X \quad \mid Y = [\mathbf{0}, x_i, x_k, \boldsymbol{\infty}], \; (i, i, k) \in \mathbf{A} \right\}$$

$$\cup \left\{ \boldsymbol{P}^{x+y}(Y) \;\#_{\mathbf{pyr}(Y)}\; \boldsymbol{T}_Y^X \;\mid Y = [\mathbf{0}, x_i, x_j, x_k, \boldsymbol{\infty}], \; (i, j, k) \in \mathbf{A} \text{ and } i \neq j \right\}$$

$$\cup \left\{ \boldsymbol{P}^{x^2}(Y) \;\#_{\mathbf{pyr}(Y)}\; \boldsymbol{T}_Y^X \quad \mid Y = [\mathbf{0}, \mathbf{1}, x_i, x_k, \boldsymbol{\infty}], \; (i, i, k) \in \mathbf{M} \right\}$$

$$\cup \left\{ \boldsymbol{P}^{x \cdot y}(Y) \;\#_{\mathbf{pyr}(Y)}\; \boldsymbol{T}_Y^X \quad \mid Y = [\mathbf{0}, \mathbf{1}, x_i, x_j, x_k, \boldsymbol{\infty}], \; (i, j, k) \in \mathbf{M} \text{ and } i \neq j \right\}$$

Each polytope $\boldsymbol{Q}_i$ in $\mathcal{C}(\mathcal{S}) = \{\boldsymbol{Q}_1, \ldots, \boldsymbol{Q}_m\}$ has a facet that is a pyramid over a $2(n+3)$-gon $\boldsymbol{G}(X)$. This facet is the "open connection" of the transmitter $\boldsymbol{T}_Y^X$ and will be called the *join* of $\boldsymbol{Q}_i$. Furthermore each of these polytopes models a particular equation of the Shor normal form by the non-prescribability of line slopes in $\boldsymbol{G}(X)$ of their join. Using $|\mathbf{A}| + |\mathbf{M}| - 1$ connectors $\boldsymbol{C}_X = \boldsymbol{C}_{2(n+3)}$ we connect all these polytopes (including $\boldsymbol{S}(\mathcal{S})$) by connected sum operations along their joins in the canonical way. The resulting polytope is called $\boldsymbol{P}(\mathcal{S})$. The following diagram illustrates the construction of $\boldsymbol{P}(\mathcal{S})$.
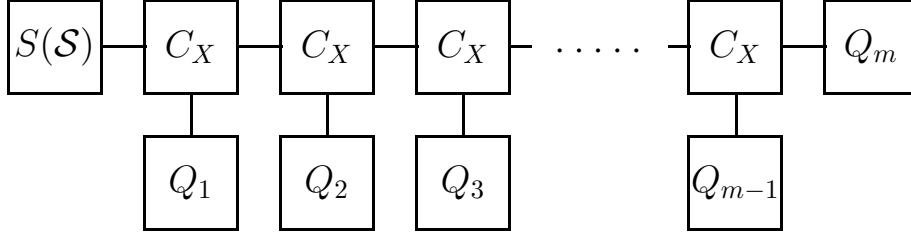
THEOREM 8.1.1. *For a given Shor normal form $\mathcal{S} = (n, \mathbf{A}, \mathbf{M})$, the polytope $\boldsymbol{P}(\mathcal{S})$ has the following properties.*

(i) *$\boldsymbol{P}(\mathcal{S})$ contains a normal computation frame $\boldsymbol{G} = \boldsymbol{G}[\mathbf{0}, \mathbf{1}, x_1, \ldots, x_n, \boldsymbol{\infty}]$.*

(ii) *For every realization of $\boldsymbol{P}(\mathcal{S})$, after standardization, the slopes of $\boldsymbol{G}$ satisfy*

$$(s_{x_1}, s_{x_2}, \ldots, s_{x_n}) \in V(\mathcal{S}).$$

(iii) *For every point $(y_1, \ldots, y_n) \in V(\mathcal{S})$ there is a realization of $\boldsymbol{P}(\mathcal{S})$ such that, after standardization, $s_{x_i} = y_i$ for $i = 1, \ldots, n$.*

PROOF. (i): The fact that $\boldsymbol{P}(\mathcal{S})$ contains a 2-face $\boldsymbol{G}[\mathbf{0}, \mathbf{1}, x_1, \ldots, x_n, \boldsymbol{\infty}]$ is clear by construction. The normality is a consequence of the fact that each of the variables is contained in at least one equation. All polytopes in $\mathcal{C}(\mathcal{S})$ contain the edge pairs labeled $\mathbf{0}$ and $\boldsymbol{\infty}$. We define the line at infinity of $\boldsymbol{G}$ to be the line ℓ joining the points $\mathbf{0} \wedge \mathbf{0}'$ and $\boldsymbol{\infty} \wedge \boldsymbol{\infty}'$. The parallelity of the remaining edge pairs is then inherited from the parallelism of the edge-pairs of the polytopes in $\mathcal{C}(\mathcal{S})$, since this projective property is not disturbed by the transmitters.

(ii): By construction the slopes of $\boldsymbol{G}$ must satisfy all equations. For each of the elementary equations in $\mathbf{A}$ and $\mathbf{M}$ this is forced by an addition or a multiplication polytope.

(iii): Conversely, assume that any normal realization of $\boldsymbol{G}$ is given that satisfies the requirements of the defining equations of $\mathcal{S}$. We use the polytope $\mathbf{pyr}(\boldsymbol{G})$ as joins for the polytopes in $\mathcal{C}(\mathcal{S})$. Since the slopes of $\boldsymbol{G}$ satisfy all equations of the Shor normal form, for any $\boldsymbol{P} \in \mathcal{C}(\mathcal{S})$ the join $\mathbf{pyr}(\boldsymbol{G})$ can by Theorem 5.3.1(i), Lemma 6.2.1(iii), Theorem 7.1.1(ii), Theorem 7.2.1(ii) or Theorem 7.2.2(ii) be always completed to a realization of $\boldsymbol{P}$. Theorem 5.1.1(i) and Lemma 3.2.4 ensure that also the corresponding connectors are realizable with this special realization on $\boldsymbol{G}$. Lemma 3.2.4 ensures that these polytopes can be composed by connected sums to a realization of $\boldsymbol{P}(\mathcal{S})$. □

8.2 The Construction Seen from a Distance

In what follows we assume that $\mathcal{S}$ is a fixed Shor normal form with n variables. So far we have constructed the polytope $\boldsymbol{P}(\mathcal{S})$ in such a way that the points

of the semialgebraic set $V(\mathcal{S})$ can be rediscovered as the line slopes of an n-gon $\boldsymbol{G}$. We will now show that the realization space of $\boldsymbol{P}(\mathcal{S})$ is indeed stably equivalent to $V(\mathcal{S})$. For this it is useful to step back and look from a general point of view how $\boldsymbol{P}(\mathcal{S})$ is constructed. For the sake of the analysis of (the stable equivalence of) the realization spaces, we neglect our knowledge about the construction structures given by the second-order building blocks like harmonic polytopes or addition/multiplication polytopes. Instead, we consider $\boldsymbol{P}(\mathcal{S})$ as a composition of its basic building blocks.

We may think of $\boldsymbol{S}(\mathcal{S}) = \mathbf{pyr}(\mathbf{pyr}(\boldsymbol{G}[X]))$ as the root of a tree of building blocks that describes $\boldsymbol{P}(\mathcal{S})$. The nodes of the tree are our basic building blocks. Two nodes are connected by an edge if the corresponding blocks are glued by a connected sum operation. Let m be the number of BBBs that have to be added. We can add the building blocks one-by-one and describe $\boldsymbol{P}(\mathcal{S})$ recursively by:

$$\begin{aligned}
\boldsymbol{P}_0 &= \boldsymbol{S}(\mathcal{S}) \\
\boldsymbol{P}_i &= \boldsymbol{P}_{i-1}\#_{F_i}\boldsymbol{B}_i \quad \text{for } i = 1,\ldots,m \\
\boldsymbol{P}(\mathcal{S}) &= \boldsymbol{P}_m
\end{aligned}$$

Here $\boldsymbol{B}_i$ represents one of the basic building blocks, and F_i represents the facet along which it is glued to the polytope $\boldsymbol{P}_{i-1}$ that has been constructed up to this point. The choice of the $\boldsymbol{B}_i$ and F_i determines the entire construction.

For any polytope $\boldsymbol{P}$ and a vertex subset $Y \subset \mathbf{vert}(\boldsymbol{P})$, we denote denote the projections of the realization space $\mathcal{R}(\boldsymbol{P})$ by

$$\mathcal{R}_Y(\boldsymbol{P}, B) = \left\{\boldsymbol{P}'\big|_Y \mid \boldsymbol{P}' \in \mathcal{R}(\boldsymbol{P}, B)\right\}.$$

Here B is a basis contained in the vertex set $Y = \mathbf{vert}(\boldsymbol{S}(\mathcal{S}))$. For $i = 0,\ldots,m$ we denote by $Y_i = \mathbf{vert}(\boldsymbol{P}_i)$ the vertex set of $\boldsymbol{P}_i$. We choose a basis $B_0 \in Y_0$. In particular we have $\mathcal{R}_{Y_m}(\boldsymbol{P}, B_0) = \mathcal{R}(\boldsymbol{P}(\mathcal{S}), B_0)$. Since the face F_i is necessarily flat it forms a facet of $\boldsymbol{P}_i$; therefore we have

$$\mathcal{R}_{Y_i}(\boldsymbol{P}, B_0) \subseteq \mathcal{R}(\boldsymbol{P}_i, B_0).$$

We are now going to prove

$$\begin{aligned}
\mathcal{R}_{Y_0}(\boldsymbol{P}(\mathcal{S}), B_0) &\approx V(\mathcal{S}) \\
\mathcal{R}_{Y_i}(\boldsymbol{P}(\mathcal{S}), B_0) &\approx \mathcal{R}_{Y_{i-1}}(\boldsymbol{P}(\mathcal{S}), B_0) \quad \text{for } i = 1,\ldots,m
\end{aligned}$$

The first equivalence is (almost) established by Theorem 8.1.1. For the second equivalence we have to inspect all cases that occur when a basic building block is added.

In our construction all facets F_i are *pyramids* over n-gons, *prism* over n-gons, or *tents* over n-gons. The $\boldsymbol{B}_i$ are $\boldsymbol{X}$-*polytopes*, $\boldsymbol{Y}$-*polytopes*, *transmitters*, *forgetful transmitters*, and *adapters*. The following table summarizes the nine possible cases of pairs $(\boldsymbol{B}_i, F_i)$ that can occur.

Case	$\boldsymbol{B}_i$	F_i
1	$\boldsymbol{X}$	$\mathbf{pyr}(1,\ldots,6)$
2	$\boldsymbol{T}_X$	$\mathbf{pyr}(X)$
3	$\boldsymbol{T}_X$	$\mathbf{prism}(X)$
4	$\boldsymbol{T}_X^Y; \quad X \subset Y$	$\mathbf{pyr}(Y)$
5	$\boldsymbol{T}_X^Y; \quad X \subset Y$	$\mathbf{pyr}(X)$
6	$\boldsymbol{Y}_8$	$\mathbf{tent}^{a,b}(1,\ldots,8)$
7	$\boldsymbol{Y}_8$	$\mathbf{prism}(G_8)$
8	$\boldsymbol{A}_8$	$\mathbf{pyr}(X)$
9	$\boldsymbol{A}_8$	$\mathbf{tent}^{a,b}(X)$

Recall that each of the basic building blocks contains at most two information frames. For a given point $(x_1,\ldots,x_n)$ of $V(\mathcal{S})$ and a corresponding realization of $\boldsymbol{P}(\mathcal{S})$, the edge slopes of <u>all</u> information frames occurring in $\boldsymbol{P}(\mathcal{S})$ are fixed (up to projective equivalence).

8.3 Proving Stable Equivalence

We now prove that our construction indeed gives a stable equivalence when adding the blocks $\boldsymbol{B}_i$. Unavoidably, this part is a bit technical, since we have to cover nine different situations. We first prove:

<u>LEMMA 8.3.1.</u> $\mathcal{R}_{Y_i}(\boldsymbol{P}(\mathcal{S}), B_0) \approx \mathcal{R}_{Y_{i-1}}(\boldsymbol{P}(\mathcal{S}), B_0)$, for every $i = 1,\ldots,m$.

PROOF. We assume that i is fixed throughout the proof. We have to provide a proof for each of the nine cases listed in the table above. For a realization $\boldsymbol{P}_{i-1} \in \mathcal{R}_{Y_{i-1}}(\boldsymbol{P}(\mathcal{S}), B_0)$, we consider its representation $\boldsymbol{P}_{i-1}^{\mathrm{hom}} \subset \mathbb{R}^{d+1}$ by homogeneous coordinates. Let

$$h_0,\ h_1,\ldots,\ h_r \in (\mathbb{R}^{d+1})^*$$

be the facet-defining linear functionals with $h_j \cdot \boldsymbol{p} \geq 0$ for $\boldsymbol{p} \in \boldsymbol{P}_{i-1}^{\mathrm{hom}}$ and $j = 1,\ldots,r$. Assume that h_0 is the facet-defining functional for the facet F_i. Furthermore, let $h_\infty = (0,\ldots,0,1) \in (\mathbb{R}^{d+1})^*$ be a functional that represents the plane at infinity. We set

$$\mathcal{A} = \{\boldsymbol{p} \in \mathbb{R}^{d+1} \mid h_i \cdot \boldsymbol{p} > 0 \text{ for } i = 1,\ldots,r \text{ and } h_0 \cdot \boldsymbol{p} < 0\}$$

and

$$\mathcal{B} = \{\boldsymbol{p} \in \mathcal{A} \mid h_\infty \cdot \boldsymbol{p} > 0\}.$$

The region $\mathcal{A}$ describes the possible locations of points $\boldsymbol{p}$ such that $\boldsymbol{P}_{i-1}^{\mathrm{hom}} \cup \{\boldsymbol{p}\}$ again represents a cone with all points in convex position containing all facets of $\boldsymbol{P}_{i-1}^{\mathrm{hom}}$ except F_i. The region $\mathcal{B}$ describes the possible locations of points $\boldsymbol{p}$ such that (after dehomogenization with the hyperplane defined by $x_{d+1} = 1$) $\boldsymbol{P}_{i-1}^{\mathrm{hom}} \cup \{\boldsymbol{p}\}$ is again a polytope with all points in convex position containing all facets of $\boldsymbol{P}_{i-1}$ except F_i.

Now for all the nine cases of the table we study how the building block $\boldsymbol{B}_i$ can be added to the already realized polytope $\boldsymbol{P}_{i-1}$ by a certain construction, and why this construction gives a stable equivalence to the semialgebraic set $V(\mathcal{S})$. In particular, homogeneous coordinates for all points that are added have to lie in the region $\mathcal{B}$, since otherwise the convexity is violated. Observe that $\mathcal{A}$ as well as $\mathcal{B}$ are the interiors of polyhedral sets, whose bounding hyperplanes depend polynomially on the coordinates of $\boldsymbol{P}_{i-1}$. We will describe how we can get homogeneous coordinates for the points that have to be added. Since all the added points have a positive x_{d+1}-coordinate, the transition to affine coordinates can be obtained by a rational equivalence (dividing by the last coordinate) that trivially gives a stable equivalence.

<u>Case 1:</u> Assume that $\boldsymbol{B}_i$ is an $\boldsymbol{X}$-polytope (compare Figure 5.4.1 for the labeling). The join F_i is given by the pyramid

$$\mathbf{pyr}(1,2,3,4,5,6) = \mathbf{pyr}(\boldsymbol{G}(1,2,3,4,5,6), \overline{y}).$$

The remaining points have to be added. The points $1 \wedge 4$, $2 \wedge 3$ and $5 \wedge 6$ are collinear, since $\boldsymbol{P}_{i-1}$ must be compatible with the polytope $\boldsymbol{P}(\mathcal{S})$. We describe how homogeneous coordinates for the remaining points a, b and $\underline{y}$ can be chosen.

  (i) Choose $\boldsymbol{p}_a$ arbitrarily in the region $\mathcal{B}$.
 (ii) Choose scalars $\lambda_1, \tau_1 > 0$ such that $\boldsymbol{p}_b = \lambda_1 \boldsymbol{p}_a + \tau_1 \sigma_1 (1 \wedge 4) \in \mathcal{B}$.
(iii) By construction the lines $(2 \wedge 3) \vee a$ and $(5 \wedge 6) \vee b$ meet in a point $\boldsymbol{q}_y$. Choose scalars $\lambda_2, \tau_2 > 0$ such that $\boldsymbol{p}_{\underline{y}} = \lambda_2 \boldsymbol{p}_{\overline{y}} + \tau_2 \sigma_2 \boldsymbol{q}_y \in \mathcal{B}$.

In the above construction we assume that the signs $\sigma_1, \sigma_2 \in \{-1, +1\}$ have been chosen appropriately. By the above construction we can reach any admissible realization of $\boldsymbol{P}_i$. In any case the regions in which the points $\boldsymbol{p}_a$, $\boldsymbol{p}_b$ and $\boldsymbol{p}_{\underline{y}}$ can be chosen are the (non-empty) interiors of polyhedral sets. The regions in steps (ii) and (iii) are non-empty since the points $\boldsymbol{p}_a$ and $\boldsymbol{p}_{\underline{y}}$ both lie in the closure of $\mathcal{B}$. This gives a stable equivalence between $\mathcal{R}_{Y_{i-1}}(\boldsymbol{P}(\mathcal{S}), B_0)$ and $\mathcal{R}_{Y_i}(\boldsymbol{P}(\mathcal{S}), B_0)$ by a sequence of stable projections.

<u>Case 2:</u> Assume that $\boldsymbol{B}_i$ is a transmitter $\boldsymbol{T}_X$ with $X = (1, \ldots, r)$ (compare Figure 5.1.1 for the labeling). The join F_i is given by the pyramid $\mathbf{pyr}(X) = \mathbf{pyr}(\boldsymbol{G}(X), \overline{y})$. First assume that a realization of $\boldsymbol{P}_i$ is already given. We define $\boldsymbol{p}_j = j \wedge (j+1)$ and $\boldsymbol{p}_{j'} = j' \wedge (j+1)'$ (indices modulo r). In any such realization of $\boldsymbol{P}_i$ the point $\boldsymbol{q}_y$ that is obtained as the common intersection of the edges $(\boldsymbol{p}_1, \boldsymbol{p}_{1'}), (\boldsymbol{p}_2, \boldsymbol{p}_{2'}), \ldots, (\boldsymbol{p}_r, \boldsymbol{p}_{r'}), (\boldsymbol{p}_{\underline{y}}, \boldsymbol{p}_{\overline{y}})$ lies in the region $\mathcal{A}$. This can be seen as follows. The (linear) hyperplanes bounding the region $\mathcal{A}$ are those coming from

facets adjacent to the facet F_i in $\boldsymbol{P}_{i-1}$ and F_i itself. For each of these hyperplanes H, there is a line segment $[\boldsymbol{p}_j, \boldsymbol{q}_y]$ with j taken from $\{1, \ldots, r, \underline{y}\}$, that strictly lies on the same side as the region $\mathcal{A}$. Therefore $\boldsymbol{q}_y$ itself lies in region $\mathcal{A}$. Now we can construct a realization of $\boldsymbol{P}_i$ starting from $\boldsymbol{P}_{i-1}$ as follows.

(i) Choose $\boldsymbol{q}_y$ arbitrarily in the region $\mathcal{A}$.

(ii) Choose a hyperplane H given by a linear functional $h \in (\mathbb{R}^{d+1})^*$, such that all the intersections $H \cap [\boldsymbol{p}_j, \boldsymbol{q}_y]$ for $j \in \{1, \ldots, r, \underline{y}\}$ lie in the region $\mathcal{B}$.

(iii) Define $\boldsymbol{p}_{j'}$ by the intersection $H \cap [\boldsymbol{p}_j, \boldsymbol{q}_y]$.

By the above construction we can reach any admissible realization of $\boldsymbol{P}_i$. In step (i) the point $\boldsymbol{q}_y$ is chosen in the interior of the polyhedral set $\mathcal{A}$. In step (ii) for each $j \in \{1, \ldots, r, \underline{y}\}$ we get a linear equation restricting the coefficients of h. However, the region in which h can be chosen is always non-empty, since we find an admissible value in an ε-neighborhood of the facet-defining functional for F_i. Therefore the region in which h can be chosen is the interior of a polyhedral set. Step (iii) describes a rational equivalence that translates h into admissible choices of the points $1', \ldots, r', y$. Altogether this construction proves the stable equivalence between $\mathcal{R}_{Y_{i-1}}(\boldsymbol{P}(\overline{\mathcal{S}}), B_0)$ and $\mathcal{R}_{Y_i}(\boldsymbol{P}(\mathcal{S}), B_0)$.

<u>Case 3:</u> Assume that $\boldsymbol{B}_i$ is a transmitter $\boldsymbol{T}_X$ with $X = (1, \ldots, r)$, and assume that the join F_i is given by the prism $\mathbf{prism}(\boldsymbol{G}(X), \boldsymbol{G}(X'))$. We define $\boldsymbol{q}_y$ as the point where the supporting lines of $(\boldsymbol{p}_1, \boldsymbol{p}_{1'}), (\boldsymbol{p}_2, \boldsymbol{p}_{2'}), \ldots, (\boldsymbol{p}_r, \boldsymbol{p}_{r'})$ meet. We can construct a realization of $\boldsymbol{P}_i$ starting from $\boldsymbol{P}_{i-1}$ as follows.

(i) Choose $\boldsymbol{p}_{\overline{y}}$ arbitrarily in the region $\mathcal{B}$.

(ii) Choose scalars $\lambda, \tau > 0$ such that $\boldsymbol{p}_{\underline{y}} = \lambda \boldsymbol{p}_{\overline{y}} + \tau \sigma \boldsymbol{q}_y \in \mathcal{B}$.

In any case the regions in which the points $\boldsymbol{p}_{\overline{y}}$ and $\boldsymbol{p}_{\underline{y}}$ can be chosen are the (non-empty) interiors of polyhedral sets. The region in step (ii) is non-empty since the points $\boldsymbol{p}_{\underline{y}}$ lies in the closure of $\mathcal{B}$. This gives a stable equivalence between $\mathcal{R}_{Y_{i-1}}(\boldsymbol{P}(\mathcal{S}), B_0)$ and $\mathcal{R}_{Y_i}(\boldsymbol{P}(\mathcal{S}), B_0)$ by a sequence of stable projections.

<u>Case 4:</u> The case where $\boldsymbol{B}_i$ is a forgetful transmitter $\boldsymbol{T}_X^Y$ with $X = (1, \ldots, r)$ and $Y = (1', \ldots, r, (r+1)')$ and where the join F_i is given by the pyramid $\mathbf{pyr}(\boldsymbol{G}(Y), \underline{y})$ is similar to Case 2 (compare Figure 5.3.1 for the labeling). The only difference is that another point x (the fourth point of the tetrahedron in which $\underline{y}, 1' \wedge (r+1)', r' \wedge (r+1)'$ are involved) has to be added. Again, this point can be chosen in an open line segment.

<u>Case 5:</u> The case where $\boldsymbol{B}_i$ is a forgetful transmitter $\boldsymbol{T}_X^Y$ with $X = (1, \ldots, r)$ and $Y = (1', \ldots, r, (r+1)')$ and where the join F_i is given by the pyramid $\mathbf{pyr}(\boldsymbol{G}(X), \overline{y})$ is similar to Case 2 (compare Figure 5.3.1 for the labeling). The only problem that arises is that a new edge $(r+1)'$ with a new direction has to be added. The direction of $(r+1)'$ is completely determined by the construction of $\boldsymbol{P}(\mathcal{S})$, because Case 5 only arises when intermediate variables are introduced in an addition or multiplication polytope. These intermediate variables are either

x^2, $-y$, or $\frac{x+y}{2}$, where x and y correspond to variables that already occurred in $\boldsymbol{G}(X)$. In any case the new direction can be computed from $\boldsymbol{G}(Y')$ in $\boldsymbol{T}_Y$ by a <u>rational</u> function (this is the reason why we avoided creating square roots in our multiplication polytope). We assume that a realization $\boldsymbol{P}_{i-1}$ is given, and start by constructing a transmitter $\boldsymbol{T}_Y$ along the join F_i, as we did in Case 2. However, we alter the procedure slightly. When we chose the cutting hyperplane H, we do not require that the vertex $\boldsymbol{p}_{r'} = r' \wedge 1'$ lies in the region $\mathcal{B}$. Instead, we require that the procedure of constructing the edge $(r+1)'$ described below can be carried out. It can easily be checked that this still describes linear constraints in the choice of H. After choosing $\boldsymbol{T}_Y$ we consider the plane H that supports the r-gon $\boldsymbol{G}(Y')$ of $\boldsymbol{T}_Y$. We now truncate one of the vertices $r' \wedge 1'$ of $\boldsymbol{G}(Y')$ by introducing a new edge $(r+1)'$. After determining the direction of the edge $(r+1)'$ we have to choose its actual position. This gives another three linear inequalities on the choice of the parameter $(r+1)'$, since it has to be positioned correctly with respect to the points $1' \wedge r'$, $1' \wedge 2'$ and $(r-1)' \wedge r'$ of $\boldsymbol{T}_Y$. After choosing the edge $(r+1)'$, we get two new points $1' \wedge (r+1)'$ and $r' \wedge (r+1)'$ by a rational equivalence. Finally, the point x (compare Figure 5.3.1) can be chosen anywhere on the open line segment connecting $1 \wedge r$ and $1' \wedge r'$. This construction again gives a stable equivalence.

<u>Case 6:</u> Assume that $\boldsymbol{B}_i$ is a $\boldsymbol{Y}_8$-polytope (compare Figure 5.6.1 for the labeling). The join F_i is given by the tent $\mathbf{tent}^{1,5}(\boldsymbol{G}(1,\ldots,8))$. For this case it is preferable to work directly in the affine case and not in the homogenized version. The region $\mathcal{B}$ here means the dehomogenized counterpart of our previous region $\mathcal{B}$.

In the realization $\boldsymbol{P}_{i-1}$, the points $1 \wedge 5$, $2 \wedge 6$, $3 \wedge 7$ and $4 \wedge 8$ lie all on one line ℓ. This line lies completely exterior to $\mathcal{B}$. We assume that a hyperplane H through ℓ is given, that intersects the region $\mathcal{B}$. After a suitable projective transformation we may assume that ℓ is mapped to infinity and that H and $\boldsymbol{G}(1,\ldots,8)$ become parallel. Our construction of the polytope $\boldsymbol{P}(\mathcal{S})$ forces the edge slopes of $\boldsymbol{G}(1,\ldots,8)$ to be in harmonic position. Now the 8-gon $\boldsymbol{G}(1',\ldots,8')$ has to be chosen on H with edges parallel to $\boldsymbol{G}(1,\ldots,8)$ and in the class that is admissible for the configuration given in section 6.1. Remember that, by Remark 6.1.2, (up to projective equivalence) this configuration was completely controlled by one parameter x that can be chosen in the open interval $]\frac{1}{3}, 1[$. We pick such an admissible parameter x and the corresponding 8-gon $\boldsymbol{G}$ as defined in Section 6.2. By a 2-dimensional projective transformation τ we can map $\boldsymbol{G}$ into the polyhedral set $H \cap \mathcal{B}$ such that the edges become parallel to the corresponding edges in $\boldsymbol{G}(1,\ldots,8)$. This transformation is uniquely determined up to a translation $t \in \mathbb{R}^2$ and a scaling $s \in \mathbb{R}$ of the image $\tau(\boldsymbol{G})$. The fact that $H \cap \mathcal{B}$ is bounded by lines gives linear constraints for the parameters t and s. After choosing the parameters x, t and s in a suitable way, by a rational equivalence we can compute the missing vertices of $\boldsymbol{G}(1',\ldots,8')$ as the vertices of $\boldsymbol{G}$. By this we can reach each realization of $\boldsymbol{P}_i$. Furthermore, since the controlling parameters H, x, t and s are all taken from interiors of polyhedral sets, and the points added are

calculated from them by invertible rational functions, we get a stable equivalence between $\mathcal{R}_{Y_{i-1}}(\boldsymbol{P}(\mathcal{S}), B_0)$ and $\mathcal{R}_{Y_i}(\boldsymbol{P}(\mathcal{S}), B_0)$.

<u>Cases 7 and 8:</u> In both cases only two points have to be added the arguments are similar to Case 3.

<u>Case 9:</u> This final case is trivial since only one point has to be added. This point may be chosen anywhere in region $\mathcal{B}$. $\square$

We now finally prove that the realizations of our starting polytope $\boldsymbol{S}(\mathcal{S})$ which are compatible with $\boldsymbol{P}(\mathcal{S})$ are stably equivalent to the semialgebraic set $V(\mathcal{S})$. Remember our definition $Y_0 = \mathbf{vert}(\boldsymbol{S}(\mathcal{S}))$.

<u>LEMMA 8.3.2.</u> $\mathcal{R}_{Y_0}(\boldsymbol{P}(\mathcal{S}), B_0) \approx V(\mathcal{S})$.

PROOF. This time we specify the basis B_0 of $\boldsymbol{P}(\mathcal{S})$ as a basis of $\boldsymbol{S}(\mathcal{S})$. The polytope $\boldsymbol{S}(\mathcal{S})$ was defined as a doubly iterated pyramid over

$$\boldsymbol{G} = \boldsymbol{G}[\mathbf{0}, \mathbf{1}, x_1, x_2, \ldots, x_n, \boldsymbol{\infty}].$$

As the basis we take the two apices of the pyramids, a and b, together with the points $\mathbf{0} \wedge \boldsymbol{\infty}'$, $\mathbf{0} \wedge \mathbf{1}$ and $\boldsymbol{\infty}' \wedge x_n'$. Since the realization space of a pyramid is isomorphic to the realization space of its basis we can restrict ourselves to the analysis of realizations of $\boldsymbol{G}$. In $\mathbb{R}^2$ we set

$$\mathbf{0} \wedge \boldsymbol{\infty}' := (0,0), \quad \mathbf{0} \wedge \mathbf{1} := (1,0), \quad \boldsymbol{\infty}' \wedge x_n' := (0,1).$$

All remaining points of $\boldsymbol{G}$ have to lie in the positive orthant of $\mathbb{R}^2$. We want to prove that, after fixing the basis, the space of all computation frames $\boldsymbol{G}$ that are compatible with $\boldsymbol{P}(\mathcal{S})$ is stably equivalent to $V(\mathcal{S})$.

By Theorem 8.1.1, (up to projective equivalence) the possible realizations of $\boldsymbol{G}$ are exactly the normalized computation frames, where the line slopes represent a point of $V(\mathcal{S})$. We first consider the case where opposite sides of $\boldsymbol{G}$ are parallel. Then $\boldsymbol{G}$ can be parameterized by the edge slopes s_i and the (oriented) distances d_i of the edge supporting lines from the origin. We define a parameterization W of all these realizations that forms a stable projection onto $V(\mathcal{S})$. We first choose a point $(y_1, \ldots, y_n) \in V(\mathcal{S})$ and the slope $s_{\mathbf{1}} \geq 0$ of the edge pair $(\mathbf{1}, \mathbf{1}')$. All remaining slopes s_{x_i} of edge pairs (x_i, x_i') are then determined by $y_i = (0, \infty \,|\, s_{\mathbf{1}}, s_{x_i})$. We then position the line supporting edge $\mathbf{1}$ with slope $s_{\mathbf{1}}$ so that it passes through the point $\mathbf{0} \wedge \mathbf{1} = (1,0)$. Similarly, we position the edge supporting line of x_n' through the point $\boldsymbol{\infty}' \wedge x_n' = (0,1)$. Starting with x_i we add in cyclic order all the remaining edge supporting lines in a way that after adding a line the vertices of $\boldsymbol{G}$ determined so far are in convex position. This defines a set of linear inequalities for each of the distances d_i. Thus the set of all realizations of $\boldsymbol{G}$ with parallel opposite edges parameterized by slopes and distances defines a stable projection onto $V(\mathcal{S})$. Then we may compute the

vertices of G by a rational equivalence (a reparametrization). We finally get the set of all realizations of G by applying a projective transformation. A projective transformation τ that leaves the points in the basis fixed is uniquely determined by the position of the image $\boldsymbol{p} = \tau(\mathbf{1} \wedge x_i)$. The region in which the image $\boldsymbol{p}$ can be chosen such that $\tau(\boldsymbol{G})$ is again convex is the interior of a convex polygon (depending on the positions of the previously chosen vertices). Another rational equivalence provides the stable equivalence between $V(\mathcal{S})$ and $\mathcal{R}_{Y_0}(\boldsymbol{P}(\mathcal{S}), B_0)$. □

UNIVERSALITY THEOREM FOR 4-POLYTOPES:
For every primary basic semialgebraic set V defined over $\mathbb{Z}$ there is a 4-polytope $\boldsymbol{P}$ whose realization space is stably equivalent to V. Moreover, the face lattice of $\boldsymbol{P}$ can be generated from the defining equations of V in polynomial time.

PROOF. By Theorem 4.1.2, there exists a Shor normal form $\mathcal{S}$ such that $V \approx V(\mathcal{S})$. Let $\boldsymbol{P}(\mathcal{S})$ be the corresponding polytope with the notations as before. By Lemma 8.3.2, we have $V(\mathcal{S}) \approx \mathcal{R}_{Y_0}(\boldsymbol{P}(\mathcal{S}), B_0)$. Lemma 8.3.1 proves that

$$\mathcal{R}_{Y_0}(\boldsymbol{P}(\mathcal{S}), B_0) \approx \mathcal{R}_{Y_1}(\boldsymbol{P}(\mathcal{S}), B_0) \approx \ldots \approx \mathcal{R}_{Y_m}(\boldsymbol{P}(\mathcal{S}), B_0) = \mathcal{R}(\boldsymbol{P}(\mathcal{S})).$$

Thus we have $V \approx \mathcal{R}(\boldsymbol{P}(\mathcal{S}))$.

By Lemma 4.1.2, $\mathcal{S}$ can be computed in polynomial time from the defining equations of V. The fact that the face lattice of $\boldsymbol{P}(\mathcal{S})$ can be computed in polynomial time from $\mathcal{S}$ is a direct consequence of our inductive construction. □

9 Complexity Results

9.1 Algorithmic Complexity

We now study the implications of the Universality Theorem for the "Algorithmic Steinitz Problem," the problem of designing algorithms that decide whether a given combinatorial polytope is realizable or not. The following lemma asserts that we can retrieve the points of the original semialgebraic set from realizations of the polytope.

LEMMA 9.1.1. *For every basic semialgebraic variety W, there exists a polynomial function f with integer coefficients and a 4-polytope $\boldsymbol{P}$ such that $f(\mathcal{R}(\boldsymbol{P})) = W$.*

PROOF. Let $\mathcal{S}(W)$ be a Shor normal form of W, and let $\boldsymbol{P} := \boldsymbol{P}(\mathcal{S}(W))$ be the polytope as constructed in Theorem 8.1.1. The slopes of edges of the central computation frame for $\mathcal{S}(W)$ can be calculated by polynomial functions from the coordinates of realizations of $\boldsymbol{P}$. By Theorem 8.1.1, this defines a polynomial function g with $g(\mathcal{R}(\boldsymbol{P})) = V(\mathcal{S}(W))$. By Lemma 4.1.2, there is another polynomial function h with $h(V(\mathcal{S}(W))) = W$. The composition $h \circ g$ is the desired function f. □

THEOREM 9.1.2.

  (i) *The realizability problem for 4-polytopes is polynomial-time equivalent to the "Existential Theory of the Reals."*

 (ii) *The realizability problem for 4-polytopes is NP-hard.*

PROOF. The "Existential Theory of the Reals" is the decision problem of whether a given set of equations and inequalities has a real solution or not. Thus it is the problem of deciding whether a basic semialgebraic set W given by its defining equations is empty or not. By replacing non-strict inequalities $a \leq b$ by equations $a = b + c^2$ with new variables c, we can restrict ourselves to the case where only strict inequalities occur.

The realizability problem for polytopes can be translated (in polynomial time) into a system of polynomial equations and inequalities. So it remains to show that the problem of finding a solution for a system of equations and strict inequalities can be (polynomial time) reduced to the realizability problem for polytopes. A Shor normal form $\mathcal{S}(W)$ can be computed in polynomial time from the defining equations of a (primary) semialgebraic set, and the face lattice of $\boldsymbol{P}(\mathcal{S})$ can be generated in polynomial time from $\mathcal{S}$. Thus the face lattice of the 4-polytope in Lemma 9.9.1 can be computed in polynomial time from the (in-)equality system that has to be solved.

Part (ii) is a consequence of the NP-hardness of the Existential Theory of the Reals and (i). □

9.2 Algebraic Complexity

So far, all known examples of non-rational 4-polytopes have been constructed by Gale diagram techniques. The smallest such example is due to Perles. It has 12 vertices in dimension 8. No examples of lower dimensions were previously known. We demonstrate here that by combining Lawrence extensions with connected sum operations one can also obtain examples of relatively small non-rational 4-polytopes.

THEOREM 9.2.1.

 (i) *For every subfield A of the real algebraic numbers, there is a 4-polytope not realizable over A.*

(ii) *There exists a non-rational 4-polytope with 33 vertices.*

To see (i), let a be any algebraic number not contained in the subfield A and $f_a(x)$ its minimal polynomial. The polytope $\boldsymbol{P} = \boldsymbol{P}(\mathcal{S}(\{x \mid f_a(x) = 0\}))$ has the desired property, since by Lemma 9.1.1 (i) there is a polynomial function f with $f(\mathcal{R}(\boldsymbol{P})) = a$.

The proof of Part (ii) will only be sketched. Consider an octagon $\boldsymbol{G} = \boldsymbol{G}(1, \dots, 8)$ for which the incidences and parallelisms indicated in Figure 9.2.1 hold.
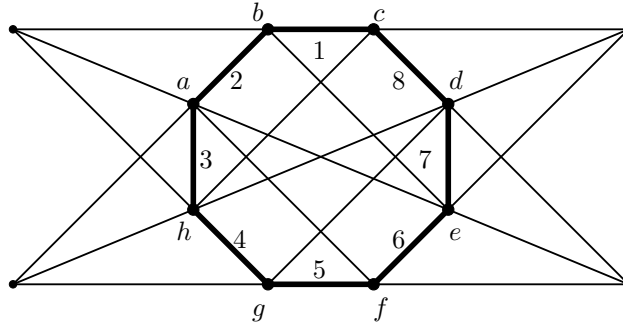
Figure 9.2.1: An incidence configuration that forces a regular octagon.

It has the following eight 3-point collinearities:

$$A = (2 \wedge 6, 3 \wedge 4, 1 \wedge 8) \qquad B = (2 \wedge 6, 4 \wedge 5, 7 \wedge 8)$$
$$C = (4 \wedge 8, 1 \wedge 2, 6 \wedge 7) \qquad D = (4 \wedge 8, 2 \wedge 3, 5 \wedge 6)$$
$$E = (4 \wedge 1, 2 \wedge 3, 7 \wedge 6) \qquad F = (8 \wedge 5, 2 \wedge 3, 7 \wedge 6)$$
$$G = (6 \wedge 1, 3 \wedge 4, 8 \wedge 7) \qquad H = (2 \wedge 5, 3 \wedge 4, 8 \wedge 7)$$

The following calculation proves that this configuration is projectively unique and is realizable only if G is projectively equivalent to a regular 8-gon. We embed G into the euclidean plane $\mathbb{R}^2$.

Up to projective equivalence we may assume that the lines $2, 4, 6$ and 8 are given by the equations $x = -1$, $y = 1$, $x = 1$ and $y = -1$, respectively. We assume that the vertices are labeled as shown in Figure 9.2.1. Using the parallelisms (collinearities $A, \ldots, D$), the points $a, \ldots, h$ get the following coordinates in $\mathbb{R}^2$:

$$a = (-1, w), \quad b = (-1, v), \quad c = (t, 1), \qquad d = (u, 1),$$
$$e = (1, v), \qquad f = (1, w), \quad g = (u, -1), \quad h = (t, -1).$$

The geometry of the configuration forces the parameters to satisfy

$$-1 < w < v < 1 \quad \text{and} \quad -1 < t < u < 1 \tag{$*$}$$

The remaining collinearities $E, \ldots, H$ are expressed by the vanishing of the following polynomials (as expansion of the corresponding Cayley algebra expressions shows):

$$E := (u - t) \ (2 - 3v + 3w - v^2 + tw - tv - vw - tv^2 + tvw)$$
$$F := (t - u) \ (2 - 3v + 3w - w^2 + uv - uw - vw + uw^2 - uvw)$$
$$G := (w - v) \ (2 - 3u + 3t - t^2 + uv - tu - tv + vt^2 - tuv)$$
$$H := (v - w) \ (2 - 3u + 3t - u^2 + tw - tu - uw - wu^2 + tuw)$$

By combining the polynomials in a suitable way we get:

$$E + F + G + H = 2(-t + u)(-v + w)(t + u + v + w)$$
$$E + F - G - H = 2(-t + u)(-v + w)(tv - uw)$$

Since by $(*)$ we have $t \neq u$ and $v \neq w$, we have for every realization:

$$t + u + v + w = 0 \quad \text{and} \quad tv = uw$$

This implies either $t = -u$ and $w = -v$ or $w = -t$ and $v = -u$. The the second case cannot occur, since then $w < v$ implies $u < t$ which is in contradiction to $(*)$. Thus we have $t = -u$ and $w = -v$. Inserting these two relations into E and F we get

$$E = 4u(1 - 3v + uv + uv^2) \quad \text{and} \quad F = 4v(-1 + 3u - uv - u^2v).$$

Adding these two equations we obtain

$$E + F = 4(u - v + u^2v - v^2u) = 4(u - v)(1 - vu).$$

Thus in every realization we have either $u = v$ or $u = 1/v$. Inserting the second statement into E we get $E = 4u(1 - 3v + 1 + v)$. Since $u \neq 0$, this implies $v = 1$ which contradicts $(*)$. Hence we are left with the case $u = v$. Inserting this into E and dividing by $4u$ we get

$$0 = 1 - 3v + v^2 + v^3 = (v - 1)(-1 + 2v + v^2)$$

This equation has the three solutions $v_1 = 1$, $v_{2,3} = -1 \pm \sqrt{2}$. The only solution compatible with $(*)$ is $v = u = -t = -w = 1 - \sqrt{2}$, which implies that $\boldsymbol{G}$ is a regular 8-gon.

As in the construction of the polytope $\boldsymbol{H}$ of Section 6, we now construct a single polytope that encodes all the collinearities $A, \ldots, H$ in its face lattice. For each single collinearity $(b \wedge d, a \wedge a + 1, c \wedge c + 1)$ (with $(a, a + 1, b, c, c + 1, d) \hookrightarrow (1, \ldots, 8)$, indices counted modulo 8), we first construct a single polytope $\boldsymbol{Z}^{a,a+1\,|\,b\,|\,c,c+1\,|\,d}(1, \ldots, 8)$ that encodes this condition by the non-prescribability of an 8-gon $\boldsymbol{G}$. We can do this in a way exactly analogous to our construction of $\boldsymbol{X}$-polytopes. We first consider the polytope $\boldsymbol{P} = \mathbf{tent}^{b,d}(\boldsymbol{G})$ and then define $\boldsymbol{Z}^{a,a+1\,|\,b\,|\,c,c+1\,|\,d}(1, \ldots, 8)$ as a suitable Lawrence extension over $\boldsymbol{P}$. We now take eight of these polytopes $\boldsymbol{Z}_A, \ldots, \boldsymbol{Z}_H$, such that $\boldsymbol{Z}_X$ represents the collinearity X of our list above. They can be composed into one single polytope by a linear chain given by the following construction diagram.

$$\boxed{Z_H} - \boxed{Z_A} = \boxed{Z_B} - \boxed{Z_C} = \boxed{Z_D} - \boxed{Z_E} = \boxed{A_8} - \boxed{Z_F} = \boxed{A_8} - \boxed{Z_G}$$
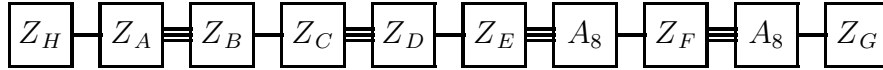
Here the $\boldsymbol{A}_8$ polytopes represent suitable adapters. The different blocks are glued along pyramids or tents. This construction requires exactly 33 vertices. The 8-gon $\boldsymbol{G}$ is shared by all $\boldsymbol{Z}$-polytopes. Each of the eight $\boldsymbol{Z}$-polytopes needs four additional vertices. One of these vertices is shared by $\boldsymbol{Z}_H$ and $\boldsymbol{Z}_A$, two by $\boldsymbol{Z}_A$ and $\boldsymbol{Z}_B$, one by $\boldsymbol{Z}_B$ and $\boldsymbol{Z}_C$, two by $\boldsymbol{Z}_C$ and $\boldsymbol{Z}_D$ and one by $\boldsymbol{Z}_D$ and $\boldsymbol{Z}_E$. The adapters do not need additional vertices. In every realization of this polytope the 8-gon $\boldsymbol{G}$ simultaneously satisfies all eight collinearities $A, \ldots, H$. Hence $\boldsymbol{G}$ is projectively equivalent to a regular 8-gon, and requires $\sqrt{2}$ to belong to the underlying coordinatization field.   □

9.3   The Sizes of 4-Polytopes

While the last section dealt with non-rational polytopes, we now consider only those d-polytopes that are realizable on a finite integer grid $G_N := \{1, 2, \ldots, N\}^d$; $N > 0$. We ask for bounds on the minimal number $\nu(n, d)$, such that every rational d-polytope with n vertices has a realization with vertex coordinates in $G_{\nu(n,d)}$. In [51] Onn and Sturmfels proved that for $d = 3$ we have $\nu(n, 3) < n^{169n^3}$; in other words the size of 3-polytopes does not grow worse than singly exponentially in the number of vertices. We now prove that the size of certain 4-polytopes with integral coordinates grows doubly exponentially with the number of vertices involved. This gives a theorem similar to a result of Goodman, Pollack and Sturmfels for line arrangements. The technique of the proof is also similar.

For this we first need an estimate on the number of vertices of $\boldsymbol{P}(\mathcal{S})$ for a given Shor normal form $\mathcal{S}$.

<u>LEMMA 9.3.1.</u>   *There is a constant $\alpha > 0$ such that, for every Shor normal form $\mathcal{S} = (n, \mathbf{A}, \mathbf{M})$ with $k = |\mathbf{A}| + |\mathbf{M}| \geq 1$ equations, the polytope $\boldsymbol{P}(\mathcal{S})$ has less then $\alpha k n^2$ vertices.*

PROOF.   Let $\mathcal{S} = (n, \mathbf{A}, \mathbf{M})$ be a Shor normal with $k = |\mathbf{A}| + |\mathbf{M}|$ equations. We set $m = 2(n + 3)$, the number of vertices of the "central computation frame" in $\boldsymbol{P}(\mathcal{S})$. Let $t = 2m + 2$ be the number of vertices of a basic forgetful transmitter from an m-gon to an $(m-1)$-gon, let $r = 2m + 4$ be the numbers of vertices of a connector $\boldsymbol{C}_m$ and let $s = m + 2$ be the number of vertices of the initial doubly iterated pyramid $\boldsymbol{S}(\mathcal{S})$. Furthermore, let a be the maximum of the numbers of vertices of the polytopes $\boldsymbol{P}^{2x}$, $\boldsymbol{P}^{x+y}$, $\boldsymbol{P}^{x^2}$ and $\boldsymbol{P}^{x \cdot y}$. To join a single addition or multiplication polytope into the construction $\boldsymbol{P}(\mathcal{S})$, we need at most one connector $\boldsymbol{C}_m$ and $2m$ basic forgetful transmitters (each of them has at most t vertices). Thus to construct $\boldsymbol{P}(\mathcal{S})$ we need at most $s + k(a + 2m \cdot t + r)$ vertices (the connected sum operations only decrease the number of points). For a sufficiently large constant $\alpha > 0$ we get $s + k(a + m \cdot t + r) < \alpha k n^2$. This proves the lemma. $\square$

One might think that by a more careful analysis of the vertex number of the polytope $\boldsymbol{P}(\mathcal{S})$ one might qualitatively improve this bound. However, by this only the size of the constant α is decreased. The main reason for the quadratic behavior in the number n of variables comes from the fact that we use a *chain* of forgetful transmitters to connect each addition or multiplication polytope to the central computation frame. There is a way to replace this chain of transmitters by a single polytope, whose number is linearly bounded in n. If one wants to model a forgetful transmitter $\boldsymbol{T}_X^Y$ with $Y \hookrightarrow X$, one starts with a transmitter $\boldsymbol{T}_Y$ and generates the edges of X that have to be "forgotten" by successive truncation of vertices. A sketch of this construction is given in Figure 9.3.1.
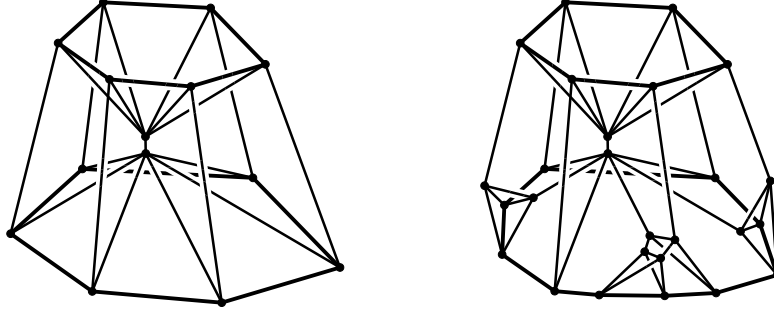
Figure 9.3.1: Alternative construction for a forgetful transmitter.

This leads to an alternative construction $P'(\mathcal{S})$ with essentially the same properties as $P(\mathcal{S})$ but fewer vertices (however it becomes technically more difficult to get the final "stable equivalence statement"). By this — without formal proof — we get:

REMARK 9.3.2.   There is a constant $\beta > 0$ such that, for every Shor normal form $\mathcal{S} = (n, \mathbf{A}, \mathbf{M})$ with $k = |\mathbf{A}| + |\mathbf{M}| \geq 1$ equations, $P'(\mathcal{S})$ has less then $\beta k n$ vertices.

We now formalize the term "size" of a rational 4-polytope P. For this let $P = (\boldsymbol{p}_1, \boldsymbol{p}_2, \ldots, \boldsymbol{p}_n) \in (\mathbb{R}^4)^n$ be any 4-polytope with n vertices $\boldsymbol{p}_i = (p_i^1, p_i^2, p_i^3, p_i^4) \in \mathbb{R}^4$. Let $\nu(P)$ be defined by

$$\nu(P) := \min \left(\max \{ \, p_i^j \mid 1 \leq i \leq n; \; 1 \leq j \leq 4 \, \} \right)$$

where the minimum is taken over all realization of P in the integer grid $(\mathbb{N}^4)^n$. If P does not have a rational realization, then $\nu(P)$ is undefined. Thus

$$\nu(n, 4) = \max \{ \, \nu(P) \mid P \text{ is a rational 4-polytope with } n \text{ vertices} \, \}$$

THEOREM 9.3.3.   *There exists a constant c such that, for infinitely many $n \in \mathbb{N}$, there is a 4-polytope P on n points with $\nu(P) \geq 2^{2^{c \sqrt[3]{n}}}$.*

PROOF.   The proof of this lower bound on $\nu(n, 4)$ is based on the following construction. For $m \in \mathbb{N}$ we consider a Shor normal form $\mathcal{S}_m$ on m variables

$$1 < x_1 < x_2 < \ldots < x_m.$$

The m equations of $\mathcal{S}_n$ are

$$\begin{aligned} x_1 &= 1 + 1 \\ x_i &= x_{i-1} \cdot x_{i-1} \quad \text{for} \quad i = 2, \ldots, m. \end{aligned}$$

This system has the unique solution $x_i = 2^{2^{i-1}}$ for $i = 1, \ldots, m$. By the Universality Theorem, $\boldsymbol{P}_m := \boldsymbol{P}(\mathcal{S}_m)$ has a realization with integral vertex coordinates. Take a realization $\boldsymbol{P}_m$ that achieves the minimum $\nu_m = \nu(\boldsymbol{P}_m)$. We may assume that $\boldsymbol{P}_m$ is chosen such that the 2-dimensional affine space supporting the central computation frame does not contain the unit vectors $e_1 = (1,0,0,0)$ and $e_2 = (0,1,0,0)$. By Lemma 9.3.1, the number of vertices $v_m = |\text{vert}(\boldsymbol{P}_m)|$ is bounded from above by the polynomial αm^3. Thus

$$v_m < \alpha m^3 \quad \implies \quad \sqrt[3]{v_m} \cdot \alpha' < m, \qquad (*)$$

with a new constant α'. If we consider the central computation frame in $\boldsymbol{P}_m$ with edges $[\boldsymbol{0}, \boldsymbol{1}, x_1, \ldots, x_m, \boldsymbol{\infty}]$, we get

$$(\boldsymbol{0}, \boldsymbol{\infty} \,|\, \boldsymbol{1}, x_m) = 2^{2^{m-1}},$$

where $(\boldsymbol{0}, \boldsymbol{\infty} \,|\, \boldsymbol{1}, x_m)$ represents the cross ratio of the slopes of the edge supporting lines. This cross ratio is well defined, since these lines are in a common plane. For $i \in \{\boldsymbol{0}, \boldsymbol{1}, x_m, \boldsymbol{\infty}\}$ let $\boldsymbol{p}_i$ and $\boldsymbol{q}_i$ be the two vertices that lie on the edge i and let $\boldsymbol{r}_i := \boldsymbol{p}_i - \boldsymbol{q}_i \in \mathbb{R}^4$. The absolute values of the coordinates of $\boldsymbol{r}_i$ are bounded by $2\nu_m$. The cross ratio $(\boldsymbol{0}, \boldsymbol{\infty} \,|\, \boldsymbol{1}, x_m)$ can be computed as

$$\frac{\det(\boldsymbol{r_0}, \boldsymbol{r_1}, e_1, e_2) \cdot \det(\boldsymbol{r_\infty}, \boldsymbol{r}_{x_m}, e_1, e_2)}{\det(\boldsymbol{r_0}, \boldsymbol{r}_{x_m}, e_1, e_2) \cdot \det(\boldsymbol{r_\infty}, \boldsymbol{r_1}, e_1, e_2)} = 2^{2^{m-1}}.$$

The numerator η is bounded from above by $64\nu_m^4$. This bound is achieved when each of the entries of r_i takes the maximal value $2\nu_m$. On the other hand it has to be at least $2^{2^{m-1}}$ since both the numerator and the denominator are integral:

$$2^{2^{m-1}} < \eta < 64\nu_m^4.$$

From this we get $2^{2^{m/2}} < \nu_m$ for sufficiently large m. Combining this equation with $(*)$ we get the desired result. $\qquad\qquad\qquad\qquad\qquad\qquad\qquad\qquad\quad\square$

This bound can be slightly improved if one uses the construction of the polytope $\boldsymbol{P}'(\mathcal{S})$ instead of $\boldsymbol{P}(\mathcal{S})$. We then get:

<u>REMARK 9.3.4.</u> There exists a constant c' such that, for infinitely many $n \in \mathbb{N}$, there is a 4-polytope $\boldsymbol{P}$ on n points with $\nu(\boldsymbol{P}) \geq 2^{2^{c'\sqrt{n}}}$.

9.4 Infinite Classes of Non-Polytopal Combinatorial 3-Spheres

We now switch to a different problem: the characterization of polytopality of combinatorial spheres. By Steinitz's Theorem every combinatorial 2-sphere is polytopal. The smallest example of a non-polytopal 3-sphere is due to Barnette, and has 8 vertices. For a long time it was believed that there might be a characterization of polytopality by excluding a finite set of "forbidden minors". We here prove that already in dimension 4 there are infinitely many minor-minimal non-polytopal combinatorial spheres. A construction presented in [57] for that purpose turned out to be incorrect (see [65]).

   If one considers minors of polytopes, one usually has to consider minors obtained by *deletion* and *contraction* of vertices. However, by contraction of a vertex of a combinatorial 3-sphere we obtain a combinatorial 2-sphere, which is polytopal by Steinitz's Theorem. Therefore we may restrict ourselves to the case of deletions only.

$\underline{\text{DEFINITION 9.3.1.}}$ Let P be a combinatorial polytope on the index set X. The *deletion* of a vertex set $A \in X$ is the face list

$$P \setminus A := \{F \mid F \in P \text{ and } A \cap F = \emptyset\}.$$

   Intuitively the deletion of a vertex set A is obtained by removing all facets that contain vertices of A from the combinatorial polytope. Notice that a deletion $P \setminus A$ is in general no longer a combinatorial polytope, since this operation "cuts a hole" into the boundary of the polytope. However, the resulting set system may appear as a subset of the face list of a larger combinatorial polytope.

$\underline{\text{THEOREM 9.3.2.}}$ *There is an infinite class of non-polytopal combinatorial 4-polytopes $\boldsymbol{P}_4$, $\boldsymbol{P}_6$, $\boldsymbol{P}_8, \ldots$ such that every minor (by deletion) of P_n that has $n-1$ elements can be completed to the facet list of a 4-polytope.*

PROOF. Let n be chosen in $\{4, 6, 8, \ldots\}$. Let $\mathcal{S}_n$ be a Shor normal form on $n+1$ variables

$$1 < x_2 < x_3 < \ldots < x_n < x_{n+1} < x'_{n+1}.$$

We set $x_1 = 1$ and define $\mathcal{S}_n$ by the following list of elementary additions:

$$
\begin{array}{rclcrcl}
x_2 & = & x_1 + x_1 & & x_3 & = & x_1 + x_2 \\
x_4 & = & x_2 + x_2 & & x_5 & = & x_3 + x_2 \\
x_6 & = & x_4 + x_2 & & x_7 & = & x_5 + x_2 \\
& \vdots & & & & \vdots & \\
x_n & = & x_{n-2} + x_2 & & x_{n+1} & = & x_{n-1} + x_2 \\
x'_{n+1} & = & x_n + x_1 & & & &
\end{array}
$$

The only solution of these equation is given by $x_i = i$ for $i = 1, \ldots, n+1$ and $x'_{n+1} = n+1$. Thus the variety $V(\mathcal{S}_n)$ is empty since we have $x_{n+1} = x'_{n+1}$ which contradicts the inequality $x_{n+1} < x'_{n+1}$. Therefore the combinatorial polytope

$\boldsymbol{P}_n = \boldsymbol{P}(\mathcal{S}_n)$ is not realizable. However, deleting any of the above equations (except for $x_2 = x_1 + x_1$) makes the whole system solvable.

For every minor $\boldsymbol{P}'$ of $\boldsymbol{P}_n$ on $n-1$ elements X', there is at least one of these equations such that X' has no vertices in the corresponding addition polytope. Therefore this minor can be completed to the facet list of $\boldsymbol{P}(\mathcal{S}'_n)$, where this equation is missing completely. This is realizable by the above observation. $\quad\square$

Using Lawrence extensions and connected sums there are many alternative ways of obtaining minor-minimal non-polytopal 3-spheres (without making the detour around encoding polynomial equations). We sketch here a particularly simple construction for this purpose.

For this we need a new basic building block $\boldsymbol{X}^+$ that is a perturbed version of the polytope $\boldsymbol{X}$ of Section 5.4. The polytope $\boldsymbol{X}^+$ contains a hexagonal 2-face $\boldsymbol{G} = \boldsymbol{G}(1,\dots,6)$ such that in *no* realization of $\boldsymbol{X}^+$ the vertices $1 \wedge 4$, $2 \wedge 3$ and $5 \wedge 6$ are collinear. (More precisely, after normalizing $\boldsymbol{G}$ by making the edges 1 and 4 parallel with infinite slope, the line $(2 \wedge 3) \vee (5 \wedge 6)$ will have positive slope.) We can construct such a polytope in a way similar to the construction of $\boldsymbol{X}$.

- Start with a hexagon $\boldsymbol{G} = \boldsymbol{G}(1,\dots,6)$, for which the edges 1 and 4 are parallel with infinite slope, and the line $(2 \wedge 3) \vee (5 \wedge 6)$ has positive slope.
- Form $\boldsymbol{P} = \mathbf{tent}^{1,4}(\boldsymbol{G})$, a tent over $\boldsymbol{G}$. If a and b are the apices of the tent, then the lines $(2 \wedge 3) \vee a$ and $(5 \wedge 6) \vee b$ do not meet in a point.
- Let $\boldsymbol{q}_y$ be a point that is on the intersection of $(2 \wedge 3) \vee a$ and the supporting plane of the triangle spanned by edge 5 and vertex b. This point does not lie on the supporting plane of the triangle spanned by edge 6 and vertex b.
- Perform a Lawrence extension at the point $\boldsymbol{q}_y$. We define

$$\boldsymbol{X}^+ = \boldsymbol{\Lambda}(\boldsymbol{P}, \{\boldsymbol{q}_y\}).$$

A proof similar to Theorem 5.4.1 shows that $\boldsymbol{X}^+$ has the claimed properties. Let $X = (1,\dots,6)$ and $n \in N$. We define the "Non-Steinitz" combinatorial sphere $\boldsymbol{NS}_n$ by

$$\boldsymbol{NS}_n := \boldsymbol{X} \; \#_X \; \underbrace{\boldsymbol{T}_X \; \#_X \; \boldsymbol{T}_X \; \#_X \; \cdots \; \#_X \; \boldsymbol{T}_X}_{n \text{ times}} \; \#_X \; \boldsymbol{X}^+.$$

A construction diagram is given below.
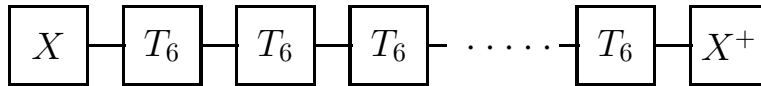
Figure 9.4.1 illustrates this chain of polytopes in a less schematic and more geometric way. Between two adjacent polytopes in the chain a connected sum operation along the prism over the hexagon has to be performed.
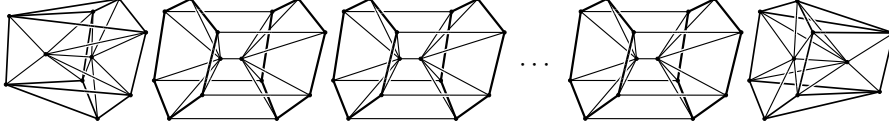
Figure 9.4.1: Construction of the non-Steinitz spheres.

<u>THEOREM 9.4.3.</u>   *For each n the combinatorial 3-sphere $\boldsymbol{NS}_n$ is not polytopal, but every minor obtained by deletion can be completed to a polytopal face lattice.*

PROOF.   Let $n \in \mathbb{N}$ be fixed. We first prove that $\boldsymbol{NS}_n$ is not realizable as the boundary complex of a polytope. For this first consider the sub-polytope

$$\boldsymbol{NS}_n' := \boldsymbol{X} \ \#_X \ \underbrace{\boldsymbol{T}_X \ \#_X \ \boldsymbol{T}_X \ \#_X \ \cdots \ \#_X \ \boldsymbol{T}_X}_{n \text{ times}}.$$

This boundary complex is realizable. To see this, take a realization of a polytope $\boldsymbol{X}$ and successively form connected sums with transmitter $\boldsymbol{T}_X$. The "open hexagon" of the final transmitter in the chain has still the projective property that is inherited from the polytope $\boldsymbol{X}$, namely that the points $1 \wedge 4$, $2 \wedge 3$ and $5 \wedge 6$ not collinear. Thus it is impossible to (geometrically) perform a connected sum operation with a realization of $\boldsymbol{X}^+$, which has the contrary property on the relevant hexagon. Thus $\boldsymbol{NS}_n$ is not realizable.

We only sketch the minor-minimality part. We simply have to check that every vertex of $\boldsymbol{NS}_n$ really plays a role in the non-polytopality. This is easily seen, since the vertices of the $\boldsymbol{X}$ and $\boldsymbol{X}^+$ polytopes are necessary to encode their projective condition. Likewise the vertices of the transmitters are essential for the transmitting property. Deleting a point of the Lawrence extension would destroy this property, since deleting a point in a hexagon would destroy the information that is "stored" in this hexagon.   □

10   Universality for 3-Diagrams and 4-Fans

10.1   3-Diagrams and 4-Fans

How far can we relax the concept of a polytope and still obtain a universality theorem? Our proof of the Universality Theorem for polytopes is essentially based on the fact that affine dependencies among the vertices of a 4-polytope may encode projective relations on vertices. A careful analysis of the basic building blocks shows that nearly all dependencies used in our construction are 2-dependencies (i.e., dependencies that force certain points to lie on a common 2-dimensional plane). The only basic building block in which 3-dependencies are actually used is the polytope X. In this section we will alter our construction of the polytope $P(S)$ slightly (by replacing the polytope X by a variant X^* that forces the same projective condition on the relevant hexagonal face). We aim for a polytope $P'(S)$ that has the following property:

> The realization space of $P'(S)$ is stably equivalent to $V(S)$ and is already determined by the 2-skeleton of $P'(S)$.

This construction allows us to transfer our results also to 3-dimensional diagrams and 4-dimensional fans (for an introduction to the theories of diagrams and fans see [31] and [65]). Thus we get "bad realization spaces," non-rational examples, NP-completeness, etc., for these objects, too. However, here we will not prove such universality theorems in their full generality (involving statements on stable equivalence), since this involves a rather technical analysis similar to the proof of Lemma 8.3.1. We restrict ourselves to the proof that all elements of a given primary semialgebraic set V can be recovered from the set of all realizations of a certain 3-diagram $\mathcal{D}(V)$ (resp. 4-fan $\mathcal{F}(V)$).

We start by formal definitions of *polytopal complexes* and *diagrams*. These objects are collections of polytopes, satisfying several "good" intersection properties. In order to express these intersection properties in the easiest way possible, we will consider a polytope P really as a "massive" convex object $\mathbf{conv}(P)$ and not just as the collection of its vertices P. So in the following definitions a *polytope P* means the convex hull of the vertex set P. By ∂P we denote the boundary of P.

<u>DEFINITION 10.1.1.</u>   A *polytopal complex* $\mathcal{C}$ is a finite collection of polytopes such that

 (i) the empty polytope is in $\mathcal{C}$,
 (ii) if $P \in \mathcal{C}$, then all faces of P are also in $\mathcal{C}$,
(iii) the intersection $P \cap Q$ of two polytopes $P, Q \in \mathcal{C}$ is a face of both P and Q.

The dimension of $\mathcal{C}$ is the largest dimension of a polytope in $\mathcal{C}$.

We may consider the set system $\mathcal{C}$ as a partially ordered set (poset, for short) where the order relation is induced by geometric inclusion. We refer to the poset $(\mathcal{C}, \subseteq)$ as the *combinatorial structure* of $\mathcal{C}$.

<u>DEFINITION 10.1.2.</u>   A *d-diagram* $\mathcal{D} = (\mathcal{C}, \boldsymbol{P})$ is a pair of a polytopal complex $\mathcal{C}$ and a polytope $\boldsymbol{P}$ such that

(i) The union $\bigcup \{ \boldsymbol{Q} \mid \boldsymbol{Q} \in \mathcal{C} \}$ of all polytopes in $\mathcal{C}$ is the polytope $\boldsymbol{P}$.

(ii) If $\boldsymbol{Q} \in \mathcal{C}$, then $\boldsymbol{Q} \cap \partial \boldsymbol{P}$ is a (possibly empty) face of $\boldsymbol{P}$.

The polytope $\boldsymbol{P}$ is called the *basis* of the diagram. The polytopes of full dimension in $\mathcal{C}$ are called *inner cells*.

Schlegel diagrams, which we used throughout the paper in order to visualize 4-polytopes, are by this definition a special kind of 3-diagrams. The facet $\boldsymbol{F}$ onto which the $(d-1)$-skeleton of $\boldsymbol{P}$ is projected then becomes the basis of the Schlegel diagram. In general a d-polytope $\boldsymbol{P}$ and a facet $\boldsymbol{F}$ do not uniquely determine a Schlegel diagram, since we have some freedom in choosing the projection. However, up to projective equivalence we can always assume that $\boldsymbol{P}$ is given in a way such that $\pi(\boldsymbol{P}) = \boldsymbol{F}$ for the orthogonal projection π onto the facet $\boldsymbol{F}$. For such a polytope $\boldsymbol{P}$, we denote by $\mathcal{D}(\boldsymbol{P}, \boldsymbol{F})$ the Schlegel diagram, which is generated by orthogonal projection of the $(d-1)$-skeleton of $\boldsymbol{P}$ onto the facet $\boldsymbol{F}$. (In fact, every Schlegel diagram can be represented in this way.)

The diagram $\mathcal{D}(\boldsymbol{P}, \boldsymbol{F})$ encodes the complete combinatorial structure of $\boldsymbol{P}$. The poset of all polytopes in $\mathcal{D}(\boldsymbol{P}, \boldsymbol{F})$ partially ordered by inclusion equals the face lattice of $\boldsymbol{P}$ after the facet $\boldsymbol{F}$ and $\boldsymbol{P}$ itself have been removed. However, not every realization of $\mathcal{D}(\boldsymbol{P}, \boldsymbol{F})$ (considered as a diagram) is actually a Schlegel diagram. Some realizations of the diagram $\mathcal{D}(\boldsymbol{P}, \boldsymbol{F})$ may be liftable to a realization of $\boldsymbol{P}$, some may be not.

We consider the collection $(\boldsymbol{p}_1, \ldots, \boldsymbol{p}_n)$ of all vertices (i.e. 0-polytopes) of $\mathcal{C}$. A *realization* of the diagram $\mathcal{D}$ is a point configuration $\boldsymbol{Q} = (\boldsymbol{q}_1, \ldots, \boldsymbol{q}_n) \in \mathbb{R}^{d \cdot n}$ that is the vertex set of a d-diagram $\mathcal{D}'$ that is combinatorially isomorphic to $\mathcal{D}$ under the canonical correspondence $\boldsymbol{q}_i \to \boldsymbol{p}_i$. (Warning: Unlike in the case of polytopes the vertex set of a diagram does not uniquely determine the combinatorial type. The same vertex set may support several combinatorially different diagrams.) For the definition of the *realization space* of a diagram we restrict ourselves to the case of d-diagrams $\mathcal{D} = (\mathcal{C}, \Delta_d)$, for which the basis is a d-simplex Δ_d (in order to have a — up to affine equivalence — unique representation of the basis of $\mathcal{D}$). We assume that $\boldsymbol{p}_1, \ldots, \boldsymbol{p}_{d+1}$ are the vertices of Δ_d. The realization space $\mathcal{R}(\mathcal{D})$ is the set of all realizations of $\mathcal{D}$ for which $\boldsymbol{p}_i = \boldsymbol{q}_i$ for $i = 1, \ldots, d+1$. Later on we will prove the following theorem:

<u>THEOREM 10.1.3.</u>   *For every Shor normal form $\mathcal{S}$ with $V(\mathcal{S}) \neq \emptyset$, there is a 3-diagram $\mathcal{D}(\mathcal{S}) = (\mathcal{C}(\mathcal{S}), \Delta_3)$ such that there exists a surjective rational map f defined on $\mathcal{R}(\mathcal{D}(\mathcal{S}))$ with $f(\mathcal{R}(\mathcal{D}(\mathcal{S}))) = V(\mathcal{S})$. Moreover, the combinatorial structure of $\mathcal{D}(\mathcal{S})$ can be generated in polynomial time from $\mathcal{S}$.*

In other words, we can recover all solutions of a given system of polynomial equations and strict inequalities by investigating the realization space of a certain 3-diagram.

<u>REMARK 10.1.4.</u> In fact, a careful analysis similar to the one used in the proof of Lemma 8.3.1 shows that $\mathcal{R}(\mathcal{D}(\mathcal{S}))$ is stably equivalent to $V(\mathcal{S})$.

Fans are the linear counterparts of polytopal complexes. A fan is composed from a collection of cones that have "nice" intersection properties. For the definition of fans we consider a cone $\boldsymbol{P}$ as "massive" object $\mathbf{pos}(\boldsymbol{P})$ and not just as a collection of its vertices. We furthermore assume that every cone $\boldsymbol{P}$ under consideration is *pointed*, i.e., there exists a linear hyperplane H such that $\boldsymbol{P} \cap H$ is the zero vector.

<u>DEFINITION 10.1.5.</u> A *fan* $\mathcal{F}$ in $\mathbb{R}^d$ is a finite collection of non-empty polyhedral cones such that

   (i) if $\boldsymbol{P} \in \mathcal{F}$, then all non-empty faces of $\boldsymbol{P}$ are also in $\mathcal{F}$,
   (ii) the intersection $\boldsymbol{P} \cap \boldsymbol{Q}$ of two cones $\boldsymbol{P}, \boldsymbol{Q} \in \mathcal{F}$ is a face both of $\boldsymbol{P}$ and of $\boldsymbol{Q}$.

The dimension of $\mathcal{F}$ is the largest dimension of a cone in $\mathcal{F}$. A fan $\mathcal{F}$ is *complete* if the union $\bigcup \{\boldsymbol{P} \mid \boldsymbol{P} \in \mathcal{F}\}$ is $\mathbb{R}^d$.

All elements of a fan $\mathcal{F}$ ordered by inclusion define a poset to which we refer as the *combinatorial type* of $\mathcal{F}$. Every d-polytope $\boldsymbol{P}$ that contains the origin $\boldsymbol{0}$ in its interior generates a corresponding d-fan $\mathcal{F}(\boldsymbol{P})$: the *face fan* of $\boldsymbol{P}$. The cones of $\mathcal{F}(\boldsymbol{P})$ are the positive hulls of faces of $\boldsymbol{P}$. However there are also fans that do not come from a polytope in that way (see [65]). The 1-dimensional cones in $\mathcal{F}$ are called the *vertices* of $\mathcal{F}$. We represent each vertex $\boldsymbol{v}$ by a point $\boldsymbol{p} \in \mathbb{R}^d$ whose positive hull is $\boldsymbol{v}$. Like a diagram, a fan is not uniquely described by its vertices. There may be different fans supported by the same vertex set.

We consider the collection $(\boldsymbol{p}_1, \ldots, \boldsymbol{p}_n) \in \mathbb{R}^{d \cdot n}$ of all vertices of a complete d-fan $\mathcal{F}$. A *realization* of $\mathcal{F}$ is a point configuration $\boldsymbol{Q} = (\boldsymbol{q}_1, \ldots, \boldsymbol{q}_n) \in \mathbb{R}^{d \cdot n}$ for which under the canonical correspondence $\boldsymbol{q}_i \to \boldsymbol{p}_i$ the configuration $\boldsymbol{Q}$ represents the vertex set of a d-fan $\mathcal{F}'$ that is combinatorially isomorphic to $\mathcal{F}$. A *basis* of $\mathcal{F}$ is a collection $B = (\boldsymbol{p}_1, \ldots, \boldsymbol{p}_d)$ of vertices of one cone in $\mathcal{F}$ that is linearly independent in every realization of $\mathcal{F}$. The *realization space* $\mathcal{R}(\mathcal{F}, B)$ is the set of all realizations $(\boldsymbol{q}_1, \ldots, \boldsymbol{q}_n)$ of $\mathcal{F}$ with $\boldsymbol{p}_i = \boldsymbol{q}_i$ for $i = 1, \ldots, d$. With this we are going to prove:

<u>THEOREM 10.1.6.</u> *For every Shor normal form $\mathcal{S}$ with $V(\mathcal{S}) \neq \emptyset$, there is a complete 4-fan $\mathcal{F}(\mathcal{S})$ with basis B such that there exists a surjective rational map g defined on $\mathcal{R}(\mathcal{F}(\mathcal{S}), B)$ with $g(\mathcal{R}(\mathcal{F}(\mathcal{S}), B)) = V(\mathcal{S})$. Moreover, the combinatorial structure of $\mathcal{F}(\mathcal{S})$ can be generated in polynomial time from $\mathcal{S}$.*

REMARK 10.1.7. Again, a careful analysis (omitted here) would prove that $\mathcal{R}(\mathcal{F}(V))$ is stably equivalent to $V(\mathcal{S})$.

The diagram $\mathcal{D}(\mathcal{S})$ whose existence is claimed in Theorem 10.1.3 arises as Schlegel diagram $\mathcal{D}(\boldsymbol{P}'(\mathcal{S}), \Delta_3)$ of the polytope $\boldsymbol{P}'(\mathcal{S})$, a slight modification of our original construction $\boldsymbol{P}(\mathcal{S})$. Here Δ_3 is any tetrahedral facet of $\boldsymbol{P}'(\mathcal{S})$ (there are many such facets already in the starting polytope $\boldsymbol{S}(\mathcal{S})$, which is a doubly iterated pyramid over an n-gon). Since we consider only the case where $V(\mathcal{S})$ is not empty there will always exist proper realizations of $\boldsymbol{P}'(\mathcal{S})$. The fan $\mathcal{F}(\mathcal{S})$, whose existence is claimed in Theorem 10.1.6, arises as face fan $\mathcal{F}(\boldsymbol{P}'(\mathcal{S}))$ of $\boldsymbol{P}'(\mathcal{S})$, where we may assume that w.l.o.g the origin lies in the interior of this polytope. We label the elements of $\mathcal{D}(\mathcal{S})$ and of $\mathcal{F}(\mathcal{S})$ in the way that is canonically inherited from the polytope $\boldsymbol{P}'(\mathcal{S})$. We will describe the precise construction of $\boldsymbol{P}'(\mathcal{S})$ in the next section. For now it is enough for us to know that $\boldsymbol{P}'(\mathcal{S})$ satisfies a statement analogous to Theorem 8.1.1 for $\boldsymbol{P}(\mathcal{S})$:

> $\boldsymbol{P}'(\mathcal{S})$ contains a normal computation frame $\boldsymbol{G}$. After standardization the slopes of $\boldsymbol{G}$ correspond to points in $V(\mathcal{S})$ and all points of $V(\mathcal{S})$ can be represented in this way. Moreover, the combinatorial type of $\boldsymbol{P}'(\mathcal{S}(V))$ can be computed in polynomial time from $\mathcal{S}$.

In $\mathcal{D}(\mathcal{S})$ there exists a 2-face $\boldsymbol{G}$ that corresponds to the computation frame in the above statement. The rational map f in Theorem 10.1.3 is simply the map that describes the process of standardization and calculating the slopes of $\boldsymbol{G}$ in $\mathcal{D}(\mathcal{S})$. To prove Theorem 10.1.3 we have to prove

$$f(\mathcal{R}(\mathcal{D}(\mathcal{S}))) \subseteq V(\mathcal{S}) \quad \text{and} \quad f(\mathcal{R}(\mathcal{D}(\mathcal{S}))) \supseteq V(\mathcal{S}).$$

The second fact follows directly from the fact that every element of $V(\mathcal{S})$ can be described by the edge slopes of $\boldsymbol{G}$ in a certain realization of $\boldsymbol{P}'(\mathcal{S})$. So it remains to prove that in every realization of $\mathcal{D}(\mathcal{S})$ (considered as diagram) after standardization the slopes of $\boldsymbol{G}$ form an element of $V(\mathcal{S})$.

The situation for Theorem 10.1.6 is similar. In $\mathcal{F}(\mathcal{S})$ we find a cone $\boldsymbol{G}$ that corresponds to the computation frame of $\boldsymbol{P}'(\mathcal{S})$. The map g in this theorem is the map that models cutting the cone $\boldsymbol{G}$ with a hyperplane, standardizing the resulting n-gon and calculating the slopes. In the proof of $g(\mathcal{R}(\mathcal{F}(\mathcal{S}), B)) = V(\mathcal{S})$ again the $\supseteq$-part is trivial and it remains to show that in every realization of $\mathcal{F}(\mathcal{S})$ (considered as fan) after cutting and standardization the slopes of $\boldsymbol{G}$ form an element of $V(\mathcal{S})$.

10.2   The Polytope $\boldsymbol{P}'(\mathcal{S})$

The basic reason that allows us to transfer the Universality Theorem to diagrams is the fact that the projective properties of the basic building blocks are determined already by their 2-skeletons. Unfortunately, this is not the case for the polytope $\boldsymbol{X}$ which was used to generate a non-prescribable hexagon.

We here present an alternative basic building block $\boldsymbol{X}^*$ that contains a hexagon $\boldsymbol{G}_6 = \boldsymbol{G}(1, \ldots, 6)$ such that in every realization of $\boldsymbol{X}^*$ the points $1 \wedge 4$, $2 \wedge 3$ and $5 \wedge 6$ are collinear. In $\boldsymbol{X}^*$ this property is already induced by the 2-skeleton, as we will see in the next section. The polytope $\boldsymbol{X}^*$ is constructed as follows:

- Start with a realization of the polytope $\boldsymbol{X}$.
- $\boldsymbol{X}$ contains two tetrahedral facets. For each of these tetrahedra form the intersection of the four adjacent facets. Call these two new points of intersection $\boldsymbol{p}$ and $\boldsymbol{q}$.
- If necessary, apply a projective transformation such that the vertices of $\boldsymbol{X}$ together with $\boldsymbol{p}$ and $\boldsymbol{q}$ lie in convex position.
- The vertices of $\boldsymbol{X}^*$ are the vertices of $\boldsymbol{X}$ together with $\boldsymbol{p}$ and $\boldsymbol{q}$.

Figure 10.2.1 shows a Schlegel diagram of $\boldsymbol{X}$ and the corresponding Schlegel diagram of $\boldsymbol{X}^*$. The polytope $\boldsymbol{X}^*$ has and 12 vertices and 8 facets (six triangular prisms, one tent over a hexagon and one more facet that can be obtained by truncating two vertices of a hexagonal pyramid).
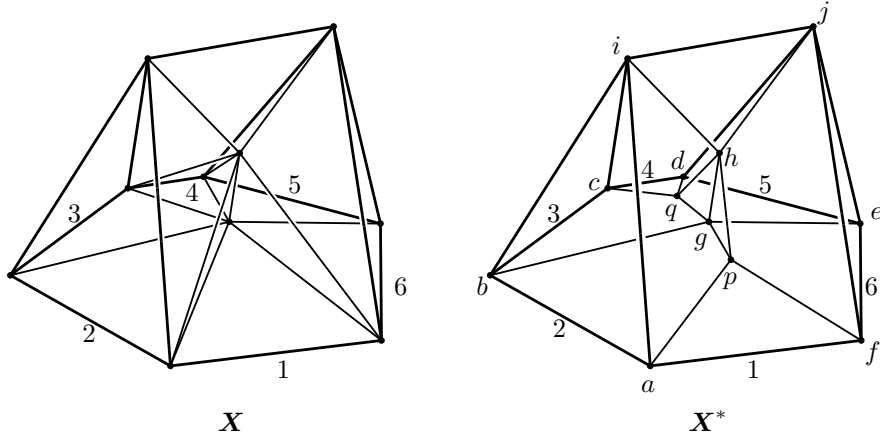
Figure 10.2.1: An alternative construction for a non-prescribable 2-face.

<u>LEMMA 10.2.1.</u> *In every realization $\boldsymbol{P}$ of $\boldsymbol{X}^*$, the points $1 \vee 4$, $2 \vee 3$ and $5 \vee 6$ are collinear.*

PROOF. After deleting the points $\boldsymbol{p}$ and $\boldsymbol{q}$ from $\boldsymbol{P}$ we are left with a realization of $\boldsymbol{X}$ which has by Theorem 5.4.1 the desired property.   □

In order to replace all occurrences of the polytope $\boldsymbol{X}$ in the construction of the polytope $\boldsymbol{P}(\mathcal{S})$ by polytopes $\boldsymbol{X}^*$ we have to use an adaptor $\boldsymbol{A}_6$, since $\boldsymbol{X}^*$

does not contain a pyramid along which we could perform the connected sum operation. Thus we set:

To obtain the polytope $\boldsymbol{P}'(\mathcal{S})$ we replace each occurrence of the polytope $\boldsymbol{X}$ in the construction diagrams by a polytope $\boldsymbol{X}'$. Since the basic properties of the polytope $\boldsymbol{X}$ (as described in Theorem 5.4.1) are also valid for the polytope $\boldsymbol{X}^*$, we can replace the role of $\boldsymbol{P}(\mathcal{S})$ in Theorem 8.1.1 by the polytope $\boldsymbol{P}'(\mathcal{S})$ and we will still obtain valid statements.

10.3   Nets

For the proofs of Theorem 10.1.3 and Theorem 10.1.6 it remains to prove that

$$f(\mathcal{R}(\mathcal{D}(\mathcal{S}))) \subseteq V(\mathcal{S}) \quad \text{and} \quad g(\mathcal{R}(\mathcal{F}(\mathcal{S}), B)) \subseteq V(\mathcal{S}).$$

Instead of working on the level of diagrams and fans directly, we introduce an intermediate structure that forms a common framework for d-fans and $(d-1)$-diagrams of polytopes: *d-nets*.

<u>DEFINITION 10.3.1.</u>   For a d-polytope $\boldsymbol{P} = (\boldsymbol{p}_1, \ldots, \boldsymbol{p}_n) \in (\mathbb{R}^d)^n$ a *d-net* of $\boldsymbol{P}$ is a point configuration $\boldsymbol{Q} = (\boldsymbol{q}_1, \ldots, \boldsymbol{q}_n) \in (\mathbb{R}^d)^n$ such that for every facet F of $\boldsymbol{P}$ the d-cone $\boldsymbol{Q}\big|_F$ is a pointed cone that is combinatorially isomorphic to $\boldsymbol{P}\big|_F$.

In other words in a d-net of a polytope $\boldsymbol{P}$ every facet of $\boldsymbol{P}$ corresponds to a (combinatorially equivalent) cone. We do not require any additional intersection properties among these cones. For instance each polytope $\boldsymbol{P}$ for which the origin does not lie on one of the hyperplanes that support the facets is automatically a net of itself. Observe that by definition multiplying a point $\boldsymbol{q}_i$ in a net $\boldsymbol{Q} = (\boldsymbol{q}_1, \ldots, \boldsymbol{q}_n)$ by a positive scalar does not change the property of being a net. If we consider the points of a d-net $\boldsymbol{Q}$ as homogeneous coordinates the net can be interpreted as a structure in which simultaneously each facet of a polytope is represented by homogeneous coordinates.

<u>LEMMA 10.3.2.</u>   *Let $\boldsymbol{P}$ be a d-polytope that contains the origin in its interior. Let $\mathcal{D} = \mathcal{D}(\boldsymbol{P}, \boldsymbol{F})$ be a Schlegel diagram of $\boldsymbol{P}$ and let $\mathcal{F} = \mathcal{F}(\boldsymbol{P})$ be the face fan of $\boldsymbol{P}$. Then the following holds.*

 (i) *For every realization $\boldsymbol{Q}$ of the diagram $\mathcal{D}$ the homogenization $\boldsymbol{Q}^{\mathrm{hom}}$ is a net of $\boldsymbol{P}$.*

 (ii) *Every realization $\boldsymbol{Q}$ of the fan $\mathcal{F}$ is a net of $\boldsymbol{P}$.*

PROOF. Let $\boldsymbol{Q}$ be a realization of $\mathcal{D}$. The vertices of $\boldsymbol{P}$ canonically correspond to the vertices of $\boldsymbol{Q}$. For every face F of $\boldsymbol{P}$ the point configuration $\boldsymbol{Q}\big|_F$ forms a realization of F (either as basis of $\mathcal{D}$ or as inner cell), and $(\boldsymbol{Q}\big|_F)^{\mathrm{hom}}$ describes this facet by homogeneous coordinates. This proves Part (i).

To see Part (ii) let $\boldsymbol{Q}$ be a realization of $\mathcal{F}$. The vertices of $\boldsymbol{P}$ canonically correspond to the vertices of $\boldsymbol{Q}$. By the definition of a fan for every face F of $\boldsymbol{P}$ the point configuration $\boldsymbol{Q}\big|_F$ represents a cone that is combinatorially equivalent to F, and therefore describes this facet by homogeneous coordinates. $\qquad\square$

If we are interested in incidence relations only (for a moment neglecting convexity) we may consider the points in a net of a d-polytope $\boldsymbol{P}$ as homogeneous coordinates in projective $(d-1)$-space. The $d-2$ faces of $\boldsymbol{P}$ then induce coplanarities of the net vertices (considered as points in projective space). With this model we prove that the main properties of our basic building blocks are also valid on the level of nets. For this we need the following simple lemma.

LEMMA 10.3.3. If h_1, h_2, and h_3 are hyperplanes in projective 3-space that have no line in common, then the lines $l_1 = h_2 \cap h_3$, $l_2 = h_1 \cap h_3$, and $l_3 = h_1 \cap h_2$ meet in a unique point $\boldsymbol{p}$.

PROOF. Since h_1, h_2, and h_3 do not have a line in common they have a unique point $\boldsymbol{p}$ of intersection. This point lies on l_1, l_2 and l_3. $\qquad\square$

We now study the nets of our basic building blocks considered as configurations in projective 3-space. Join and meet operations, coplanarity conditions, projective equivalences, etc. are always considered on this level. For sake of simplicity we label the vertices of a net of $\boldsymbol{P}$ in the way that is inherited from $\boldsymbol{P}$ (compare Section 5).

LEMMA 10.3.4. Let $\boldsymbol{Q}$ be a net of the polytope $\boldsymbol{T}_X$, where $X = (1,\ldots,n)$. Then the vertices of the n-gon $\boldsymbol{G}(X)$ and the vertices of the $\boldsymbol{G}(X')$ in $\boldsymbol{Q}$ are projectively equivalent (under the canonical combinatorial isomorphism).

PROOF. We refer to Figure 5.1.1 for the labeling. We consider $\boldsymbol{Q}$ as configuration in projective 3-space. We set $\boldsymbol{q}_i = (i-1,i) \wedge (i,i+1)$ and $\boldsymbol{q}_i' = ((i-1)',i) \wedge (i,(i+1)')$ for $i = 1,\ldots,n$, indices counted modulo n. For $i = 1,\ldots,n-1$ the following quadruples of points in $\boldsymbol{Q}$ are coplanar: $(\boldsymbol{q}_i, \boldsymbol{q}_{i+1}, \boldsymbol{q}_i', \boldsymbol{q}_{i+1}')$, $(\boldsymbol{q}_i, \underline{y}, \boldsymbol{q}_i', \overline{y})$ and $(\boldsymbol{q}_{i+1}, \underline{y}, \boldsymbol{q}_{i+1}', \overline{y})$. Furthermore, all $\boldsymbol{q}_i$ are coplanar and all $\boldsymbol{q}_i'$ are coplanar. By Lemma 10.3.1, the lines $\boldsymbol{q}_i \wedge \boldsymbol{q}_i'$, $\boldsymbol{q}_{i+1} \wedge \boldsymbol{q}_{i+1}'$, and $\underline{y} \wedge \overline{y}$ meet in a unique point $\boldsymbol{p}_i$, for $i = 1,\ldots,n-1$. Since each pair of such lines has a unique point of intersection, all points $\boldsymbol{p}_i$ must coincide. This common point of intersection forms the center of a projection that maps the vertices of $\boldsymbol{G}(X)$ to the vertices of $\boldsymbol{G}(X')$ (under the canonical combinatorial isomorphism). $\qquad\square$

LEMMA 10.3.5.   Let $\boldsymbol{Q}$ be a net of the polytope $\boldsymbol{T}_X^Y$, where $X = (1, \ldots, n)$ and $Y = (1', \ldots, (n+1)')$. Then the sets $\boldsymbol{L}_1$ and $\boldsymbol{L}_2$ of lines supporting the edges $1, \ldots, n$ and $1', \ldots, n'$ in $\boldsymbol{Q}$, respectively, are projectively equivalent (under the canonical combinatorial isomorphism).

PROOF. The proof is analogous to the proof of Lemma 10.3.4. $\square$

LEMMA 10.3.6.   Let $\boldsymbol{Q}$ be a net of the polytope $\boldsymbol{Y}_8^{1,5}$. Then the supporting lines of the edges $1, 1', 5$ and $5'$ in $\boldsymbol{Q}$ meet in a point.

PROOF. We refer to Figure 5.6.1 for the labeling. By Lemma 10.3.1 the supporting lines of the edges 1, $1'$ and $(y, \overline{y})$ in $\boldsymbol{Q}$ meet in a point. A similar statement holds for the edge triples $(5, 5', (y, \overline{y}))$, $(1, 5, (y, \overline{y}))$, and $(1', 5', (y, \overline{y}))$. Hence all these points of intersection coincide. This proves the lemma. $\square$

The above lemmas form the counterparts of Theorem 5.1.1, Theorem 5.3.1, and Theorem 5.6.1 on the level of nets. The only basic building blocks left now are adaptors and the polytope $\boldsymbol{X}^*$. We do not have to treat the adaptors, since they do not encode any projective condition. Treating the polytope $\boldsymbol{X}^*$ is a bit more elaborate.

LEMMA 10.3.7.   Let $\boldsymbol{Q}$ be a net of the polytope $\boldsymbol{X}^*$. Then the points $1 \vee 4$, $2 \vee 3$ and $5 \vee 6$ in $\boldsymbol{Q}$ are collinear.

PROOF. We refer to the vertex labeling given in Figure 10.2.1. By Lemma 10.3.1 we can conclude that the two triples of lines

$$(a \vee p, b \vee g, i \vee h), \ (f \vee p, e \vee g, j \vee h).$$

are both concurrent. We call the two corresponding points of intersection x and y, respectively. The points x and y lie on the three planes spanned by the triples of points

$$(i, j, h), \ (a, f, p), \ (b, e, g).$$

Therefore these three planes have a line ℓ in common. The three planes spanned by (i, j, h, x, y), (a, f, p, x, y) and (i, j, a, f) have a unique point z in common. At the point z the lines $i \vee j$, $a \vee f$ and ℓ intersect. Similarly, the three planes spanned by (b, e, g, x, y), (a, f, p, x, y) and (b, e, a, f) have a unique point z' in common. At the point z' the lines $b \vee e$, $a \vee f$ and ℓ intersect. Thus, z and z' coincide and the three lines $i \vee j$, $b \vee e$, $a \vee f$ are concurrent. By a symmetric argument one can show that $i \vee j$, $b \vee e$, $c \vee d$ are concurrent. This proves the claim. $\square$

We are now ready to prove the missing piece of the proofs of Theorem 10.1.3 and Theorem 10.1.6. The following lemma together with Lemma 10.3.2 implies these theorems immediately.

<u>LEMMA 10.3.8.</u> *Let $\mathcal{S}$ be a Shor normal form with $V(\mathcal{S}) \neq \emptyset$ and let $\boldsymbol{Q}$ be a net of the polytope $\boldsymbol{P}'(\mathcal{S})$. The vertices $\boldsymbol{q}_1, \ldots, \boldsymbol{q}_k \in \mathbb{R}^4$ of $\boldsymbol{Q}$ that correspond to the vertices of the central computation frame $\boldsymbol{G}$ of $\boldsymbol{P}'(\mathcal{S})$ satisfy:*

  (i) *There is an affine hyperplane $H \subset \mathbb{R}^4$ such that $\boldsymbol{G}' = H \cap \mathbf{pos}(\{\boldsymbol{q}_1, \ldots, \boldsymbol{q}_k\})$ is a convex k-gon.*
 (ii) *After standardization the slopes of $\boldsymbol{G}'$ satisfy*

$$(s_{x_1}, s_{x_2}, \ldots, s_{x_k}) \in V(\mathcal{S}).$$

PROOF. The point configuration $\boldsymbol{Q}$ was assumed to be a net of $\boldsymbol{P}'(\mathcal{S})$. By definition, for every facet of $\boldsymbol{P}$ there exists a hyperplane that truncates the positive hull of the corresponding points in $\boldsymbol{Q}$. Any such hyperplane of a facet that contains $\boldsymbol{G}$ satisfies the requirement of Part (i).

Part (ii) follows since the nets of our basic building blocks induce (by Lemma 10.3.4 up to Lemma 10.3.7) the same projective conditions on their information frames as the corresponding polytopes. Hence our constructions of polytopes given in Section 6 up to Section 8 apply word-by-word on the level of nets. $\square$

<u>REMARK 10.5.2.</u> There are two ways to prove the stronger version of the above Theorems stated in Remark 10.1.4 and Remark 10.1.7. One way is to make a detailed analysis (on the level of diagrams and fans) about the vertex loci that are allowed when successively adding basic building blocks (as we did in Lemma 8.3.1). The other way is to prove that every realization of the diagram $\mathcal{D}(\boldsymbol{P}'(\mathcal{S}), \Delta_3)$ is indeed a Schlegel diagram. This implies that the realization spaces $\mathcal{R}(\boldsymbol{P}'(\mathcal{S}))$ and $\mathcal{R}(\mathcal{D}(\boldsymbol{P}'(\mathcal{S}), \Delta_3))$ are stably equivalent.

10.4   The Corollaries

We can also apply the results of Section 9 to obtain immediately the following corollaries for fans and diagrams.

<u>COROLLARY 10.4.1.</u>

  (i) *All algebraic numbers are needed to coordinatize all 3-diagrams (4-fans).*
 (ii) *The realizability problem for 3-diagrams (4-fans) is NP-hard.*
(iii) *The realizability problem for 3-diagrams (4-fans) is (polynomial time) equivalent to the "Existential Theory of the Reals" (see [53]).*
 (iv) *There is a 3-diagram (4-fan) for which the shape of a 2-face cannot be arbitrarily prescribed.*
  (v) *Combinatorial types of 3-diagrams (4-fans) cannot be characterized by excluding a finite set of "forbidden minors."*
 (vi) *The maximum size of a 3-diagram (4-fan) with n vertices with integral coordinates is bounded from below by a doubly exponential function in n.*

PROOF. Part (i) is proved analogously to Theorem 9.2.1(i). Parts (ii) and (iii) are proved analogously to Theorem 9.1.2. Part (iv) is proved by the existence of the polytope $\boldsymbol{X}^*$, one of its Schlegel diagrams and its face fan. Part (v) is proved analogously to Theorem 9.3.2. Part (vi) is proved analogously to Theorem 9.2.3. $\square$

11 The Universal Partition Theorem for 4-Polytopes

This section deals with an interesting strengthening of the Universality Theorem:
the *Universal Partition Theorem.*

While the Universality Theorem dealt with a single primary semialgebraic
set, the Universal Partition Theorem is concerned with a family of such sets that
are nested in a complicated way. The main statement of the Universal Partition
Theorem is that (up to stable equivalence) one can recover certain families of
semialgebraic sets as a family of realization spaces of polytopes. These realization
spaces are nested in a way that is topologically equivalent to the nesting of the
original semialgebraic sets. A similar statement on the level of oriented matroids
was stated by Mnëv [50]. However, for a long time no proof was available. A proof
of a slightly weaker statement has recently been provided by Günzel [34, 52]. The
main difficulty in the proof of such a kind of statement is that one has to keep
track of many semialgebraic sets at the same time, encoding them all into the
same geometric situation.

11.1 Semialgebraic Families and Partitions

For an exact statement of a Universal Partition Theorem, we have to introduce
the concept of simultaneous stable equivalence of a family of basic semialgebraic
sets. For this, once again, we go back to the level of stable projections and rational
equivalences. We call a finite (ordered) collection $(V_1, \ldots, V_m)$ of pairwise disjoint
basic semialgebraic sets $V_i \subseteq \mathbb{R}^n$ a *semialgebraic family.* Let $\mathcal{V} = (V_1, \ldots, V_m)$
with $V_i \subseteq \mathbb{R}^n$ and let $\mathcal{W} = (W_1, \ldots, W_m)$ with $W_i \subseteq \mathbb{R}^{n+d}$ be semialgebraic
families with $\pi(W_i) = V_i$ for $i = 1, \ldots, n$, where π is the canonical projection
$\pi : \mathbb{R}^{n+d} \to \mathbb{R}^d$ that deletes the last d coordinates. $\mathcal{V}$ is a *stable projection* of $\mathcal{W}$
if for $i = 1, \ldots, m$ the W_i have the form

$$W_i = \left\{ (\boldsymbol{v}, \boldsymbol{v}') \in \mathbb{R}^{n+d} \mid \boldsymbol{v} \in V_i \text{ and } \phi_j^{\boldsymbol{v}}(\boldsymbol{v}') > 0; \ \psi_k^{\boldsymbol{v}}(\boldsymbol{v}') = 0 \text{ for all } j \in X; \ k \in Y \right\}.$$

Here X and Y denote finite (possibly empty) index sets. For $j \in X$ and $k \in$
Y the functions $\phi_j^{\boldsymbol{v}}$ and $\psi_k^{\boldsymbol{v}}$ are affine functionals whose parameters depend
polynomially on V. Thus we have

$$\phi_j^{\boldsymbol{v}}(\boldsymbol{v}') = \langle (\phi_j^1(\boldsymbol{v}), \ldots, \phi_j^d(\boldsymbol{v}))^T, \boldsymbol{v}' \rangle + \phi_j^{d+1}(\boldsymbol{v})$$

$$\psi_k^{\boldsymbol{v}}(\boldsymbol{v}') = \langle (\psi_k^1(\boldsymbol{v}), \ldots, \psi_k^d(\boldsymbol{v}))^T, \boldsymbol{v}' \rangle + \psi_k^{d+1}(\boldsymbol{v})$$

with polynomial functions $\phi_j^1(\boldsymbol{v}), \ldots, \phi_j^{d+1}(\boldsymbol{v})$ and $\psi_k^1(\boldsymbol{v}), \ldots, \psi_k^{d+1}(\boldsymbol{v})$.

Two semialgebraic families $\mathcal{V}$ and $\mathcal{W}$ are *rationally equivalent* if there exists
a homeomorphism $f : \bigcup_{i=1}^m V_i \to \bigcup_{i=1}^m W_i$ such that both f and f^{-1} are rational
functions and $f(V_i) = W_i$ for $i = 1, \ldots, m$.

<u>DEFINITION 11.1.1.</u> Two semialgebraic families $\mathcal{V}$ and $\mathcal{W}$ are *stably equivalent*, denoted $\mathcal{V} \approx \mathcal{W}$, if they are in the same equivalence class with respect to the equivalence relation generated by stable projections and rational equivalence.

These definitions are almost word-by-word repetitions of the corresponding definitions for basic semialgebraic sets. The only essential difference is that for semialgebraic families the functions ϕ_j, ψ_k and f are defined on $\bigcup_{i=1}^{m} V_i$ and identically used for all V_i. In particular $\mathcal{V} = (V_1, \ldots, V_m) \approx (W_1, \ldots, W_m) = \mathcal{W}$ implies $V_i \approx W_i$ for all $i = 1, \ldots, m$. Furthermore the topological structure of all sets V_i taken together is identical (up to a trivial fibration) to the topological structure of all sets W_i taken together.

<u>DEFINITION 11.1.2.</u> Let $V \in \mathbb{R}^n$ be a primary semialgebraic set and let $f_i, \ldots, f_m \in \mathbb{Z}[x_1, \ldots, x_n]$ be polynomial functions on $\mathbb{R}^n$. For $\sigma \in \{-1, 0, +1\}^m$ we abbreviate

$$V_\sigma := \{\boldsymbol{v} \in V \mid \mathbf{sign}(f_i(\boldsymbol{v})) = \sigma_i \text{ for all } i = 1, \ldots, m\}.$$

The collection of primary semialgebraic sets $(V_\sigma)_{\sigma \in \{-1,0,+1\}^m}$ is called a *partition* of V.

In particular, partitions are special semialgebraic families. Moreover, we can recover any primary semialgebraic set $W \in \mathbb{R}^n$ as a component of a partition of $\mathbb{R}^n$. To see this, we simply consider the partition that is induced by the polynomials of the defining equations $f_1(\boldsymbol{v}) = 0, \ldots, f_k(\boldsymbol{v}) = 0$ and defining strict inequalities $f_{k+1}(\boldsymbol{v}) > 0, \ldots, f_m(\boldsymbol{v}) > 0$ of W. We then have $W = V_\sigma$ with $\sigma = (\underbrace{0, \ldots, 0}_{k \text{ times}}, \underbrace{+1, \ldots, +1}_{m-k \text{ times}})$.

Figure 11.1.1 illustrates a partition $\mathcal{V}$ of $\mathbb{R}^2$ that is induced by two linear polynomials (the two lines) and two quadratic polynomials (the circle and the hyperbola). The elements of $\mathcal{V}$ that have maximal dimension are marked by the letters $a, \ldots, m$. In particular the sets $a, b, \ldots, e$ are disconnected.

The Universal Partition Theorem for 4-polytopes may now be stated as follows.

<u>THEOREM 11.1.3.</u> *For any partition* $\mathcal{V} = (V_\sigma)_{\sigma \in \{-1,0,+1\}^m}$ *of* $\mathbb{R}^n$ *there is a collection of (combinatorial) 4-polytopes* $(\boldsymbol{P}_\sigma)_{\sigma \in \{-1,0,+1\}^m}$ *with common basis* B *such that*

$$\mathcal{V} \approx (\mathcal{R}(\boldsymbol{P}_\sigma, B))_{\sigma \in \{-1,0,+1\}^m}.$$

In particular this theorem implies the Universality Theorem for 4-polytopes. We will give the proof of the Universal Partition Theorem for polytopes in the next few subsections. The proof given there does not rely on a Shor normal form. Thus we also have a second proof of the Universality Theorem that does not need Shor normal forms.
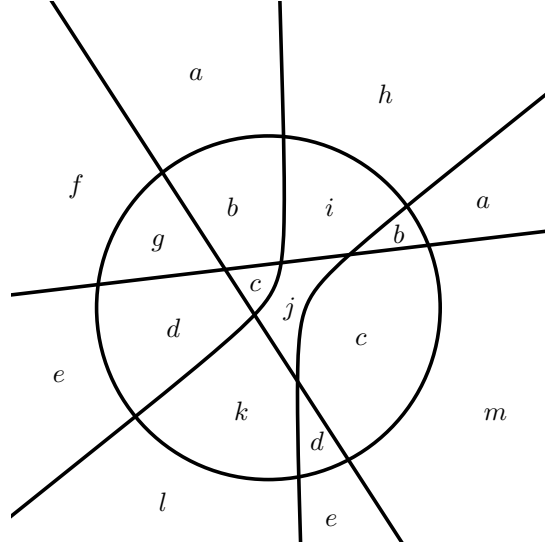
Figure 11.1.1: A partition of $\mathbb{R}^2$ by four polynomials.

11.2   Shor's Normal Form Versus Quadrilateral Sets

Why can't we give a proof of the Universal Partition Theorem based on a Shor normal form? In principle we could. However, unlike in the proof of the Universality Theorem we cannot use just the final result of Shor's Theorem. To obtain a proof of the Universal Partition Theorem, we would have to know exactly which of the inequalities in the chain $x_1 < x_2 < \ldots < x_n$ correspond to the inequalities in the original system of polynomials. Also we have to locate the places, at which the original equality signs are encoded. This requires detailed structural insight into the construction of a Shor normal form. Moreover, we would have to find a way to encode the choice of the signs into a class of polytopes that are related by a "small" change of their combinatorial structure. In particular these polytopes should have identical numbers of vertices. In the Shor normal form the number of variables involved (hence the number of vertices in a corresponding polytope) decreases if we replace an inequality by the corresponding equation.

How can we avoid all these problems and get a conceptually simple approach to the Universal Partition Theorem? The key idea for the Shor normal form is to have a total ordering on the variables and to have only additions and multiplications as elementary operations. We had to represent the additions $x + y = z$ (or the multiplications $x \cdot y = z$) as relations of x, y and z to the basis elements of the projective scale $\mathbf{0}, \mathbf{1}, \boldsymbol{\infty}$. The projective relations that correspond to this are known as *quadrilateral set relations*. So, in principle our polytopes for addition and multiplications were nothing else but constructions that (after

standardization) force quadrilateral set relations on the slopes of the edges of a 2-face.

If we use quadrilateral set relations directly as basic operations (rather than additions and multiplications) we obtain normal forms that are much closer related to the original system of polynomials. In the next few sections we aim for a normal form that has the following properties.

- The variables that occur are strictly totally ordered.
- The only relations that occur are quadrilateral set relations and "perturbed" quadrilateral set relations.
- Additions, multiplications, and equalities are represented by quadrilateral set relations.
- Inequalities are represented by perturbed quadrilateral set relations.

The resulting normal form may be considered as a structure in which each variable, each elementary addition or multiplication, each equation, and each inequality is represented by a "cluster" of points that forms an individual projective scale and encodes the corresponding relation. Within each cluster the points are totally ordered as a consequence of the construction. We obtain an overall total ordering on the variables by simply lining up all the individual clusters one after the other. The elements of different clusters will be linked by quadrilateral set relations.

We now come to the formal definition of quadrilateral set relations. Like harmonic relations they form projective invariants.

<u>DEFINITION 11.2.1.</u>   A 6-tuple of numbers $(a, b, c, d, e, f) \in \mathbb{R}^6$ forms a *quadrilateral set* provided

$$q(a, b, c, d, e, f) := \frac{(a - d)(c - f)(e - b)}{(a - f)(c - b)(e - d)} = 1.$$

The number $q(a, b, c, d, e, f)$ is called the *quadrilateral ratio* and is a projective invariant for six points $a, \ldots, f$ on a line. In particular we get

$$\lim_{e \to \infty} q(a, b, c, d, e, f) = \frac{(a - d)(c - f)}{(a - f)(c - b)} \quad \text{and} \quad \lim_{e, f \to \infty} q(a, b, c, d, e, f) = \frac{a - d}{c - b}.$$

Five numbers in a quadrilateral set uniquely determine the sixth number. Since the formula q involves only differences between the indeterminants, we have

$$q(a, b, c, d, e, f) = q(a + t, b + t, c + t, d + t, e + t, f + t),$$

for any number $t \in \mathbb{R}$. This effect can be also considered as a consequence of the fact that translation by a scalar t is a projective transformation. We cover the limit case by setting $\infty + t = \infty$. In particular, addition and multiplication is modeled by the following quadrilateral set relations:

$$q(x, y, 0, x+y, \infty, \infty) = 1, \qquad q(x, y, 1, x \cdot y, \infty, 0) = 1.$$

For the Universal Partition Theorem for polytopes, we make use of the following quadrilateral set relations and their translates:

$$
\begin{aligned}
q(0, 0, -x, x, \infty, \infty) &= 1 \\
q(0, y, -x, x+y, \infty, \infty) &= 1 \\
q(1, 1, 1/x, x, \infty, 0) &= 1 \\
q(1, y, 1/x, x \cdot y, \infty, 0) &= 1
\end{aligned}
$$

11.3   Computations of Polynomials

The first steps of our approach to a normal form follow the approach of Günzel [34] for the oriented matroid case. We first observe that it is sufficient to restrict our considerations to partitions of the set $(1, \infty)^n$ consisting of all vectors of $\mathbb{R}^n$ with all entries strictly greater than 1.

<u>LEMMA 11.3.1.</u>   *For any partition $\mathcal{V} = (V_\sigma)_{\sigma \in \{-1, 0, +1\}^m}$ of $\mathbb{R}^n$ there is a partition $\mathcal{W} = (W_\sigma)_{\sigma \in \{-1, 0, +1\}^m}$ of $(1, \infty)^{2n}$ such that $\mathcal{V} \approx \mathcal{W}$.*

PROOF. Let $f_1(\boldsymbol{x}), \ldots, f_m(\boldsymbol{x}) \in \mathbb{Z}[x_1, \ldots, x_n]$ be the defining equations of $\mathcal{V}$. Then the defining equations of $\mathcal{W}$ are

$$f_1(\boldsymbol{u} - \boldsymbol{v}), \ldots, f_m(\boldsymbol{u} - \boldsymbol{v}) \in \mathbb{Z}[u_1, \ldots, u_n, v_1, \ldots, v_n]$$

together with the inequalities $u_i > 1$ and $v_i > 1$ for all $i = 1, \ldots, n$. We show this by proving $\mathcal{V} \approx_1 \mathcal{W}' \approx_2 \mathcal{W}$, where $\approx_1$ is a stable projection and $\approx_2$ is a rational equivalence. The partition $\mathcal{W}'$ is a partition of the semialgebraic set

$$\widetilde{\mathbb{R}}^{2n} := \Big\{ (\boldsymbol{x}, \boldsymbol{y}) \in \mathbb{R}^n \times \mathbb{R}^n \mid \boldsymbol{x} \in \mathbb{R}^n \text{ and } y_i > x; \ y_i > -x_i \text{ for } i = 1, \ldots, n \Big\}.$$

The defining equations for $\mathcal{W}'$ are given by the polynomials

$$f_1(\boldsymbol{x}), \ldots, f_m(\boldsymbol{x}) \in \mathbb{Z}[x_1, \ldots, x_n, y_1, \ldots, y_n].$$

By definition this gives a stable projection from $\mathcal{W}'$ to $\mathcal{V}$. The rational equivalence between $\mathcal{W}'$ and $\mathcal{W}$ is given by the affine transformation

$$
\begin{aligned}
T \colon \mathbb{R}^{2n} &\longrightarrow \mathbb{R}^{2n} \\
(\boldsymbol{x}, \boldsymbol{y}) &\longmapsto (\frac{\boldsymbol{x} + \boldsymbol{y}}{2} + 1, \frac{-\boldsymbol{x} + \boldsymbol{y}}{2} + 1).
\end{aligned}
$$

We have $T(\widetilde{\mathbb{R}}^{2n}) = (1, \infty)^{2n}$. If $(\boldsymbol{u}, \boldsymbol{v}) = T(\boldsymbol{x}, \boldsymbol{y})$, we get $\boldsymbol{x} = \boldsymbol{u} - \boldsymbol{v}$. $\qquad \square$
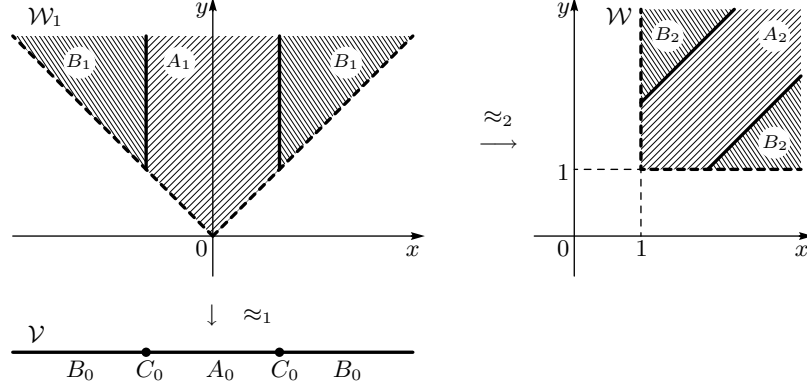
Figure 11.3.1: Stable equivalence of $\mathbb{R}$ and $(1,\infty)^2$.

Figure 11.3.1 illustrates the equivalences of the last proof in a simple example. The original partition is 1-dimensional and is defined by one polynomial $f(x) = x^2 - 1$. The corresponding partition consists of three semialgebraic sets

$$A_0 = \{x \mid x^2 - 1 < 0\}, \quad B_0 = \{x \mid x^2 - 1 > 0\}, \quad C_0 = \{x \mid x^2 - 1 = 0\}.$$

A_0 is just an open line segment, B_0 consists of two open intervals and C_0 consists of two points. The stable projection $\approx_1$ increases the dimension of each of the sets by one. The semialgebraic sets that are stably equivalent to A_0 and B_0 are marked A_1 and B_1, respectively. By the stable projection $\approx_1$ the wedge $\widetilde{\mathbb{R}}^2$ is mapped onto $\mathbb{R}$. Finally, the affine transformation T rotates and shifts $\widetilde{\mathbb{R}}^2$ and maps it to $(1,\infty)^2$. The corresponding cells of full dimensions are marked A_2 and B_2.

Now we consider a partition $\mathcal{V}$ of $(1,\infty)^n$ by polynomials $f_1, \ldots, f_m \in \mathbb{Z}[x_1, \ldots, x_n]$. Each such polynomial f_i can be written as $f_i^+ - f_i^-$ with $f_i^+, f_i^- \in \mathbb{N}[x_1, \ldots, x_n]$. The polynomial f_i^+ collects all terms of f_i with positive coefficients, the polynomial f_i^- collects all terms with negative coefficients.

The computation of a polynomial $f(x_1, \ldots, x_n) \in \mathbb{N}[x_1, \ldots, x_n]$ can be decomposed into a sequence of elementary additions and multiplications that start from the values $1, x_1, \ldots, x_n$ and compute f step by step. We consider f as bracketed in a way in which each bracket contains exactly one elementary addition or multiplication. The integral coefficients may be decomposed into a summation of ones. For instance, the polynomial $x^2 + 3y^3$ can be bracketed as

$$x^2 + 3y^3 \;=\; ((x \cdot x) + (((1+1)+1) \cdot ((y \cdot y) \cdot y))).$$

For each bracket $\alpha = (\ldots)$ that occurs we introduce an additional variable V_α. In our example we get

$$V_{x^2} = x \cdot x, \; V_{y^2} = y \cdot y, \; V_{y^3} = V_{y^2} \cdot y,$$

$$V_2 = 1 + 1, \ V_3 = V_2 + 1, \ V_{3y^3} = V_3 \cdot V_{y^3}, \ V_{x^2+3y^3} = V_{x^2} \cdot V_{3y^3}.$$

We call such a decomposition of f a *computation of f*. If all variables $x_1, \ldots, x_n$ are greater than one, then (since the coefficients of f are also greater than one) the values of all intermediate variables V_α are greater than one, as well. Compared to the Shor normal form, a computation of a polynomial does not provide any control on the order of intermediate variables (except that they are all greater than one). For instance if we consider $x + y = z$ we do not know whether $x < y$ or $y < x$.

<u>LEMMA 11.3.2.</u> *For each polynomial $f \in \mathbb{N}[x_1, \ldots, x_n]$ there is*

- *an integer $k \geq n$,*
- *additional variables $x_{n+1}, \ldots, x_k$,*
- *a collection $A \subset \{ \text{"}x + y = z\text{"} \mid x, y, z \in (0, 1, x_1, \ldots, x_k) \}$ of additions, and*
- *a collection $M \subset \{ \text{"}x \cdot y = z\text{"} \mid x, y, z \in (0, 1, x_1, \ldots, x_k) \}$ of multiplications*

such that for every "input" $(x_1, \ldots, x_n) \in (1, \infty)^n$ a solution of the system $A \cup M$

- *determines all variables $x_1, \ldots, x_k$,*
- *satisfies $(x_1, \ldots, x_k) \in (1, \infty)^k$, and*
- *satisfies $x_k = f(x_1, \ldots, x_n)$.*

PROOF. The statement is a summary of the properties of the stepwise decomposition of f into elementary additions and multiplications which we just presented. □

<u>REMARK 11.3.3.</u> Under complexity theoretical aspects, the decomposition of integers into a summation of ones is by far not optimal. It creates a number of intermediate variables that is exponential in the bit coding length of the integers. If one is heading for good complexity bounds, one can bypass this problem by choosing a more efficient coding method that does use additions *and* multiplications. Using binary coding mechanisms one can in principle achieve that the number of intermediate variables is linear in the bit coding length of the integers.

We now model a computation of polynomials by introducing "clusters" of variables that are related by quadrilateral set operations.

<u>DEFINITION 11.3.3.</u> Let $Y = (0, 1, x_1, \ldots, x_k)$ be a set of formal variables. A *cluster* $\mathcal{B} = (X, \mathcal{Q})$ is a pair consisting of an ordered collection $X = (x'_0, \ldots, x'_l)$ of variables that satisfies $\{0, 1\} \subseteq \{x'_0, \ldots, x'_l\} \subseteq Y$ and a (possibly empty) set $\mathcal{Q}$ of signed quadrilateral set relations

$$\mathcal{Q} \subset \Big\{ \text{"}\mathbf{sign}(q(a, b, c, d, e, f) - 1) = \sigma\text{"} \mid a, b, c, d, e, f \in X \text{ and } \sigma \in \{-1, 0, +1\} \Big\}.$$

We set $\mathcal{B}^{\downarrow} = x'_0$ and $\mathcal{B}^{\uparrow} = x'_l$. Concrete values $x'_0, \ldots, x'_l \in \mathbb{R}$ *satisfy* a cluster $\mathcal{B} = (X, \mathcal{Q})$ if the are totally ordered by $x'_0 < x'_1 < \ldots x'_l$, and they fulfill the requirements in $\mathcal{Q}$.

We now consider the original (partition defining) polynomial system

$$f_1, \ldots, f_m \in \mathbb{Z}(x_1, \ldots, x_n),$$

where the input values of the x_i may be taken in $(1, \infty)$. The next lemma is proved by modeling a computation of all polynomials $f_1, \ldots, f_m$ by a collection of clusters.

LEMMA 11.3.4. *For any partition* $\mathcal{V} = (V_\sigma)_{\sigma \in \{-1,0,+1\}^m}$ *of* $(1, \infty)^n$ *induced by polynomials* $f_1, \ldots, f_m \in \mathbb{Z}[x_1, \ldots, x_n]$ *there exists integers* K *and* N, *such that the semialgebraic family*

$$\mathcal{W} = \Big(\Big\{ \boldsymbol{y} = (y_1, \ldots, y_N) \in \mathbb{R}^N \,\big|\, 1 < y_1 < y_2 < \ldots < y_N \text{ and }$$
$$q_i(\boldsymbol{y}) = 1 \text{ for } i = 1, \ldots, K \text{ and }$$
$$\mathbf{sign}(\overline{q}_i(\boldsymbol{y}) - 1) = \sigma_i \text{ for } i = 1, \ldots, m \Big\} \Big)_{\sigma \in \{-1,0,+1\}^m}$$

is stably equivalent to $\mathcal{V}$. *Here* q_i *and* $\overline{q}_i$ *denote quadrilateral ratios on certain 6-tuples in* $\{-1, 0, 1, y_1, \ldots, y_N, \infty\}$.

PROOF. For each polynomial $f_1^+, f_1^-, \ldots, f_m^+, f_m^-$ we consider the decomposition into elementary additions and multiplications given in Lemma 11.3.2. We collect all n_V intermediate variables that occur in all calculations into a set $Y = \{0, 1, x_1, \ldots, x_n, x_{n+1}, \ldots, x_{n_V}\}$. We assume that there are $n_A + n_M$ elementary operations altogether; n_A additions and n_M multiplications. Furthermore, we have to implement $n_S = m$ sign conditions. We fix a certain sign vector $\sigma \in \{-1, 0, +1\}^m$ and consider the following collection of clusters:

(0): We set $\mathcal{B}_0 = ((V_{-1}^0, 0^0, 1^0), \ \{q(0^0, 0^0, V_{-1}^0, 1^0, \infty, \infty) = 0\})$.

(V): For each variable x_i with $i \in \{x_1, \ldots, x_{n_V}\}$ we introduce a cluster

$$\mathcal{B}_i = (\ (\ V_{-x_i}^i, 0^i, V_{1/x_i}^i, 1^i, x_i^i\ ),$$
$$\{\ q(0^i, 0^i, V_{-x_i}^i, x_i^i, \infty, \infty) = 1,$$
$$q(1^i, 1^i, V_{1/x_i}^i, x_i^i, \infty, 0^i) = 1\ \}\ ).$$

(A): For the i-th ($i \in \{1, \ldots, n_A\}$) elementary addition $x_a + x_b = x_c$ we set $j = n_V + i$ and introduce a cluster

$$\mathcal{B}_j = (\ (\ V_{-x_a}^j, 0^j, x_b^j, x_c^j\ ),$$
$$\{\ q(x_b^j, 0^j, V_{-x_a}^j, x_c^j, \infty, \infty) = 1\ \}\ ).$$

(M): For the i-th ($i \in \{1, \ldots, n_M\}$) elementary multiplication $x_a \cdot x_b = x_c$ we set $j = n_V + n_A + i$ and introduce a cluster

$$\mathcal{B}_j = (\, (\, 0^j, V_{1/x_a}^j, 1^j, x_b^j, x_c^j \,),$$
$$\{\, q(1^j, x_b^j, V_{1/x_a}^j, x_c^j, \infty, 0^j) = 1 \,\} \,).$$

(S): For the i-th ($i \in \{1, \ldots, n_S\}$) polynomial $f_i = f_i^+ - f_i^-$ with $x_a = f_i^+$ and $x_b = f_i^-$ we set $j = n_V + n_A + n_M + i$ and introduce a cluster

$$\mathcal{B}_j = (\, (\, V_{-x_a}^j, 0^j, x_b^j \,),$$
$$\{\, \mathbf{sign}(q(0^j, 0^j, V_{-x_a}^j, x_b^j, \infty, \infty) - 1) = \sigma_i \,\} \,).$$

In the above description 0^i and 1^i represent formal variables that (together with ∞) form a projective scale for the cluster $\mathcal{B}_i$. We set $M = n_V + n_A + n_M + n_S$. For each pair of cluster variables W^i, W^j with

$$W \in \{0, 1, V_{-1}, x_1, V_{-x_1}, V_{1/x_1}, \ldots, x_k, V_{-x_k}, V_{1/x_k}\}$$

and $i, j \in \{0, \ldots, N\}$ with $i \neq j$, we also introduce a quadrilateral relation

$$q(0^i, W^j, 0^j, W^i, \infty, \infty) = 1. \tag{$*$}$$

These last *linking relations* force that $W^i - 0^i = W^j - 0^j$, i.e., the variable W has identical values with respect to the projective scales of the clusters $\mathcal{B}_i$ and $\mathcal{B}_j$. Obviously, some of these linking relations are redundant. However, since we do not aim for complexity theoretic results, we may neglect this redundancy. Finally, we identify $\mathcal{B}_{i-1}^{\uparrow} = \mathcal{B}_i^{\downarrow}$ for $i = 1, \ldots, N$, i.e., the "last" point of the cluster $\mathcal{B}_i$ is the "first" point of the cluster $\mathcal{B}_{i+1}$. We set $0^0 = 0$ and $1^0 = 1$ and $x_i^i - 0^i = x_i$.

For a given "input" $\boldsymbol{x} = (x_1, \ldots, x_n) \in (1, \infty)^n$ the conditions of the clusters **(0)** – **(M)** together with the linking relations $(*)$ uniquely determine all variables that occur in the clusters. Moreover, within each cluster $\mathcal{B}_i = ((x_0', x_1', \ldots, x_l'), \mathcal{Q}_i)$ the variables are consistently ordered: $x_0' < x_1' < \ldots < x_l'$. Thus all cluster variables taken together form a strictly ordered chain $V_{-1} < 0 < 1 < y_1 < y_2 < \ldots < y_N$. Finally, the requirements given by the clusters in **(S)** encode the sign conditions σ on the polynomials $f_1, \ldots, f_m$. Thus all quadrilateral set conditions are satisfied simultaneously if and only if $\boldsymbol{x} \in V_{\sigma}$. We denote the set of all points $(y_1, \ldots, y_n)$ in $\mathbb{R}^N$ satisfying all of the above requirements by W_{σ}. The values of $(y_1, \ldots, y_n) \in W_{\sigma}$ are given by a rational function $f: V_{\sigma} \to W_{\sigma}$ in the values $(x_1, \ldots, x_n) \in V_{\sigma}$. The inverse function f^{-1} is given by $x_i = x_i^i - 0^i$. Thus V_{σ} and W_{σ} are rationally equivalent. Since f and f^{-1} are the same for all $\sigma \in \{-1, 0, +1\}^m$ we have $\mathcal{V} \approx \mathcal{W}$. $\qquad \square$

We close this section by exemplifying the concept of clusters in the easiest possible example. We consider the partition of $\mathbb{R}$ given by the polynomial $g(x) = x + 1$. Applying the technique of Lemma 11.3.1, this translates to a partition of

$(1, \infty)^2$ defined by the polynomial $f(x_1, x_2) = x_1 - x_2 + 1$. A decomposition of this polynomial into a positive and a negative part consists only of elementary expressions already. We set

$$f^+(x_1, x_2) = x_1 + 1 = x_3 \quad \text{and} \quad f^-(x_1, x_2) = x_2.$$

So, we have to encode three variables, one addition and one comparison. The next figure shows the corresponding collection of cluster variables. The variables are illustrated as points in their final total ordering. Observe that the last variable of the cluster $\mathcal{B}_i$ and the first variable of the cluster $\mathcal{B}_{i+1}$ are identified.
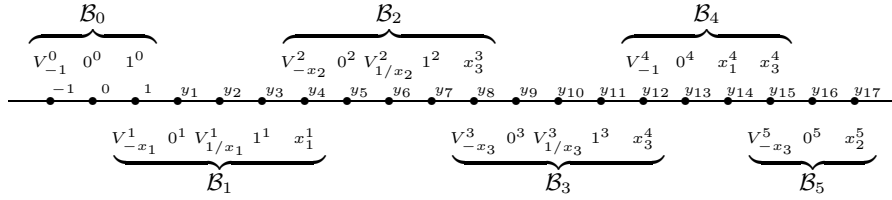
Figure 11.3.2

After relabeling, this translates into 17 variables $y_1, \ldots, y_{17}$ altogether (plus additional points for -1, 0, 1, and ∞). The clusters **(0)** – **(M)** taken together force 8 quadrilateral set relations on these variables. After deleting redundancies, the linking relations force 8 additional quadrilateral set relations. Finally, the sign condition is expressed as one perturbed quadrilateral set relation $\mathbf{sign}(q(y_{16}, y_{16}, y_{15}, y_{17}, \infty, \infty) - 1) = \sigma$.

11.4 Encoding Quadrilateral Sets into Polytopes

Taking Lemma 11.3.1 and Lemma 11.3.4 together, we see that for every partition $\mathcal{V} = (V_\sigma)_{\sigma \in \{-1,0,+1\}^m}$ of $\mathbb{R}^n$ there is a normal form that defines a stably equivalent semialgebraic family $\mathcal{W} = (W_\sigma)_{\sigma \in \{-1,0,+1\}^m}$ such that all variables $y_1, \ldots, y_N$ of $\mathcal{W}$ are totally linearly ordered and the only relations that occur are quadrilateral set relations and signed quadrilateral set relations. The semialgebraic family $\mathcal{W}$ is contained in $(1, \infty)^N$ and is stably equivalent to $\mathcal{V}$.

We now have to encode this structure into a class of 4-dimensional polytopes $(\boldsymbol{P}_\sigma)_{\sigma \in \{-1,0,+1\}^m}$. We fix a certain σ and explain the construction of $\boldsymbol{P}_\sigma$. As in the proof of the Universality Theorem we encode the variables $-1, 0, 1, y_1, \ldots, y_N, \infty$ into a $(2(N+4))$-gon $\boldsymbol{G} = \boldsymbol{G}[-\mathbf{1}, \mathbf{0}, \mathbf{1}, y_1, \ldots, y_N, \boldsymbol{\infty}]$ whose opposite sides are parallel (after standardization) and whose edge slopes represent the values of the variables. We start with a doubly iterated pyramid $\boldsymbol{S} = \mathbf{pyr}(\mathbf{pyr}(\boldsymbol{G}))$. We first construct a polytope $\boldsymbol{P}'$ that forces all quadrilateral set relations **(0)** – **(M)** together with the linking relations $(*)$. The structure of $\boldsymbol{P}'$ does not depend on the choice of σ. We do this by gluing polytopes $\boldsymbol{P}^{2x}$, $\boldsymbol{P}^{x+y}$, $\boldsymbol{P}^{x^2}$ and $\boldsymbol{P}^{x \cdot y}$ to $\boldsymbol{S}$ by suitable connectors and forgetful transmitters.

(0): $q(0^0, 0^0, V^0_{-1}, 1^0, \infty, \infty) = 1$ is forced by $\boldsymbol{P}^{2x}[V^0_{-1}, 0^0, 1^0, \infty]$.

(V): $q(0^i, 0^i, V^i_{-x_i}, x^i_i, \infty, \infty) = 1$ is forced by $\boldsymbol{P}^{2x}[V^i_{-x}, 0^i, x^i_i, \infty]$.

$\qquad q(1^i, 1^i, V^i_{1/x_i}, x^i_i, \infty^i, 0^i) = 1$ is forced by $\boldsymbol{P}^{x^2}[0^i, V^i_{1/x}, 1^i, x^i_i, \infty]$.

(A): $q(x^j_b, 0^j, V^j_{-x_a}, x^j_b, \infty, \infty) = 1$ is forced by $\boldsymbol{P}^{x+y}[V^j_{-x_a}, 0^j, x^j_b, x^j_c, \infty]$.

(M): $q(1^j, x^j_b, V^j_{1/x_a}, x^j_c, \infty, 0^j) = 1$ is forced by $\boldsymbol{P}^{x \cdot y}[0^j, V^j_{1/x_a}, 1^j, x^j_b, x^j_c, \infty]$.

(∗): $q(0^i, W^j, 0^j, W^i, \infty, \infty) = 1;\ i < j$ is forced by $\boldsymbol{P}^{x \cdot y}[0^i, W^i, 0^j, W^j, \infty]$.

Connecting all these polytopes to the construction forces that in $\boldsymbol{P}'$ the intersection of opposite edge-supporting lines of $\boldsymbol{G}$ are collinear.

We now finally have to add polytopes to $\boldsymbol{P}'$ that encode the actual sign conditions **(S)**. The signed quadrilateral set relations

$$\mathbf{sign}(q(0^j, 0^j, V^j_{-x_a}, x^j_b, \infty, \infty) - 1) = \sigma_i$$

that correspond to the clusters in **(S)** can equivalently be considered as signed harmonic relations on the elements $V^j_{-x_a}, x^j_b, 0, \infty$. In the next section we construct "switch polytopes" $\boldsymbol{H}^+$, $\boldsymbol{H}^-$ and $\boldsymbol{H}^0$ that force signed harmonic relations on the slopes of a octagon. These polytopes have to be added (depending on the choice of $\sigma \in \{-1, 0, +1\}^m$) to the polytope $\boldsymbol{P}'$ in order to obtain $\boldsymbol{P}_\sigma$.

11.5 The "Switch Polytope"

Recall the construction of our perturbed $\boldsymbol{X}$-polytope $\boldsymbol{X}^+$ as given in Section 9.3. Both polytopes $\boldsymbol{X}$ and $\boldsymbol{X}^+$ can be generated in the following way:

- Start with a hexagon $\boldsymbol{G} = \boldsymbol{G}(1, 2, 3, 4, 5, 6)$ (in counterclockwise order) where both edges 1 and 4 are parallel and have infinite slopes. Let 1 be left of 4.
- Perform a Lawrence extension at the intersection $1 \vee 4$.
- Label the two new points by a and b such that $(2, a)$, $(3, a)$, $(5, b)$ and $(6, b)$ span triangles of the resulting 3-polytope (compare the labeling of Figure 5.4.1 and of Figure 11.5.1, which shows only the hexagon).
- Perform a Lawrence extension at the intersection $\boldsymbol{p}_y$ of the planes spanned by $(2, a)$, $(3, a)$ and $(5, b)$.
- Label the two new points by $\overline{y}$ and $\underline{y}$ such that the pyramid spanned by $\boldsymbol{G}$ and $\overline{y}$ is a facet.
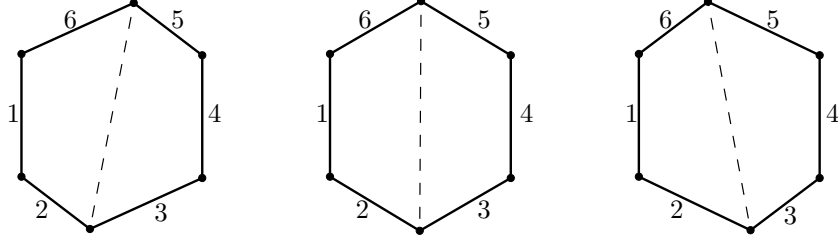
Figure 11.5.1: The three possible states of a hexagon.

The combinatorial type of the resulting polytope depends on the position of the two points $\boldsymbol{p}_{2,3} = 2 \vee 3$ and $\boldsymbol{p}_{5,6} = 5 \vee 6$ only. Let $x_{2,3}$ and $x_{5,6}$ be the x-coordinates of these two points. The three cases $x_{2,3} < x_{5,6}$, $x_{2,3} = x_{5,6}$, and $x_{2,3} > x_{5,6}$ generate the different combinatorial types of the polytopes. We call the three resulting polytopes $\boldsymbol{X}^-$, $\boldsymbol{X}^0$ and $\boldsymbol{X}^+$, respectively. The polytope $\boldsymbol{X}^0$ is our original polytope $\boldsymbol{X}$. The combinatorial type of the resulting polytope depends on the relative position of the point $\boldsymbol{p}_y$ and the supporting plane H of the triangle $(6, b)$. In the case where $x_{2,3} = x_{5,6}$ the point $\boldsymbol{p}_y$ is incident to the plane H. This results in the fact that in $\boldsymbol{X}^0$ the edge 5 together with the vertices b, $\overline{y}$ and $\underline{y}$ spans a facet F_1 as well as the edge 6 together with the vertices b, $\overline{y}$ and $\underline{y}$) spans a facet F_2. As a consequence these two facets are both pyramids over a square (along which they are joined). In the perturbed situations the vertices of F_1 still form a facet (a bi-pyramid over a triangle), while the pyramid F_2 breaks up into two tetrahedra. Figure 11.5.2 illustrates this effect by showing just the relevant part of the corresponding Schlegel diagrams.
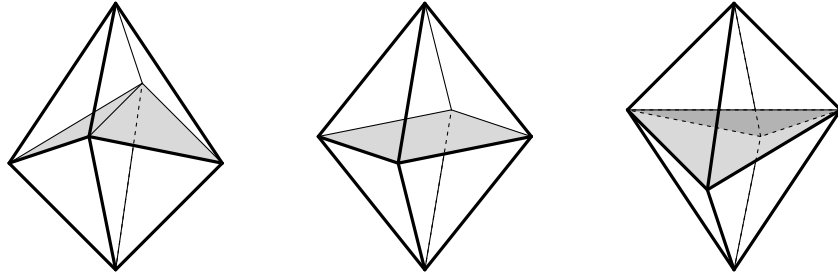
Figure 11.5.2: The three possible states of the switch polytope.

<u>LEMMA 11.5.1.</u> *Let $\sigma \in \{-1, 0, +1\}$ and let $\boldsymbol{X}'$ be a realization of the polytope $\boldsymbol{X}^\sigma$. We normalize $\boldsymbol{X}'$ by mapping $\boldsymbol{G}(1, \ldots, 6)$ into the (x, y)-plane with infinite slopes for edges 1 and 4, with 1 left of 4 and 1 up to 6 in counterclockwise order. Then with the notation above we get $\mathbf{sign}(x_{2,3} - x_{5,6}) = \sigma$. Moreover, every realization of $\boldsymbol{G}(1, \ldots, 6)$ normalized in such a way with $\mathbf{sign}(x_{2,3} - x_{5,6}) = \sigma$ can be completed to a realization of $\boldsymbol{X}^\sigma$.*

PROOF. The proof is completely analogous to the proof of Theorem 5.4.1. □

We now use these polytopes to construct three polytopes $\boldsymbol{H}^-$, $\boldsymbol{H}^0$, $\boldsymbol{H}^+$ which form the "harmonic switches" we need. Consider the octagon $\boldsymbol{G} = \boldsymbol{G}(1,\ldots,8)$ shown in Figure 11.5.3 where we assume that the additional collinearities $(1\vee 5, 2\vee 3, 7\vee 8)$, $(1\vee 5, 3\vee 4, 6\vee 7)$ and $(3\vee 7, 1\vee 8, 5\vee 6)$ hold and where we furthermore assume that opposite sides are parallel with 3 and 7 having infinite slope and 3 being left of 7. Let $x_{1,2}$ and $x_{4,5}$ be the x coordinates of $1\vee 2$ and $4\vee 5$.
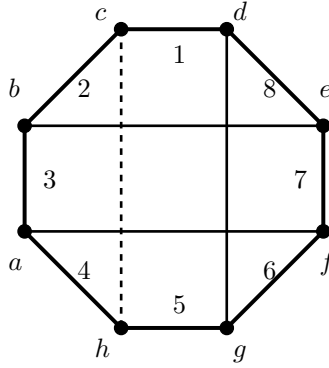
Figure 11.5.3: The octagon $\boldsymbol{G} = \boldsymbol{G}(1,\ldots,8)$.

LEMMA 11.5.2.   *With the above settings we get*

$$\mathbf{sign}(x_{1,2} - x_{4,5}) = \mathbf{sign}((s_1, s_3 \mid s_2, s_4) - 1).$$

PROOF. We may assume that $h = (u,0)$, $a = (0,v)$, $f = (1,v)$, $g = (w,0)$, $d = (w,1)$, $e = (x,1)$, $e = (x,0)$, $c = (1,y)$ with $u,v,w,x,y > 0$. For the slopes we assume that $s_1 = s_5 = 0$, $s_3 = s_7 = \infty$, $s_2 = s_6 = \alpha > 0$ and $s_4 = s_8 = -\beta < 0$. So we have $(s_1, s_3 \mid s_2, s_4) = \alpha/\beta$. Using the parallelism we can successively compute $v = u\beta$, $w = 1 - u\beta/\alpha$, $x = 1 - u\beta^2/\alpha$ and $y = u\beta^2/\alpha^2$. Since u,y,β and α are all positive we conclude $\mathbf{sign}(y - u) = \mathbf{sign}(y/u - 1) = \mathbf{sign}(\beta^2/\alpha^2 - 1) = \mathbf{sign}(\beta/\alpha - 1)$, which proves the claim. □

With the above considerations in mind we provide an explicit construction diagram for the polytopes $\boldsymbol{H}^\sigma$. They encode the configuration discussed in Lemma 11.5.2. $\boldsymbol{X}$-polytopes are used to encode the collinearities and $\boldsymbol{X}^\sigma$-polytopes are used to encode the sign condition.
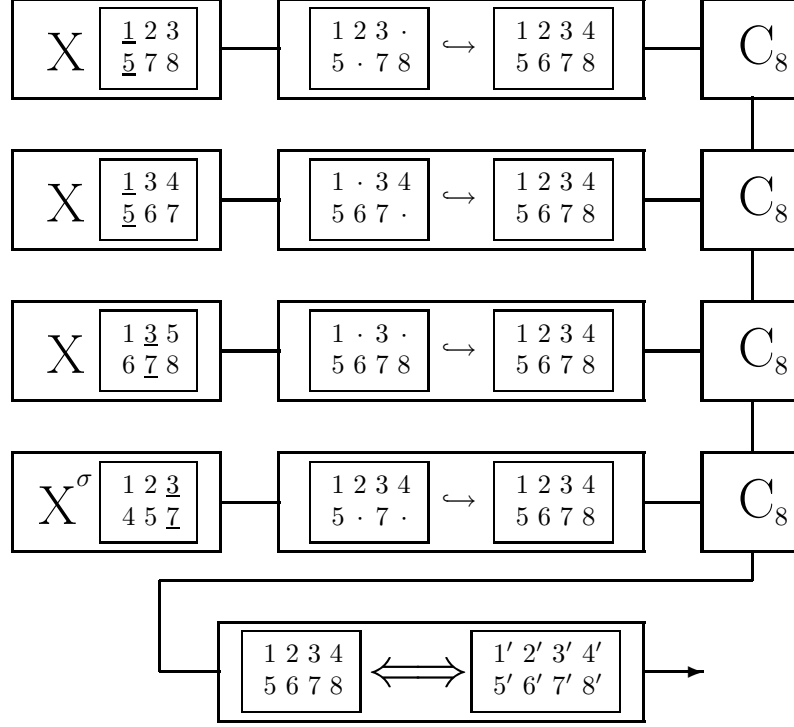
<u>Lemma 11.5.3.</u> *Let* $\sigma \in \{-1, 0, +1\}$ *and let* $\boldsymbol{H}'$ *be a realization of the polytope* $\boldsymbol{H}^\sigma$. *After pre-standardization the slopes of* $\boldsymbol{G}(1, \ldots, 8)$ *satisfy* $\sigma = \mathbf{sign}((s_1, s_3 \,|\, s_2, s_4) - 1)$. *Every normal pre-standardized octagon* $\boldsymbol{G}(1, \ldots, 8)$ *with* $\sigma = \mathbf{sign}((s_1, s_3 \,|\, s_2, s_4) - 1)$ *can be completed to a realization of* $\boldsymbol{H}^\sigma$.

Proof. By applying Lemma 11.5.1 and Lemma 11.5.2, the proof is analogous to the proof of Lemma 6.2.1.   □

11.6   The Universal Partition Theorem

We now have collected all the pieces that are necessary to construct the polytopes $\boldsymbol{P}_\sigma$ from our already constructed $\boldsymbol{P}'$. For each of the m sign conditions given by $\sigma \in \{-1, 0, +1\}^m$

$$\mathbf{sign}(q(0^j, 0^j, V^j_{-x_a}, x^j_b, \infty, \infty) - 1) = \sigma_i$$

we add (by suitable connectors and forgetful transmitter polytopes) a polytope $\boldsymbol{H}^\sigma[0^j, V^j_{-x_a}, x^j_b, \infty]$ to the polytope $\boldsymbol{P}'$. The resulting polytope is $\boldsymbol{P}_\sigma$. The face lattices of the (combinatorial) polytopes $(\boldsymbol{P}_\sigma)_{\sigma \in \{-1, 0, +1\}^m}$ differ by m choices as indicated in Figure 11.5.2. Since the construction of $\boldsymbol{P}'$ already implies that

the central computation frame is normal, Lemma 11.5.3 applies, and the $\boldsymbol{H}^\sigma$-polytopes encode the correct sign conditions. We now complete the proof of the Universal Partition Theorem for 4-polytopes.

PROOF OF THEOREM 11.1.3. It remains to show that the partition $\mathcal{W} = (W_\sigma)_{\sigma\in\{-1,0,+1\}^m}$ that was defined in Section 11.4 is stably equivalent to the family of realization spaces

$$(\mathcal{R}(\boldsymbol{P}_\sigma, B))_{\sigma\in\{-1,0,+1\}^m}.$$

Here B is a basis of points that are already in the starting polytope $\boldsymbol{S}$ and therefore contained in each of the polytopes $\boldsymbol{P}_\sigma$. By construction for every realization of $\boldsymbol{P}_\sigma$ (after standardization) the slopes s_{y_i} of the edges in the central computation frame $\boldsymbol{G} = \boldsymbol{G}[-\mathbf{1}, \mathbf{0}, \mathbf{1}, y_1, \ldots, y_N, \boldsymbol{\infty}]$ correspond to a point in W_σ. Conversely, for every point in $(y_1, \ldots, y_N) \in W_\sigma$ there is a corresponding realization of $\boldsymbol{P}_\sigma$ such that, after standardization, $y_i = s_{y_i}$ for $i = 1, \ldots, N$ (compare the proof of Theorem 8.1.1).

Finally, we have to prove that we get indeed a stable equivalence of the corresponding semialgebraic families. For this observe that as in the proof of the Universality Theorem we may consider the polytopes $\boldsymbol{P}_\sigma$ to be constructed by a sequence of connected sums, where in each step another basic building block is added. Thus an almost word-by-word repetition of the proofs of Lemma 8.3.1 and Lemma 8.3.2 (where we proved the corresponding fact for the polytope $\boldsymbol{P}(\mathcal{S})$) applies. The only difference is that we have to take special care of the polytopes $\boldsymbol{X}^\sigma$. We must make sure that when adding the remaining points a, b, and $\underline{y}$ this can be done by the same sequence of rational equivalences and stable projections, independent of the choice of σ. Here only stable projections are needed. The proof is given by an almost literal repetition of Case 1 in the proof of Lemma 8.3.1. Just the decisive construction sequence has to be altered slightly.

(i) Choose $\boldsymbol{p}_a$ arbitrarily in the region $\mathcal{B}$.

(ii) Choose scalars $\lambda_1, \tau_1 > 0$ such that $\boldsymbol{p}_b = \lambda_1 \boldsymbol{p}_a + \tau_1 \sigma_1 (1 \wedge 4) \in \mathcal{B}$.

(iii) Define $\boldsymbol{p}_y$ as the intersection of the planes spanned by $(2, a)$, $(3, a)$ and $(5, b)$. Choose scalars $\lambda_2, \tau_2 > 0$ such that $\boldsymbol{p}_{\underline{y}} = \lambda_2 \boldsymbol{p}_{\overline{y}} + \tau_2 \sigma_2 \boldsymbol{q}_y \in \mathcal{B}$.

This sequence models the construction of $\boldsymbol{X}^\sigma$ starting from $\mathbf{pyr}(\boldsymbol{G}(1, \ldots, 6), \overline{y})$. The addition of the points forms a sequence of stable projections independent of the choice of σ. Thus we get

$$\mathcal{W} = (W_\sigma)_{\sigma\in\{-1,0,+1\}^m} \approx (\mathcal{R}(\boldsymbol{P}_\sigma, B))_{\sigma\in\{-1,0,+1\}^m}.$$

This completes the proof of the Universal Partition Theorem for 4-Polytopes. $\square$

11.7   The Universal Partition Theorem for Point Configurations

We close this chapter with a proof of a closely related problem the *Universal Partition Theorem for oriented matroids* as it was originally stated my Mnëv [50]. Our method of encoding a partition of $\mathbb{R}^n$ into a sequence of clusters allows to give an elegant proof of this theorem, as well. In fact, we obtain an even stronger version as the one that has been proven by Günzel [34]. The statement there gives only a proof where stable equivalence is obtained up to the product of the semialgebraic sets with a non-controllable smooth manifold. We here prove the original statement as it was claimed by Mnëv.

Oriented matroids and their close relatives chirotopes encode the combinatorial structure of point configurations in $\mathbb{R}^n$ (compare [7]). We can restrict ourselves to the case of 2-dimensional affine point configurations, and start with the basic definitions on the level of chirotopes.

<u>DEFINITION 11.7.1.</u>   Let $\boldsymbol{P} = (\boldsymbol{p}_1, \ldots, \boldsymbol{p}_n) \in \mathbb{R}^{2 \cdot n}$ be a finite 2-dimensional point configuration on an index set X. We set $\boldsymbol{p}_i = (x_i, y_i)$, for $i = 1, \ldots, n$. The map

$$\chi \colon X^3 \quad \longrightarrow \quad \{-1, 0, 1\}$$

$$(i, j, k) \quad \longmapsto \quad \boldsymbol{\det} \begin{pmatrix} 1 & x_i & y_i \\ 1 & x_j & y_j \\ 1 & x_k & y_k \end{pmatrix}$$

is called the *chirotope* of $\boldsymbol{P}$. A point configuration $\boldsymbol{P}$ is called a *realization* of a map $\chi \colon X^3 \longrightarrow \{-1, 0, 1\}$ if $\chi^{\boldsymbol{P}} = \chi$. The triple (i, j, k) is called a *basis* of χ if $\chi(i, j, k) \neq 0$. If $\chi(i, j, k) = +1$, then the *realization space* $\overline{\mathcal{R}}(\chi, (i, j, k))$ is the set of all realizations $\boldsymbol{P}$ of χ with $\boldsymbol{p}_i = (0, 0)$, $\boldsymbol{p}_j = (1, 0)$, and $\boldsymbol{p}_k = (0, 1)$.

The map $\chi^{\boldsymbol{P}}$ indicates for any triple of points whether they are clockwise oriented, counterclockwise oriented, or collinear. An alternating map $\chi \colon X^3 \to \{-1, 0, 1\}$ is called *non-realizable* if there is no point configuration $\boldsymbol{P}$ with $\chi^{\boldsymbol{P}} = \chi$.

In general an alternating map $\chi \colon X^3 \to \{-1, 0, 1\}$ is a chirotope when additional conditions (known as Grassmann-Plücker relations) are satisfied. We will omit the detailed definition here. However, these relations are always fulfilled if χ comes from a point configuration. All sign maps, that play a role in this section are indeed chirotopes. The Universal Partition Theorem for point-configurations now states.

<u>THEOREM 11.7.2.</u>   *For any partition* $\mathcal{V} = (V_\sigma)_{\sigma \in \{-1, 0, +1\}^m}$ *of* $\mathbb{R}^n$ *there is an index set X and a collection of alternating sign maps*

$$(\chi_\sigma \colon X^3 \to \{-1, 0, 1\})_{\sigma \in \{-1, 0, +1\}^m}$$

with common basis B such that

$$\mathcal{V} \approx (\overline{\mathcal{R}}(\chi_\sigma, B))_{\sigma \in \{-1, 0, +1\}^m}.$$

PROOF.   With the method of encoding of a partition into a collection of clusters as given by Lemma 11.4.3, our proof is almost finished. It remains to apply a standard construction that encodes quadrilateral sets into point configurations and thereby fixes the orientations. This process was already described by Mnëv [48, 49] and by Shor [53]. In principle this can be done by a slightly refined "von Staudt construction". We consider our variables together with -1, $\mathbf{0}$, $\mathbf{1}$, and $\boldsymbol{\infty}$ as points on a line and consider the projective scale defined by $\mathbf{0}$, $\mathbf{1}$, and $\boldsymbol{\infty}$. We have to implement the quadrilateral set relations of Lemma 11.4.3 by suitable point configurations. This can be done by intersecting the sides of a complete quadrilateral with a line (that is where the name "quadrilateral set" comes from). Up to translation, the only cases that occur are

$$\begin{aligned} q(0,0,-x,x,\infty,\infty) &= 1, & q(0,y,-x,x+y,\infty,\infty) &= 1, \\ q(1,1,1/x,x,\infty,0) &= 1, & q(1,y,1/x,x\cdot y,\infty,0) &= 1, \end{aligned}$$

and the sign conditions $\mathbf{sign}(q(0,0,-x,y,\infty,\infty)-1)=\sigma$.

The corresponding point configurations are shown in Figure 11.7.1. In each of the cases four new points labeled $a,\dots,d$ are introduced. Each of these configurations contains an "information line" ℓ, on which the values of the variables are represented by points. Points a and b lie on a line ℓ'. The position of the points c and d as well as all orientations are fixed by the incidence structure of the configuration and the ordering of the points on ℓ and on ℓ'. Observe that, by choosing b very close to a one can achieve that the points b, c, and d are in an ε-neighborhood of a, for arbitrary small $\varepsilon > 0$.
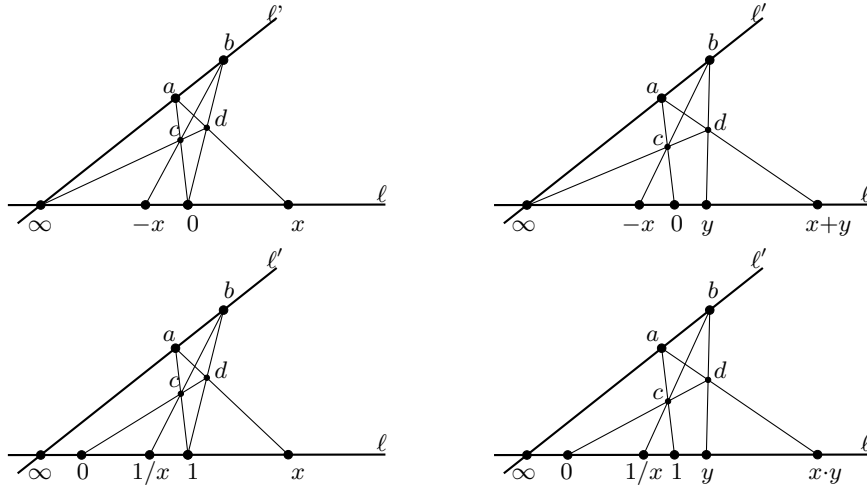
Figure 11.7.1: Von Staudt constructions for addition and multiplication.

The sign conditions can be encoded into perturbed versions of the right upper configuration of Figure 11.7.1. For this the points c, d, and $\boldsymbol{\infty}$ are no longer assumed to be collinear. Depending on the orientation of the triple $(c,d,\boldsymbol{\infty})$ we

get either $x < y$, $x > y$, or $x = y$. The two perturbed situations are shown in Figure 11.7.2.
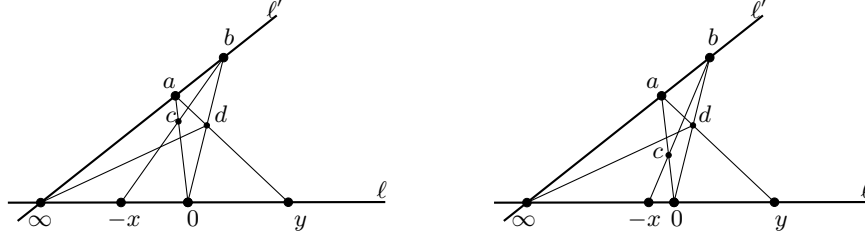
Figure 11.7.2: Encoding of inequalities.

Finally, all the necessary quadrilateral set relations have to be encoded into one point configuration, thereby fixing all the orientations. We start with the line ℓ, which we identify with the x-axis, and a line ℓ', which we identify with the y-axis. The origin is labeled ∞. All points in the final configuration will have non-negative x and y coordinates. First the quadrilateral set relations $q_1, \ldots, q_K$ corresponding to our classes **(0)** – **(M)** together with the linking relations $(*)$ are encoded. We take concrete values $\boldsymbol{y} = (y_1, y_2, \ldots, y_N)$ that satisfy $q_1, \ldots, q_K$, and are totally ordered $y_1 < y_2 < \ldots < y_N$. By a projective transformation we map the points $-1, 0, 1, y_1, \ldots, y_N, \infty$ onto the line ℓ such that ∞ becomes the origin and the sequence $-1, 0, 1, y_2, \ldots, y_N$ starts to the right from the origin. We assume that the point labeled -1 has coordinates $(1, 0)$. Now we iteratively add the point configurations that encode the quadrilateral set relations. For each q_i we introduce four new points $a_i, \ldots, d_i$ in the following way. We set $a_1 = (0, 1)$ and $b_1 = (0, 2)$. The points c_1 and d_1 are chosen according to the point configuration of Figure 11.7.1 that encodes q_1. For $i = 2, \ldots, K$ we set $a_i = (0, \alpha_i)$ where $\alpha_i > 0$ is chosen large enough that it is above all the lines spanned by points that are already constructed (except for line ℓ' itself on which a_i lies). Now let $b_i = (0, \alpha_i + \varepsilon_i)$ where $\varepsilon_i > 0$ is a very small number. We construct c_i and d_i according to the configuration that encodes q_i. Choosing ε_i small enough we can achieve that all lines that are spanned by points that are so far constructed (except of those passing through the origin) have negative slope (i.e., they intersect ℓ' above the origin). For small ε_i it happens as well that the signs of all orientations involving one of the points b_i, c_i, or d_i are completely determined by the type of the quadrilateral set relation q_i and do not depend on the actual choice of $\boldsymbol{y}$. This can be shown by a simple case analysis. The obstructions to the choices of the α_i and the ε_i can be expressed as stable projections. Finally, we have to add our m sign conditions. For each of the relations $\overline{q}_i$ in Lemma 11.3.4., with $i = 1, \ldots, m$, we add a configuration of the incidence type as given in Figure 11.7.2. We do this by adding points $a_{K+i}, \ldots, d_{K+i}$ in the same way as described above. We call the oriented matroid of the resulting point configuration $\chi[\boldsymbol{y}]$. The construction fixes all orientation except of $\chi[\boldsymbol{y}](\infty, c_{K+i}, d_{K+i})$, for $1 = 1, \ldots, m$. These signs are dependent on the choice of our input parameters $\boldsymbol{y}$. The construction forces

$$\chi[\boldsymbol{y}](\boldsymbol{\infty}, c_{K+i}, d_{K+i}) = \mathbf{sign}(\overline{q}_i(\boldsymbol{y}) - 1),$$

for $i = 1, \ldots, m$. Hence the orientations of $\chi[\boldsymbol{y}]$ depend just on the choice of the input parameters $\boldsymbol{y}$. We now define χ_σ as an alternating sign function on

$$X^3 = \{-\mathbf{1}, \mathbf{0}, \mathbf{1}, y_1, \ldots, y_N, \boldsymbol{\infty}, a_1, b_1, \ldots, c_{K+m}, d_{K+m}\}^3.$$

The labels of X are equipped with a total order "$\prec$". The map χ_σ is the determined by its values $\chi_\sigma(i, j, k)$ with $i \prec j \prec k$. For this we define

$$\chi_\sigma(i, j, k) = \begin{cases} \chi[\boldsymbol{y}](i, j, k), & \text{if } (i, j, k) \neq (\boldsymbol{\infty}, c_l, d_l), \ K < l \leq K + m, \\ \sigma_i, & \text{if } (i, j, k) = (\boldsymbol{\infty}, c_l, d_l), \ K < l \leq K + m. \end{cases}$$

By construction this choice of χ_σ has the desired properties: if $\boldsymbol{y} \in W_\sigma$ (with the W_σ of Lemma 11.3.4), then we have $\chi_\sigma = \chi[\boldsymbol{y}]$; if W_σ is empty, then χ_σ is non-realizable. As common basis of all χ_σ we choose $B = (\boldsymbol{\infty}, -\mathbf{1}, a_0)$. The desired stable equivalence between the realization spaces $\overline{\mathcal{R}}(\chi_\sigma, B)$ and the sets W_σ are given by the stable projections that determine the values α_i and ε_i and the rational equivalence that describes the actual construction of the points. $\square$

Part IV: Three-dimensional Polytopes

It is the purpose of this part to give a proof of Steinitz's Theorem: *A graph G is the edge graph of a polytope if (and only if) it is planar and 3-connected.* We here concentrate on the harder "if"-part of the theorem. In principle there are three (known) different approaches to build up a proof:

- Steinitz's classical approach [55, 56] starts with a tetrahedron and proceeds by iteratively adding (triangular) facets and (3-valent) vertices until a polytope with edge graph G is obtained. Here the main technical difficulty lies in the fact that one has to be very careful not to run into dead ends. A well written modern proof that follows these classical lines can be found in [65].

- A second principle approach comes from the Koebe-Andreev-Thurston *Circle Packing Theorem*. This theorem states that every planar 3-connected graph can be represented as a *coin graph* in $\mathbb{R}^2$: a set of non-overlapping discs (one for each vertex) such that two disks touch if and only if the corresponding vertices are joined by an edge. Via stereographic projection the coin graph can be mapped onto the 2-sphere. Considering the planes spanned by the circles on the 2-sphere leads to an embedding of the corresponding polytope. The realization that is obtained by this method is essentially unique (up to Möbius transformations). It has the additional nice property that all edges are tangent to the 2-sphere. A proof of the Circle Packing Theorem can be found for instance in [54].

- The approach that we will follow here is originated in the theory of *equilibrium stresses* in graphs (see for instance [23, 36, 45, 46]). An assignment of weights to the edges of a drawing of a planar graph is called a *self-stress* (or *equilibrium load*) if these weights interpreted as forces induce an equilibrium at every vertex. There is a remarkable correspondence between Schlegel diagrams of 3-dimensional polytopes and graph drawings that admit a self-stress: *A planar drawing of a 3-connected planar graph admits a self-stress with positive weights on all interior edges, if and only if it is a Schlegel diagram.* Applying this theorem we can find a polytope representation by first finding a self-stress for a graph and then lifting the Schlegel diagram.

Our proof will be constructive. We start with the combinatorial description of a 3-connected planar graph. We select a cell to be exterior and fix the positions of its vertices. Then we produce a drawing of the graph with this exterior cell and

with a self-stress given by preassigned weights. After this we can apply the above theorem and explicitly produce a polytopal lifting of the drawing. This approach does not only lead to just one realization. By varying the weights one can (up to projective equivalence) generate all realizations of the corresponding polytope. Using this fact we will prove that the realization space of any 3-polytope is a open ball of dimension $e - 6$, where e is the number of edges. Moreover following the details of the construction we will derive a singly exponential upper bound for the minimal grid size on which the polytope can be realized.

12   Graphs

12.1   Preliminaries from Graph Theory

Our objective is to go from graphs to graph representations to polytope realizations. We will need only very little of graph theory. We recall only the basic definitions that are of relevance for our purposes. The facts that we need are all standard in graph theory. Proofs can be found for instance in [19] or [61].

DEFINITION 12.1.1.   A *graph* is a pair $G = (V, E)$ where $V = 1, \ldots, n$ is a finite set of *vertices*, and $E \subseteq \{\{v, w\} \mid v, w \in V; v \neq w\}$ is a set of *edges* between the vertices.

Our graphs are by definition loopless (no edges that join an element with itself) and they do not contain parallel edges (no multiple edges between pairs of points). A graph may be visualized by a set of disjoint points in the plane (the vertices) and a collection of (Jordan-)arcs connecting certain pairs of them (the edges). The next definition summarizes basic vocabulary of graph theory that will be needed for our treatment of 3-polytopes. By $\mathcal{P}(V, 2)$ we denote the set of all (unordered) pairs of elements from V.

DEFINITION 12.1.2.   Let $G = (V, E)$ be a graph.

- The *degree* of a vertex $v \in V$ is the number of edges in E that contain v.
- The graph obtained from G by *deleting* a vertex set $W \subseteq V$ is defined as the restriction of G to the vertex set $V' = V \setminus W$. We formally write $G \setminus W = (V', E \cap \mathcal{P}(V', 2))$.
- A graph $G' = (V', E')$ is a *subgraph* of G, if $V' \subseteq V$ and $E' \subseteq E$. We then write $G' \subseteq G$.

We will need three important types of subgraphs:

- A *path* between two vertices v_1 and v_k in G is a subgraph $G' \subseteq G$ with $V' = \{v_1, v_2, v_3, \ldots, v_k\}$ and $E' = \{\{v_1, v_2\}, \{v_2, v_3\}, \ldots, \{v_{k-1}, v_k\}\}$. We write $G' = G_{v_1}^{v_k}$.
- A *k-cycle* in G is a subgraph $G' \subseteq G$ with $V' = \{v_1, v_2, v_3, \ldots, v_k\}$ and $E' = \{\{v_1, v_2\}, \{v_2, v_3\}, \ldots, \{v_{k-1}, v_k\}, \{v_k, v_1\}\}$.

- A Y-*graph* in G that connects $v_1, v_2, v_3 \in V$ is a subgraph $G' \subseteq G$ such that there exists a vertex $w \in V \setminus \{v_1, v_2, v_3\}$ and paths $G_{v_1}^w$, $G_{v_2}^w$, and $G_{v_3}^w$ that are disjoint except for the common endpoint w.

In addition we need the concept of connectivity.

- A graph G is 1-*connected* (or just connected) if it has at least one edge, and for any disjoint pair of vertices $v, w \in V$ there is a path G_v^w connecting them.
- A graph G is k-*connected* for $k > 1$, if for every $v \in V$ the graph $G \setminus v$ is $(k-1)$-connected.

We will often notate paths (or cycles) by simply giving the sequence of the vertices in which they occur in the path (or cycle). Thus $(1, 2, \ldots, m)$ may represent the path $(\{1, \ldots, m\}, \{\{1, 2\}, \{2, 3\}, \ldots, \{m-1, m\}\}) = (V, E)$ or the cycle $(V, E \cup \{m, 1\})$.

Graphs are very intuitive objects. We may draw a graph in the plane by identifying each vertex $v \in V$ with a point $\boldsymbol{p}_v \in \mathbb{R}^2$. Edges are represented by (Jordan-)arcs connecting corresponding vertices. In Figure 12.1.1 a path, a cycle and a Y-graph of some graph are emphasized.
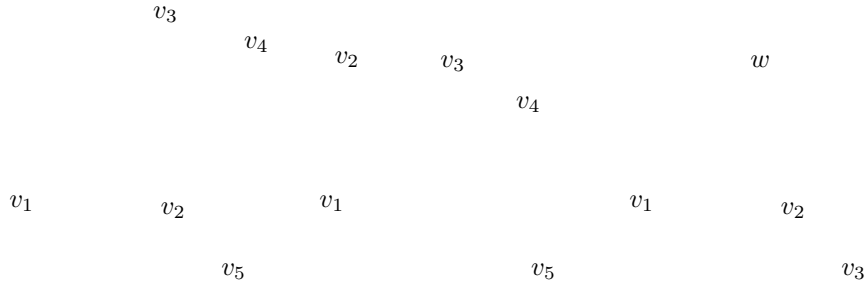
Figure 12.1.1: A path a cycle and a Y-graph.

<u>DEFINITION 12.1.3.</u> A graph $G = (E, V)$ with $E = \{1, \ldots, n\}$ is *planar* if it can be drawn in the plane such that the interiors of the edges do not intersect and the vertices are represented by disjoint points in $\mathbb{R}^2$.

The definition of planarity does not require that the edges are represented by straight line segments. However, a classical result (that was independently proved by Wagner 1936 [60] and by Fáry 1948 [26]) states that it is equivalent to require this stronger condition, too.

For a planar drawing of a graph G let $\mathcal{D} \subset \mathbb{R}^2$ be the union of all edge-representing arcs (including their endpoints: the vertex-representing points). Informally speaking, $\mathcal{D}$ is the black part in an ink drawing of G on a white sheet of

paper. The complement of $\mathcal{D}$ may have several connected components: the *cells* of $\mathcal{D}$. If G is at least 2-connected then each cell has a boundary that corresponds to a cycle in G. There is exactly one infinite cell (the exterior of $\mathcal{D}$). Also this cell has such a boundary. We will treat the infinite cell in the same way as the interior cells. (If one prefers a compactified situation one may equivalently map the drawing onto the 2-sphere by a stereographic projection. The infinite cell is then mapped to a finite cell on the sphere.) To a pair $(G, \mathcal{D})$ where G is planar and 2-connected and $\mathcal{D}$ is a planar drawing of G we associate the set:

$$\mathbf{cells}(G, \mathcal{D}) = \{G' \subseteq G \mid G' \text{ bounds a cell in the complement of } \mathcal{D}\}.$$

Figure 12.1.2 shows a planar drawing of a planar 3-connected graph. The cycles that correspond to the cells are $(1, 2, 3, 4, 5)$, $(3, 6, 4)$, $(1, 7, 8, 2)$, $(2, 8, 9, 6, 3)$, $(6, 9, 10)$, $(4, 6, 10, 11, 5)$, $(1, 5, 11, 7)$, and $(7, 8, 9, 10, 11)$.
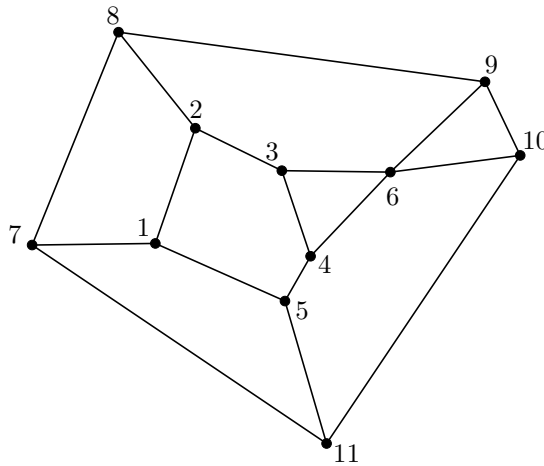
Figure 12.1.2: A 3-connected planar graph.

The *edge graph* $G(P)$ of a polytope P is the graph whose vertex set is the vertex set of the polytope P. Two vertices form an edge of the graph $G(P)$, if they are the endpoints of a 1-face (i.e, an edge) of P. Note that we have to distinguish carefully between the vertices and edges of P and of $G(P)$. We now can formally state Steinitz's Theorem:

THEOREM 12.1.4, (STEINITZ'S THEOREM).   *A finite graph is the edge-graph of a 3-polytope if and only if it is planar and 3-connected.*

Here we will only prove the "if-part" of this theorem. The other direction is not too difficult to prove. To see that the edge graph of a 3-polytope is planar, simply draw a Schlegel diagram. The 3-connectivity of the edge-graph follows for

instance from Balinski's Theorem that states that the edge graph of a d-polytope is d-connected. A proof of Balinski's Theorem can be found in [65].

The cells of a planar drawing of a graph will play the role of the facets of the corresponding 3-polytope. The graph in the last example is the edge graph of a cube where two adjacent vertices have been truncated and the truncation planes meet. Figure 12.1.3 illustrates the essence of Steinitz's Theorem.
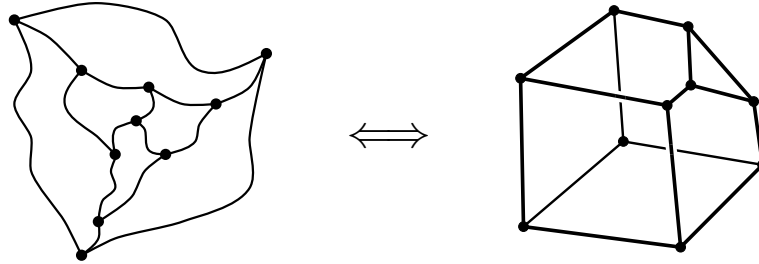
Figure 12.1.3: The essence of Steinitz's Theorem.

For the proof of Steinitz's Theorem we will rely on the following facts from graph theory that deal with planarity and connectivity.

THEOREM 12.1.5. *Let G be a graph.*

(i) *(Menger's Theorem) If G is 3-connected, then between any pair of vertices there are three paths G_1, G_2, and G_3 in G that are disjoint except for the endpoints.*

(ii) *If there are three vertices u, v, w that are connected by three different Y-graphs Y_1, Y_2, and Y_3 that are disjoint except for u, v, w, then G is not planar.*

(iii) *(Whitney's Theorem) If G is planar and 3-connected then the set $\mathbf{cells}(G, \mathcal{D})$ is independent on the particular choice of a drawing $\mathcal{D}$ of G.*

(iv) *(Euler's Theorem) If G is planar and 2-connected and $\mathcal{D}$ is a drawing of G, then the numbers of cells $c = |\mathbf{cells}(G, \mathcal{D})|$, vertices $v = |V|$, and edges $e = |E|$ are related by*
$$v + c = e + 2$$

PROOF. Proofs for all of these facts may be found in [61]. We here just give references. (i) is [19, Corollary 11.5], it can easily be proved by induction on the size of G. (ii) follows immediately from [19, Corollary 11.5]. Thus it is a consequence of the fact that the complete bipartite graph $K_{3,3}$ (one of the Kuratiowski Graphs) is not planar. (iii) is [61, Example 7.1.9]. Whitney's Theorem follows from the fact that in 3-connected planar graphs the cells are characterized as the non (edge-)separating cycles. (iv) is [19, Theorem 9.5]. Also Euler's Theorem can be proved by induction on the size of G. □

<u>REMARK 12.1.6.</u> One can also interpret Whitney's Theorem in a topological way. Let G be planar and 3-connected, and let $\mathcal{D}_1$ and $\mathcal{D}_2$ be two drawings of G for which the exterior cell corresponds to the same cycle in G. Then there is a continuous deformation (a self-homeomorphism) of $\mathbb{R}^2$ that maps $\mathcal{D}_1$ either to $\mathcal{D}_2$ or to a mirror image of $\mathcal{D}_2$. Thus Whitney's Theorem implies that no matter how we draw a planar representation of the graph in Figure 12.1.2, we will always get the same set of cycles that correspond to cells.

12.2   Tutte's Theorem on Stresses in Graphs

How can we find a drawing of a 3-connected planar graph in which the edges are represented by a single line segment, and in which all cells are realized as convex polygons? A beautiful construction that provides such an embedding was given in 1962 by W.T. Tutte [59]. The background of this construction is of almost physical nature: Assume that the edges of the graph G are made from rubber bands. Take the vertices that correspond to one particular cell c_0 whose cycle has m vertices. Pin down these vertices in the plane $\mathbb{R}^2$ such that c_0 is realized as a convex m-gon and such that all interior rubber bands are under tension. Then the figure that one gets is a planar embedding of G in which all the remaining cells $c_1, c_2, \ldots$ are realized as convex polygons. The interiors of these polygons do not overlap.

For us the crucial point is that this particular graph representation satisfies even more nice properties. If c_0 is a triangle, then the resulting figure is a Schlegel diagram of a 3-polytope with edge graph G. Figure 12.2.1 illustrates the sequence how to produce a 3-polytope from the combinatorial data of the graph G. In the first step an equilibrium representation of the graph is generated. This representation is then interpreted as a Schlegel diagram (second arrow). Then this Schlegel diagram is finally lifted to 3-space.
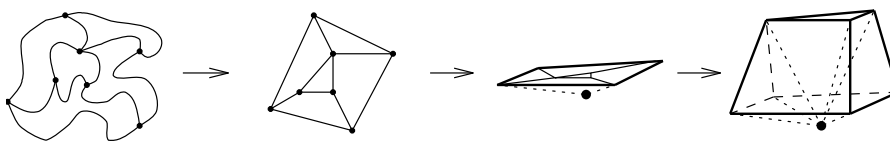
Figure 12.2.1: From graphs via stressed graph representations to polytopes.

In this section we concentrate on the first arrow in the above sequence of pictures. We give a proof of Tutte's theorem, which states that the above construction generates indeed non-overlapping convex interior cells. To proceed more formally we introduce a notion that models rubber bands in mathematical terms. To each edge $\{v, w\} \in E$ we assign a weight $\omega_{v,w} \in \mathbb{R}$ that represents the elasticity constant of the corresponding rubber band. Since $\omega_{v,w}$ is supposed

to be indexed by the *set* $\{v, w\}$, we in addition require the symmetry condition $\omega_{v,w} = \omega_{w,v}$.

<u>DEFINITION 12.2.1.</u> Let $G = (V, E)$ be a graph and $\omega \colon E \to \mathbb{R}$ be an assignment of weights to the edges. Furthermore, let $\boldsymbol{p} \colon V \to \mathbb{R}^2$ be an assignment of positions in $\mathbb{R}^2$ for the vertices of G. A vertex $v \in V$ is in *equilibrium* if

$$\sum_{\{v,w\} \in E} \omega_{v,w} (\boldsymbol{p}_v - \boldsymbol{p}_w) = 0.$$
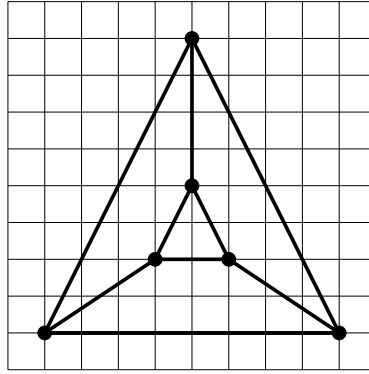
Figure 12.2.2: A graph in equilibrium.

From now on we assume that G is planar and 3-connected and that the vertices are labeled by $V = \{1, \ldots, n\}$ so that the last $k+1$ vertices $c_0 = (k+1, \ldots, n)$ are a cell of G (in this order). The cell c_0 will play the role of the external boundary of a drawing of G. We will realize c_0 as a (strictly) convex $(n-k)$-gon $\mathcal{G}$. All the remaining vertices will be forced (by the equilibrium condition) to have positions in the interior of $\mathcal{G}$. For this reason we call $V' = \{1, \ldots, k\}$ the *interior vertices*, and $V'' = \{k+1, \ldots, n\}$ the *peripheral vertices*. The *interior edges* $E' = E \setminus (V'')^2$ are those that contain at least one interior vertex. Edges between peripheral points are called *peripheral*. Figure 12.2.2 shows a situation where by setting the weights of all interior edges to "1" equilibrium for all interior vertices is obtained. We may achieve equilibrium for the peripheral vertices as well if we choose the weights of peripheral edges to "$-\frac{1}{4}$".

<u>THEOREM 12.2.2.</u> *(Tutte, 1962) Let $G = (\{1, \ldots, n\}, E)$ be a 3-connected, planar graph that has a cell $(k+1, \ldots, n)$ for some $k < n$. Let $\boldsymbol{p}_{k+1}, \ldots, \boldsymbol{p}_n$ be the vertices (in this order) of a convex $(n-k)$-gon. Let $\omega \colon E' \to \mathbb{R}^+$ be an assignment of positive weights to the internal edges.*

(i) *There are unique positions $\boldsymbol{p}_1, \ldots, \boldsymbol{p}_k \in \mathbb{R}^2$ for the interior vertices such that all interior vertices are in equilibrium.*

(ii) *All cells $c_1, c_2, \ldots$ of G are then realized as non-overlapping convex polygons.*

Actually the original proof of Tutte treated only the case where all weights are equal to one. Then each interior point is in the barycenter of its neighbors. However, Tutte's proof can literally be translated to the case of general positive weights. Here we present a complete proof of Tutte's Theorem (using an approach that is different from Tutte's).

PROOF OF EXISTENCE AND UNIQUENESS (see also [36].) Assume that the positions of the peripheral points $\boldsymbol{p}_v = (x_v, y_v)$; $v \in \{k+1, \ldots, n\}$ are given. We have to prove that suitable positions $\boldsymbol{p}_v = (x_v, y_v)$; $v \in \{1, \ldots, k\}$ for the interior vertices exist and that these positions are unique. W.l.o.g. we may assume that $\boldsymbol{p}_n = (0, 0)$. Consider the function

$$
\begin{aligned}
E(x_1, \ldots, x_k, y_1, \ldots, y_k) &= \tfrac{1}{2} \sum_{\{v,w\} \in E'} \omega_{v,w}((x_v - x_w)^2 + (y_v - y_w)^2) \\
&= \tfrac{1}{2} \sum_{\{v,w\} \in E'} \omega_{v,w} \|\boldsymbol{p}_v - \boldsymbol{p}_w\|^2.
\end{aligned}
$$

E is a quadratic function that is non-negative everywhere. Assume that $z = (x_1, \ldots, x_k, y_1, \ldots, y_k)$ has at least one entry (say x_i) with large absolute value. This implies that $\boldsymbol{p}_i$ is far away from the peripheral point $\boldsymbol{p}_n = (0, 0)$. Since G is connected, there is a path that connects $\boldsymbol{p}_i$ with $\boldsymbol{p}_n$ and for at least one edge (v, w) in this path the distance $\|\boldsymbol{p}_v - \boldsymbol{p}_w\|$ is large. Since the squared distances are weighted with positive coefficients also $E(z)$ is large. Thus for sufficiently large $\alpha > 0$, $|z| > \alpha$ implies $E(z) > E(0)$. Since E is quadratic this implies that E is strictly convex (non-degenerate with a positive definite Hessian) and thus takes its unique minimum on $\{z \mid |z| < \alpha\}$. The assertion follows from the observation that the condition for a critical point ($\nabla E = 0$) of E is

$$
\frac{\partial E}{\partial x_i} = \sum_{\{v,w\} \in E'} \omega_{v,w}(x_v - x_w) = 0 \quad \text{and} \quad \frac{\partial E}{\partial y_i} = \sum_{\{v,w\} \in E'} \omega_{v,w}(y_v - y_w) = 0
$$

for all $i \in \{1, \ldots, k\}$. This is exactly the equilibrium condition for the interior vertices. □

We proceed with the proof that in the equilibrium situation the cells are represented by non-overlapping convex polygons. For this assume that the positive weights and the position of the peripheral points $\boldsymbol{p}_{k+1}, \ldots, \boldsymbol{p}_n$ are chosen. The positions for the points $\boldsymbol{p}_1, \ldots, \boldsymbol{p}_k$ are (uniquely) determined according to the equilibrium conditions. Such a point configuration will be called an *equilibrium representation* of G. We dissect the proof into several smaller claims. Our strategy is to first prove that certain degenerate situations cannot occur and then to use a global consistency argument in order to show that all the cells are indeed convex. By $N(v) = \{w \mid (v, w) \in E\}$ we denote the set of *neighbors* of a vertex v of $G = (V, E)$. We will also use the operator N to specify the positions of corresponding embedded vertices. We define $N(\boldsymbol{p}_v) = \{\boldsymbol{p}_w \mid w \in N(V)\}$. By abuse of language we will often identify a vertex $v \in V$ with its image $\boldsymbol{p}_v$.

The *relative interior* of a collection of points $\boldsymbol{P} := \{\boldsymbol{p}_1, \ldots, \boldsymbol{p}_n\} \subset \mathbb{R}^2$ is defined by

$$\mathbf{relint}(\boldsymbol{P}) = \{\sum_{v=1}^{n} \lambda_v \boldsymbol{p}_v \mid \sum_{v=1}^{n} \lambda_v = 1 \text{ and } \lambda_v > 0 \text{ for all } v = 1, \ldots, n\}.$$

This concept will play a crucial role in our considerations. The main properties of the **relint** operator are summarized in the following two lemmas.

<u>LEMMA 12.2.3.</u> Let $\boldsymbol{p} \in \mathbf{relint}(\boldsymbol{p}_1, \ldots, \boldsymbol{p}_m)$ with $\boldsymbol{p}, \boldsymbol{p}_1, \ldots, \boldsymbol{p}_m \in \mathbb{R}^2$, and let ϕ be a linear functional on $\mathbb{R}^2$.

 (i) If there exists a $v \in \{1, \ldots, m\}$ with $\phi(\boldsymbol{p}) < \phi(\boldsymbol{p}_v)$ then there exists also a $w \in \{1, \ldots, m\}$ with $\phi(\boldsymbol{p}) > \phi(\boldsymbol{p}_w)$
 (ii) If $(\boldsymbol{p}_1, \ldots, \boldsymbol{p}_m)$ affinely spans $\mathbb{R}^2$ then

$$\mathbf{relint}(\boldsymbol{p}_1, \ldots, \boldsymbol{p}_m) = \mathbf{int}(\mathbf{conv}(\boldsymbol{p}_1, \ldots, \boldsymbol{p}_m)).$$

PROOF. We have $\boldsymbol{p} = \sum_{i=1}^{m} \lambda_i \boldsymbol{p}_i$, with all $\lambda_i > 0$. Consider the expression $\phi(\boldsymbol{p} - \sum_{i=1}^{m} \lambda_i \boldsymbol{p}_i) = 0$. Linearity of ϕ yields $\sum_{i=1}^{m} \lambda_i \phi(\boldsymbol{p} - \boldsymbol{p}_i) = 0$. If the term $\phi(\boldsymbol{p} - \boldsymbol{p}_v)$ is negative, then there must be at least one $w \in \{1, \ldots, m\}$ for which $\phi(\boldsymbol{p} - \boldsymbol{p}_w)$ is positive.

A proof of part (ii) requires a few considerations of elementary linear algebra. We leave the proof to the reader. $\qquad\square$

<u>LEMMA 12.2.4.</u> The set of all configurations $(\boldsymbol{p}_0, \boldsymbol{p}_1, \ldots, \boldsymbol{p}_m) \in \mathbb{R}^{2(m+1)}$ for which

 (i) $\boldsymbol{p}_1, \ldots, \boldsymbol{p}_m$ affinely span $\mathbb{R}^2$, and
 (ii) $\boldsymbol{p}_0 \in \mathbf{relint}(\boldsymbol{p}_1, \ldots, \boldsymbol{p}_m)$

is an open subset of $\mathbb{R}^{2(m+1)}$.

PROOF. (i) is an open condition. If (i) holds then by Lemma 2.3.(ii) condition (ii) is also open. $\qquad\square$

The following isolates the crucial property (for Tutte's Theorem) of equilibrium representations.

<u>LEMMA 12.2.5.</u> Let $\boldsymbol{P} := (\boldsymbol{p}_1, \ldots, \boldsymbol{p}_n) \in \mathbb{R}^{2n}$ be an equilibrium representation (with positive weights) of the vertices of G. Then for every interior vertex $\boldsymbol{p}$ we have $\boldsymbol{p} \in \mathbf{relint}(N(\boldsymbol{p}))$.

PROOF. Let $\boldsymbol{p}_v$ be an interior vertex. The equilibrium condition states

$$\sum_{\{v,w\}\in E} \omega_{v,w}(\boldsymbol{p}_v - \boldsymbol{p}_w) = 0$$

for every interior point v (with positive $\omega_{v,w}$). This rewrites to

$$\boldsymbol{p}_v = \frac{1}{\sum_{\{v,w\}\in E}\omega_{v,w}} \cdot \Big(\sum_{\{v,w\}\in E} \omega_{v,w}\boldsymbol{p}_w\Big).$$

Hence $\boldsymbol{p}_v$ is a convex combination of its neighbors with strictly positive coefficients. $\qquad\square$

DEFINITION 12.2.6. Let G be a 3-connected, planar graph on n vertices such that the vertices $k+1,\ldots,n$ (in this order) are a cell in G. A point configuration $\boldsymbol{P} := (\boldsymbol{p}_1,\ldots,\boldsymbol{p}_n) \in \mathbb{R}^{2n}$ is called a *good representation* for G, if the following properties are satisfied

(i) $\boldsymbol{p}_{k+1},\ldots,\boldsymbol{p}_n$ (in this order) realize a convex $(n-k)$-gon,
(ii) For $v = 1,\ldots,k$ we have $\boldsymbol{p}_v \in \mathbf{relint}(N(\boldsymbol{p}_v))$.

Lemma 12.2.5 states that equilibrium representations are good. Tutte's Theorem will be an immediate consequence of the following assertion and Lemma 12.2.5.

THEOREM 12.2.7. *Let $\boldsymbol{P} \in \mathbb{R}^{2n}$ be a good representation of a 3-connected, planar graph $G = (V,E)$, then $\boldsymbol{P}$ is a planar embedding of G in which all interior cells are realized as non-overlapping convex polygons.*

We assume that a 3-connected, planar graph G together with a good representation $\boldsymbol{P} := (\boldsymbol{p}_1,\ldots,\boldsymbol{p}_n) \in \mathbb{R}^{2n}$ are given. For a line $\ell = \{\boldsymbol{x} \mid \phi(\boldsymbol{x}) = d\} \subseteq \mathbb{R}^2$ a vertex $\boldsymbol{a}$ which is on ℓ is *ℓ-active* if not all its neighbors are on ℓ, too. Here ϕ is a suitable linear functional. We call a vertex $\boldsymbol{p}_v$ *degenerate* if the set of its neighbors $N(\boldsymbol{p}_v)$ does not affinely span $\mathbb{R}^2$. Our first aim is to show that degenerate situations cannot occur.

CLAIM 1. *Let $\boldsymbol{P}$ be a good representation of a 3-connected planar graph G. Then $\boldsymbol{P}$ has no degenerate vertices.*

PROOF. The peripheral vertices are non-degenerate by definition (they are the vertices of a strictly convex polygon). Assume $\boldsymbol{p}$ is a degenerate, interior vertex in $\boldsymbol{P}$. If $\boldsymbol{p}$ is degenerate, then there is a line $\ell = \{\boldsymbol{x} \mid \phi(\boldsymbol{x}) = d\}$ such that $\boldsymbol{p}$ and all its neighbors $N(\boldsymbol{p})$ are contained in ℓ.

Let $\boldsymbol{q}$ be a point of $\boldsymbol{P}$ that is not on ℓ. Since G is 3-connected, by Menger's Theorem (Theorem 12.1.5.(i)) there are three paths A, B, and C from $\boldsymbol{p}$ to

q which have disjoint edges and vertices (except for the endpoints p and q). Each of these paths must contain at least one ℓ-active vertex (since at some point the path has to leave the line ℓ). Let a be the first ℓ-active point in the path A that comes after p. Thus the initial segment of the path A is of the form $A^0 = (p, a_1, \ldots, a_l, a)$. All the points in A^0 are on ℓ. We define b and c respectively as the first ℓ-active points on B and C that come after p. Likewise B^0 and C^0 are the initial segments of the paths. All the edges of A^0, B^0 and C^0 taken together form a Y-graph Y^0 with endpoints a, b and c. All the edges of Y^0 are on ℓ.

We now prove that there are also Y-graphs Y^+ and Y^- with the same endpoints a, b and c, for which all edges are above (respectively below) the line ℓ. We only show the existence of the Y-graph Y^+ for which all edges are above ℓ. The existence of Y^- is proved analogously.

Among the points a, b, and c there are at most two peripheral points, since at most two of the vertices of the bounding polygon can lie on ℓ. Assume that a is an interior point. For any interior point q of P we have by definition $q \in \mathbf{relint}(N(q))$. This implies by Lemma 12.2.3.(i) that the following property for the interior points holds (remember that ℓ was of the form $\{x \mid \phi(x) = d\}$):

($*$) If there is a $q_- \in N(q)$ with $\phi(q) > \phi(q_-)$, then there exists also a $q_+ \in N(q)$ with $\phi(q) < \phi(q_+)$.

This property also holds for peripheral points that are not maximal with respect to ϕ. Since a is ℓ-active there is either a point $a_+ \in N(a)$ with $\phi(a) < \phi(a_+)$ or there is $a_- \in N(a)$ with $\phi(a) > \phi(a_-)$. In the second case property ($*$) implies the existence of an a_+ with $\phi(a) < \phi(a_+)$. Applying property ($*$) iteratively, we can generate a path $A^+ = (a_0^+, a_1^+, \ldots, a_l^+)$ that connects $a = a_0^+$ with a peripheral point $a_l^+ = a^+$ that is maximal with respect to ϕ. We apply the same reasoning and define paths B^+ and C^+ starting from b and c connecting them to ϕ-maximal peripheral points b^+ and c^+. There are at most two such ϕ-maximal peripheral points. The case of two ϕ-maximal peripheral points occurs, when the peripheral polygon has an edge on which ϕ is maximal and constant). So either a^+, b^+ and c^+ are all identical or they correspond to two points that are connected by an edge. If we consider the subgraph G^+ of G that contains the paths A^+, B^+ and C^+ with all the corresponding vertices and edges this part of G is connected. The three ℓ-active vertices a, b and c have degree one in G^+. Thus the component G^+ contains a Y graph Y^+ with endpoints a, b and c. By a similar reasoning we see that there is a a Y graph Y^- with endpoints a, b and c and all edges below ℓ.

We have proved the existence of three edge-disjoint a Y graphs Y^0, Y^+, and Y^- with endpoints a, b and c. This together with Theorem 12.1.5.(ii) contradicts the planarity of the graph G. $\qquad\square$

Figure 12.2.3. illustrates the construction of the Y-graphs Y^+ and Y^-. The arrows point in direction of increasing ϕ. The example has two ϕ-maximal points.
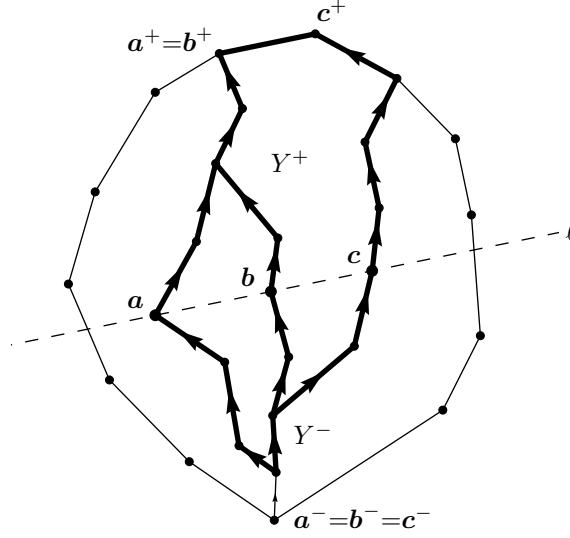
Figure 12.2.3: The construction of the graphs Y^+ and Y^-.

Claim 1 implies that for every interior point $\boldsymbol{p}_i$ the convex hull of its neighbors is 2-dimensional. This immediately gives the following assertion.

<u>CLAIM 2.</u> *For a given 3-connected planar graph G the set of all good representations $\boldsymbol{P} := (\boldsymbol{p}_1, \ldots, \boldsymbol{p}_n) \in \mathbb{R}^{2n}$ is an open subset of $\mathbb{R}^{2n}$.*

PROOF. The set of all configurations $\boldsymbol{P} \in \mathbb{R}^{2n}$ that satisfy condition (i) of Definition 12.2.5 is an open set. (The condition that the vertices $\boldsymbol{p}_{k+1}, \ldots, \boldsymbol{p}_n$ form a convex polygon is stable under small perturbations of the points). Claim 1 states that none of the interior points is degenerate. Thus we may replace condition (ii) of Definition 12.2.5 by the k conditions

   (ii)$_i$ $\boldsymbol{p}_i \in \mathbf{relint}(N(\boldsymbol{p}_i))$ and $N(\boldsymbol{p}_i)$ affinely spans $\mathbb{R}^2$,

for $i = 1, \ldots, k$. Lemma 12.2.4 states that the set of configurations $\boldsymbol{P} \in \mathbb{R}^{2n}$ for which (ii)$_i$ holds is open (i.e. it is stable under small perturbations of the points). Hence the set of all good representations of G is the intersection of $k+1$ open sets and therefore itself is open. □

To proceed, we introduce an operator $\Omega(\boldsymbol{p}_v)$ that measures the sum of absolute values of angles around a point of a good representation $\boldsymbol{P}$. This operator will be used for a "global consistency" argument that proves that the cells are convex and non-overlapping. The operator Ω will only be defined (and needed) for graphs G', for which except for the bounding polygon all cells are triangles. Furthermore, we require that no three points of an interior triangle in $\boldsymbol{P}$ are collinear (i.e. affinely dependent). Such representations of G' will be called *very good*.

Let G' be a 3-connected, planar graph, for which at most one cell is not a triangle. We assume that G' has n vertices and that $k + 1, \ldots, n$ (the exterior cell) forms the possibly non-triangular cell. By Whitney's Theorem (Theorem 12.1.5.(iii), Remark 12.1.6) the combinatorial structure of a planar drawing of a 3-connected, planar graph is independent of a particular embedding. This is resembled by the fact that around each vertex the cyclic order of its neighbors in an embedding is unique. Two vertices $v_1, v_2 \in N(V)$ are *adjacent at* a vertex v (with respect to this order) if there is a cell that contains $\{v, v_1, v_2\}$. We consider a particular planar embedding of G' and around each vertex v we take the counterclockwise cyclic order $(v^1, \ldots, v^{|N(v)|})$ of its neighbors. Thus v^i and v^{i+1} are adjacent at v for $i = 1, \ldots, |N(v)|$, indices modulo $|N(v)|$.

Now let $\boldsymbol{P}$ be a very good representation of G' (i.e. no three points of a triangle are collinear). We set $\alpha^i(\boldsymbol{p}_v) = \angle(\boldsymbol{p}_v; \boldsymbol{p}_{v^i}, \boldsymbol{p}_{v^{i+1}})$. Here $\angle(\boldsymbol{p}_v; \boldsymbol{p}_{v^i}, \boldsymbol{p}_{v^{i+1}})$ denotes the angle between $\boldsymbol{p}_{v^i}, \boldsymbol{p}_{v^{i+1}}$ seen from the point $\boldsymbol{p}_v$. Angles are always understood as values between $-\pi$ and $+\pi$. We define the operator $\Omega(\boldsymbol{p}_v)$ by

$$\Omega(\boldsymbol{p}_v) = \sum_{i=1}^{|N(v)|} |\alpha^i(\boldsymbol{p}_v)|.$$

$$\Omega(\boldsymbol{p}_0)=2\pi \qquad \Omega(\boldsymbol{p}_0)>2\pi \qquad \Omega(\boldsymbol{p}_0)<2\pi$$
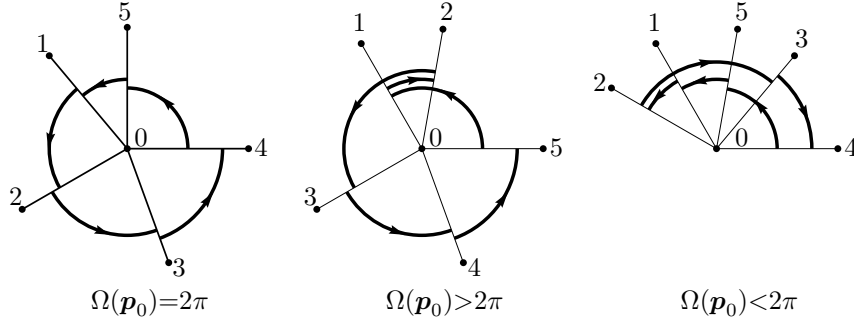
Figure 12.2.4: Examples for values of $\Omega(\boldsymbol{p}_0)$.

Thus $\Omega(\boldsymbol{p})$ measures the sum of the absolute values of the angles between adjacent neighbors of $\boldsymbol{p}$. Figure 12.2.4 shows three situations of a vertex with 5 neighbors $(1, 2, 3, 4, 5)$ (in this order). In the first picture $\Omega(\boldsymbol{p}_0)$ is 2π (the neighbors come in the correct order). In the second picture $\Omega(\boldsymbol{p}_0)$ is larger than 2π. In the third picture $\Omega(\boldsymbol{p}_0)$ is smaller than 2π.

<u>CLAIM 3.</u> *Let $\boldsymbol{P}$ be a very good representation of G.*

(i) *If $\boldsymbol{p}_v$ is a peripheral point then $\Omega(\boldsymbol{p}_v) \geq 2|\beta_v|$, where β_v is the angle between the two neighbors of $\boldsymbol{p}_v$ in the peripheral polygon.*

(ii) *If $\boldsymbol{p}_v$ is an interior point, then $\Omega(\boldsymbol{p}_v) \geq 2\pi$.*

PROOF. Observe that $\sum_{i=1}^{|N(v)|} \alpha^i(\boldsymbol{p}_v)$ (the sum over the values of the angles — *not* over their absolute values) is of the form $j \cdot 2\pi$ for an integer j. If $j \neq 0$ we

are done in both cases. So we restrict ourselves to the case $\sum_{i=1}^{|N(v)|} \alpha^i(\boldsymbol{p}_v) = 0$. To see (i) note that β_v is a summand (say $\alpha^1(\boldsymbol{p}_v)$) of this sum. We get

$$\Omega(\boldsymbol{p}_v) \geq |\beta_v| + |\sum_{i=2}^{|N(v)|} \alpha^i(\boldsymbol{p}_v)| = |\beta_v| + |-\beta_v| = 2|\beta_v|.$$

Part (ii) follows by similar reasoning from the fact that each interior point is in the relative interior of its neighbors. ☐

CLAIM 4. *With all settings as above (there are $(n-k)$ peripheral vertices, and all interior cells are triangles) there are exactly $n+k-2$ interior cells.*

PROOF. Let e be the number of edges and t be the number of interior cells (i.e. one less than the total number of cells). By Euler's Theorem (Theorem 12.1.5.(iv)) we have $n + t = e + 1$. On the other hand we have $2e = 3t + (n - k)$, since each edge is counted twice if we sum over all edges of different cells. Combining these two equations gives $t = n + k - 2$. ☐

CLAIM 5. *Let $\boldsymbol{P}$ be a very good representation of G'. Then*

$$\sum_{v=1}^{n} \Omega(\boldsymbol{p}_v) = (2n - 4)\pi.$$

PROOF. Since $\sum = \sum_{v=1}^{n} \Omega(\boldsymbol{p}_v)$ runs over all points, this sum is the sum of all absolute angles at vertices of cells of G'. Thus we may compute $\sum$ by summing up for all cells the sum of the internal angles at the vertices. All interior cells are triangles and each of these triangles accounts to a summand of π in $\sum$. By Claim 4 the number of interior triangles of G is $n + k - 2$. Thus from the interior cells we get an overall number of $(n + k - 2)\pi$.

The peripheral $(n - k)$-gon is convex. Thus from this we get a summand $(n - k - 2)\pi$. Combining the two terms we get $\sum = (2n - 4)\pi$ as desired. ☐

CLAIM 6. *Let $\boldsymbol{P}$ be a very good representation of G' then for every interior point $\boldsymbol{p}_v$ we have $\Omega(\boldsymbol{p}_v) = 2\pi$. For every peripheral point $\boldsymbol{p}_v$ we have $\Omega(\boldsymbol{p}_v) = 2|\beta_v|$*

PROOF. Claim 3 shows that in a very good representation we have

    (∗): $\Omega(\boldsymbol{p}_v) \geq 2\pi$ for the interior points, and
    (∗∗): $\Omega(\boldsymbol{p}_v) \geq 2|\beta_v|$ for the peripheral points.

There are k interior points and there are $(n-k)$ peripheral points. Thus we have

$$\sum_{v=1}^{n} \Omega(\boldsymbol{p}_v) \geq 2k\pi + 2(\sum_{v=k+1}^{n} |\beta_v|) = 2k\pi + 2(n-k-2)\pi = (2n-4)\pi.$$

Equality holds if and only if we have equality in all the expressions $(*)$ and $(**)$. On the other hand we have equality by Claim 5. This implies the desired result. $\square$

CLAIM 7.   *For three non-collinear points* $\boldsymbol{a}$, $\boldsymbol{b}$, $\boldsymbol{c}$ *the angles* $\angle(\boldsymbol{a};\boldsymbol{b},\boldsymbol{c})$, $\angle(\boldsymbol{b};\boldsymbol{c},\boldsymbol{a})$, *and* $\angle(\boldsymbol{c};\boldsymbol{a},\boldsymbol{b})$ *are either all positive or all negative.*

PROOF.   Draw a picture. $\square$

CLAIM 8.   *Let* $\boldsymbol{P}$ *be a very good representation of* G'. *Except for the angles between peripheral points (the* β_v) *all* $\alpha^i(\boldsymbol{p}_v)$ *are positive.*

PROOF.   By our convention on the orientation of the peripheral points the β_v are all negative. Claim 6 implies that the absolute values of the remaining angles at a peripheral point $\boldsymbol{p}_v$ must exactly sum up to β_v. This can only happen if they all are non-negative. Since we assumed that no three points are collinear we know that these angles are indeed positive. Claim 6 also implies that at an interior point either all angles are positive or all angles are negative. Repeated application of this fact together with Claim 7 proves the claim. $\square$

We call the angles that are determined by Claim 8 *interior angles* We now have collected all pieces to finally prove Theorem 12.2.7 (our missing piece to complete the proof of Tutte's Theorem).

PROOF OF THEOREM 12.2.7. Let $G = (V, E)$ be a planar and 3-connected graph together with a selection of a peripheral cell $(n - k, \ldots, n)$, and let $\boldsymbol{P}$ be a good representation of G. We add interior edges to G to obtain a graph $G' = (V, E') \supseteq G$ that is still planar but for which all interior cells are (combinatorially) triangles. We can always achieve this by further subdividing non-triangular interior cells. The configuration $\boldsymbol{P}$ is also a good representation of G'. We represent the interior triangles $T_1, \ldots, T_t$ of G' by 3-cycles $T_i = (v_i^1, v_i^2, v_i^3)$. We assume that the orientation of the cycles is chosen consistently such that adjacent triangles traverse their common edge in opposite direction. This can be done by orienting each triangle counterclockwise (in an original planar drawing of G' with the same peripheral polygon).

We first prove that in the representation $\boldsymbol{P}$ the vertices of each triangle of G' are affinely independent. Assume on the contrary that there is a triangle (v^1, v^2, v^3) with collinear points $\boldsymbol{p}_{v^1}$, $\boldsymbol{p}_{v^2}$, $\boldsymbol{p}_{v^3}$. Then we can perturb the position of the vertices to obtain a very good representation of G' in which at least one of

the interior angles is negative (by Claim 2 the set of all good representations of G' is open). This contradicts Claim 8. Thus none of the triangles is degenerate. Claim 8 now proves that since $\boldsymbol{P}$ is a very good representation all interior angles are strictly positive.

For a particular representation $\boldsymbol{P}$ and a triangle $T_i = (v_i^1, v_i^2, v_i^3)$ we consider its oriented area $\mathbf{vol}(T)$. This area is positive if $(\boldsymbol{p}_{v_1}, \boldsymbol{p}_{v_1}, \boldsymbol{p}_{v_1})$ come in counterclockwise order, and negative if they come in clockwise order. The fact that all interior angles are strictly positive translates to the fact that all areas are positive.

Independent of the position of the interior vertices the area of the peripheral polygon c_0 can be calculated as

$$\mathbf{vol}(c_0) = \sum_{i=1}^{t} \mathbf{vol}(T_i).$$

(This is a consequence of our orientation convention.) The triangles cover the peripheral polygon. If two triangles would overlap (in a region of positive measure) the overlapping region would be counted twice in the volume formula. Since all triangle volumes are positive this cannot happen. Thus no two triangles do overlap. This property is (by Claim 2) even stable for small perturbations of the points in $\boldsymbol{P}$. Thus if we consider the points in $\boldsymbol{P}$ together with the edges that are induced by G' we obtain a proper triangulation of the peripheral polygon. From this we conclude that (if we just consider the edges of G) we get a drawing of G in which the cells are realized by non-overlapping polygons. Since each internal vertex lies in the relative interior of its neighbors the cell must be convex. $\square$

Figure 12.2.5 Shows a good representation of a planar 3-connected graph G. Also a possible triangulation (the graph G') is given.

Figure 12.2.5: A good representation of G and its subdivision G'.

13   3-Polytopes

13.1   From Stressed Graphs to Polytopes

In this section we prove that every representation of a graph that is generated by Tutte's Theorem is the projection of a piecewise linear convex surface that sits above the peripheral polygon $\mathcal{G}$. If the bounding polygon is a triangle, the region that is enclosed by the surface and the triangle is a 3-polytope.

It was first observed by Maxwell in 1864 [45, 46] that the projection of the skeleton of a 3-dimensional polytope forms a graph representation that admits an equilibrium. The converse of this fact is slightly more subtle since one has to take care of the signs of the weights to maintain convexity. A first detailed analysis of the situations that occur was given by Crapo and Whiteley [23]. Nice treatments of this subjects from slightly different points of view are also given by Hopcroft & Kahn [36] (emphasizing the homological background) and by McMullen [47] (with emphasis on the structure of tilings. McMullen studies also higher dimensional versions). We here want to go the way that leads directly to a proof of Steinitz's Theorem, neglecting all the subtleties that play a role in the more general setting of Crapo and Whiteley.

In the sequel we assume that a 3-connected, planar graph G is given together with a choice of a peripheral polygon and an assignment of positive weights to the interior edges. We assume that the peripheral cell is realized as a convex polygon $\mathcal{G} = \mathbf{conv}(\boldsymbol{p}_{n-k}, \ldots, \boldsymbol{p}_n)$. The configuration $\boldsymbol{P} = (\boldsymbol{p}_1, \ldots, \boldsymbol{p}_n)$ is the unique equilibrium configuration that is generated by Tutte's Theorem. So far we have proved that the interior cells form a proper cell decomposition of $\mathcal{G}$ by convex polygons. We assume that the plane in which the points of $\boldsymbol{P}$ are located is already embedded in $\mathbb{R}^3$ at the plane $z = 1$. Thus we interpret $\boldsymbol{P}$ as a configuration in $\mathbb{R}^{3 \cdot n}$. Each $\boldsymbol{p}_i$ has (homogenized) coordinates $(x_i, y_i, 1)$. Let the interior cells c_i be indexed by $1, \ldots, m$, and let c_0 be the cell that corresponds to the peripheral polygon. For an oriented interior edge (i, j) of our graph there is (by Tutte's Theorem) a unique adjacent cell L to the left of it, and there is a unique adjacent cell R to the right of it. We call the (ordered) quadruple $(b, t | L, R)$ an *oriented patch* of $(G, \boldsymbol{P})$. If $(b, t | L, R)$ is an oriented patch then, $(t, b | R, L)$ is an oriented patch as well. (The letters are chosen as mnemonics for $t = top$, $b = bottom$, $L = left$, $R = right$.) To each interior cell c_i we associate a vector $\boldsymbol{q}_i \in \mathbb{R}^3$ by setting

(i) $\boldsymbol{q}_1 = (0, 0, 0)$

(ii) $\boldsymbol{q}_L = \omega_{b,t}(\boldsymbol{p}_b \times \boldsymbol{p}_t) + \boldsymbol{q}_R$ if $(b, t | L, R)$ is an oriented patch of $(G, \boldsymbol{P})$.

<u>LEMMA 13.1.1.</u>   *The vectors $\boldsymbol{q}_i$ are well defined.*

PROOF. First observe that the two oriented patches $(b, t | L, R)$ and $(t, b | R, L)$ define a consistent relation between $\boldsymbol{p}_b$, $\boldsymbol{p}_t$, $\boldsymbol{q}_L$, and $\boldsymbol{q}_R$, since

$$\boldsymbol{q}_L = \omega_{b,t}(\boldsymbol{p}_b \times \boldsymbol{p}_t) + \boldsymbol{q}_R \quad \Longleftrightarrow \quad \boldsymbol{q}_R = \omega_{t,b}(\boldsymbol{p}_t \times \boldsymbol{p}_b) + \boldsymbol{q}_L.$$

The value of a vector $\boldsymbol{q}_j$ with $j \in \{2, \dots, m\}$ can be computed by first choosing a sequence of cells

$$c_1 = c_{L_1}, c_{L_2}, \dots, c_{L_l} = c_j$$

such that for $i = 1, \dots, l-1$ the cells $c_{L_i}, c_{L_{i+1}} = c_{R_i}$ are both adjacent to an edge (b_i, t_i) of G. We then have oriented patches $(b_i, t_i | L_i, R_i)$ and can calculate the value of $\boldsymbol{q}_{L_{i+1}}$ from the value of $\boldsymbol{q}_{L_i}$. (Each such sequence corresponds to a path that connects the interior of c_1 to the interior of c_j by successively crossing edges of G.) Figure 13.1.1 shows two different paths P_1, and P_2 that connect the same pair of cells c_1, c_j.
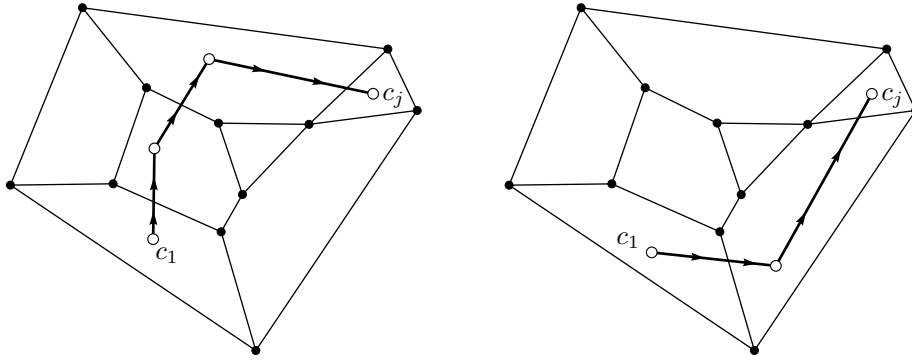
Figure 13.1.1: Two paths connecting c_1 and c_j.

It remains to show that no matter which sequence (i.e. path) we have chosen we end up with the same value for $\boldsymbol{q}_j$. To a path P_i^j from a cell c_i to a cell c_j we associate the difference vector $\boldsymbol{d}_{P_i^j} = \boldsymbol{q}_j - \boldsymbol{q}_i$ that is determined by the above procedure. We denote the reversed path from c_j to c_i by P_j^i. We have $\boldsymbol{d}_{P_j^i} = -\boldsymbol{d}_{P_i^j}$. We have to show that for any two different paths P_i^j, and Q_i^j from c_i to c_j we have $\boldsymbol{d}_{P_i^j} = \boldsymbol{d}_{Q_i^j}$. In other words the "round trip" R_i^i generated by first following P_i^j and then following the reversed path Q_j^i must generate a vanishing difference vector

$$\boldsymbol{d}_{R_i^i} = \boldsymbol{d}_{P_i^j} - \boldsymbol{d}_{Q_i^j} = (0, 0, 0).$$

The difference vector of each round trip R_i^i can be generated by summing up the difference vectors of round trips around all the vertices that are enclosed by R_i^i (compare Figure 13.1.2).

Thus it is sufficient to show that any round trip around an interior vertex generates a difference vector $(0, 0, 0)$. Let $\boldsymbol{p}_0$ be an interior point and let (with a new distribution of indices) $\boldsymbol{p}_1, \dots, \boldsymbol{p}_l$ be the cyclic sequence of its neighbors.

We get

$$
\begin{aligned}
\sum_{i=1}^{l} \omega_{0,i}(\boldsymbol{p}_0 \times \boldsymbol{p}_i) &= \sum_{i=1}^{l} \omega_{0,i}((\boldsymbol{p}_0 \times \boldsymbol{p}_i) - (\boldsymbol{p}_0 \times \boldsymbol{p}_0)) \\
&= \sum_{i=1}^{l} \omega_{0,i}(\boldsymbol{p}_0 \times (\boldsymbol{p}_i - \boldsymbol{p}_0)) \\
&= \boldsymbol{p}_0 \times \sum_{i=1}^{l} \omega_{0,i}(\boldsymbol{p}_i - \boldsymbol{p}_0) \\
&= \boldsymbol{p}_0 \times (0,0,0) \\
&= (0,0,0)
\end{aligned}
$$

The first equation holds since the $\boldsymbol{p}_0 \times \boldsymbol{p}_0$ is always zero. The second and third equation hold by the linearity of the cross product. The fourth equation holds since around every interior point we had an equilibrium. $\square$
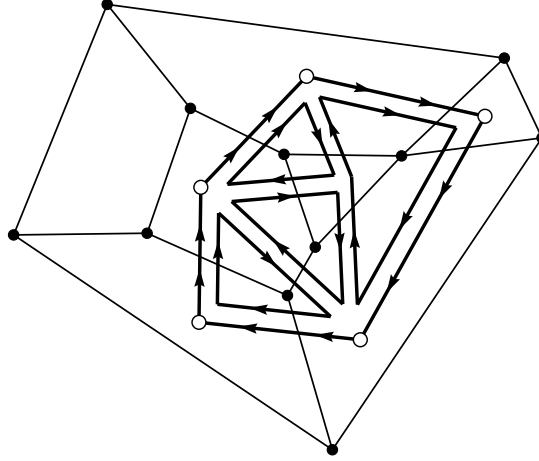
Figure 13.1.2: A "round trip" is the sum of small cycles.

The vectors $\boldsymbol{q}_i$ are now used to define a lifting function for the vectors $\boldsymbol{q}_i$. We define a piecewise linear function $f \colon \mathcal{G} \to \mathbb{R}$ from the convex hull of our drawing $\mathcal{G} = \mathbf{conv}(\boldsymbol{p}_{n-k}, \ldots, \boldsymbol{p}_n)$ to $\mathbb{R}$. This function f is defined by

$$f(\boldsymbol{x}) = \langle \boldsymbol{x}, \boldsymbol{q}_i \rangle \text{ if } \boldsymbol{x} \in c_i.$$

LEMMA 13.1.2.   *The function f is well defined.*

PROOF. The only fact that we have to show is that for adjacent cells c_L and c_R the functions $\langle \boldsymbol{x}, \boldsymbol{q}_L \rangle$ and $\langle \boldsymbol{x}, \boldsymbol{q}_R \rangle$ agree along the common edge e. Let $(b,t|L,R)$ be the corresponding oriented patch. A point on the edge e can be written as $\boldsymbol{p} = \lambda \boldsymbol{p}_b + (1-\lambda)\boldsymbol{p}_t$. Since the scalar product is linear it is sufficient to show that the two functions agree on $\boldsymbol{p}_b$ and $\boldsymbol{p}_t$.

$$\langle \boldsymbol{p}_b, \boldsymbol{q}_L \rangle = \langle \boldsymbol{p}_b, \omega_{b,t}(\boldsymbol{p}_b \times \boldsymbol{p}_t) + \boldsymbol{q}_R \rangle = \omega_{b,t}\langle \boldsymbol{p}_b, (\boldsymbol{p}_b \times \boldsymbol{p}_t) \rangle + \langle \boldsymbol{p}_b, \boldsymbol{q}_R \rangle = \langle \boldsymbol{p}_b, \boldsymbol{q}_R \rangle.$$

A similar relation holds for $\boldsymbol{p}_t$.   □

The last lemma implies that f defines a unique height for each of the vertices $\boldsymbol{p}_1, \ldots, \boldsymbol{p}_n$. The following lemma shows that we have local convexity.

LEMMA 13.1.3.   *For adjacent interior cells c_L, and c_R let ℓ be the line that supports the edge $c_L \cap c_R$. Every point $\boldsymbol{x}$ that is on the same side of ℓ as $\boldsymbol{q}_L$ satisfies $\langle \boldsymbol{x}, \boldsymbol{q}_L \rangle > \langle \boldsymbol{x}, \boldsymbol{q}_R \rangle$.*

PROOF. Let $(b, t | L, R)$ be the corresponding oriented patch. We have

$$\langle \boldsymbol{x}, \boldsymbol{q}_L \rangle - \langle \boldsymbol{x}, \boldsymbol{q}_R \rangle = \langle \boldsymbol{x}, \omega_{b,t}(\boldsymbol{p}_b \times \boldsymbol{p}_t) \rangle = \omega_{b,t} \cdot \mathbf{det}(\boldsymbol{x}, \boldsymbol{p}_b, \boldsymbol{p}_t) > 0,$$

by our orientation convention and the fact that the weight $\omega_{b,t}$ is positive.   □

Finally, we prove global convexity by using Tutte's Theorem.

LEMMA 13.1.4.   *At a point $\boldsymbol{x} \in \mathbf{int}(c_i)$ the value $\langle \boldsymbol{x}, \boldsymbol{q}_i \rangle$ is greater than all values $\langle \boldsymbol{x}, \boldsymbol{q}_j \rangle$ with $i \neq j$.*

PROOF. To compare $\langle \boldsymbol{x}, \boldsymbol{q}_i \rangle$ with some $\langle \boldsymbol{x}, \boldsymbol{q}_j \rangle$, with $j \neq i$ take a line ℓ that connects $\boldsymbol{x}$ with an interior point $\boldsymbol{y}$ of c_j, such that ℓ does not path through any of the points in $\boldsymbol{P}$. Moving along ℓ from $\boldsymbol{x}$ to $\boldsymbol{y}$ defines (since by Tutte's Theorem all cells are convex and decompose $\mathcal{G}$) a sequence of cells

$$c_i = c_{L_1}, c_{L_2}, \ldots, c_{L_l} = c_j.$$

By Lemma 13.1.3 we have

$$\langle \boldsymbol{x}, \boldsymbol{q}_i \rangle > \langle \boldsymbol{x}, \boldsymbol{q}_{L_1} \rangle > \langle \boldsymbol{x}, \boldsymbol{q}_{L_2} \rangle > \ldots > \langle \boldsymbol{x}, \boldsymbol{q}_{L_l} \rangle = \langle \boldsymbol{x}, \boldsymbol{q}_j \rangle.$$

This proves the claim.   □

Lemma 13.1.4 and Lemma 13.1.2 show that the set

$$\mathcal{X} = \{\boldsymbol{x} \in \mathbb{R}^3 \mid \langle \boldsymbol{x}, \boldsymbol{q}_i \rangle \geq 0 \text{ for } i = 1, \ldots, m\} \cap \{(x, y, z) \in \mathbb{R}^3 \mid (x, y, 1) \in \mathcal{G}\}$$

forms an (unbounded) polyhedral set in the cylinder $\{(x, y, z) \in \mathbb{R}^3 \mid (x, y, 1) \in \mathcal{G}\}$. Each of the equations $\langle \boldsymbol{x}, \boldsymbol{q}_i \rangle = 0$ supports a facet of $\mathcal{X}$ that projects to the corresponding cell in our representation of G. The vertices of $\mathcal{X}$ are of the form $\boldsymbol{p}'_i = (x_i, y_i, \langle \boldsymbol{p}_i, \boldsymbol{q}_j \rangle)$ where c_j is a cell that contains the point $\boldsymbol{p}_i = (x_i, y_i, 1)$. It is not true that in general the lifted *peripheral* points $\boldsymbol{p}'_{n-k}, \ldots, \boldsymbol{p}'_n$ are automatically coplanar. This is only the case if we can chose weights for the peripheral edges such that also the peripheral vertices are in equilibrium. However if the peripheral cell is a triangle then the three lifted points are automatically coplanar. So we obtain immediately:

COROLLARY 13.1.5. *If a graph G is planar, 3-connected and contains a triangular cell, then it is the edge graph of a 3-polytope.*

PROOF. Chose the triangular cell as the peripheral polygon, chose positive weights for the interior edges, find the equilibrium, and apply our lifting procedure. The resulting set $\mathcal{X}$ has to be intersected with a closed halfspace bounded by the plane that supports the lifted peripheral triangle in order to obtain the desired polytope. ◻

The last corollary is already the statement of Steinitz's Theorem for the special case when G contains a triangle. The following considerations show how to proceed if this is not the case.

LEMMA 13.1.6. *A planar and 3-connected graph G contains either a triangular cell or a vertex of degree 3.*

PROOF. Let v, c, and e be the numbers of vertices, cells, and edges, respectively. Let α_v be the average vertex degree and α_c the average number of sides per cell. Since each edge is incident to exactly two vertices, we get $\alpha_v v = 2e$. Since each edge is adjacent to exactly two cells, we get $\alpha_c c = 2e$. Adding these two equations and inserting Euler's formula we get:

$$\alpha_v v + \alpha_c c = 4e = 4v + 4c - 8.$$

This implies that at least one of the numbers α_v or α_c is less than 4. Since each vertex degree is at least 3 and each cell has at least 3 sides, there is either a triangle or a vertex of degree 3. ◻

The last lemma allows us to use polarity to prove the general Steinitz's Theorem. If G is a 3-connected planar graph with cells $c_0, \ldots, c_m$, then the *polar graph* G^Δ of G is graph $G^\Delta = (\{0, \ldots, m\}, E^\Delta)$. The pair $\{i, j\}$ is an edge in E^Δ if c_i and c_j have an edge in common in G. The following lemma summarizes the main properties of polarity of graphs and polytopes.

LEMMA 13.1.7. *Let $\boldsymbol{P}$ be a polytope and G be a 3-connected planar graph.*

 (i) G^Δ *is a 3-connected planar graph.*
(ii) $G^{\Delta\Delta} = G$.
(iii) *If G is the edge graph of $\boldsymbol{P}$ then G^Δ is the edge graph of $\boldsymbol{P}^\Delta$.*

PROOF. Proofs of these standard facts may be found in [65]. ◻

We finally prove Steinitz's Theorem.

THEOREM 13.1.8 (STEINITZ'S THEOREM). *If a graph G is planar and 3-connected, then it is the edge graph of a 3-polytope.*

PROOF. If G contains a triangular cell, then we are done by Corollary 13.1.5. Otherwise Lemma 13.1.6 implies that G has a vertex v of degree 3. In the polar graph G^Δ this vertex corresponds to a triangular cell. Thus we can realize by Corollary 13.1.5 a polytope $\boldsymbol{P}'$ with edge graph G^Δ. Applying a translation, if necessary, we may assume that $\boldsymbol{P}'$ contains the origin in its interior. The polar $\boldsymbol{P}'^\Delta$ has edge graph $(G^\Delta)^\Delta = G$.   □

EXAMPLE 13.1.9. This example demonstrates the different states of the construction for the case of a cube with one truncated vertex. The unique triangular cell is taken as the peripheral polygon. With the labels of Figure 13.1.3 the cells are:

$$(2, 7, 9, 10, 5), (3, 5, 10, 8, 5), (4, 6, 8, 9, 7),$$

$$(1, 2, 5, 3), (1, 3, 6, 4), (1, 4, 7, 2), (8, 9, 10).$$

We set $\boldsymbol{p}_8 = (0,0)$, $\boldsymbol{p}_9 = (1,0)$, $\boldsymbol{p}_{10} = (0,1)$, and chose the weights of the interior edges to be 1. The positions of the interior edges can then be calculated by solving the equations $M \cdot \boldsymbol{x} = \boldsymbol{b}_x$ and $M \cdot \boldsymbol{y} = \boldsymbol{b}_y$. Here $\boldsymbol{x} = (x_1, \ldots, x_7)^T$ and $\boldsymbol{y} = (y_1, \ldots, y_7)^T$ are the x- and y-coordinates of the seven interior points. The matrix M (the stress matrix) and the vectors $\boldsymbol{b}_x$ and $\boldsymbol{b}_y$ are given by

$$
M = \begin{pmatrix}
-3 & 1 & 1 & 1 & 0 & 0 & 0 \\
1 & -3 & 0 & 0 & 1 & 0 & 1 \\
1 & 0 & -3 & 0 & 1 & 1 & 0 \\
1 & 0 & 0 & -3 & 0 & 1 & 1 \\
0 & 1 & 1 & 0 & -3 & 0 & 0 \\
0 & 0 & 1 & 1 & 0 & -3 & 0 \\
0 & 1 & 0 & 1 & 0 & 0 & -3
\end{pmatrix} ; \quad
\boldsymbol{b}_x = \begin{pmatrix} 0 \\ 0 \\ 0 \\ 0 \\ 0 \\ 0 \\ 1 \end{pmatrix} ; \quad
\boldsymbol{b}_x = \begin{pmatrix} 0 \\ 0 \\ 0 \\ 0 \\ 1 \\ 0 \\ 0 \end{pmatrix} .
$$

Solving this system of linear equations and embedding the points in the $z = 1$ plane we get

$$\boldsymbol{p}_1 = (\tfrac{1}{3}, \tfrac{1}{3}, 1), \ \boldsymbol{p}_2 = (\tfrac{3}{8}, \tfrac{3}{8}, 1), \ \boldsymbol{p}_3 = (\tfrac{1}{4}, \tfrac{3}{8}, 1), \ \boldsymbol{p}_4 = (\tfrac{3}{8}, \tfrac{1}{4}, 1),$$

$$\boldsymbol{p}_5 = (\tfrac{5}{24}, \tfrac{7}{12}, 1), \ \boldsymbol{p}_6 = (\tfrac{5}{24}, \tfrac{5}{24}, 1), \ \boldsymbol{p}_7 = (\tfrac{7}{12}, \tfrac{5}{24}, 1),$$
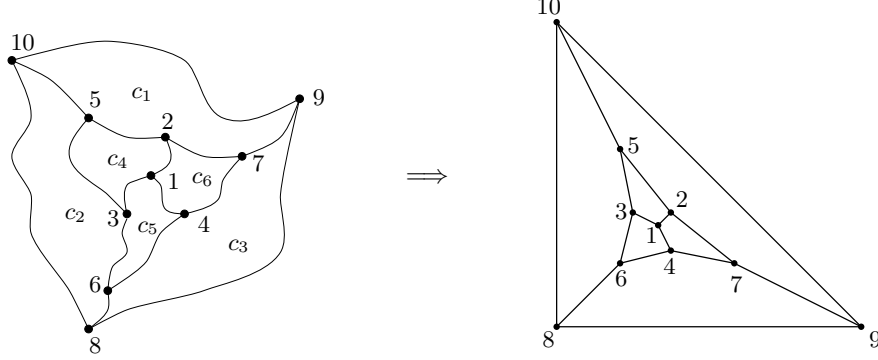
Figure 13.1.3: A graph and its stressed embedding.

To calculate the heights of the points in a corresponding lifting we first have to calculate the vectors $\boldsymbol{q}_1, \ldots, \boldsymbol{q}_6$ that are associated to the cells. We get

$$
\begin{aligned}
\boldsymbol{q}_1 &= (0,0,0) \\
\boldsymbol{q}_2 &= \boldsymbol{q}_1 + \boldsymbol{p}_{10} \times \boldsymbol{p}_5 &&= \left(\tfrac{5}{12}, \tfrac{5}{24}, -\tfrac{5}{24}\right) \\
\boldsymbol{q}_3 &= \boldsymbol{q}_1 + \boldsymbol{p}_7 \times \boldsymbol{p}_9 &&= \left(\tfrac{5}{24}, \tfrac{5}{12}, -\tfrac{5}{24}\right) \\
\boldsymbol{q}_4 &= \boldsymbol{q}_1 + \boldsymbol{p}_5 \times \boldsymbol{p}_2 &&= \left(\tfrac{5}{24}, \tfrac{1}{6}, -\tfrac{9}{64}\right) \\
\boldsymbol{q}_5 &= \boldsymbol{q}_4 + \boldsymbol{p}_3 \times \boldsymbol{p}_1 &&= \left(\tfrac{1}{4}, \tfrac{1}{4}, -\tfrac{35}{192}\right) \\
\boldsymbol{q}_6 &= \boldsymbol{q}_1 + \boldsymbol{p}_2 \times \boldsymbol{p}_7 &&= \left(\tfrac{1}{6}, \tfrac{5}{24}, -\tfrac{9}{64}\right)
\end{aligned}
$$

It is easy to check that we get the same values independent from the particular sequences that we have chosen to calculate the $\boldsymbol{q}_i$. Now we get the heights by forming scalar products of the $\boldsymbol{q}_i$ and the $\boldsymbol{p}_v$. We get

$$
\begin{aligned}
h_1 &= \langle \boldsymbol{p}_1, \boldsymbol{q}_4 \rangle &&= -\tfrac{1}{64}, & h_2 &= \langle \boldsymbol{p}_2, \boldsymbol{q}_1 \rangle &&= 0, \\
h_3 &= \langle \boldsymbol{p}_3, \boldsymbol{q}_2 \rangle &&= -\tfrac{5}{192}, & h_4 &= \langle \boldsymbol{p}_4, \boldsymbol{q}_3 \rangle &&= -\tfrac{5}{192}, \\
h_5 &= \langle \boldsymbol{p}_5, \boldsymbol{q}_1 \rangle &&= 0, & h_6 &= \langle \boldsymbol{p}_6, \boldsymbol{q}_2 \rangle &&= -\tfrac{5}{64}, \\
h_7 &= \langle \boldsymbol{p}_7, \boldsymbol{q}_1 \rangle &&= 0, & h_8 &= \langle \boldsymbol{p}_8, \boldsymbol{q}_2 \rangle &&= -\tfrac{5}{24}, \\
h_9 &= \langle \boldsymbol{p}_9, \boldsymbol{q}_1 \rangle &&= 0, & h_{10} &= \langle \boldsymbol{p}_{10}, \boldsymbol{q}_1 \rangle &&= 0.
\end{aligned}
$$

Again it is easy to test the consistency of all possible ways to calculate the h_i. If one prefers positive integers for the heights one can also multiply by a factor of -192 to obtain:

$$
h_1 = 3, \ h_2 = 0, \ h_3 = 5, \ h_4 = 5, \ h_5 = 0,
$$

$$
h_6 = 15, \ h_7 = 0, \ h_8 = 40, \ h_9 = 0, \ h_{10} = 0.
$$

13.2 A Quantitative Analysis

This section is devoted to the question of the size $f(n)$ of a minimal grid $\{1, 2, \ldots, f(n)\}^3$ on which all combinatorial types of 3-polytopes with n vertices can be realized. Following the construction steps from a graph to a concrete polytope leads to an upper bound for this minimal grid size. The bound that we achieve will be singly exponential in n for the case of simplicial polytopes and it will be singly exponential in n^2 for the general case. This improves the upper bound of n^{169n^3} that was computed by Onn and Sturmfels [51]. We first calculate a bound for the case when the polytope P contains a triangle. For this we first compute an upper bound for the grid size that is needed for an equilibrium representation of the edge graph of P.

LEMMA 13.2.1. *Let G be a planar 3-connected graph. G has at most $2|V| - 4$ cells. The average degree α_v of the vertices of G is less than 6.*

PROOF. Let v, c, and e be the numbers of vertices, cells, and edges, respectively. Since c as well as α_v is increased if we add edges to the graph we may assume that all cells of G are triangles. Since all cells are triangles and each cell is adjacent to exactly 2 edges we have $2e = 3c$. Combining this fact with Euler's equation $(v + c = e + 2)$ we get $c = 2v - 4$, which proves the first claim. Since each edge is incident to exactly two vertices we have $\alpha_v \cdot v = 2e = 3c$. Thus we have $\alpha_v \cdot v = 6v - 12$, and thus $\alpha_v < 6$. $\qquad\square$

LEMMA 13.2.2. *Let G be a 3-connected planar graph with a triangular cell c_0 and n vertices. There is an equilibrium embedding $\boldsymbol{P}$ of G on the integer grid $\{0, 1, 2, \ldots, (6.5)^{n-3}\}^2$.*

PROOF. Let G be a 3-connected planar graph with n vertices and with a triangular cell $(n-2, n-1, n)$. We set $k = n-3$. We consider the equilibrium embedding in which all interior weights have been chosen to be 1. The triangular cell is chosen as peripheral polygon with coordinates $\boldsymbol{p}_{n-2} = (0,0)$, $\boldsymbol{p}_{n-1} = (N,0)$, $\boldsymbol{p}_n = (0, N)$. Where N is a positive integer that will be determined later. The equilibrium condition for the internal points $\boldsymbol{p}_v = (x_v, y_v)$ is then written as

$$\sum_{\{v,w\} \in E} x_v - x_w = 0 \quad \text{and} \quad \sum_{\{v,w\} \in E} y_v - y_w = 0.$$

In matrix-form this can be written as $M \cdot \boldsymbol{x} = \boldsymbol{b}_x$ and $M \cdot \boldsymbol{y} = \boldsymbol{b}_y$. Here $\boldsymbol{x} = (x_1, \ldots, x_k)^T$ and $\boldsymbol{y} = (y_1, \ldots, y_k)^T$. Let λ_v be the degree of the vertex v in G. The matrix M has size $k \times k$. The v-th row of the matrix M contains an entry $-\lambda_v$ at position v (on the diagonal) and an entry 1 at positions w whenever $\{v, w\}$ is an edge of G. All other entries are zero. The entry $(\boldsymbol{b}_x)_v$ is N if $\{v, n-1\}$ is an edge of G, and zero otherwise. Similarly, the entry $(\boldsymbol{b}_y)_v$ is N if $\{v, n\}$ is an edge of G, and zero otherwise. The matrix M is the *stress-matrix* of G. The

values for $\boldsymbol{x}$ and $\boldsymbol{y}$ are by Tutte's Theorem uniquely determined. This results in the fact that M has rank k. The value x_v can be determined by Cramer's rule as $x_v = \det(M_v)/\det(M)$, where M_v is the obtained from M by replacing the v-th column by $\boldsymbol{b}_x$. Since $\boldsymbol{b}_x$ is N times an integer vector and all matrix entries are integers we get integral values for the x_i if we chose $N := \det(M)$. A similar consideration holds for the values of $\boldsymbol{y}$. All entries of $\boldsymbol{x}$ and $\boldsymbol{y}$ will then be integer numbers in the interval $[0, N]$, since all interior vertices are in the interior of the peripheral triangle. Thus we have to find an upper bound for the value of $\det(M)$. This value can by Hadamard's theorem be bounded by

$$\det(M) \leq \prod_{i=1}^{k} \sqrt{(\lambda_i^2 + \lambda_i)}.$$

The term

$$\sqrt{(\lambda_i^2 + \lambda_i)} = (\lambda_i^2 + \underbrace{1^2 + \ldots + 1^2}_{i \text{ times}})^{\frac{1}{2}}$$

bounds the euclidean length of the i-th row vector of M from above, since this vector has one entry $-\lambda_i$ on the diagonal and at most λ_i entries of 1 elsewhere. By observing $(\lambda_i^2 + \lambda_i) < (\lambda_i + \frac{1}{2})^2$ and applying Lemma 13.2.1 we obtain the chain of inequalities

$$\det(M) \ \leq \ \prod_{i=1}^{k} \sqrt{(\lambda_i^2 + \lambda_i)} \ \leq \ \prod_{i=1}^{k} (\lambda_i + \tfrac{1}{2}) \ \leq \ (\alpha_v + \tfrac{1}{2})^k \ = \ (6.5)^k.$$

The third inequality holds by the standard relation between the geometric and the arithmetic mean. $\qquad\square$

The last lemma shows that we can embed equilibrium representations in grids whose size is singly exponential in the number of vertices.

REMARK 13.2.3.   It is not clear at all whether one can find weights such that only a polynomial grid size is needed. If this were the case, this would be the key to a polynomial upper bound for the grid size that is needed for 3-polytopes.

So far we have already determined the maximal size of the x-coordinates and of the y-coordinates of a realization of the polytope that corresponds to G. We now have to study, how large the z-coordinate can get during our lifting process.

LEMMA 13.2.4.   Let P be a (combinatorial) 3-polytope that has a triangular facet f_0 and n vertices. There is a realization of P with integral vertex coordinates of absolute values less than 43^n

PROOF. Let $\boldsymbol{P}$ be the equilibrium representation from Lemma 13.3.2, of the edge graph of P. We assume that $\boldsymbol{P}$ is embedded in the plane $z = 1$. The z coordinate to which a point $\boldsymbol{p}_v$ is lifted is calculated by $\langle \boldsymbol{p}_v, \boldsymbol{q}_j \rangle$. Here $\boldsymbol{q}_j$ is the

vector that is associated to a cell c_j that contains $\boldsymbol{p}_v$ via Lemma 13.1.1. The vector $\boldsymbol{q}_j$ is calculated as the sum

$$\boldsymbol{q}_j = \sum_{i=1}^{l}(\boldsymbol{p}_{b_i} \times \boldsymbol{p}_{t_i}).$$

Here $(b_i, t_i | L_i, R_i)$ is a sequence of oriented patches with $L_1 = 1$, $R_l = j$, and $R_i = L_{i+1}$ for $i = 1, \ldots, l-1$. We need at most $2n - 4$ summands since by Lemma 13.2.1 the graph G has at most that many cells. Expanding $\langle \boldsymbol{p}_v, \boldsymbol{q}_j \rangle$ we get

$$\langle \boldsymbol{p}_v, \boldsymbol{q}_j \rangle = \langle \boldsymbol{p}_v, \sum_{i=1}^{l}(\boldsymbol{p}_{b_i} \times \boldsymbol{p}_{t_i}) \rangle = \sum_{i=1}^{l} \det(\boldsymbol{p}_v, \boldsymbol{p}_{b_i}, \boldsymbol{p}_{t_i}).$$

Each of these determinants is an integer number of size at most $((6.5)^{n-3})^2$ (it correspond to twice the area of the triangle spanned by $\boldsymbol{p}_v$, $\boldsymbol{p}_{b_i}$, and $\boldsymbol{p}_{t_i}$.) Thus we obtain

$$\langle \boldsymbol{p}_v, \boldsymbol{q}_j \rangle \leq ((6.5)^{n-3})^2 \cdot (2n - 4) < 43^n$$

$\square$

This Lemma already establishes the upper bound, if G contains a triangle for the general case we have to analyze how the process of polarizing influences the vertex coordinates.

LEMMA 13.2.5. *Let P be a (combinatorial) polytope that has a triangular facet f_0 and n vertices. There is a realization of P with integral vertex coordinates of absolute values less than 43^n that contains the origin in its interior.*

PROOF. The bounding triangle is again realized by the homogenized points $\boldsymbol{p}_{n-2} = (0, 0, 1)$, $\boldsymbol{p}_{n-1} = (N, 0, 1)$, $\boldsymbol{p}_n = (0, N, 1)$, such that N is the determinant of the stress matrix. We choose the cell c_1 as the interior cell adjacent to the two points $\boldsymbol{p}_{n-1}$ and $\boldsymbol{p}_n$ and apply the lifting construction. The coordinate bound is achieved by the last lemma. We now prove that the polytope that is generated contains a grid point in its interior. For this we reconstruct the vector $\boldsymbol{q}_0$ that describes the lifting function of the exterior triangle c_0. Let $\boldsymbol{p}_1, \ldots, \boldsymbol{p}_l$ be the interior points that are adjacent to $\boldsymbol{p}_n$, such that $\boldsymbol{p}_1$ is the point that is contained in c_1. The heights of the peripheral vertices are $h_{n-2} = H$, $h_{n-1} = 0$, $h_n = 0$ with

$$H = \langle \sum_{i=1}^{l}(\boldsymbol{p}_i \times \boldsymbol{p}_n), \boldsymbol{p}_{n-2} \rangle = \sum_{i=1}^{l} \det(\boldsymbol{p}_i, \boldsymbol{p}_n, \boldsymbol{p}_{n-2}) = \sum_{i=1}^{l} \det \begin{pmatrix} x_i & 0 & 0 \\ y_i & N & 0 \\ 1 & 1 & 1 \end{pmatrix} > N.$$

The vector $\boldsymbol{q}_0$ such that $h_i = \langle \boldsymbol{q}_0, \boldsymbol{p}_i \rangle$ for $i = n-2, \ldots, n$ is then uniquely given by $\boldsymbol{q}_0 = (-\frac{H}{N}, -\frac{H}{N}, H)$. The point $\boldsymbol{p}_1 = (x_1, y_1, 1)$ is in c_1 and therefor is lifted to a height 0. Since $\boldsymbol{p}_1$ is interior we have $x_1 + x_2 < N$. Since x_1 and x_2 are integers we even have $N - x_1 - x_2 \geq 1$. On the other hand

$$\langle \boldsymbol{q}_0, \boldsymbol{p}_1 \rangle = -\frac{H}{N}x_1 - \frac{H}{N}y_1 + H = H \cdot \frac{N - x_1 - x_2}{N} \geq \frac{H}{N} \geq 1.$$

So, the ray that is vertically above $(x_1, y_1, 0)$ contains a grid point $\boldsymbol{g}$ in $\boldsymbol{P}$. Applying a translation that moves $\boldsymbol{g}$ to the origin gives the result. $\qquad\square$

<u>LEMMA 13.2.6.</u> *Let P be a polytope that has no triangular facet and n vertices. There is a realization of P with positive integral vertex coordinates of values less than 2^{18n^2}.*

PROOF. Let G be the edge graph of G and let G^Δ be its polar. The graph G^Δ contains a triangle. Thus we can apply Lemma 13.2.5 to G^Δ and get a realization $\boldsymbol{P}^\Delta = (\boldsymbol{p}_0, \ldots, \boldsymbol{p}_m)$ of the polar of a realization of P. The hyperplanes that support the faces $f_1, \ldots, f_n$ of this polytope that is generated in Lemma 13.2.5 are of the form

$$H_i := \left\{ (x, y, z) \in \mathbb{R}^3 \mid a_i x + b_i y + c_i z + 1 = 0 \right\}.$$

(a_i, b_i, c_i) for $i = 1, \ldots, n$ are the vertices of the desired realization $\boldsymbol{P}$ of P. They can be calculated by solving the system of equations $a_i x_{i_j} + b_i y_{i_j} + c_i h_{i_j} + 1 = 0$. Here $(x_{i_j}, y_{i_j}, h_{i_j})$ for $j = 1, \ldots, 3$ are the coordinates of points in $\boldsymbol{P}^\Delta$ that lie on f_i. Solving these equations by Cramer's rule leads to coefficients a_i, b_i, and c_i of the form

$$\mathbf{det}\begin{pmatrix} * & * & * \\ * & * & * \\ 1 & 1 & 1 \end{pmatrix} \Big/ \mathbf{det}\begin{pmatrix} * & * & * \\ * & * & * \\ * & * & * \end{pmatrix}.$$

Here $*$ are entries of absolute value less than 43^n. The divisor is always identical for a fixed index i. The dividend and the divisor are of absolute value less than $6 \cdot 43^{3n}$. Multiplying all points (a_i, b_i, c_i) by the divisors of the remaining points, we can transform the rational coordinates into integral coordinates of absolute value less than $(6 \cdot 43^{3n})^n = (\sqrt{6} \cdot 43^3)^{n^2} < 194752^{n^2} < 2^{18n^2}$. The last inequality is rough enough even to allow a translation that makes all coordinate entries positive. $\qquad\square$

Summarizing the last two results we get:

<u>THEOREM 13.2.7.</u>

- (i) *All combinatorial types of 3-polytopes with n vertices can be realized on an integer grid $\{0, 1, \ldots, 2^{18n^2}\}$.*
- (ii) *All combinatorial types of simplicial 3-polytopes with n vertices can be realized on an integer grid $\{0, 1, \ldots, 43^n\}$.*

<u>REMARK 13.2.8.</u> A slightly more careful analysis of the construction proves that also a bound of 2^{13n^2} can be obtained for the coordinate size of general 3-polytopes.

13.3   The Structure of the Realization Space

In this section we finally prove that the structure of the realization space of a 3-polytope is essentially trivial. If a polytope $\boldsymbol{P}$ has e edges the realization space $\mathcal{R}(\boldsymbol{P})$ is an open ball of dimension $e - 6$. It is a remarkable fact that this result was already known to Steinitz (compare [56]). We will prove a slightly stronger result that this realization space is in addition stably equivalent to $\{0\}$ (i.e. it is a trivial semialgebraic set). We again restrict ourselves first to the case that $\boldsymbol{P}$ contains a triangle. The general case is later proved by polarity arguments.

Let $\boldsymbol{P}$ be a 3-polytope with n vertices that contains a triangle $\boldsymbol{p}_1, \boldsymbol{p}_2, \boldsymbol{p}_3$, and let P be its combinatorial type. Furthermore, let $\boldsymbol{p}_4$ be another point of $\boldsymbol{P}$ that is joined to $\boldsymbol{p}_1$ by an edge. Then $(\boldsymbol{p}_1, \boldsymbol{p}_2, \boldsymbol{p}_3, \boldsymbol{p}_4)$ forms a basis for $\boldsymbol{P}$. We set $\boldsymbol{e}_1 = (0,0,0)$, $\boldsymbol{e}_2 = (1,0,0)$, $\boldsymbol{e}_3 = (0,1,0)$, $\boldsymbol{e}_4 = (0,0,1)$. For an arbitrary realization $\boldsymbol{P} = (\boldsymbol{p}_1, \ldots, \boldsymbol{p}_n)$ of P we set $\boldsymbol{p}_i = (x_i, y_i, h_i)$. We will refer to the entry h_i as the *height* of $\boldsymbol{p}_i$. We define

$$\mathcal{R}_{\mathrm{pos}}(P) := \{\boldsymbol{P} \in \mathbb{R}^{3n} \mid \boldsymbol{P} \text{ realizes } P \text{ and } \boldsymbol{p}_1 = \boldsymbol{e}_1,\ \boldsymbol{p}_2 = \boldsymbol{e}_2,\ \boldsymbol{p}_3 = \boldsymbol{e}_3,\ h_4 > 0\}$$

$$\mathcal{R}(P) := \{\boldsymbol{P} \in \mathcal{R}_{\mathrm{pos}}(P) \mid \boldsymbol{p}_4 = \boldsymbol{e}_4\}$$

$$\mathcal{R}_{\mathrm{lift}}(P) := \{\boldsymbol{P} \in \mathcal{R}_{\mathrm{pos}}(P) \mid x_i > 0, y_i > 0, x_i + y_i < 0 \text{ for } i = 4, \ldots, n\}$$

We clearly have

$$\mathcal{R}(P) \subseteq \mathcal{R}(P)_{\mathrm{pos}} \quad \text{and} \quad \mathcal{R}_{\mathrm{lift}}(P) \subseteq \mathcal{R}_{\mathrm{pos}}(P).$$

In all these definitions the points $\boldsymbol{p}_1$, $\boldsymbol{p}_2$, and $\boldsymbol{p}_3$ form a fixed triangle $\mathcal{T} = (\boldsymbol{e}_1, \boldsymbol{e}_2, \boldsymbol{e}_3)$ in the plane $H = \{(x, y, h) \in \mathbb{R}^3 \mid h = 0\}$. By abuse of language we use the symbol $\mathcal{T}$ for both, the convex hull $\mathbf{conv}(\mathcal{T})$ and for the set of its vertices. The space $\mathcal{R}(P)$ is just the usual realization space as defined in Section 2. Here the point $\boldsymbol{p}_4$ is fixed at the position $\boldsymbol{e}_4$. $\mathcal{R}_{\mathrm{pos}}(P)$ is a superset of $\mathcal{R}(P)$. The condition for the position of $\boldsymbol{p}_4$ is relaxed. All points with positive heights are allowed. Hence $\mathcal{R}_{\mathrm{pos}}(P)$ consists of all realizations of $\boldsymbol{P}$ (with the fixed triangle) that lie in the closed halfspace $H^+ = \{(x, y, h) \in \mathbb{R}^3 \mid h \geq 0\}$. The space $\mathcal{R}_{\mathrm{lift}}(P)$ consists of all realizations in $\mathcal{R}_{\mathrm{pos}}(P)$ that project orthogonaly down to the triangle $\mathcal{T}$. Our first aim is to show that the space $\mathcal{R}_{\mathrm{lift}}(P)$ corresponds to the space of all realizations that are obtained by our self-stress/lifting constructions. It will be shown to be rationally equivalent to the space of all possible choices of weights for the interior edges (with peripheral triangle $\mathcal{T}$). We assume that P has e edges and set $\mathbb{R}^+ = \{x \mid x > 0\}$.

<u>LEMMA 13.3.1.</u>   *The space $\mathcal{R}_{\mathrm{lift}}(P)$ is rationally equivalent to $(\mathbb{R}^+)^{e-3}$.*

PROOF. Let G be the edge graph of P. If we fix positive weights and realize P by our self-stress/lifting construction with peripheral triangle $\mathcal{T} = (\boldsymbol{e}_1, \boldsymbol{e}_2, \boldsymbol{e}_3)$ we obtain a realization $\boldsymbol{P}$ that projects orthogonally onto the triangle $\mathcal{T}$. For given weights $\Omega \in (\mathbb{R}^+)^{e-3}$ let

$$\boldsymbol{P}(\Omega) = (\boldsymbol{p}_1(\Omega), \ldots, \boldsymbol{p}_n(\Omega)) \in \mathbb{R}^{3n}$$

be the realization of P that comes from the self-stress/lifting construction. We assume that the cell c_1 corresponds to the facet that is adjacent to the facet $(1,2,3)$ along the edge $(1,2)$. We furthermore assume that $\boldsymbol{p}_4$ belongs to the facet c_1. We then have $\boldsymbol{p}_1(\Omega) = (0,0,0)$, $\boldsymbol{p}_2(\Omega) = (1,0,0)$, $\boldsymbol{p}_3 = (0,1,h_3(\Omega))$, and $\boldsymbol{p}_3 = (x_4(\Omega), y_4(\Omega), 0)$ for all $\Omega \in (\mathbb{R}^+)^{e-3}$. The invertible rational function $f_\Omega(x_i, y_i, h_i) := (x_i, y_i, h_i) - (0, 0, y_i \cdot h_3(\Omega))$ applied to each point associates to every realization of the type $\boldsymbol{P}(\Omega)$ a realization in $\mathcal{R}_{\text{lift}}(P)$. Actually, f_Ω is an affine transformation. We have to prove that $g(\Omega) = f_\Omega(\boldsymbol{P}(\Omega))$ is a rational equivalence between $(\mathbb{R}^+)^{e-3}$ and $\mathcal{R}_{\text{lift}}(P)$.

We first prove that $\boldsymbol{P}(\Omega)$ is injective. Let $\Omega, \Omega' \in (\mathbb{R}^+)^{e-3}$ be two assignments of weights with $\boldsymbol{P} = \boldsymbol{P}(\Omega) = \boldsymbol{P}(\Omega') = \boldsymbol{P}'$. Both assignments of weights generate identical equilibrium representations of the graph G. Assume that $\boldsymbol{P}$ has facets labeled by $0, \ldots, m$ with $\mathcal{T}$ corresponding to the index 0. Let $\boldsymbol{q}_1, \ldots, \boldsymbol{q}_m$ be the facet vectors (as used in Section A.3) in the self-stress/lifting construction from Ω and let $\boldsymbol{q}'_1, \ldots, \boldsymbol{q}'_m$ be the corresponding vectors for Ω'. For any oriented patch $(b, t | L, R)$ we have

$$\omega_{b,t}(\boldsymbol{p}_b \times \boldsymbol{p}_t) = \boldsymbol{q}_L - \boldsymbol{q}_R = \boldsymbol{q}'_L - \boldsymbol{q}'_R = \omega'_{b,t}(\boldsymbol{p}_b \times \boldsymbol{p}_t).$$

This implies $\Omega = \Omega'$. If $g(\Omega) = g(\Omega')$ we must have in particular $\boldsymbol{P}(\Omega) = \boldsymbol{P}(\Omega')$, which proves that G is injective.

We now prove the existence of a rational inverse g^{-1} of g. We do this by determining a rational construction that associates to every polytope $\boldsymbol{P}'$ in $\mathcal{R}_{\text{lift}}(P)$ a choice of positive weights Ω with $g(\Omega) = \boldsymbol{P}'$. We do this by just reversing our construction (actually this is in principle the construction that was already known to Maxwell more than 100 years ago). We first apply an affine transformation that leaves $\boldsymbol{p}'_1$, and $\boldsymbol{p}'_2$ invariant and moves $\boldsymbol{p}'_4 = (x_4, y_4, h_4)$ into the position $(x_4, y_4, 0)$. The resulting polytope is called $\boldsymbol{P}$. The projection of the edge skeleton of $\boldsymbol{P}$ to $\mathcal{T}$ is a planar representation of G with boundary $\mathcal{T}$. By $\boldsymbol{p}_i^*$ we denote the point $(x_i, y_i, 1)$ (the homogenization of the projection of $\boldsymbol{p}_i$.) To each facet f_i we associate the corresponding cell c_i, and determine the (unique) vector $\boldsymbol{q}_i$ such that $(x, y) \mapsto \langle (x, y, 1), \boldsymbol{q}_i \rangle$ describes the lifting function from c_i to f_i in the realization $\boldsymbol{P}$. We obtain our weights Ω by assigning to each each oriented patch $(b, t | L, R)$ a weight $\omega_{b,t}$ by $\boldsymbol{q}_L - \boldsymbol{q}_R = \omega_{b,t}(\boldsymbol{p}_b^* \times \boldsymbol{p}_t^*)$. This is possible since $\boldsymbol{q}_L - \boldsymbol{q}_R$ is a scalar multiple of $\boldsymbol{p}_b^* \times \boldsymbol{p}_t^*$, since the lifting functions for f_L and f_R agree on the points $\boldsymbol{p}_b^*$ and $\boldsymbol{p}_t^*$ (compare the calculation of Lemma 13.1.1). Reversing the argumentation of Lemma 13.1.2 we see that we have equilibrium around every interior vertex. Reversing the argumentation of Lemma 13.1.3 shows that the convexity of $\boldsymbol{P}$ translates to the fact that the weights are positive. $\qquad\square$

We now compare the spaces $\mathcal{R}_{\text{lift}}(P)$ and $\mathcal{R}(P)$. Let $\boldsymbol{P} = (\boldsymbol{p}_1, \ldots, \boldsymbol{p}_n) \in \mathcal{R}(P)$ be a realization of P. For $i = 1, \ldots, n$ we set $\boldsymbol{p}_i^{\text{hom}} = (x_i, y_i, h_i, 1)$ — the homogenization of $\boldsymbol{p}_i$.

A projective transformation of the points in $\boldsymbol{P}$ may be expressed by multiplying $\boldsymbol{P}^{\text{hom}}$ by a non-degenerate 4×4 matrix and then dehomogenizing by

dividing by the 4-th coordinate. If $z \neq 0$, we denote this process of dehomogenization by $(x, y, h, z)^{\mathrm{dehom}} = (x/z, y/z, h/z)$. We consider a class of special projective transformations

$$\tau_{a,b,c} = \begin{pmatrix} 1 & 0 & a & 0 \\ 0 & 1 & b & 0 \\ 0 & 0 & 1 & 0 \\ 0 & 0 & c & 1 \end{pmatrix}.$$

All such transformations $\tau_{a,b,c}$ leave the plane $H = \{(x, y, 0) \in \mathbb{R}^3\}$ invariant. The determinant of the transformation matrix is 1, thus the transformations preserve orientation. We consider the set

$$\mathcal{R}^*(P) := \Big\{ (\tau_{a,b,c}(\boldsymbol{P}^{\mathrm{hom}}))^{\mathrm{dehom}} \mid a, b, c \in \mathbb{R}; \ \boldsymbol{P} \in \mathcal{R}(P) \text{ and}$$
$$\langle \tau_{a,b,c}(\boldsymbol{p}_i^{\mathrm{hom}}), (0, 0, 0, 1) \rangle > 0, \ \langle \tau_{a,b,c}(\boldsymbol{p}_i^{\mathrm{hom}}), (1, 0, 0, 0) \rangle > 0,$$
$$\langle \tau_{a,b,c}(\boldsymbol{p}_i^{\mathrm{hom}}), (0, 1, 0, 0) \rangle > 0, \ \langle \tau_{a,b,c}(\boldsymbol{p}_i^{\mathrm{hom}}), (-1, -1, 0, 1) \rangle > 0;$$
$$\text{for } i = 4, \ldots, n \Big\}.$$

The dehomogenization is always possible since the z-coordinate is forced to be positive by the first inequality. The other three inequalities encode the condition that for $\boldsymbol{P} \in \mathcal{R}^*(P)$ the points $\boldsymbol{p}_4, \ldots, \boldsymbol{p}_n$ project orthogonally to $\mathcal{T}$.

<u>LEMMA 13.3.2.</u>

(i) $\mathcal{R}^*(P) \approx \mathcal{R}(P)$,
(ii) $\mathbf{dim}(\mathcal{R}^*(P)) = \mathbf{dim}(\mathcal{R}(P)) + 3$,
(iii) $\mathcal{R}^*(P) = \mathcal{R}_{\mathrm{lift}}(P)$.

PROOF. By $\mathbf{A}(\boldsymbol{P})$ we denote the set of all (a, b, c) that are admissible for the choice of $\tau_{a,b,d}$ for given $\boldsymbol{P}$ in the definition of $\mathcal{R}^*(P)$. This set is bounded by $4(n-4)$ linear equations. We have $\tau_{a,b,d}(x_i, y_i, h_i, 1) = (x_i + h_i a, y_i + h_i b, h_i, 1 + h_i c)$. The set $\mathbf{A}(\boldsymbol{P})$ is never empty, since for sufficiently large $\lambda > 0$ the vector $\lambda(1/3, 1/3, 1) = (a, b, c)$ satisfies all inequalities (since the h_i are all positive). Hence, the set $\mathcal{R}(P)$ is a stable projection of the set

$$\overline{\mathcal{R}}(P) := \{(\boldsymbol{P}, (a, b, c)) \mid \boldsymbol{P} \in \mathcal{R}(P) \text{ and } (a, b, c) \in \mathbf{A}(\boldsymbol{P})\}.$$

The dimension of $\overline{\mathcal{R}}(P)$ is $\mathbf{dim}(\mathcal{R}(P)) + 3$. Performing the projective transformation and the dehomogenization is an invertible rational operation. Thus $\overline{\mathcal{R}}(P)$ and $\mathcal{R}^*(P)$ are rationally equivalent. This proves (i) and (ii).

By definition we have $\mathcal{R}^*(P) \subseteq \mathcal{R}_{\mathrm{lift}}(P)$. To see $\mathcal{R}^*(P) \supseteq \mathcal{R}_{\mathrm{lift}}(P)$ We must find for every $\boldsymbol{P} \in \mathcal{R}_{\mathrm{lift}}(P)$ a $\boldsymbol{P}' \in \mathcal{R}(P)$ and an admissible $(a, b, c) \in \mathbf{A}(\boldsymbol{P})$ such that $(\tau_{a,b,c}(\boldsymbol{P}^{\mathrm{hom}}))^{\mathrm{dehom}} = \boldsymbol{P}$. For $\boldsymbol{P} \in \mathcal{R}_{\mathrm{lift}}(P)$ with $\boldsymbol{p}_4 = (x_4, y_4, h_4)$ we set $(a, b, c) = (x_4/h_4, y_4/h_4, (1/h_4 - 1))$. We then have

$$
\begin{aligned}
(\tau_{a,b,c}(\boldsymbol{e}_4^{\mathrm{hom}}))^{\mathrm{dehom}} &= (\tau_{a,b,c}(0,0,1,1))^{\mathrm{dehom}} \\
&= (x_4/h_4, y_4/h_4, 1, 1/h_4)^{\mathrm{dehom}} \\
&= (x_4, y_4, h_4).
\end{aligned}
$$

We finally set $\boldsymbol{P}' = (\tau_{a,b,c})^{-1}(\boldsymbol{P})$. The polytope $\boldsymbol{P}'$ is the desired element from $\mathcal{R}(P)$. This proves (iii) $\qquad\square$

Combining Lemma 13.3.1 and Lemma 13.3.2 we get.

THEOREM 13.3.3. *For a 3-polytope P with e edges the realization space $\mathcal{R}(P)$ is an open ball of dimension $e - 6$. $\mathcal{R}(P)$ is a trivial semialgebraic set.*

PROOF. If P contains a triangle we can apply Lemma 13.3.1 and Lemma 13.3.2. The dimension count is $\mathbf{dim}(\mathcal{R}(P)) = \mathbf{dim}(\mathcal{R}_{\mathrm{lift}}(P)) - 3 = e - 6$ Since $\mathcal{R}(P) \approx \mathcal{R}_{\mathrm{lift}}(P) \approx (\mathbb{R}^+)^{e-6} \approx \{0\}$ the space $\mathcal{R}(P)$ is trivial.

If P does not contain a triangle then by Lemma 13.1.6 it has a vertex of degree 3. Then P^Δ contains a triangle. Theorem 2.6.3 states that the realization spaces of P and P^Δ are stably equivalent and have the same dimension. $\qquad\square$

PART V: ALTERNATIVE CONSTRUCTION TECHNIQUES

During the process of "cooking up" the proof of the Universality Theorem many nice constructions were explored that are of interest on their own right. It is the purpose of this part to sketch the two most beautiful such constructions. Both lead to weaker results than the Universality Theorem as proved in the main part of this monograph. However in both cases the construction relies on structural properties of polytopes that are different from the tools that have been used there.

The first construction provides a class of polytopes that prove a Non-Steinitz Theorem in dimension 5. It makes use of Ziegler's example of a 5-polytope containing a hexagon all whose vertices must lie on a conic. Many copies of Ziegler's example are glued in a completely symmetric way along a polytope that encodes an incidence theorem concerning conics. Local perturbations in this class of examples gives the desired class of combinatorial polytopes.

The second construction leads to a Universality Theorem for polytopes in dimension six. It establishes a relatively simple and symmetric way to use Mnëv's Universality Theorem for oriented matroids as a starting point that can be translated into a corresponding theorem for polytopes. This construction makes use of the fact that realizable oriented matroids correspond to zonotopes (a special class of polytopes).

14 Generalized Adapter Techniques

Before we go into the details of the "alternative constructions," we discuss a method that makes their description a bit easier. When we introduced our Basic Building Block "transmitter for line slopes" in Section 5.7, we were faced with the problem of gluing polytopes along facets that were not combinatorially equivalent. We solved this problem by inserting intermediate polytopes called "adapters" (compare Section 5.5). This method also works in more general settings. We will make use of this refined method in the following two sections.

Recall that every face of a combinatorial d-polytope is characterized by its vertex set. For a k_1-face F^{k_1} and a k_2-face F^{k_2} of a combinatorial d-polytope with $0 \leq k_1 < k_2 \leq d$ we have $F^{k_1} \subset F^{k_2}$ if F^{k_1} is a proper face of F^{k_2}. Let P^d and Q^d be two (combinatorial) d-polytopes and let F^k be a k-face that occurs in both polytopes P and Q. Our aim is to find a polytope $P^d \stackrel{\sim}{\#}_{F^k} Q^d$ that

contains the polytopes P^d and Q^d as summands of connected sums, such that they are identified along the face F^k. Let

$$F^k = F_P^k \subset F_P^{k+1} \subset \ldots \subset F_P^d = P^d$$

be a maximal chain of faces in P and let

$$F^k = F_Q^k \subset F_Q^{k+1} \subset \ldots \subset F_Q^d = Q^d$$

be a maximal chain of faces in Q. Furthermore, assume that F_P^{d-1} and F_Q^{d-1} are necessarily flat. By $\mathbf{pyr}_i(F)$ we denote the i-times iterated pyramid over F (the polytope $\mathbf{pyr}_3(F)$ is the pyramid of the pyramid of the pyramid of F; the polytope $\mathbf{pyr}_0(F)$ is F itself). Consider the combinatorial polytopes

$$P_j^i = \mathbf{pyr}_j(F_P^i) \quad \text{and} \quad Q_j^i = \mathbf{pyr}_j(F_Q^i)$$

for $i = k, \ldots, d$ and $j = 0, \ldots, d - k$. P_j^i is the j-times iterated pyramid over F_P^i. In particular, $P_0^i = F_P^i$ and $P_0^d = P$. P_{d-i}^i is a d-polytope. The combinatorial polytope P_{d-i}^i contains P_{d-i-1}^i (for $i = d-1, \ldots, k$) and P_{d-i}^{i-1} (for $i = d, \ldots, k+1$) as facets. A similar statement holds for the polytopes Q_j^i. We also have $P_{d-k-1}^k = Q_{d-k-1}^k$. All these polytopes of the types P_{d-i-1}^i or Q_{d-i-1}^i are necessarily flat (either they are pyramids or they are F_P^{d-1} or F_Q^{d-1}). We can generate the desired polytope $P^d \mathbin{\widetilde{\#}}_{F^k} Q^d$ by forming a chain of connected sums as indicated by the following construction diagram. Although the construction depends on the chains of facets that have been chosen, we use the ambiguous notation $P^d \mathbin{\widetilde{\#}}_{F^k} Q^d$.
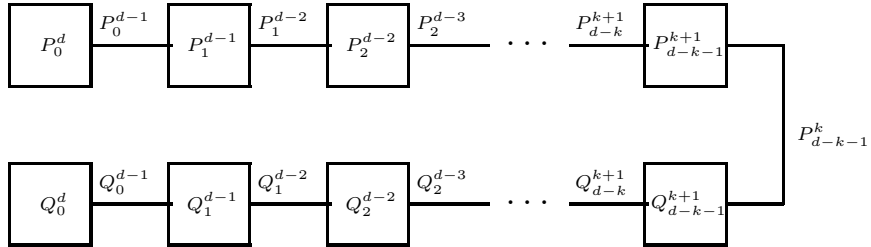
Iterative application of Lemma 3.2.4 shows

LEMMA 14.1.1. Let $R = P \mathbin{\widetilde{\#}}_F Q$ and let $\boldsymbol{P}$ and $\boldsymbol{Q}$ be realizations of combinatorial d-polytopes P and Q, respectively. If the face $\boldsymbol{P}\big|_F$ is projectively equivalent to the face $\boldsymbol{Q}\big|_F$, then there exists a projective transformation τ such that $\mathbf{conv}(\boldsymbol{P} \cup \tau(\boldsymbol{Q}))$ is a realization of R.

15 A Non-Steinitz Theorem in Dimension Five

The construction presented here provides a proof that *there is no local characterization for boundary complexes of 5-polytopes.* (This construction was the origin of the further investigations that led to the complete Universality Theorem.) The construction proceeds as follows:

- First we provide a class of incidence theorems of the following form: *Let $\boldsymbol{p}_1, \ldots, \boldsymbol{p}_k$ be a collection of points in $\mathbb{R}^d$. If for a certain collection of 6-tuples the points in each 6-tuple are coplanar and lie on a conic, then another 6-tuple of points also lies on a conic.* All the points involved lie on the edge skeleton of an embedded, triangulated, orientable 2-manifold M. Exactly two of the points lie on each edge of M. The 6-tuples of points under consideration are those coming from faces of M.

- We embed a certain class of such manifolds M^n ($n = 6, 8, 10 \ldots$) in 4-polytopes and perform a truncation operation such that the vertices of the incidence theorem become vertices of a polytope $\boldsymbol{P}_{M^n}$. This polytope $\boldsymbol{P}_{M^n}$ contains n hexagonal 2-faces $\mathcal{H}_1, \ldots, \mathcal{H}_n$. All realizations $\boldsymbol{P}$ of $\boldsymbol{P}_{M^n}$ share the following property: *If the six vertices of each $\mathcal{H}_1, \ldots, \mathcal{H}_{n-1}$ lie on a conic then the vertices of $\mathcal{H}_n$ lie on a conic as well.*

- Finally, we consider the pyramid $\boldsymbol{P}'_{M^n}$ over $\boldsymbol{P}_{M^n}$ (a 5-dimensional polytope). Along each of the hexagons $\mathcal{H}_i$ for $i = 1, \ldots, n-1$ we glue (using connected sums, and generalized adapter techniques) a copy of Ziegler's polytope $\boldsymbol{P}_Z$ (as described in Example 3.4.3), which forces the vertices of $\mathcal{H}_i$ to lie on a conic. Along $\mathcal{H}_n$ we (combinatorially) glue a copy of a perturbed version $\boldsymbol{P}'_Z$ of $\boldsymbol{P}_Z$ that forces the vertices of $\mathcal{H}_n$ *not* to lie on a conic.

- The resulting (combinatorial) polytope is not realizable, since on the one hand the vertices of $\mathcal{H}_n$ must lie on a conic (as a consequence of the incidence theorem), and on the other hand they cannot lie on a conic, since they must satisfy the condition forced by $\boldsymbol{P}'_Z$. However, the global construction is responsible for the non-realizability. If we delete one of the (essential) points then we can complete the remainder of the face lattice to a realizable polytope. This provides a *Non-Steinitz Theorem !*

15.1 Conics and Incidence Theorems

We start with some considerations about conics in the plane. Conics are an intrinsically projective concept, therefore it is convenient to study them using homogeneous coordinates.

<u>DEFINITION 15.1.1.</u> Let $\lambda_1, \ldots, \lambda_6 \in \mathbb{R}$ be six real numbers at least one of which is non-zero. The set $\{(x, y, z) \in \mathbb{C}^3 \mid \lambda_1 x^2 + \lambda_2 y^2 + \lambda_3 z^2 + \lambda_4 yz + \lambda_5 xz + \lambda_6 xy = 0\}$ is a *quadratic cone.*

In other words, a quadratic cone is an algebraic set that is obtained by solving a single homogeneous quadratic equation. The set of solutions may have no non-zero real solutions at all (for instance consider the equation $x^2 + y^2 + z^2 = 0$). However, we will be interested only in the real part of the solution. If a quadratic equation can be written as the product of two real linear factors, then the corresponding quadratic cone degenerates into two linear hyperplanes (which may even coincide). If we dehomogenize a real non-degenerate quadratic cone by intersecting with an affine hyperplane H we obtain a planar conic. Depending on the position of H, we get either an *ellipse*, a *parabola*, or a *hyperbola*.

<u>LEMMA 15.1.2.</u> *Let* $(x_1, y_1, z_1), \ldots, (x_6, y_6, z_6) \in \mathbb{R}^3$ *be homogeneous coordinates for six planar points. The points lie on a common conic if and only if*

$$\mathcal{C}(1,2,3,4,5,6) := \det \begin{pmatrix} x_1^2 & y_1^2 & z_1^2 & y_1 z_1 & x_1 z_1 & x_1 y_1 \\ x_2^2 & y_2^2 & z_2^2 & y_2 z_2 & x_2 z_2 & x_2 y_2 \\ x_3^2 & y_3^2 & z_3^2 & y_3 z_3 & x_3 z_3 & x_3 y_3 \\ x_4^2 & y_4^2 & z_4^2 & y_4 z_4 & x_4 z_4 & x_4 y_4 \\ x_5^2 & y_5^2 & z_5^2 & y_5 z_5 & x_5 z_5 & x_5 y_5 \\ x_6^2 & y_6^2 & z_6^2 & y_6 z_6 & x_6 z_6 & x_6 y_6 \end{pmatrix} = 0.$$

PROOF. A point with homogeneous coordinates (x, y, z) is on a conic with parameters $\lambda_1, \ldots, \lambda_6$ if (x, y, z) satisfies the corresponding equation from Definition 15.1.1. Thus six points $(x_1, y_1, z_1), \ldots, (x_6, y_6, z_6)$ are on a common conic if and only if there are parameters $\lambda_1, \ldots, \lambda_6$ such that all (x_i, y_i, z_i) satisfy the corresponding quadratic equation. We may write the quadratic equations as the scalar product

$$\langle (\lambda_1, \ldots, \lambda_6), (x_i^2, y_i^2, z_i^2, y_i z_i, x_i z_i, x_i y_i) \rangle = 0$$

of the parameters with the quadratic coordinates. Thus there is a set of parameters as desired if and only if the quadratic coordinates are linearly dependent. This happens if and only if the determinant in the lemma vanishes.   □

We now switch to the special case, in which the cutting hyperplane of homogenization/dehomogenization chosen is $H = \{(x, y, z) \in \mathbb{R}^3 \mid x + y + z = 1\}$. Furthermore, we assume that the six points $\boldsymbol{x}_1, \ldots, \boldsymbol{x}_6$ are chosen on the sides of the triangle $(\boldsymbol{e}_1, \boldsymbol{e}_2, \boldsymbol{e}_3) = ((1,0,0), (0,1,0), (0,0,1))$ – two points on each side. By this (in homogeneous coordinates) each of the points $\boldsymbol{x}_1, \ldots, \boldsymbol{x}_6$ has at least one zero entry. We furthermore assume that no two points coincide. The special choice of coordinates is not a serious restriction since any situation can be transformed to this special case by a change of coordinate system. The determinant of the last lemma becomes much simpler and factors nicely. For the labeling of the coordinates in the following Lemma we refer to Figure 15.1.1.

<u>LEMMA 15.1.3.</u> *Six mutually distinct points $\boldsymbol{x}_1, \ldots, \boldsymbol{x}_6 \in \mathbb{R}^3$ on the edges of a triangle $(\boldsymbol{e}_1, \boldsymbol{e}_2, \boldsymbol{e}_3)$ — as in Figure 15.1.1 — are on a conic if and only if*

$$a_2 b_2 c_2 d_2 e_2 f_2 - a_1 b_1 c_1 d_1 e_1 f_1 = 0.$$

PROOF. With our special choice of coordinates, the condition of Lemma 15.1.2 translates to:

$$\mathcal{C}(1, \ldots, 6) = \mathbf{det} \begin{pmatrix} a_1^2 & a_2^2 & 0 & 0 & 0 & a_1 a_2 \\ b_1^2 & b_2^2 & 0 & 0 & 0 & b_1 b_2 \\ 0 & c_1^2 & c_2^2 & c_1 c_2 & 0 & 0 \\ 0 & d_1^2 & d_2^2 & d_1 d_2 & 0 & 0 \\ e_2^2 & 0 & e_1^2 & 0 & e_1 e_2 & 0 \\ f_2^2 & 0 & f_1^2 & 0 & f_1 f_2 & 0 \end{pmatrix}$$

$$= (a_1 b_2 - a_2 b_1)(c_1 d_2 - c_2 d_1)(e_1 f_2 - e_2 f_1)(a_2 b_2 c_2 d_2 e_2 f_2 - a_1 b_1 c_1 d_1 e_1 f_1).$$

Since the points $\boldsymbol{x}_1, \ldots, \boldsymbol{x}_6$ are all distinct, the first three factors (actually 2×2 determinants that indicate whether the two points on an edge are identical) are all non-zero. Therefore the entire expression is zero if and only if the last factor is zero. □
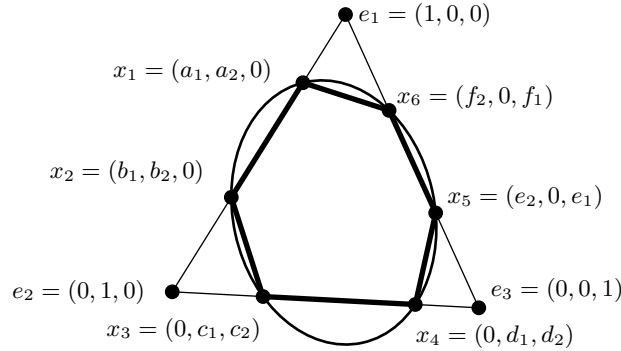
Figure 15.1.1: Six points on the edges of triangle that lie on a conic.

We end with another more euclidean characterization for six points on a conic. The characterization follows directly from Lemma 15.1.3. We introduce some notation, which will also be needed later.

Let $\boldsymbol{x}$ and $\boldsymbol{y}$ be the endpoints of an (oriented) line segment $s = (\boldsymbol{x}, \boldsymbol{y})$ and $\boldsymbol{p}$ be a point on s. We define

$$r_s(\boldsymbol{p}) := \frac{||\boldsymbol{y}, \boldsymbol{p}||}{||\boldsymbol{x}, \boldsymbol{p}||},$$

where $||\boldsymbol{a}, \boldsymbol{b}||$ denotes the oriented euclidean distance between $\boldsymbol{a}$ and $\boldsymbol{b}$.

<u>LEMMA 15.1.4.</u> *Let $(\boldsymbol{q}_1, \boldsymbol{q}_2, \boldsymbol{q}_3)$ be the vertices of a planar triangle T with two additional points $\boldsymbol{a}_i, \boldsymbol{b}_i$ on each of the sides $s_i = (\boldsymbol{q}_i, \boldsymbol{q}_{i+1})$, with indices modulo 3. Assume that the points are pairwise distinct. The points $\boldsymbol{a}_1, \boldsymbol{b}_1, \boldsymbol{a}_2, \boldsymbol{b}_2, \boldsymbol{a}_3, \boldsymbol{b}_3$ are on a conic if and only if*

$$r_{s_1}(\boldsymbol{a}_1) \cdot r_{s_1}(\boldsymbol{b}_1) \cdot r_{s_2}(\boldsymbol{a}_2) \cdot r_{s_2}(\boldsymbol{b}_2) \cdot r_{s_3}(\boldsymbol{a}_3) \cdot r_{s_3}(\boldsymbol{b}_3) = 1.$$

PROOF. After a suitable affine transformation, which does not change the value of the functions $r(\dots)$, we may assume that T is an equilateral triangle. If we use the hyperplane $H = \{(x, y, z) \mid x + y + z = 1\}$ for the homogenization, we may represent the vertices $\boldsymbol{q}_1, \boldsymbol{q}_2, \boldsymbol{q}_3$ by unit vectors $\boldsymbol{e}_1, \boldsymbol{e}_2, \boldsymbol{e}_3 \in \mathbb{R}^3$, respectively. Homogeneous coordinates for the points $\boldsymbol{a}_i$ and $\boldsymbol{b}_i$ are then given by

$$\begin{pmatrix} \boldsymbol{a}_1 \\ \boldsymbol{b}_1 \\ \boldsymbol{a}_2 \\ \boldsymbol{b}_2 \\ \boldsymbol{a}_3 \\ \boldsymbol{b}_3 \end{pmatrix} = \begin{pmatrix} r_{s_1}(\boldsymbol{a}_1) & 1 & 0 \\ r_{s_1}(\boldsymbol{b}_1) & 1 & 0 \\ 0 & r_{s_2}(\boldsymbol{a}_2) & 1 \\ 0 & r_{s_2}(\boldsymbol{b}_2) & 1 \\ 1 & 0 & r_{s_3}(\boldsymbol{a}_3) \\ 1 & 0 & r_{s_3}(\boldsymbol{b}_3) \end{pmatrix}.$$

The condition in Lemma 15.1.3 translates to:

$$r_{s_1}(\boldsymbol{a}_1) \cdot r_{s_1}(\boldsymbol{b}_1) \cdot r_{s_2}(\boldsymbol{a}_2) \cdot r_{s_2}(\boldsymbol{b}_2) \cdot r_{s_3}(\boldsymbol{a}_3) \cdot r_{s_3}(\boldsymbol{b}_3) = 1$$

This proves the lemma.   ☐

Using this characterization we now prove an incidence theorem concerning conics on 2-manifolds.

<u>DEFINITION 15.1.5.</u> Let M be an oriented simplicial 2-manifold with (triangular) 2-faces $f_1, \dots, f_n$, edges $e_1, \dots, e_m$ and vertex set $V = (\boldsymbol{q}_1, \dots, \boldsymbol{q}_l) \in \mathbb{R}^{d \cdot l}$. Let $\boldsymbol{P} := \{\boldsymbol{a}_1, \dots, \boldsymbol{a}_m, \boldsymbol{b}_1, \dots, \boldsymbol{b}_m\}$ be distinct additional points such that $\boldsymbol{a}_i$ and $\boldsymbol{b}_i$ lie on the edge e_i for $i = 1, \dots, m$. Such a manifold together with the additional points $\boldsymbol{a}_i, \boldsymbol{b}_i$ in the specified order will be called an *ab-manifold* $\overline{M}$.

For each 2-face f_i there are exactly six such additional points in $\boldsymbol{P}$ incident with f_i. They will be called the *hexagon* of f_i.

<u>THEOREM 15.1.6.</u> *Let $\overline{M}$ be an ab-manifold and for $i = 1, \dots, n$ let $\mathcal{H}_i$ be the hexagon of f_i. If for $i = 1, \dots, n-1$ the vertices of $\mathcal{H}_i$ lie on a conic, then the vertices of $\mathcal{H}_n$ lie also on a conic.*

PROOF. Let $\overline{M}$ be the *ab*-manifold equipped with a consistent orientation on the faces (for each edge the adjacent triangles should induce opposite orientations). For a triangle f_i we assume that $(\boldsymbol{q}_{i,1}, \boldsymbol{q}_{i,2}, \boldsymbol{q}_{i,3})$ are its vertices ordered consistently with the given orientation. We get a set of three oriented

edges $E_i := \{(\boldsymbol{q}_{i,1}, \boldsymbol{q}_{i,2}), (\boldsymbol{q}_{i,2}, \boldsymbol{q}_{i,3}), (\boldsymbol{q}_{i,3}, \boldsymbol{q}_{i,1})\}$ around the face f_i. If two 2-faces f_{i_1} and f_{i_2} have two vertices $\boldsymbol{x}, \boldsymbol{y}$ in common and $s = (\boldsymbol{x}, \boldsymbol{y}) \in E_{i_1}$ then $\overline{s} = (\boldsymbol{y}, \boldsymbol{x}) \in E_{i_2}$. By $\boldsymbol{a}_s$ and $\boldsymbol{b}_s$ we denote the two points that lie on the edge s. We have

$$r_s(\boldsymbol{a}_s) = r_{\overline{s}}(\boldsymbol{a}_s)^{-1} \quad \text{and} \quad r_s(\boldsymbol{b}_s) = r_{\overline{s}}(\boldsymbol{b}_s)^{-1}.$$

This implies

$$\prod_{i=1}^{n} \prod_{s \in E_i} (r_s(\boldsymbol{a}_s) \cdot r_s(\boldsymbol{b}_s)) = 1,$$

since each of the edges is used exactly once in both possible orientations. If for $i = 1, \ldots, n-1$ the vertices of $\mathcal{H}_i$ lie on a conic, then we have

$$\prod_{s \in E_i} (r_s(\boldsymbol{a}_s) \cdot r_s(\boldsymbol{b}_s)) = 1,$$

for $i = 1, \ldots, n-1$, by Lemma 15.1.4. Combining these equations with the above expression gives

$$\prod_{s \in E_n} (r_s(\boldsymbol{a}_s) \cdot r_s(\boldsymbol{b}_s)) = 1.$$

Thus the points of $\mathcal{H}_n$ are on a conic, by Lemma 15.1.4. $\square$

Figure 15.1.2 (a) shows part of a typical ab-manifold. Figure 15.1.2 (b) shows the same part of the ab-manifold together with some of the conics that are relevant for Theorem 15.1.6.

(a)   (b)

Figure 15.1.2: Part of an ab-manifold, with and without conics.

The smallest case of this theorem, where M is the boundary of a tetrahedron, is illustrated in Figure 15.1.3. If for three facets of the tetrahedron the vertices of the hexagon lie on a conic, then this is also the case for the last facet.
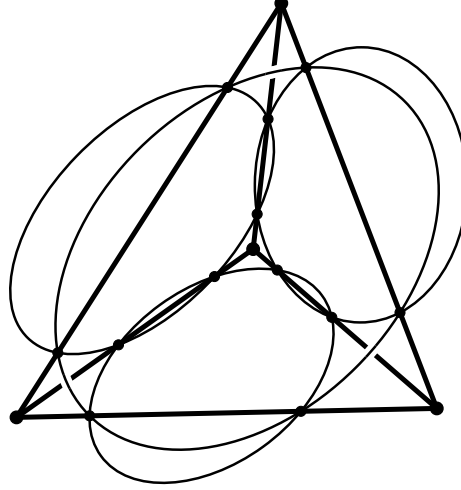
Figure 15.1.3: An incidence theorem on the boundary of a tetrahedron.

15.2   An Incidence Theorem for 4-Polytopes

Our last theorem indicates how to encode incidence theorems about conics into the boundary of a polytope. Unfortunately Theorem 15.1.6 tells us nothing about the shape of specific hexagonal faces of a *polytope*, since the vertices $\boldsymbol{a}_i, \boldsymbol{b}_i$ are not *vertices* of the underlying manifold. We now provide one special class of 4-polytopes $(\boldsymbol{P}^n)_{n \geq 3}$ that realize incidence theorems on hexagonal 2-faces. The polytope $\boldsymbol{P}^n$ contains $m = 2n$ hexagonal 2-faces with the property that co-conicality of the vertices of $m - 1$ hexagons implies co-conicality of the last one. Actually there are many ways of constructing such polytopes. For later use we pick out one special class which satisfies certain additional symmetry properties.

We start by describing these polytopes by explicit (homogeneous) coordinates. For $n \geq 3$ the polytope $\boldsymbol{P}^n$ has $6n + 2$ vertices. To construct $\boldsymbol{P}^n$ we start with the vertices

$$\boldsymbol{p}_n(i) = (1, \cos(\frac{2i\pi}{n}), \sin(\frac{2i\pi}{n}), 0, 0) \quad \text{ for } i = 1, \dots, n$$

of a regular convex n-gon (embedded by homogeneous coordinates in $\mathbb{R}^5$). Furthermore we need the vertices $\boldsymbol{x}' = (1, 0, 0, 1, 0)$ and $\boldsymbol{y}' = (1, 0, 0, 0, 1)$. All these vertices lie on the linear hyperplane $H = \{\boldsymbol{x} \in \mathbb{R}^5 \mid x_1 = 1\}$. Thus the vertices span a positive cone. Cutting this cone with the hyperplane H gives us a convex polytope $\boldsymbol{P}_A^n$. In what follows we will identify the vertices of the polytopes with their homogeneous coordinates. The transition from homogeneous coordinates of a vertex $\boldsymbol{v}$ to the vertex can be always made by cutting the positive span $\mathbb{R}^+\boldsymbol{v}$ with the hyperplane H.

For fixed n the convex hull of the vertices $\boldsymbol{p}_n(1),\ldots,\boldsymbol{p}_n(n),\boldsymbol{x}',\boldsymbol{y}'$ forms a pyramid over the pyramid over an n-gon. The 3-faces of $\boldsymbol{P}_A^n$ are two pyramids over an n-gon

$$\left(\boldsymbol{p}_n(1)\ldots\boldsymbol{p}_n(n),\boldsymbol{x}'\right),\ \left(\boldsymbol{p}_n(1)\ldots\boldsymbol{p}_n(n),\boldsymbol{y}'\right)$$

and a ring of n tetrahedra

$$\left(\boldsymbol{p}_n(i),\boldsymbol{p}_n(i+1),\boldsymbol{x}',\boldsymbol{y}'\right).$$

We now take this polytope $\boldsymbol{P}_A^n$ and "truncate" each single vertex $\boldsymbol{v}$. We can do this by replacing the vertex $\boldsymbol{v}$ (of edge-degree k) by k vertices $\boldsymbol{v}_1,\ldots,\boldsymbol{v}_k$ on a hyperplane such that the new vertices are close to $\boldsymbol{v}$ and lie on the k edges that are incident with $\boldsymbol{v}$. This truncation corresponds to the intersection of the polytope $\boldsymbol{P}_A^n$ with a halfspace that contains all vertices except for $\boldsymbol{v}$. By truncating all vertices we generate a polytope that has two points on each edge of $\boldsymbol{P}_A^n$. Actually, in our case we can make the "close to" part of this construction very rough. For an edge $(\boldsymbol{v}_1,\boldsymbol{v}_2)$ the point "close to" $\boldsymbol{v}_1$ will be chosen at homogeneous coordinates $2\boldsymbol{v}_1+\boldsymbol{v}_2$. The resulting polytope $\boldsymbol{P}^n$ has the following vertices:

$$\begin{aligned}
\boldsymbol{a}_n(i) &= 2\boldsymbol{p}_n(i)+\boldsymbol{p}_n(i+1), &\quad \boldsymbol{b}_n(i) &= \boldsymbol{p}_n(i)+2\boldsymbol{p}_n(i+1),\\
\boldsymbol{c}_n(i) &= 2\boldsymbol{p}_n(i)+\boldsymbol{x}', &\quad \boldsymbol{d}_n(i) &= \boldsymbol{p}_n(i)+2\boldsymbol{x}',\\
\boldsymbol{e}_n(i) &= 2\boldsymbol{p}_n(i)+\boldsymbol{y}', &\quad \boldsymbol{f}_n(i) &= \boldsymbol{p}_n(i)+2\boldsymbol{y}',
\end{aligned}$$

for $i = 1,\ldots,n$, and the two vertices

$$\boldsymbol{x} = 2\boldsymbol{x}'+\boldsymbol{y}',\quad \boldsymbol{y} = 2\boldsymbol{y}'+\boldsymbol{x}'.$$

The vertices $(\boldsymbol{d}_n(1)\ldots\boldsymbol{d}_n(n),\boldsymbol{x})$ are those close to our original point $\boldsymbol{x}'$. They all lie on the hyperplane $\{(x_1,\ldots,x_5)\in\mathbb{R}^5\mid 2x_1=3x_4\}$, and form a facet which is a pyramid over an n-gon. The vertices $(\boldsymbol{f}_n(1)\ldots\boldsymbol{f}_n(n),\boldsymbol{y})$ are the vertices close to our original point $\boldsymbol{y}'$. The vertices close to the original point $\boldsymbol{p}_n(i)$ are $(\boldsymbol{a}_n(i),\boldsymbol{b}_n(i-1),\boldsymbol{c}_n(i),\boldsymbol{e}_n(i))$, where indices are taken modulo n. These facets are tetrahedra.

The remaining facets of $\boldsymbol{P}^n$ have the vertex sets:

$$\begin{aligned}
X_n &= \left(\boldsymbol{x},\boldsymbol{c}_n(1)\ldots\boldsymbol{c}_n(n),\boldsymbol{d}_n(1)\ldots\boldsymbol{d}_n(n),\boldsymbol{a}_n(1)\ldots\boldsymbol{a}_n(n),\boldsymbol{b}_n(1)\ldots\boldsymbol{b}_n(n)\right),\\
Y_n &= \left(\boldsymbol{y},\boldsymbol{e}_n(1)\ldots\boldsymbol{e}_n(n),\boldsymbol{f}_n(1)\ldots\boldsymbol{f}_n(n),\boldsymbol{a}_n(1)\ldots\boldsymbol{a}_n(n),\boldsymbol{b}_n(1)\ldots\boldsymbol{b}_n(n)\right),\\
T_n(i) &= \left(\boldsymbol{x},\boldsymbol{y},\boldsymbol{a}_n(i),\boldsymbol{b}_n(i),\boldsymbol{c}_n(i),\boldsymbol{c}_n(i+1),\boldsymbol{d}_n(i),\boldsymbol{d}_n(i+1),\right.\\
&\qquad\qquad \left.\boldsymbol{e}_n(i),\boldsymbol{e}_n(i+1),\boldsymbol{f}_n(i),\boldsymbol{f}_n(i+1)\right).
\end{aligned}$$
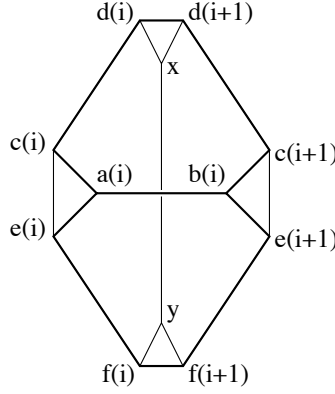
Figure 15.2.1:   The labeling of $T_n(i)$.

The facets $T_n(i)$ arise from tetrahedra by truncating all vertices. Similarly, the faces X_n and Y_n are obtained by truncating the vertices of a pyramid over an n-gon.

Figure 15.2.1 shows the vertex labeling of the face $T_n(i)$. In Figure 15.2.2 we show a special projection of the edge graph of P^7, and a 3-dimensional Schlegel diagram for P^{12}. For a visualization purposes we have chosen the cutting hyperplanes closer to the original vertices.
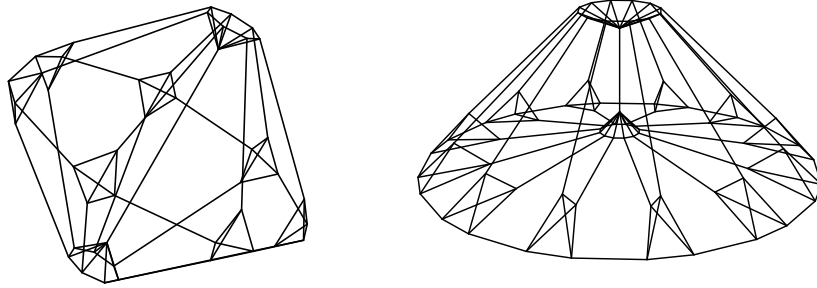
Figure 15.2.2:   The polytopes P^7 and P^{12}.

The polytope $\boldsymbol{P}^n$ contains the following hexagons, which are 2-faces (facets of $T_n(i)$). For $i = 1, \ldots, n$:

$$\begin{aligned}
\mathcal{H}_n^x(i) &= \Big(\boldsymbol{a}_n(i), \boldsymbol{b}_n(i), \boldsymbol{c}_n(i+1), \boldsymbol{d}_n(i+1), \boldsymbol{d}_n(i), \boldsymbol{c}_n(i)\Big), \\
\mathcal{H}_n^y(i) &= \Big(\boldsymbol{b}_n(i), \boldsymbol{a}_n(i), \boldsymbol{e}_n(i), \boldsymbol{f}_n(i), \boldsymbol{f}_n(i+1), \boldsymbol{e}_n(i+1)\Big).
\end{aligned}$$

<u>THEOREM 15.2.1.</u> *For $n \geq 3$ let $\boldsymbol{P}$ be a polytope combinatorially equivalent to $\boldsymbol{P}^n$. If the points of the hexagons $\mathcal{H}_n^x(1), \ldots, \mathcal{H}_n^x(n), \mathcal{H}_n^y(1), \ldots, \mathcal{H}_n^y(n-1)$ are on a conic then the points of $\mathcal{H}_n^y(n)$ are also on a conic.*

PROOF. The main idea of the proof is to take a realization $\boldsymbol{P}$ of $\boldsymbol{P}^n$ and to reconstruct the original points before the truncation. Then we consider a certain substructure of $\boldsymbol{P}_A^n$ together with the vertices of $\boldsymbol{P}^n$ as an ab-manifold and apply Theorem 15.1.6.

Let $\boldsymbol{P}$ be any realization of $\boldsymbol{P}^n$. During this proof we label the vertices and faces of $\boldsymbol{P}$ by the letters $\boldsymbol{a}(i), \boldsymbol{b}(i), \boldsymbol{c}(i), \boldsymbol{d}(i), \boldsymbol{e}(i), \boldsymbol{f}(i), \boldsymbol{x}, \boldsymbol{y}, T(i), X, Y$ consistent with our original labeling of the vertices of $\boldsymbol{P}^n$. The hyperplanes supporting the faces $T(i), T(i+1), X, Y$ of $\boldsymbol{P}$ meet in a common point $\boldsymbol{p}(i)$. In particular, the point $\boldsymbol{p}(i)$ lies on the support of the edges

$$\begin{aligned} T(i) \cap X \cap Y &= (\boldsymbol{a}(i), \boldsymbol{b}(i)), \\ T(i+1) \cap X \cap Y &= (\boldsymbol{a}(i+1), \boldsymbol{b}(i+1)), \\ T(i) \cap T(i+1) \cap X &= (\boldsymbol{c}(i), \boldsymbol{d}(i)), \\ T(i) \cap T(i+1) \cap Y &= (\boldsymbol{e}(i), \boldsymbol{f}(i)). \end{aligned}$$

Furthermore the supports of all 3-faces $T(1), \ldots, T(n)$ meet in a line, since these 3-faces share the edge $(\boldsymbol{x}, \boldsymbol{y})$. Hence the supports of the faces $T(1), \ldots, T(n), X$ meet in one point $\boldsymbol{x}'$, which lies on all the supports of all edges $(\boldsymbol{c}(i), \boldsymbol{d}(i))$ for $i = 1, \ldots, n$. Similarly, all faces $T(1), \ldots, T(n), Y$ meet in one point $\boldsymbol{y}'$, which lies on all the supports of all edges $(\boldsymbol{e}(i), \boldsymbol{f}(i))$ for $i = 1, \ldots, n$. Now consider the oriented 2-manifold M that is formed by the vertices

$$\boldsymbol{p}(1), \ldots, \boldsymbol{p}(n), \boldsymbol{x}', \boldsymbol{y}'$$

and the (oriented) triangles

$$\left(\boldsymbol{p}(i), \boldsymbol{p}(i+1), \boldsymbol{x}'\right) \text{ and } \left(\boldsymbol{p}(i+1), \boldsymbol{p}(i), \boldsymbol{y}'\right)$$

for $i = 1, \ldots, n$, indices counted modulo n. Actually, M has the combinatorial type of a double pyramid over an n-gon. Together with our vertices

$$\boldsymbol{a}(i), \boldsymbol{b}(i), \boldsymbol{c}(i), \boldsymbol{d}(i), \boldsymbol{e}(i), \boldsymbol{f}(i)$$

for $i = 1, \ldots, n$, which lie on the edges of M, the manifold M forms an ab-manifold with hexagons $\mathcal{H}^x(i)$, and $\mathcal{H}^y(i)$, for $i = 1, \ldots, n$. Theorem 15.1.6 proves the desired result. □

<u>LEMMA 15.2.2.</u> *The special realization $\boldsymbol{P}^n$ realizes the case, in which the vertices of each hexagon $\mathcal{H}_n^x(i)$ and $\mathcal{H}_n^y(i)$ lie on a conic.*

PROOF. The result is clear by the symmetry of the chosen coordinates. We could also prove this fact by explicitly using the criterion of Lemma 15.1.5. □

15.3   The Non-Steinitz Theorem

Combining the polytopes $\boldsymbol{P}^n$ with Ziegler's polytope $\boldsymbol{P}_{\mathrm{Z}}$ that forces six points to lie on a conic, we are almost done. We recall the properties of the 5-polytope $\boldsymbol{P}_{\mathrm{Z}}$ (compare Example 3.4.3).

- $\boldsymbol{P}_{\mathrm{Z}}$ contains a hexagonal 2-face $\mathcal{H}$,
- in every realization of $\boldsymbol{P}_{\mathrm{Z}}$ the vertices of $\mathcal{H}$ are on a conic,
- every hexagon whose vertices are on a conic can be completed to a realization of $\boldsymbol{P}_{\mathrm{Z}}$.

Recall that $\boldsymbol{P}_{\mathrm{Z}}$ was constructed as a three-fold Lawrence extension over a drawing of Pascal's Theorem (compare Figure 3.4.3). To emphasize the symmetric structure of $\boldsymbol{P}_{\mathrm{Z}}$ we also give here a set of "nice" homogeneous coordinates for a realization and the vertex/facet incidence table.

$$\begin{pmatrix} 2 & 1 & 0 & 0 & 0 & 0 \\ 1 & 2 & 0 & 0 & 0 & 0 \\ 0 & 2 & 1 & 0 & 0 & 0 \\ 0 & 1 & 2 & 0 & 0 & 0 \\ 1 & 0 & 2 & 0 & 0 & 0 \\ 2 & 0 & 1 & 0 & 0 & 0 \\ 1 & 0 & 0 & 1 & 0 & 0 \\ 0 & 1 & 0 & 0 & 1 & 0 \\ 0 & 0 & 1 & 0 & 0 & 1 \\ 0 & 0 & 1 & 1 & 0 & 0 \\ 1 & 0 & 0 & 0 & 1 & 0 \\ 0 & 1 & 0 & 0 & 0 & 1 \end{pmatrix}$$

	f_0	f_1	f_2	f_3	f_4	f_5	f_6	f_7	f_8	f_9
z_1		×	×					×	×	×
z_2			×	×				×	×	×
z_3				×	×			×	×	×
z_4					×	×		×	×	×
z_5						×	×	×	×	×
z_6		×					×	×	×	×
z_7	×	×	×	×			×		×	×
z_8	×		×	×	×	×		×		×
z_9	×	×			×	×	×	×		
z_{10}	×				×	×	×	×		×	×
z_{11}	×	×	×			×	×	×		×
z_{12}	×	×	×	×	×			×	×	

We obtain a perturbed version $\boldsymbol{P}_{\mathrm{Z}}'$ of $\boldsymbol{P}_{\mathrm{Z}}$ if we start with a hexagon whose points do not lie on a conic. The six points of the Lawrence extensions are then no longer on a single facet. The facet f_0 of $\boldsymbol{P}_{\mathrm{Z}}$ is then broken into three tetrahedra. This is the only change in the face lattice.

We relabel the hexagons of $\boldsymbol{P}^n$ that are involved in our construction by

$$F_1 = \mathcal{H}_n^x(1), \ldots, F_n = \mathcal{H}_n^x(n), \ F_{n+1} = \mathcal{H}_n^y(1), \ldots, F_{2n} = \mathcal{H}_n^y(n).$$

Using the generalized adaptor techniques from Section 14 we perform connected sums that glue to each of the hexagons $F_1, \ldots, F_{2n-1}$ a copy of the polytope $\boldsymbol{P}_{\mathrm{Z}}$. Along $F_{2n} = \mathcal{H}_n^y(n)$ we glue the perturbed polytope $\boldsymbol{P}_{\mathrm{Z}}'$. We call the resulting (combinatorial) polytope P_{R}^n. The $2n-1$ copies of $\boldsymbol{P}_{\mathrm{Z}}$ are $\boldsymbol{P}_{\mathrm{Z}}^1 \ldots \boldsymbol{P}_{\mathrm{Z}}^{2n-1}$. The vertices of each of these copies has to be relabeled properly to fit to the corresponding hexagon F_i. Formally we may write

$$P_{\mathrm{R}}^n = \boldsymbol{P}^n \ \widetilde{\#}_{F_1} \ \boldsymbol{P}_{\mathrm{Z}}^1 \ \widetilde{\#}_{F_2} \ \ldots \ \widetilde{\#}_{F_{2n-1}} \ \boldsymbol{P}_{\mathrm{Z}}^{2n-1} \ \widetilde{\#}_{F_{2n}} \ \boldsymbol{P}_{\mathrm{Z}}'.$$

<u>THEOREM 15.3.1.</u>

(i) P_{R}^n is not polytopal.

(ii) Every minor of P_{R}^n can be completed to a polytopal face lattice.

PROOF. For part (i) assume that there is a realization $\boldsymbol{P}$ of P_{R}^n. In $\boldsymbol{P}$ all the hexagons $\mathcal{H}_n^x(1), \ldots, \mathcal{H}_n^x(n), \mathcal{H}_n^y(1), \ldots, \mathcal{H}_n^y(n-1)$ have their vertices on a conic, since they are part of the summands $\boldsymbol{P}_{\mathrm{Z}}^i$. By Theorem 15.2.1 this implies that the vertices of $\mathcal{H}_n^y(n)$ are on a conic, since all the hexagons are part of the summand $\boldsymbol{P}^n$. This contradicts the fact that this hexagon is part of the summand $\boldsymbol{P}_{\mathrm{Z}}'$, which forces the vertices not to lie on a conic.

Part (ii) of this theorem (the minor minimality) is really technical. We omit it here. In principle it is a consequence of the fact that the non-realizability of P_{R}^n is forced by the *global* structure of the face lattice. Each point contributes to the non-realizability. Deleting any point allows us to find a realization of the remaining part of the face lattice that can be completed to a polytope. $\square$

16   The Universality Theorem in Dimension 6

In the main part of this monograph we proved the Universality Theorem for 4-polytopes "from scratch". We gave explicit constructions that model multiplication and addition on the level of realizations of polytopes. In contrast to that, for a long time it was believed that the easiest approach to a Universality Theorem for polytopes in fixed dimension must be based on *oriented matroids*. As previously mentioned, Mnëv proved (already in 1986) the Universality Theorem for oriented matroids [49, 52] (we presented a relatively simple proof of this theorem "en passant" in Section 11.7). Mnëv used his Universality Theorem combined with Gale Diagram techniques to prove a Universality Theorem for polytopes without a fixed bound on the dimension (compare Section 3). To prove such a theorem for *fixed* dimension d, all that was missing, one thought, was some construction that associates to a given oriented matroid $\mathcal{M}$ a d-polytope $P(\mathcal{M})$, for some fixed d, such that the realization spaces of $\mathcal{M}$ and $P(\mathcal{M})$ are stably equivalent. Here we present such a construction. Unfortunately, this does not lead to the Universality Theorem in its strongest form. The technique presented here is simple and elegant, but it produces 6-dimensional polytopes rather than 4-dimensional polytopes. A similar construction for 4-dimensional polytopes is still not known. Here is a sketch of the 6-dimensional construction.

- For every real spanning vector configuration $\boldsymbol{V} = (\boldsymbol{v}_1, \ldots, \boldsymbol{v}_n) \in (\mathbb{R}^d)^n$ there is an associated zonotope

$$\boldsymbol{Z}(\boldsymbol{V}) = \sum_{i=1}^{n} [-\boldsymbol{v}_i, +\boldsymbol{v}_i],$$

  that is the Minkowski sum of the line segments $[-\boldsymbol{v}_i, +\boldsymbol{v}_i]$. $\boldsymbol{Z}(\boldsymbol{V})$ is a certain d-dimensional polytope. The faces of the zonotope $\boldsymbol{Z}(\boldsymbol{V})$ are naturally labeled by the covectors of $\boldsymbol{V}$. The amazing connection between oriented matroids and zonotopes is that for two vector configurations (without parallel elements or loops) $\boldsymbol{V}, \boldsymbol{V}' \in (\mathbb{R}^d)^n$ the (labeled) zonotopes $\boldsymbol{Z}(\boldsymbol{V})$ and $\boldsymbol{Z}(\boldsymbol{V}')$ are isomorphic if and only if the oriented matroids $\mathcal{M}_{\boldsymbol{V}}$ and $\mathcal{M}_{\boldsymbol{V}'}$ are the same.

- As a consequence, the realization space of the zonotope $\boldsymbol{Z}(\boldsymbol{V})$ in the class of *zonotopes* is stably equivalent to the realization space of the oriented matroid $\mathcal{M}_{\boldsymbol{V}}$. From a realization of $\boldsymbol{Z}(\boldsymbol{V})$ as a zonotope the configuration $\boldsymbol{V}$ can be reconstructed. However, the realization space of $\boldsymbol{Z}(\boldsymbol{V})$ considered as a *polytope* is in general not stably equivalent to the realization space of $\mathcal{M}_{\boldsymbol{V}}$.

- We need a construction that embeds $\boldsymbol{Z}(\boldsymbol{V})$ as a face of a polytope $\boldsymbol{P} = \boldsymbol{P}(\boldsymbol{V})$, in such a way that in every realization $\boldsymbol{P}'$ of $\boldsymbol{P}$ the corresponding face $\boldsymbol{Z}'$ is again (nearly) a zonotope from which a realization $\boldsymbol{V}'$ of $\mathcal{M}_{\boldsymbol{V}}$ can be reconstructed. Such a construction can be made by performing Lawrence extensions on $\boldsymbol{Z}(\boldsymbol{V})$ for all non-bases of $\mathcal{M}_{\boldsymbol{V}}$, and gluing all polytopes that arise this way along the face $\boldsymbol{Z}(\boldsymbol{V})$.

- If we now want to encode a given system of polynomial equations and inequalities S, we start with the oriented matroid $\mathcal{M}$ that comes from Mnëv's construction applied to S (or from our construction provided in Section 11.7). If S has no solution at all then we can associate to S any non-realizable combinatorial polytope. Otherwise $\mathcal{M}$ is realizable by a configuration $\boldsymbol{V}$. By construction, the realization space of the polytope $\boldsymbol{P}(\boldsymbol{V})$ is stably equivalent to the solution space of S. Since $\mathcal{M}$ has rank 3 the zonotope $\boldsymbol{Z}(\boldsymbol{V})$ has dimension 3. The Lawrence extension increases the dimension by 3. Thus $\boldsymbol{P}(\boldsymbol{V})$ is a 6-polytope.

16.1 Oriented Matroids

Compared to our approach in Section 11.7 this time we need slightly more terminology from oriented matroid theory. Another difference from our approach in Section 11.7 is that we use a linear setting rather than an affine setting, since this fits better into the context of zonotopes. The 2-dimensional affine point configurations used there can be transformed into 3-dimensional linear vector configurations by the usual embedding into the $x_3 = 1$ plane. We use "+" and "−" as shorthand for "+1" and "−1".

To a vector configuration $\boldsymbol{V} = (\boldsymbol{v}_1, \ldots, \boldsymbol{v}_n) \in \mathbb{R}^{d \cdot n}$ with index set $X = \{1, \ldots, n\}$ and rank d we associate its *chirotope*:

$$\begin{aligned}
\chi_{\boldsymbol{V}} \colon X^d &\rightarrow \{-, 0, +\} \\
(\lambda_1, \ldots, \lambda_d) &\mapsto \mathbf{sign}(\mathbf{det}(\boldsymbol{v}_{\lambda_1}, \ldots, \boldsymbol{v}_{\lambda_d})).
\end{aligned}$$

The chirotope of $\boldsymbol{V}$ encodes the orientations of triples of vectors in $\boldsymbol{V}$. The integer d is the *rank* of the chirotope. As already mentioned, a general chirotope is an alternating sign map $\chi \colon X^d \to \{-, 0, +\}$ that satisfies certain axioms, which model the behavior of determinants on a combinatorial level. A vector configuration $\boldsymbol{V}$ is a realization of χ if $\chi_{\boldsymbol{V}} = \chi$. (For the rank 3 case there is a nice characterization of general chirotopes in terms of local realizability: an alternating sign map $\chi \colon X^3 \to \{-, 0, +\}$ is a chirotope if and only if all restrictions to six elements of X are realizable).

Chirotopes are closely related to *oriented matroids*. There are many cryptomorphic data representations and axiomatizations for oriented matroids. We here use the encoding by *covectors*. Again $X = \{1, \ldots, n\}$. The oriented matroid of a rank d vector configuration $\boldsymbol{V} \in \mathbb{R}^{d \cdot n}$ is the pair $\mathcal{M}_{\boldsymbol{V}} := (X, \mathcal{L}_{\boldsymbol{V}})$, such that

$$\mathcal{L}_{\boldsymbol{V}} = \Big\{ (\mathbf{sign}\langle \boldsymbol{v}_1, \boldsymbol{y} \rangle, \ldots, \mathbf{sign}\langle \boldsymbol{v}_n, \boldsymbol{y} \rangle) \mid \boldsymbol{y} \in \mathbb{R}^d \Big\}.$$

Each single covector is a sign vector that encodes how a linear hyperplane

$$H(\boldsymbol{y}) := \{ \boldsymbol{x} \in \mathbb{R}^d \mid \langle \boldsymbol{x}, \boldsymbol{y} \rangle = 0 \}$$

partitions the vectors in $\boldsymbol{V}$ (with the only exception that $H(0, \ldots, 0)$ is the entire space, and not a hyperplane). The vectors *on* $H(\boldsymbol{y})$ are marked "0", those vectors

on the *positive* side of $H(\boldsymbol{y})$ are marked "+", and those vectors on the *negative* side of $H(\boldsymbol{y})$ are marked "−". The set $\mathcal{L}_{\boldsymbol{V}}$ gives the complete collection of all such partitions. In general, an oriented matroid is a pair $\mathcal{M} := (\{1, \ldots, n\}, \mathcal{L})$, with $\mathcal{L} \subseteq \{-, 0, +\}^X$ that satisfies a system of axioms. The partial order on $\mathcal{L}$ that is induced by the order relations "$- \prec 0$" and "$+ \prec 0$" becomes a lattice $(\mathcal{L}, \prec)$, if we add an artificial minimal element.

There is a straightforward translation from chirotopes to oriented matroids. For a chirotope χ on n elements, consider the set

$$\mathcal{C}_\chi^* = \Big\{ (\chi(\lambda, 1), \chi(\lambda, 2), \ldots, \chi(\lambda, n)) \mid \lambda \in X^{d-1} \Big\}.$$

These sign vectors correspond to the partitions by hyperplanes that are spanned by $d - 1$ elements (together with the zero vector $(0 \ldots 0)$). To get partitions from general hyperplanes we need the composition operator for two sign vectors $C, D \in \{-, 0, +\}^X$:

$$(C \circ D)_i = \left\{ \begin{array}{ll} C_i & \text{if } C_i \neq 0 \\ D_i & \text{if } C_i = 0 \end{array} \right.$$

The set of covectors of χ is then defined by

$$\mathcal{L}(\chi) = \Big\{ C_1 \circ C_2 \circ \ldots \circ C_k \mid C_1, \ldots, C_k \in \mathcal{C}_\chi^* \Big\}.$$

It is an easy task to check

$$\mathcal{L}(\chi_{\boldsymbol{V}}) = \mathcal{L}_{\boldsymbol{V}}.$$

The following lemma characterizes the relationship between oriented matroids and chirotopes.

<u>LEMMA 16.1.1.</u> *If $\mathcal{L}$ is the set of covectors of an oriented matroid, then there is a chirotope χ with $\mathcal{L} = \mathcal{L}(\chi)$. Furthermore, if $\mathcal{L}(\chi) = \mathcal{L}(\chi')$ then either $\chi = \chi'$ or $\chi = -\chi'$.*

An oriented matroid (or equivalently a chirotope) can — in the realizable case — be considered as the *combinatorial type* of the corresponding point configuration (in the same way as a face lattice is the combinatorial type of a polytope). In particular, the oriented matroid $\mathcal{M}_{\boldsymbol{V}}$ completely describes which subsets of $\boldsymbol{V}$ form a linear basis. For a basis $b = (b_1, \ldots, b_d)$ the realization space of $\mathcal{M}$ w.r.t. b is the set

$$\mathcal{R}(\mathcal{M}, b) := \Big\{ V \in \mathbb{R}^{n \cdot d} \mid \mathcal{M} = \mathcal{M}_{\boldsymbol{V}} \text{ and } \boldsymbol{v}_{b_i} = \boldsymbol{e}_i \text{ for } i = 1, \ldots, d \Big\}.$$

In Section 11.7 we proved that the realization spaces of oriented matroids are universal.

16.2   Zonotopes and Planets

We now associate to a vector configuration $\boldsymbol{V}$ a second object, the *zonotope* $\boldsymbol{Z}(\boldsymbol{V})$. A zonotope is a special type of polytope. Here are four different (but equivalent) characterizations.

- A zonotope is the Minkowski sum of finitely many line segments.
- A zonotope is a polytope for which all faces are centrally symmetric.
- A zonotope is a polytope for which all 2-faces are centrally symmetric.
- A zonotope is a polytope for which all 2-faces have an even number of edges, with opposite sides parallel and of equal length.

The last characterization shows that for each edge there is a complete "belt" of edges of equal length and direction in the zonotope. They are all translates of a corresponding generating line segment in the Minkowski sum representation. The zonotope of a vector configuration $\boldsymbol{V} \in \mathbb{R}^{d \cdot n}$ indexed by $X = \{1, \ldots, n\}$ is defined by

$$\boldsymbol{Z}(\boldsymbol{V}) := \sum_{i \in X} [-\boldsymbol{v}_i, +\boldsymbol{v}_i].$$

Here $[-\boldsymbol{v}_i, +\boldsymbol{v}_i]$ is the line segment between $-\boldsymbol{v}_i$ and $+\boldsymbol{v}_i$ in $\mathbb{R}^d$, and the sum is interpreted as the Minkowski sum. Equivalently we could write

$$\boldsymbol{Z}(\boldsymbol{V}) := \Big\{ \sum_{i \in X} \lambda_i \boldsymbol{v}_i \mid -1 \leq \lambda_i \leq +1 \text{ for } i \in X \Big\}.$$

To avoid unnecessary technicalities caused by degenerate situations, from now on we assume that our vector configurations contain no *loops* (i.e. vectors $\boldsymbol{v} = (0, \ldots, 0)$) and contain no pairs of *parallel elements* (i.e. vectors $\boldsymbol{v}_i = \lambda \boldsymbol{v}_j$ with $i \neq j$). There is a close relationship between the oriented matroid $\mathcal{M}_{\boldsymbol{V}}$ and the face lattice of $\boldsymbol{Z}(\boldsymbol{V})$. For a sign-vector $\sigma \in \{-, 0, +\}^X$ we define

$$\boldsymbol{Z}(\boldsymbol{V})_\sigma := \sum_{\sigma_i = +} \boldsymbol{v}_i - \sum_{\sigma_i = -} \boldsymbol{v}_i + \sum_{\sigma_i = 0} [-\boldsymbol{v}_i, +\boldsymbol{v}_i].$$

In particular, $\boldsymbol{Z}(\boldsymbol{V})_{(0,\ldots,0)} = \boldsymbol{Z}(\boldsymbol{V})$. The following theorem is the well known standard connection between zonotopes and oriented matroids.

<u>THEOREM 16.2.1.</u>   *The faces of $\boldsymbol{Z}(\boldsymbol{V})$ are exactly the sets $\boldsymbol{Z}(\boldsymbol{V})_\sigma$ with $\sigma \in \mathcal{L}_{\boldsymbol{V}}$.*

PROOF. We show that the covectors in $\mathcal{L}_{\boldsymbol{V}}$ are in bijection with the faces of $\boldsymbol{Z}(\boldsymbol{V})$. The sign vector $\sigma \in \{-, 0, +\}^X$ is a covector of $\boldsymbol{V}$ if and only if there is a $\boldsymbol{y} \in \mathbb{R}^d$ with $\sigma = (\mathbf{sign}\langle \boldsymbol{v}_1, \boldsymbol{y} \rangle, \ldots, \mathbf{sign}\langle \boldsymbol{v}_n, \boldsymbol{y} \rangle)$. Let $F(\boldsymbol{y})$ be the set consisting of all $\boldsymbol{x} \in \boldsymbol{Z}(\boldsymbol{V})$ for which $\langle \boldsymbol{x}, \boldsymbol{y} \rangle$ is maximal. The faces of $\boldsymbol{Z}(\boldsymbol{V})$ are exactly the sets of the form $F(\boldsymbol{y})$. It remains to prove that that

$$F(\boldsymbol{y}) = \boldsymbol{Z}(\boldsymbol{V})_\sigma = \sum_{\sigma_i = +} \boldsymbol{v}_i - \sum_{\sigma_i = -} \boldsymbol{v}_i + \sum_{\sigma_i = 0} [-\boldsymbol{v}_i, +\boldsymbol{v}_i].$$

For this we are looking for all choices for $-1 \leq \lambda_i \leq +1$ that maximize

$$\langle \sum_{i \in X}^{n} \lambda_i \boldsymbol{v}_i, \boldsymbol{y} \rangle = \sum_{i \in X}^{n} \lambda_i \langle \boldsymbol{v}_i, \boldsymbol{y} \rangle.$$

If $\langle \boldsymbol{v}_i, \boldsymbol{y} \rangle$ is positive we must choose $\lambda_i = 1$. If it is negative we must choose $\lambda_i = -1$. If $\langle \boldsymbol{v}_i, \boldsymbol{y} \rangle = 0$ the value of λ_i does not influence the scalar product at all, and it may be chosen arbitrarily in $[-1, +1]$. This proves the claim. $\square$

The last theorem shows that it is natural to label the faces of $\boldsymbol{Z}(\boldsymbol{V})$ by the covectors of $\mathcal{M}_{\boldsymbol{V}}$. The face lattice of $\boldsymbol{Z}(\boldsymbol{V})$ is therefore isomorphic to the lattice $(\mathcal{L}, \prec)$. A face $\boldsymbol{Z}(\boldsymbol{V})_{\sigma_1}$ is contained in $\boldsymbol{Z}(\boldsymbol{V})_{\sigma_2}$ if and only if $\sigma_1 \prec \sigma_2$. The vertices of $\boldsymbol{Z}(\boldsymbol{V})$ correspond to the sign vectors $\sigma \in \mathcal{L}_{\boldsymbol{V}} \cap \{-,+\}^X$ (the atoms of $(\mathcal{L}, \prec)$). The facets of $\boldsymbol{Z}(\boldsymbol{V})$ correspond to the cocircuits in $\mathcal{L}_{\boldsymbol{V}}$ (the coatoms of $(\mathcal{L}, \prec)$). Up to translation any zonotope is of the form $\boldsymbol{Z}(\boldsymbol{V})$. Thus also for a general zonotope it is natural to label the faces by the covectors of $\boldsymbol{V}$. Figure 16.2.1 demonstrates the connection between the vector configuration, its covectors and the corresponding zonotope. Here the vector configuration consists of 4 non-parallel vectors in $\mathbb{R}^2$. The corresponding zonotope $\boldsymbol{Z}$ turns out to be an 8-gon. The faces of $\boldsymbol{Z}$ are labeled by the covectors. The entire zonotope gets a label (0000).
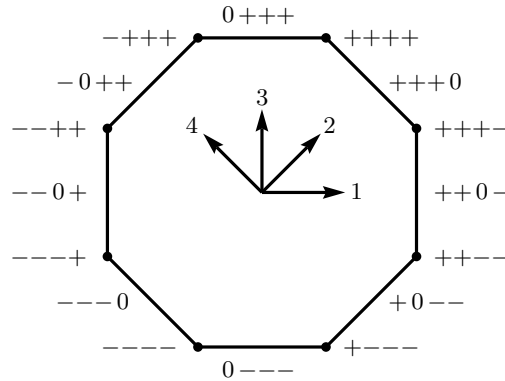
Figure 16.2.1: A vector configuration and its zonotope.

Closely related to zonotopes is the concept of *planets*. Planets arise from zonotopes by parallel displacements of the facets. The face lattices of planets are identical to the face lattices of zonotopes. Planets as well as zonotopes have belts of parallel edges. However, in comparison to zonotopes, it is not required that the edges in a belt have equal lengths. Formally, we may define planets by a relaxation of our last characterization of zonotopes.

- A planet is a polytope for which all 2-faces have an even number of edges, and opposite sides of a 2-face are parallel.
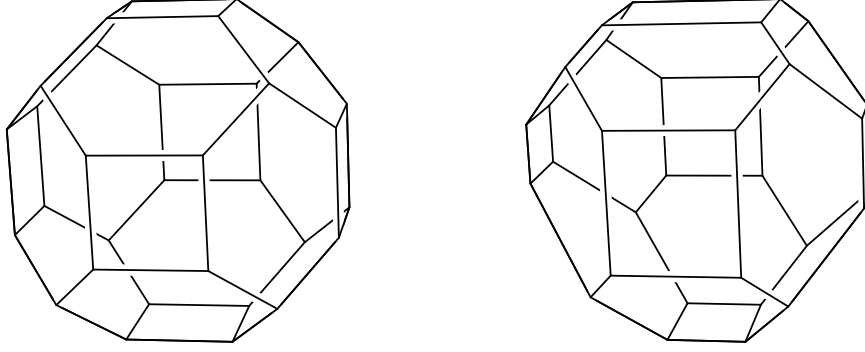
Figure 16.2.2: The permutahedron and a corresponding planet.

It is not too difficult to prove that for every planet there is a zonotope with identical face lattice. However, we will omit this here, since all the planets that are relevant for us by definition come from face lattices of zonotopes $\boldsymbol{Z}(\boldsymbol{V})$. By the coincidence of the face lattices, we may in a natural way label the faces of a planet by the covectors $\mathcal{L} = \mathcal{L}_{\boldsymbol{V}}$. Figure 16.2.2 shows a zonotope (the permutahedron) and a planet whose face lattice is isomorphic to the face lattice of the permutahedron.

<u>DEFINITION 16.2.2.</u> Let Z be the face lattice of a zonotope and B be a (polytope) basis of Z. The *planet realization space* $\mathcal{P}(Z, B) \subseteq \mathcal{R}(Z, B)$ is the space of all planets in $\mathcal{R}(Z, B)$.

The following theorem expresses the relation between the planet realization space and the realization space of an oriented matroid. Although this theorem is true in general rank, we state and prove it only for the rank 3 case. The technical difficulties in the following proof arise from the very restrictive definition of stable equivalence.

<u>THEOREM 16.2.3.</u> Let $\boldsymbol{V} \in \mathbb{R}^{3n}$ be a vector configuration without loops or parallel elements, and let $Z_{\boldsymbol{V}}$ be the face lattice of $\boldsymbol{Z}(\boldsymbol{V})$. Let b be a basis of $\boldsymbol{V}$ and B be a (polytope) basis of Z. Then

$$\mathcal{R}(\mathcal{M}_{\boldsymbol{V}}, b) \approx \mathcal{P}(Z_{\boldsymbol{V}}, B).$$

PROOF. The spaces $\mathcal{R}(\mathcal{M}_{\boldsymbol{V}}, b)$ and $\mathcal{P}(Z_{\boldsymbol{V}}, B)$ do not depend (up to stable equivalence) on the choice of the particular bases. As affine polytope basis of $Z_{\boldsymbol{V}}$ we take a 3-valent vertex $\boldsymbol{p}_0$ of $Z_{\boldsymbol{V}}$ and all its neighbors $\boldsymbol{p}_1, \boldsymbol{p}_2, \boldsymbol{p}_3$ (such a vertex does always exist, compare [7]). The planet realization space then consists of all planets $\boldsymbol{P}$ with face lattice $Z_{\boldsymbol{V}}$ such that $\boldsymbol{p}_0 = (0, 0, 0)$ and

$\boldsymbol{p}_1 = \boldsymbol{e}_1, \ldots, \boldsymbol{p}_d = \boldsymbol{e}_3$. Each of the edges $(\boldsymbol{p}_0, \boldsymbol{p}_i)$ for $i = 1, 2, 3$ corresponds to an element (say i) in $\mathcal{M}_{\boldsymbol{V}}$. We set $b = (1, 2, 3)$. The triple b is an oriented matroid basis of $\mathcal{M}_{\boldsymbol{V}}$ since the vectors $\boldsymbol{p}_0 - \boldsymbol{p}_1$, $\boldsymbol{p}_0 - \boldsymbol{p}_2$, $\boldsymbol{p}_0 - \boldsymbol{p}_3$ linearly span $\mathbb{R}^3$.

We now describe a chain of stably equivalent spaces

$$\mathcal{R}(\mathcal{M}_{\boldsymbol{V}}, b) = \mathcal{R}_0 \approx \mathcal{R}_1 \approx \mathcal{R}_2 \approx \mathcal{R}_3 \approx \mathcal{R}_4 \approx \mathcal{R}_5 \approx \mathcal{R}_6 \approx \mathcal{R}_7 = \mathcal{P}(Z_{\boldsymbol{V}}, B)$$

Each pair of consecutive spaces in this chain is either related by a stable projection or by a rational equivalence.

We start by describing the space $\mathcal{R}_2$ which is a normalization of $\mathcal{R}_0$. The space $\mathcal{R}_0$ is the space of all $d \times n$ matrices that form a realization of $\mathcal{M}_{\boldsymbol{V}}$ and satisfy $\boldsymbol{v}_1 = \boldsymbol{e}_1, \ldots, \boldsymbol{v}_3 = \boldsymbol{e}_3$. A particular entry $v_{1,j}$ in this matrix V can be written as

$$v_{i,j} = \mathbf{det}(\boldsymbol{v}_j, \boldsymbol{e}_2, \boldsymbol{e}_3).$$

Similar statements hold for entries $v_{2,j}$ and $v_{3,j}$. Thus the signs of the entries (in particular the positions of zeros) are already determined by the bases orientations of $\mathcal{M}_{\boldsymbol{V}}$. For a vector $\boldsymbol{v} = (v_1, v_2, v_3) \in \mathbb{R}^3 \setminus \mathbf{0}$ let $\alpha(\boldsymbol{v})$ be the unique coordinate entry which is non-zero and has minimal index. We set $\overline{\boldsymbol{v}} = \boldsymbol{v}/|\alpha(\boldsymbol{v})|$. We define

$$\mathcal{R}_2 = \{(\overline{\boldsymbol{v}_1}, \ldots, \overline{\boldsymbol{v}_n}) \mid (\boldsymbol{v}_1, \ldots, \boldsymbol{v}_n) \in \mathcal{R}_0\}.$$

We furthermore set $\mathcal{R}_1 = \mathcal{R}_2 \times (\mathbb{R}^+)^{n-3}$. $\mathcal{R}_0 \approx \mathcal{R}_1$ is a rational equivalence: We can express any element of $\mathcal{R}_0$ as $(\boldsymbol{e}_1, \ldots, \boldsymbol{e}_3, \alpha_4 \boldsymbol{v}_4, \ldots, \alpha_n \boldsymbol{v}_n)$ such that $(\boldsymbol{e}_1, \ldots, \boldsymbol{e}_3, \boldsymbol{v}_4, \ldots, \boldsymbol{v}_n) \in \mathcal{R}_2$ and $\alpha_4, \ldots, \alpha_n \in \mathbb{R}^+$. $\mathcal{R}_1 \approx \mathcal{R}_2$ is a trivially a stable projection.

Assume that $\mathcal{M}_{\boldsymbol{V}}$ has m cocircuits $C^1, \ldots, C^m$. They correspond to hyperplanes spanned by elements in $\boldsymbol{V}$. For each cocircuit C^i we choose two distinct elements $a_i, b_i \in 1, \ldots, n$ with $C_{a_i}^i = C_{b_i}^i = 0$. Thus $\overline{\boldsymbol{v}_{a_i}}$ and $\overline{\boldsymbol{v}_{b_i}}$ span the corresponding (linear) hyperplane H_i. We define $f_i(\boldsymbol{V}) = \overline{\boldsymbol{v}_{a_i}} \times \overline{\boldsymbol{v}_{b_i}}$. The vector $f_i(\boldsymbol{V})$ is a normal vector of H_i. We set $f(\boldsymbol{V}) = (f_1(\boldsymbol{V}), \ldots, f_n(\boldsymbol{V}))$ and $\mathcal{R}_3 = f(\mathcal{R}_2)$. $\mathcal{R}_2 \approx \mathcal{R}_3$ is a rational equivalence, since f is a rational map with a rational inverse f^{-1}. This inverse can be taking the cross product of two hyperplanes that meet in a vector $\boldsymbol{v}_i$ and normalizing this vector.

The elements in $\mathcal{R}_3$ are the normal vectors of the facets of the planets in $\mathcal{P}(Z_{\boldsymbol{V}}, B)$. For a collection of scalars $A = (a_1, \ldots, a_m) \in \mathbb{R}^m$ and an $Y = (\boldsymbol{y}_1, \ldots, \boldsymbol{y}_m) \in \mathcal{R}_3$ we set

$$Z(Y, A) = \{\boldsymbol{x} \in \mathbb{R}^3 \mid \langle \boldsymbol{x}, \boldsymbol{y}_i \rangle \le a_i \text{ for } i = 1, \ldots, m\}, \quad \text{and}$$

$$\mathcal{R}_4 = \{(Y, A) \mid Y \in \mathbb{R}_3 \text{ and } Z(Y, A) \text{ is a planet in } \mathcal{P}(Z_{\boldsymbol{V}}, B).$$

$\mathcal{R}_3 \approx \mathcal{R}_4$ is a stable projection, since, the set of all $(a_1, \ldots, a_m)$ that lead to realizations of $Z_{\boldsymbol{V}}$ for given $\boldsymbol{y}_1, \ldots, \boldsymbol{y}_m$ is bounded by linear constraints that polynomially depend on the $\boldsymbol{y}_i$. (Each such constraint is either of the form $\mathbf{sign}(\mathbf{det}((\boldsymbol{y}_{i_1}, \alpha_{i_1}), \ldots, (\boldsymbol{y}_{i_4}, a_{i_4}))) = \sigma$ or of the form $\langle \boldsymbol{y}_i, \boldsymbol{p}_j \rangle = a_i$, such that $\boldsymbol{p}_i$ is a point of the basis and i is a facet that should be incident to it).

The elements $((\boldsymbol{y}_1, a_1), \ldots, (\boldsymbol{y}_m, a_m))$ are the homogeneous coordinates of facets of planets in $\mathcal{P}(Z_{\boldsymbol{V}}, B)$. By forming suitable exterior products we can calculate homogeneous coordinates of the corresponding vertices. This process can be expressed by an invertible map g and we define $\mathcal{R}_5 = g(\mathcal{R}_4)$. The inverse function can be carried out for instance by taking an element from $\mathcal{R}_5$, then calculating the vectors $\boldsymbol{v}_1, \ldots, \boldsymbol{v}_n$ at infinity, then normalizing them, then calculate the corresponding normal vectors $\boldsymbol{y}_1, \ldots, \boldsymbol{y}_m$, and finally use them to determine the α_i. Thus $\mathcal{R}_4 \approx \mathcal{R}_5$ is a rational equivalence.

To get from $\mathcal{R}_5$ to $\mathcal{R}_7 = \mathcal{P}(Z_{\boldsymbol{V}}, B)$ we simply have to a do a homogenization/dehomogenization process. As usual this van be done by first performing a rational equivalence $\mathcal{R}_5 \approx \mathcal{R}_6 = \mathcal{R}_7 \times (\mathbb{R}^+)^k$ and then a trivial stable projection $\mathcal{R}_6 \approx \mathcal{R}_7$. □

16.3   The Construction

Having established the last theorem, the construction that transfers universality results from oriented matroids to polytopes is not too complicated. The problem is that in general there are realizations of $Z_{\boldsymbol{V}}$ as *polytopes* that are not *planets*. This implies that the corresponding spaces $\mathcal{R}(Z, B)$ and $\mathcal{P}(Z, B)$ are not at all stably equivalent. For instance, an oriented matroid $\mathcal{M}$ that comes from our construction in Section 11.7 has rank 3. The corresponding zonotope Z has dimension 3. Thus the space $\mathcal{P}(Z, B)$ may be arbitrary complicated, while the space $\mathcal{R}(Z, B)$ is trivial (as the realization space of a 3-polytope).

We will construct a 6-polytope $P(\mathcal{M})$ that contains Z as 3-face F_Z. The structure of $P(\mathcal{M})$ will force that in every realization of $P(\mathcal{M})$ the face F_Z is indeed a planet. The construction again goes via Lawrence extensions and connected sums. We will make use of the following decisive property of the oriented matroids constructed in Section 11.7.

<u>LEMMA 16.3.1.</u>   *Let $\mathcal{M} = (X, \mathcal{L})$ be an oriented matroid as constructed in Section 11.7, let $NB(\mathcal{M}) \subseteq X^3$ be the set of non-bases of $\mathcal{M}$, and let $d > 3$. Every configuration of vectors $(\boldsymbol{v}_i)_{i \in X} \in \mathbb{R}^{d \cdot |X|}$ that satisfies*

$$\mathbf{dim}(\boldsymbol{v}_i, \boldsymbol{v}_j, \boldsymbol{v}_k) = 2 \Longleftrightarrow (i, j, k) \in NB$$

has linear dimension 3.

PROOF. Consider the construction (and pictures) of Section 11.7. Let $\mathcal{M}$ be an oriented matroid constructed there. The lines ℓ and ℓ' have the point ∞ in common. Hence the subconfiguration that consists only of the points on ℓ and ℓ' has linear dimension 3. Every additional point i is contained in a non-basis (i, j, k) that has one point i in $\ell - \{\infty\}$ and one point k in $\ell' - \{\infty\}$. Thus it is contained in the linear span of the points on ℓ and ℓ'. □

In other words, a configuration that only forces the non-bases of $\mathcal{M}$ to be the dependent sets of size 3 is automatically flat. We now describe the construction

of our desired polytope $P(\mathcal{M})$. We may restrict ourselves to the case that $\mathcal{M}$ is realizable. (In the non-realizable case we may associate to $\mathcal{M}$ any non-polytopal combinatorial 6-polytope). Let $\boldsymbol{V}$ be a realization of $\mathcal{M} = (X, \mathcal{L})$ and let Z be the face lattice of $\boldsymbol{Z}(\boldsymbol{V})$. We may represent the vertices of $\boldsymbol{Z}(\boldsymbol{V})$ by homogeneous coordinates $\boldsymbol{p}_\sigma = (x_\sigma, y_\sigma, z_\sigma, 1)$. To each element of X there corresponds a belt of parallel edges in $\boldsymbol{Z}(\boldsymbol{V})$. The supporting lines of these edges intersect in a point at infinity $\boldsymbol{q}_i := (v_{i,1}, v_{i,2}, v_{i,3}, 0) = (\boldsymbol{v}_i, 0)$. For a non-basis $(i, j, k) \in NB(\mathcal{M})$ we consider the Lawrence extension

$$\boldsymbol{P}_{(i,j,k)} := \boldsymbol{\Lambda}(\boldsymbol{Z}(\boldsymbol{V}), \{\boldsymbol{q}_i, \boldsymbol{q}_j, \boldsymbol{q}_k\}).$$

The polytope $\boldsymbol{P}_{(i,j,k)}$ has dimension 6 and contains Z as a 3-face. In any realization of $\boldsymbol{P}_{(i,j,k)}$ the supporting lines of the edges of the belts of i, j and k intersect in three points $\boldsymbol{q}'_i$, $\boldsymbol{q}'_j$, and $\boldsymbol{q}'_k$, respectively. These three points are (projectively) collinear.
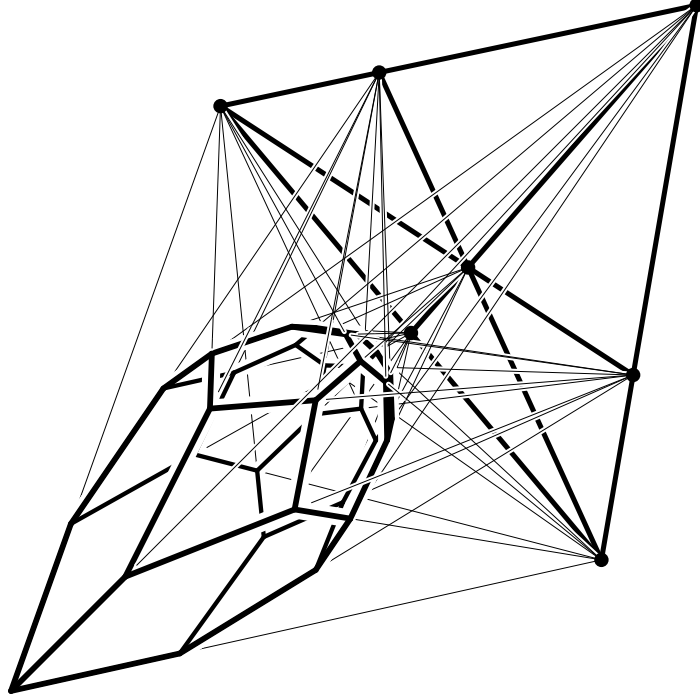
Figure 16.3.1:   The entire construction applied to the permutahedron.

Let $b_1, \ldots, b_k$ be the set of non-bases of $\mathcal{M}$. We define

$$P(\mathcal{M}) = \boldsymbol{P}_{b_1} \stackrel{\sim}{\#}_Z \boldsymbol{P}_{b_2} \stackrel{\sim}{\#}_Z \ldots \stackrel{\sim}{\#}_Z \boldsymbol{P}_{b_k}.$$

Here we use the generalized adapter methods of Section 14. The construction as written down here is a bit ambiguous and may need an explanation.

Each of the polytopes $\boldsymbol{P}_{(i,j,k)}$ contains Z as a 3-face and has three necessarily flat facets that contain Z (namely $\boldsymbol{\Lambda}(\boldsymbol{Z}(\boldsymbol{V}), \{\boldsymbol{q}_i, \boldsymbol{q}_j\})$, $\boldsymbol{\Lambda}(\boldsymbol{Z}(\boldsymbol{V}), \{\boldsymbol{q}_i, \boldsymbol{q}_k\})$, and $\boldsymbol{\Lambda}(\boldsymbol{Z}(\boldsymbol{V}), \{\boldsymbol{q}_j, \boldsymbol{q}_k\})$). Along these facets we may perform generalized connected sums as introduced in Section 14. The way in which this gluing is performed is ambiguous, and it depends on the particular choice of the chain of faces. We therefore once and forever fix the (combinatorial) way in which the gluing is performed and keep this for the rest of our considerations. The resulting polytope $P(\mathcal{M})$ has again Z as a 3-face. Moreover all the obstructions of the different polytopes $\boldsymbol{P}_{b_i}$ are present in $P(\mathcal{M})$. Let B' be a basis of $P(\mathcal{M})$ that is obtained by extending the polytope basis B for Z chosen in Lemma 16.2.3. and let b be the corresponding basis of $\mathcal{M}$.

Figure 16.3.1 shows a projective deformation of the permutahedron, together with the supporting lines of the edges. One can clearly see the seven points at which Lawrence extensions are performed.

LEMMA 16.3.2. *The polytope $P(\mathcal{M})$ described above has the following properties.*

(i) *In every realization of $P(\mathcal{M})$ the 3-face Z is projectively equivalent to a planet.*

(ii) *Every planet in $\mathcal{P}(Z, B)$ can be extended to a realization of $P(\mathcal{M})$.*

(iii) $\mathcal{R}(\mathcal{M}, b) \approx \mathcal{R}(P(\mathcal{M}), B)$.

PROOF. Let $\boldsymbol{P}$ be a realization of $P(\mathcal{M})$, and let $\boldsymbol{Z}$ be the substructure of $\boldsymbol{P}$ that corresponds to the 3-face Z. The points of $\boldsymbol{Z}$ affinely span $\mathbb{R}^3$. The supporting lines of the belts of edges in $\boldsymbol{Z}$ meet in points $\boldsymbol{q}_1, \ldots, \boldsymbol{q}_n$ (as a consequence of the Lawrence extensions). For each non-basis (i, j, k) the three points $\boldsymbol{q}_i$, $\boldsymbol{q}_j$, $\boldsymbol{q}_k$ are (projectively) collinear. By Lemma 16.3.1 all points $\boldsymbol{q}_1, \ldots, \boldsymbol{q}_n$ are (projectively) coplanar. After a projective transformation we may assume that the corresponding plane on which these points lie is at infinity. Hence, $\boldsymbol{Z}$ is projectively equivalent to a planet. This proves (i).

To see (ii), simply observe that every planet in $\mathcal{P}(Z, B)$ can be extended to a realization of each of the polytopes $\boldsymbol{P}_b$, with $b \in NB(\mathcal{M})$. All these realizations can be glued to form a realization of $P(\mathcal{M})$.

Let $\widehat{\mathcal{P}}(Z, B) \subseteq \mathcal{R}(Z, B)$ denote the subset of $\mathcal{R}(Z, B)$ that corresponds to the projective deformations of the planets $\mathcal{P}(Z, B)$. We have $\widehat{\mathcal{P}}(Z, B) \approx \mathcal{R}(Z, B)$. Part (i) implies that the deletion map that maps $\mathcal{R}(P(\mathcal{M}), B')$ to $\mathcal{R}(Z, B)$ has $\widehat{\mathcal{P}}(Z, B)$ as image. Part (ii) implies that the map onto $\widehat{\mathcal{P}}(Z, B)$ is surjective. An analysis similar to the one given in Section 8 shows that indeed the fibers over $\widehat{\mathcal{P}}(Z, B)$ behave nicely. We get

$$\mathcal{R}(P(\mathcal{M}), B') \approx \widehat{\mathcal{P}}(Z, B) \approx \mathcal{R}(Z, B) \approx \mathcal{R}(\mathcal{M}, b)$$

The last equivalence holds by Lemma 16.2.3. □

As an immediate consequence we obtain:

THEOREM 16.3.3 (UNIVERSALITY FOR 6-POLYTOPES). *For every basic primary semialgebraic set V over $\mathbb{Z}$ there is a 6-polytope whose realization space is stably equivalent to V.*

PROOF. We simply take the corresponding oriented matroid $\mathcal{M}$ that is constructed in Section 11.7 with $\mathcal{R}(\mathcal{M}, b) \approx V$. Applying Lemma 16.3.2 we get $\mathcal{R}(P(\mathcal{M}), B') \approx \mathcal{R}(\mathcal{M}, b) \approx V$.   □

17 Open Problems on Polytopes and Realization Spaces

17.1 Universality Theorems for Simplicial Polytopes

Our construction of the universality polytopes $P(\mathcal{S})$ in Section 8 generates polytopes that are of a particularly simple type: the only facets that occur are *pyramids*, *prisms* and *tents* (the tetrahedra that occur are special kinds of pyramids). Nonetheless, it is also desirable to obtain a universality theorem for simplicial polytopes, i.e. polytopes for which all faces are *simplices*. For this situation we cannot expect a universality theorem that states that we can encode both equations and strict inequalities. For a simplicial polytope P^{simp} one can always displace each vertex within an ε-neighborhood of itself and still have the same combinatorial type of the polytope (in other words the vertices of $\mathcal{R}(P^{\mathrm{simp}})$ can always be chosen to be in general position). Thus the realization space $\mathcal{R}(P^{\mathrm{simp}})$ is always an open semialgebraic set, and it is impossible to encode polynomial equations.

However, there is evidence that already in the case of 4-dimensional simplicial polytopes there are constructions that provide *open* variants of the Universality Theorem for realization spaces.

- The 4-polytope P_{BEK} of Bokowski, Ewald and Kleinschmidt [15, 16] that has disconnected realization space is *simplicial*. By forming connected sums of P_{BEK} with copies of itself one can prove that, for every $n \in \mathbb{N}$, there is a simplicial 4-polytope P_{BEK}^n with 2^n connected components.

- In the case of oriented matroids the original construction of Mnëv for the Universality Theorem for oriented matroids can be perturbed to obtain a corresponding universality theorem for *uniform* oriented matroids (i.e. all points are in general position). *For every open semialgebraic set V there is a uniform oriented matroid whose realization space is stably equivalent to V* [48]. This result makes use of a tricky perturbation technique due to Sturmfels and White [38], that replaces each point by four new points.

Thus we are lead to

CONJECTURE 17.1.1. *For every open primary semialgebraic set V (defined by strict inequalities only) there is a simplicial 4-polytope whose realization space is stably equivalent to V.*

173

However, there seems to be no direct way to perturb the polytopes $\boldsymbol{P}(\mathcal{S})$ and thus prove the above conjecture. The properties of the polytopes $\boldsymbol{P}(\mathcal{S})$ directly rely on affine dependences on the set of vertices. The *information frames* that are used to encode the values of the variables are n-gons and therefore have dependent vertex sets. The projective properties that are used to encode polynomials into the boundary structure of $\boldsymbol{P}(\mathcal{S})$ have their origin in the dependence of points in the 2-faces that are generated by Lawrence extensions. A suitable perturbation technique must be such that the polytope $\boldsymbol{P}(\mathcal{S})$ can be reconstructed from its perturbed companion.

A similar universality theorem is desirable in the cases of simplicial 3-diagrams and simplicial 4-fans. Is there a construction that provides a universality theorem for these structures? It is not clear at all how a positive answer to the above conjecture could imply an answer to this question. A universality construction for 4-fans would be important in relation to Cairns' smoothing theory [21].

17.2   Small Non-Rational 4-Polytopes

Our construction of a non-rational 4-polytope with 33 vertices is in a sense very artificial. We encode a planar incidence configuration by explicitly expressing each incidence as the non-prescribability of a 2-face in a polytope, and then combine all these polytopes via connected sums. By this many dependences of points occur that have their origin in the underlying construction, and not in the incidence configuration that is encoded. Compared to this, Perles' original example of a non-rational 8-polytope with only 12 vertices [31] essentially only uses dependences that are directly related to the underlying incidence configuration. It is very likely that the knowledge of a non-rational 4-polytope with minimal number of vertices will lead to new geometric insights on how to encode incidence relations into the boundary structure of a polytope.

<u>PROBLEM 17.2.1.</u>   Construct a 4-polytope $\boldsymbol{P}$ with a minimal number of vertices such that all realizations of $\boldsymbol{P}$ require non-rational vertex coordinates.

17.3   Many Polytopes

Are there asymptotically more non-realizable combinatorial 3-spheres or realizable ones?

Let $c(d,n)$ be the number of combinatorial types of (labeled) d-polytopes with n vertices, and let $c_s(d,n)$ be the corresponding number for simplicial polytopes. Analogously, let $s(d,n)$ be the number of (labeled) combinatorial $(d-1)$-spheres with n vertices, and let $s_s(d,n)$ be the corresponding number for simplicial combinatorial spheres. Much effort has been spent on computing these numbers for small values of n and d and on describing their asymptotic behavior. The enumerations of $c(n,d)$ for $d=3$ and small n already took place in the nineteenth century. Brückner [20] determined $c_s(n,3)$ for $n \leq 10$ and and

Hermes [35] determined $c(n, 3)$ for $n \leq 8$. More recently it was proved for the 4-dimensional case that $c_s(8, 4) = 37$ (Grünbaum, Sreedharan [32]), $s_s(8, 4) = 39$ (Barnette [9]), $s_s(9, 4) = 1296$ (Altshuler, Steinberg [3]), $c_s(9, 4) = 1142$ (Altshuler, Bokowski, Steinberg [5]), and $c(8, 4) = 1294$, $s(8, 4) = 1336$ (Altshuler, Steinberg [2, 4]).

These small values do not tell anything about the asymptotic behavior of these functions. For the case $d = 3$, we have $c(n, 3) = s(n, 3)$ and $c_s(n, 3) = s_s(n, 3)$, since by Steinitz's Theorem all combinatorial 2-spheres are realizable. By the results of Mani [44] and Kleinschmidt [41], we have similar statements for $n = d + 3$. For a long time the best known upper bound for $c_s(n, d)$ in general was $n^{cn^{d/2}}$, as a consequence of the upper bound theorem. A breakthrough in the question of determining the asymptotic behavior of $c_s(n, d)$ was achieved by Goodman and Pollack [27, 28], who proved that $c_s(n, d) \leq n^{d(d+1)n}$; this considerably improved the known upper bounds. A comparable result for $c(n, d)$ was proved by Alon [1], who asserted that $c(n, d) \leq (n/d)^{d^2(1+o(1))}$ as $n/d \to \infty$.

If one compares the number of combinatorial types of d-polytopes with the number of types of combinatorial $(d-1)$-spheres, Kalai proved [39] that for the simplicial case there are asymptotically many more triangulated non-polytopal spheres than polytopes. For $d \geq 5$, he proved that $\lim_{n \to \infty}(c_s(n, d)/s_s(n, d)) = 0$. The case $d = 4$ and the non-simplicial case is still open.

<u>PROBLEM 17.3.1.</u> Is it true that $\lim_{n \to \infty}(c_s(n, 4)/s_s(n, 4)) = 0$?

17.4   The Sizes of Polytopes

We have seen that the size of certain classes of 4-polytopes grows doubly exponentially in the number of vertices. Is this still true for simplicial polytopes? This question also seems to depend on perturbation techniques that generate simplicial polytopes from the polytopes $\boldsymbol{P}(\mathcal{S})$. For the case of oriented matroids for which corresponding results were proved by Goodman, Pollack and Sturmfels [29], the perturbation technique of Sturmfels and White [38] mentioned in 17.1.1 is applicable. Using this it is proved that, for the representation of planar, rational and uniform oriented matroids on n-elements, a grid size of at least $2^{2^{c_1 n}}$ is needed (c_1 is a suitable constant). In the uniform case, one can also apply a general result of Grigor'ev and Vorobjov on the size of solutions of polynomial inequalities [30]. This leads to an upper bound of the same asymptotic size. Every planar, rational and uniform oriented matroid on n-elements can be represented in a grid of size $2^{2^{c_2 n}}$ (with appropriate constant c_2) [29].

Neither a result for the simplicial case nor an upper bound are so far available for 4-polytopes.

<u>PROBLEM 17.4.1.</u> Find an upper bound for the number $\nu(n, 4)$, the grid size such that every rational 4-polytope with n vertices has a realization in $\{1, 2, \ldots, \nu(n, 4)\}^4$.

PROBLEM 17.4.2.   Find upper and lower bounds for the $\nu_s(n,4)$, the grid size such that every simplicial 4-polytope with n vertices has a realization in $\{1, 2, \ldots, \nu_s(n,4)\}^4$.

In the 3-dimensional case it is also not clear what is the actual asymptotic behavior of $\nu(n,3)$. In Section 13.2 we proved that $\nu(n,3) \leq 2^{18n^2}$. It is still open whether $\nu(n,3)$ grows polynomially or singly exponential.

PROBLEM 17.4.3.   Either construct a class of 3-polytopes $\boldsymbol{P}_n$ with $\nu(\boldsymbol{P}_n) > 2^{cn}$ for a suitable constant c, or prove that $\nu(\boldsymbol{P})$ is bounded from above by a polynomial in the number of vertices of $\boldsymbol{P}$.

17.5   Rational Realizations of 3-Polytopes

We have seen that, as a consequence of Steinitz's Theorem, every 3-polytope is realizable with rational vertex coordinates. However, there are other parameters of 3-polytopes that are interesting to investigate. The dimension of the realization space of a 3-polytope $\boldsymbol{P}$ is closely related to the number of edges e of $\boldsymbol{P}$. We have $\dim(\mathcal{R}(\boldsymbol{P})) = e - 6$. So it seems reasonable that the realization space can be parameterized by the lengths of the edges. This is true for the simplicial case but not in general, as the example of a 3-cube shows (there are many realization of the cube with all edges having unit length).

PROBLEM 17.5.1.   Does every 3-polytopes admit a realization with all edge lengths being rational?

PROBLEM 17.5.2.   For fixed $\boldsymbol{P}$ are the realizations of $\boldsymbol{P}$ with rational edge lengths dense in the set of all realizations?

The above considerations about the 3-cube show that these questions are closely related to questions of rigidity of polytopes. We may also combine rationality for edge lengths and vertex coordinates.

PROBLEM 17.5.3.   Does every 3-polytopes admit a realization with all edge lengths and all vertex coordinates being rational?

17.6   The Steinitz Problem for Triangulated Tori

We close our list of open problems with another question in 3-dimensional space. Steinitz's Theorem gives a complete characterization of embeddability of 2-dimensional combinatorial spheres. Topologically the next class of objects having higher complexity are tori. We may ask whether all polytopal complexes topologically equivalent to tori are embeddable without self-intersections in $\mathbb{R}^3$. In general, this question has to be answered in the negative. The following figure

shows a polytopal complex that represents a torus (we have to identify points labeled identically and the corresponding edges). This combinatorial complex is not embeddable in 3-space since by a incidence theorem coplanarity of the vertices of the eight flat quadrangles forces coplanarity of the broken quadrangle [18].
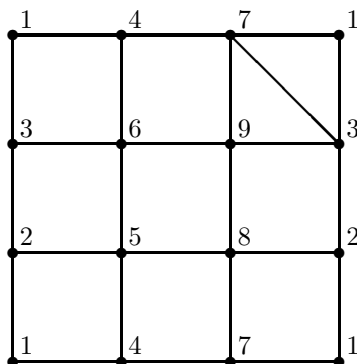
Figure 17.6.1: A non-embeddable cell decomposition of the torus.

However, so far it is not known whether there exist non-embeddable triangulated tori.

PROBLEM 17.6.3.   Does there exist a triangulation of a torus that has no embedding in $\mathbb{R}^3$ with flat triangles and without self-intersections?

Bibliography

[1] N. Alon, *The number of polytopes, configurations and real matroids, Mathematika* **33** (1986), 62–71.

[2] A. Altshuler & L. Steinberg, *Enumeration of the quasi-simplicial* 3*-spheres and* 4*-polytopes with eight vertices, Pacific J. Math.* **113** (1984), 269–288.

[3] A. Altshuler & L. Steinberg, *Enumeration of the combinatorial* 3*-manifolds with nine vertices, Discrete Math.* **16** (1976), 113–137.

[4] A. Altshuler & L. Steinberg, *The complete enumeration of the* 4*-polytopes and* 3*-spheres with eight vertices, Pacific J. Math.* **118** (1985), 1–16.

[5] A. Altshuler, J. Bokowski & L. Steinberg, *The classification of simplicial* 3*-spheres with nine vertices into polytopes and non-polytopes, Discrete Math.* **31** (1980), 115–125.

[6] M. Bayer & B. Sturmfels, *Lawrence polytopes, Can. J. Math* **42** (1990), 62–79.

[7] A. Björner, M. Las Vergnas, B. Sturmfels, N. White & G.M. Ziegler, *Oriented Matroids, Encyclopedia of Mathematics*, Vol. 46, Cambridge University Press 1993.

[8] D.W. Barnette, *Diagrams and Schlegel Diagrams,* in: *Combinatorial Structures and Their Applications*, Gorden and Breach 1970, 1–4.

[9] D.W. Barnette, *The triangulations of the* 3*-sphere with up to* 8 *vertices, J. Combinatorial Theory Ser.* **A 14** (1973), 37–52.

[10] D.W. Barnette, *Preassigning the shape of projections of convex polytopes, J. Combinatorial Theory Ser.* **A 42** (1986), 293–295.

[11] D.W. Barnette, *Two "simple"* 3*-spheres, Discrete Math.* **67** (1987), 97–99.

[12] D.W. Barnette & B. Grünbaum, *Preassigning the shape of a face, Pacific J. Math* **32** (1970), 299–302.

[13] L.J. Billera & B.S. Munson, *Polarity and inner products in oriented matroids, European J. Combinatorics*, **5** (1984), 293–308.

[14] A. Björner, *Topological methods,* in: *Handbook of Combinatorics* (R. Graham, M. Grötschel, L. Lovász, eds.), North Holland 1994, to appear.

[15] J. Bokowski, G. Ewald & P. Kleinschmidt, *On combinatorial and affine automorphisms of polytopes, Israel J. Math* **47** (1984), 123–130.

179

[16] J. Bokowski & A. Guedes de Oliveira, *Simplicial convex 4-polytopes do not have the isotopy property,* Portugaliae Mathematica **47** (1990), 309–318.

[17] J. Bokowski & B. Sturmfels, *Polytopal and nonpolytopal spheres - an algorithmic approach,* Israel J. Math., **57** (1987), 257–271.

[18] J. Bokowski & B. Sturmfels, *Computational Synthetic Geometry,* Lecture Notes in Mathematics, **1355**, Springer-Verlag, Berlin Heidelberg 1989.

[19] J.A. Bondy & U.S.R. Murty, *Graph Theory with Applications,* MacMillan and American Elsevier, New York 1976.

[20] J.M. Brückner, *Vielecke und Vielflache. Ihre Theorie und Geschichte,* Leipzig 1900.

[21] S.S. Cairns, *Homeomorphisms between topological manifolds and analytic manifolds,* Ann. of Math. **41** (1940), 796–808.

[22] R. Conelly, *Rigidity and Energy,* Invent. Math. **66** (1982), 11–33.

[23] H. Crapo & W. Whitely, *Statics of frameworks and motions of panel structures, a projective geometric introduction,* Structural Topology **6** (1982), 42–82.

[24] J. Edmonds & A. Mandel, *Topology of oriented matroids,* Ph.D. Thesis of A. Mandel, University of Waterloo 1982, 333 pages.

[25] G. Ewald, P. Kleinschmidt, U. Pachner & C. Schulz, *Neuere Entwicklungen in der kombinatorischen Konvexgeometrie,* in: *Contributions to Geometry* (J. Tölke, J. Wills, eds.), *Proc. Geometry Symposium Siegen 1978,* Birkhäuser, Basel (1979), pp. 131–163.

[26] I. Fáry, *On straight line representations of planar graphs,* Acta Sci. Math. (Szeged), **11** (1948), 229–233.

[27] J.E. Goodman & R. Pollack, *There are asymptotically far fewer polytopes than we thought,* Bull. Amer. Math. Soc **14** (1986), 127–129.

[28] J.E. Goodman & R. Pollack, *Upper bounds for configurations and polytopes in* $\mathbb{R}^d$, Discrete Comput. Geometry **1** (1986), 219–227.

[29] J.E. Goodman, R. Pollack & B. Sturmfels, *The intrinsic spread of a configuration in* $\mathbb{R}^d$, Journal Amer. Math. Soc. **3** (1990), 639–651.

[30] D.Yu. Grigor'ev & N.N. Vorobjov, *Solving systems of polynomial inequalities in subexponential time,* J. Symbolic Comput. **5** (1988), 37–64.

[31] B. Grünbaum, *Convex Polytopes,* Interscience Publ., London 1967; revised edition (V. Klee, P. Kleinschmidt, eds.), Springer-Verlag, in preparation.

[32] B. Grünbaum & V. Sreedharan, *An enumeration of simplicial 4-polytopes with 8 vertices,* J. Combin. Theory **2** (1967), 437–465.

[33] H. Günzel, R. Hirabayashi & H.Th. Jongen, *Multiparametric optimization: On stable singularities occurring in combinatorial partition codes,* Control & Cybernetics **22** (1994), 153–167

[34] H. GÜNZEL, *The universal partition theorem for oriented matroids,* Preprint TH-Aachen (1994), 29p.; *Discrete Comput. Geometry,* to appear.

[35] O. HERMES, *Die Formen der Vielflache, J. Reine Angew. Math.* **120** (1899), 27–59; **122** (1900), 124–154; **123** (1901), 312–342.

[36] J.E. HOPCROFT & P.J. KAHN *A Paradigm for robust geometric algorithms, Algorithmica* **7** (1992), 339–380.

[37] J.F.P. HUDSON, *Piecewise Linear Topology,* Benjamin, New York 1969.

[38] B. JAGGI, P. MANI-LEVITSKA, B. STURMFELS & N. WHITE, *Constructing uniform oriented matroids without the isotopy property, Discrete Comput. Geometry* **4** (1989), 97–100.

[39] G. KALAI, *Many triangulated spheres, Discrete Comput. Geometry* **3** (1988), 1–14.

[40] P. KLEINSCHMIDT, *On facets with non-arbitrary shapes, Pacific J. Math.,* **65** (1976), 511–515.

[41] P. KLEINSCHMIDT, *Sphären mit wenigen Ecken, Geometriae Dedicata,* **5** (1976), 97–101.

[42] P. KLEINSCHMIDT & U. PACHNER, *Shadow-boundaries and cuts of convex polytopes, Mathematika,* **27** (1980), 58–63.

[43] N. LINIAL, L. LOVÁSZ & A. WIDGERSON, *Rubber bands, convex embeddings and graph connectivity, Combinatorica,* **8** (1988), 91–102.

[44] P. MANI, *Spheres with few vertices, J. Combinatorial Geometry Ser. A,* **13** (1972), 346–352.

[45] J.C. MAXWELL, *On reciprocal figures and diagrams of forces, Philos. Mag.,* **4** (1864), 250–261.

[46] J.C. MAXWELL, *On reciprocal figures, frames and diagrams of forces, Trans. Royal Soc. Edinburgh,* **26** (1869–1971), 1–40.

[47] P. MCMULLEN, *Duality, sections and projections of certain euclidean tilings, Geometriae Dedicata,* **49** (1994), 183–202.

[48] N.E MNËV, *On manifolds of combinatorial types of projective configurations and convex polyhedra, Soviet Math. Doklady,* **32** (1985), 335–337.

[49] N.E MNËV, *The universality theorems on the classification problem of configuration varieties and convex polytopes varieties,* in: Viro, O.Ya. (ed.): *Topology and Geometry — Rohlin Seminar,* Lecture Notes in Mathematics **1346**, Springer, Heidelberg 1988, 527–544.

[50] N.E MNËV, *The universality theorems on the oriented matroid stratification of the space of real matrices,* in: *Applied Geometry and Discrete Mathematics – The Victor Klee Festschrift* (P. Gritzmann, B. Sturmfels, eds.), DIMACS Series in Discrete Mathematics and Theoretical Computer Science, Amer. Math. Soc., Providence, RI, **6** (1991), 237–243.

[51] S. ONN & B. STURMFELS, *A quantitative Steinitz' theorem, Beiträge zur Algebra und Geometrie* **35** (1994), 125–129.

[52] J. Richter-Gebert, *Mnëv's universality theorem revisited,* Proceedings of the Séminaire Lotaringien de Combinatorie 1995, 211–225.

[53] P. Shor, *Stretchability of pseudolines is NP–hard,* in: *Applied Geometry and Discrete Mathematics – The Victor Klee Festschrift* (P. Gritzmann, B. Sturmfels, eds.), DIMACS Series in Discrete Mathematics and Theoretical Computer Science, Amer. Math. Soc., Providence, RI, **4** (1991), 531–554.

[54] O. Schramm, *How to cage an egg, Inventiones Math.* **107** (1992), 543–560.

[55] E. Steinitz & H. Rademacher, *Vorlesungen über die Theorie der Polyeder,* Springer Verlag, Berlin 1934; reprint, Springer Verlag 1976.

[56] E. Steinitz, *Polyeder und Raumeinteilungen,* in: *Encyclopädie der Mathematischen Wissenschaften.* Band 3 (Geometrie) Teil 3AB12, 1–139, 1922.

[57] B. Sturmfels, *Boundary complexes of convex polytopes cannot be characterized locally, Bull. London Math. Soc.,* **35** (1987), 314–326.

[58] B. Sturmfels, *Some applications of affine Gale diagrams to polytopes with few vertices, SIAM J. Discrete Math.,* **1** (1988), 121–133.

[59] W.T. Tutte, *How to draw a graph, Proc. London Math. Soc.,* **13** (1963), 743–767.

[60] K. Wagner, *Bemerkungen zum Vierfarbenproblem, Jahresbericht der Deutschen Mathematiker-Vereinigung,* **46** (1936), 26–32.

[61] D.B. West, *Introduction to Graph Theory,* Prentice Hall, Upper Saddle River 1996.

[62] W. Whitely, *Motions and stresses of projected polyhedra, Structural Topology* **7** (1982), 13–38.

[63] E.C. Zeemann, *Seminar on Combinatorial Topology,* mimeographed notes, Inst. des Hautes Études Sci., Paris 1963.

[64] G.M. Ziegler, *Three problems about 4-polytopes,* in: *Polytopes: Abstract, Convex and Computational* (T. Bisztriczky, P. McMullen, R. Schneider & A. Weiss, eds.), Kluwer, Dordrecht 1994, 499–502.

[65] G.M. Ziegler, *Lectures on Polytopes,* Graduate Texts in Mathematics **152**, Springer-Verlag New York 1995. Corrections, updates, and more, `http://www.math.tu-berlin.de/~ziegler`

INDEX

183